Polyelectrolyte Microcapsules for controlled cargo-release and sensing applications in living cells

Dissertation
zur
Erlangung des Doktorgrades
der Naturwissenschaften
(Dr. rer. nat.)

dem
Fachbereich Physik
der Philipps-Universität Marburg

vorgelegt von

Markus Ochs

aus
Frielendorf

Marburg/Lahn, 2012

Vom Fachbereich Physik der Philipps-Universität
als Dissertation angenommen am 30.04.2013

Erstgutachter: Prof. Dr. Wolfgang J. Parak
Zweitgutachter: Prof. Dr. Kerstin Volz
Prüfer : Prof. Dr. Reinhard Noack
Prüfer: Prof. Dr. Eric Meggers

Tag der mündlichen Prüfung: 08.05.2013
Hochschulkennziffer 1180

Die vorliegende Arbeit wurde am Fachbereich Physik
der Philipps-Universität Marburg unter Anleitung von

Herrn Prof. Dr. Wolfgang J. Parak

in der Zeit von August 2010 bis Januar 2013 angefertigt.

Zusammenfassung

Inhalt dieser mehrschichtigen Arbeit ist es, multifunktionale Mikrokapseln aus polymeren Materialien für biologische und biomedizinische Anwendungen zu präparieren. Die Herstellung solcher Kapseln basiert auf der schichtweisen Adsorption von entgegengesetzt geladenen Polymeren, sog. Polyelektrolyten, auf geladen Oberflächen (Layer-by-Layer assembly). Als sphärische Basis für die Kapselherstellung wurden poröse Kalciumcarbonat-Partikel verwendet. Wegen der vorhandenen Oberflächenladung dieser, wenige Mikrometer großen Partikel, haften neben den geladenen Polymeren auch weitere geladene Moleküle wie Farbstoffe, Proteine oder auch hydrophile Nanopartikel an der Oberfläche. Diese zusätzlich eingebauten Materialien verleihen der Polymerhülle weitere Eigenschaften wie Fluoreszenz, paramagnetisches Verhalten oder das Vermögen, Licht Energie in Hitze umzuwandeln. Diese Funktionalisierungen spielten für die Realisierung der angestrebten Anwendungsbereiche eine entscheidende Rolle.

Neben der Funktionalisierung der Hülle spielt bei der vorliegenden Arbeit auch das Füllen der Kapseln eine entscheidende Rolle. Die Kavitäten wurden mit verschiedensten Materialien angereichert. Hierzu wurden insgesamt drei Füllmechanismen herangezogen und auf die Anforderungen der jeweiligen Anwendung angepasst. So können die Kapseln schon bei der Herstellung der Kerne durch Ausfällen der einzukapselnden Moleküle gefüllt werden. Weiterhin können „leere“ Kapseln erzeugt und nach ihrer Fertigstellung via Schrumpfverfahren mit dem Gewünschten Cargo angereichert werden. Als letzte, und relativ neue Methode wurde ein Imprägnierverfahren angewandt, welches durch Anhaften oder Einfangen der Füllstoffe an amphiphilen Polymer-Mizellen realisiert wird. Hierbei können in die Kavität eingebaute Mizellen sowohl kleine hydrophile als auch hydrophobe Moleküle einlagern und später gezielt freisetzen.

Nach der Charakterisierung der hergestellten Materialien mittels Spektroskopischer, Licht- und Elektronenmikroskopischer Analyse wurden die Kapseln gezielt auf die vorgesehenen Anwendungen getestet. Hierbei wurde ein besonderer Schwerpunkt auf die intrazelluläre Freisetzung der Füllstoffe gelegt. Mit zahlreichen Experimenten wurde die Freigabe der Cargo-Moleküle nachgewiesen. Zudem wurden mit den freigegebenen Materialien Reaktionen in den Zellen ausgelöst. Reaktive Substanzen, welche getrennt eingekapselt wurden konnten erfolgreich intrazellulär freigesetzt und die Reaktion miteinander nachgewiesen werden. Desweiteren konnten Nukleinsäureketten (sog. mRNS) erfolgreich eingekapselt, gezielt freigesetzt und die biologische Produktion der kodierten Proteine demonstriert werden.

Ein weiterer Punkt der Untersuchung betrachtete die Möglichkeit, Kapseln zu lenken oder zu platzieren. Mit Hilfe einer Flusskammer wurde der Blutstrom in lebenden Organismen simuliert und mit Hilfe von Magnetfeldern konnten die Kapseln gezielt auf einer Zellschicht abgelagert werden. Hierdurch konnten ebenso großflächige Bereiche belegt, als auch Strukturen in Mikrometer Skala erzeugt werden.

Neben der Freisetzung von Materialien und gelenkten Deponierung von Kapseln untersucht die vorliegende Arbeit aber auch die mögliche Nutzung von Mikrokapseln als Sensoren für die Zusammensetzung der Umgebung. Diese Sensoreigenschaften wurden auf Basis von ionenselektiven Fluoreszenzfarbstoffen im extrazellulären, als auch im intrazellulären Raum getestet.

Zusammenfassend stellen die hier vorgestellten polymeren Mikrokapseln einen fortschrittlichen und vielfältig anwendbaren Ansatz im Hinblick auf bio-medizinische Anforderungen zur Wirkstoffübermittlung und Sensorik dar.

Summary

Topic of the presented work is the preparation of multifunctional polymer microcapsules for biological and biomedical applications. The fabrication of such capsules is based on the layered adsorption of oppositely charged polymers, the so-called polyelectrolytes, onto charged templates (layer-by-layer assembly). As spherical base for the capsules porous calcium carbonate particles have been used. In addition to molecules that were encapsulated into the final polymer capsules further properties such as fluorescence, paramagnetic behavior or the ability to convert light energy into heat were embedded into the polymer shell by implementing nanoparticles. These functional groups were crucial for the realization of the experimental demands on the microsystems.

In addition to the functionalization of the shell an efficient filling of the capsules with a multitude of different molecules was one of the major developments. Besides a co-precipitation method (pre-filling of the templates), a post-loading technique as well as the enrichment of the capsules with amphiphilic polymer micelles were used for loading the capsules. This last approach even allowed for filling both, hydrophilic and hydrophobic molecules into the the polymer microcapsules.

The prepared materials were observed via absorbance or fluorescence spectroscopy or electron- and optical microscopy, the capsules were tested specifically for their intended applications. Here, special emphasis was placed on the intracellular release of the encaged cargo materials. Numerous experiments were performed to test the release of the cargo molecules within living cells. The efficient release via external laser-triggered heating was proven and improved by variation of gold-nanoparticle concentration attached to the polymer shells. In addition, the released content distributed into the cells, was observed to react after its liberation. Reactive substances, which have been separately encapsulated could successfully be released intracellularly and the occurring reactions were detected. Furthermore, nucleic acid chains (mRNA) could be encapsulated and successfully be released within cells. The cellular production of the RNA-encoded proteins was demonstrated. Another aim of the study was the targeted delivery of capsules to a desired place. In a flow chaannel, the flow of blood in living organisms was simulated. Capsules modified with iron-oxide nanoparticles could be deposited selectively on a cell layer with the help of magnetic field gradients. This enabled for deposition of capsules on a large scale area as well as on on small, sub-millimeter patterns.

Additionally to the release of materials and controlled deposition of capsules, the presented work is also studying the possible use of microcapsules as sensors for the composition of the environmental solution. These sensor properties were tested on the basis of ion-selective fluorescent dyes in the extracellular as well as in the intracellular space.

In summary, the presented polymer microcapsules were proven as an advanced and versatile approach towards bio-medical requirements for drug delivery and sensing applications.

Acknowledgement / Danksagung

I want to thank Professor Wolfgang Parak for giving me the possibility to perform my PhD-thesis in a very, pleasent and friendly atmosphere of the Biophotonics workgroup. I wouldlike to thank him and my supervisor Dr. Susana Carregal-Romero for all the helpful and constructive discussions.
Related to the unresting help not only concerning the work, offered to me by Loretta, I want to send special thanks to her.
I am grateful for all the support and benefits I got from the whole Biophotonic workgroup.
Special thanks to Christian, Moritz, Raimo and Dominik, always available for constructive discussions and supporting me in all questions of labwork.
I also thank Xiang for preparing TEM pictures and Pilar for giving technical understanding of the microscopes.
Great thanks again to Christian for proofreading this thesis.
I offer my regards and blessings to all of those who supported me in any respect during the completion of this work.

Ganz besonderen Dank richte ich an dieser Stelle an meine Familie, die zu jeder Zeit hinter mir stand und mir, nicht zuletzt durch die finanzielle Unterstützung während des Studiums die Realisierung meiner Doktorarbeit ermöglichte.

Contents

1. Introduction and Goals

During the last decades, medical and pharmaceutical applications were facilitated due to developments and evolutions in drug composition, fabrication and administration. New technologies, e.g. nanoparticle-based drug delivery, complexation or nano- and microencapsulation of active substances led to a whole new field of applications in medical and biological investigations[1]. Delivery applications still are under major focus of a huge community of researchers that investigate new possible pathways of active compounds like drugs, nucleic acids, proteins or sensor materials into biological tissues or cells. Additional to the delivery of material, the carrier systems should be capable of further functionality like sensing ability, multiplexing sub-structures or anti clearing modification.

The presented work was focused on the development of polymer microcapsules as multifunctional sensing and drug delivery tool. The potential of nano- or microcapsules for encapsulating various compounds and efficiently protect them from intracellular or other defense mechanism (e.g. immuno clearing)[2-4] makes them an interesting approach towards drug delivery. This is an important requirement for advanced delivery tools as it could significantly decrease the administered dose. Furthermore, a protective shell around the cargo substance would reduce side effects in the organism. One keyword concerning encapsulation of molecules is functionalization. Additional to the (active) substances that are delivered through the system other functional groups or active sites could be embedded within the capsules. These would allow for additional applications or simultaneous observation of the spatial position, the activity of the released compounds or medically interesting factors on the spot. The use of biodegradable materials for the composition of capsule walls potentially allows for intracellular release of encapsulated compounds without external trigger[5]. Modifications of the capsules with fluorescent probes, quantum dots (QDs), metallic nanoparticles (NPs) or other nano-materials have been shown to be efficient technologies for embedding further functionalities into such systems. Labeling, sensing, controlled release or targeting could sufficiently be addressed by embedding such materials into microcapsule systems. Especially the controlled release of material in living cells and the targeting or guidance of delivery vehicles to a spot of interest are major requirements for sophisticated delivery or sensing tools that could be applied in modern medicine.

The presented work focused on the development of such multifunctional delivery vehicles with additional ability for sensing[6-8]. Capsules were fabricated basing on calcium carbonate ($CaCO_3$) microspheres. These microparticles could easily be produced and filled via precipitation method. The fabrication of a polymer shell was realized via so-called layer-by-layer assembly (LbL) of a polyelectrolyte multilayer (PEM) shell.[9-14] Due to electrostatic attractions between the charged core and differently charged polymer chains alternately mixed with the particles[15, 16], a coating layer assembled around the $CaCO_3$ template. After removing the solid core by chelating agents (in mild conditions) a cavity was obtained that was protected by the PEM shell. In addition the physicochemical[17, 18], the mechanical[19] and permeability[6, 7, 20, 21] properties of these capsules have been investigated.

For the filling of the cavity, depending on the desired cargo material that should be encapsulated, different loading methods could be selected[22-26]. These methods will be described more detailed in section 2.1-2.3 and the assets and drawbacks as well as the

potential of the respective methods will be presented. The selection of encapsulation technique according to the desired cargo turned out to be one crucial step towards efficient filling of the core and subsequent release of the cargo to living cells. Previous work concerning $CaCO_3$-based microcapsules showed limitations of the filling capacity depending on the size of encapsulated molecules. Especially material with low molecular weight could only be kept inside such multilayer capsules non satisfactory. The new investigations presented here show the possibility to efficiently load such capsules with huge macromolecules as well as small cargo like single dye molecules and even hydrophobic materials. Furthermore, the data show that the materials are not only accumulated within the capsules but also being released efficiently from the cavities after intracellular opening of the shell.

The next key step for the capsules was the composition and functionalization of the multilayer polyelectrolyte shell. The embedding of fluorescent probes but especially the addition of a variety of nanoparticles into the shell were important prerequisites for the functions of the final capsules. The uptake of fluorescent dyes or particles into/onto the coating layers provided spectral and spatial separation of different capsules and their cargo[27]. In particular this was necessary for multiplexed sensing applications (section 3.1). One major advantage of the presented capsules was demonstrated with the fabrication of several ion-selective sensor capsules which were proven to act together as multiplexing ion sensor tool. A large variety of nanoparticles could be selected to be implemented into the microcapsules to fulfill different functions. Fluorescent quantum dots worked as a staining or "bar-code" of the capsules[28]. Gold nanoparticles (AuNPs) were embedded for efficient energy conversion[29] from light into heat. This made the so-modified capsules heat sensitive and adressable for externally triggered opening[30, 31]. Magnetic nanoparticles consisting of iron oxide colloids provided magnetic susceptibility to the capsules. Such micro containers could be guided via magnetic fields and be deposited along specified target areas[32]. This approach in combination with intracellular triggered release meant a huge step towards targeted drug delivery and showed great potential towards future in vivo applications. Intracellular release of ion sensitive substances as active sensor compounds enabled for real-time observation of extra- or intracellular environmental conditions. Individual or sequential delivery of one or more active substances via light-controlled release and demonstration of intracellular activity were major aims of the work. Especially the delivery of nucleic acids and their subsequent translation into proteins as well as the observation of time kinetics were investigated. Control experiments observing the release from non-controlled and untargeted delivery systems [33, 34] should point out the advantages of the fabricated PEM microcapsules. Another experiment was based on the sequential release of two compounds that, after being liberated into the cytosol of a cell, react and form a fluorescent product. This approach demonstrated the possibility of performing intracellular reactions from two (or more) remotely delivered materials.

Concluding the results of the presented work, the PEM microcapsules based on spherical $CaCO_3$ templates and capable of various modifications in the polyelectrolyte shell should demonstrate a highly versatile system for a multitude of applications. The combination of various materials that can be embedded into the polymer shell brought high functionality to the capsules. Together with a multitude of cargo molecules that were proven to be embedded

within the cavities of the capsules the presented capsule based system acts as a multifunctional tool for a high variety of applications in biology and medicine[35].
Nevertheless, the data presented here show also the difficulties and drawbacks of a highly modified system like the microcapsules. The huge number of different materials that have to be assembled in the right sequence and in appropriate concentrations also mean a multitude of adjustment steps. Furthermore, interactions between two or more of the used materials could occur. Efficient filling of microcapsules turned out to be very challenging. However, this is one of the major requirements to a delivery system. One further demand on biological compatible tools is a high control over the size. As the size of the $CaCO_3$ templates is limited to the range of few micrometers, this demand is fulfilled only to a certain point. Future applications based on polyelectrolyte multilayer capsules should also focus on more control over template diameter. Final aim for future investigations could be a nano-sized capsule system with the same or comparable properties like for the micro-sized capsules.

2. Experimental Section

2.1 Fabrication of PEM capsules filled with various cargo materials

Microcapsules based on spherical $CaCO_3$ templates and consisting of polyelectrolyte multilayers have become a very versatile tool for encapsulating any kind of cargo. Small molecules as single fluorophores can be loaded into such capsules as well as macromolecules with a high molecular weight and a branched structure[17]. Also hydrophobic materials can be enriched inside PEM microcapsules and be combined with hydrophilic molecules to fulfill multifunctional tasks. Furthermore, any kind of charged material like fluorophores, macromolecules as well as nanoparticles can be embedded into the multilayer shell to combine the functionality of material that is loaded in the cavity and the components that stick to the shell (surface) of the capsule.

To encapsulate huge macromolecules like Proteins or branched polymers (like dextrane or dextrane-conjugates) a so-called co-precipitation approach can be applied[36]. Here the material that should be encaged in the capsules is mixed with one of the precursors of the $CaCO_3$ ($CaCl_2$ or Na_2CO_3)[1, 10]. By mixing the two precursors rapidly, the fast supersaturation of the solution leads to the formation of small $CaCO_3$ seeds that afterwards grow in a porous-spherical structure until they reach a final size of a few micrometers (cf. Figure 1). The resulting microspheres have a porous structure full of pores in which the macromolecular cargo material can stick. Due to charge interaction of the $CaCO_3$ and the cargo during the sphere-growth the huge molecules that should be loaded into the capsules are entering the pores and are being entrapped by the growing $CaCO_3$ template. In this way a pre-filled particle that is enriched with the desired cargo (mostly with a molecular weight above 50 kDa) can be produced. After the coating of the particles with several layers of polyelectrolytes of alternating charge, the surrounding polymer shell has reached a thickness of few nanometers. Though its porosity is high enough to ensure the permeation of solvent molecules, ions and small molecules with a low molecular weight, it is tight enough to retain the huge macromolecular cargo inside the cavity after removal of the core material via chelating agent Ethylenediaminetetraacetic acid

(EDTA). This complexation of the Ca^{2+} ions leads to complete dissolution of the $CaCO_3$ and retains only the entrapped macromolecular cargo within the cavities of the capsules.

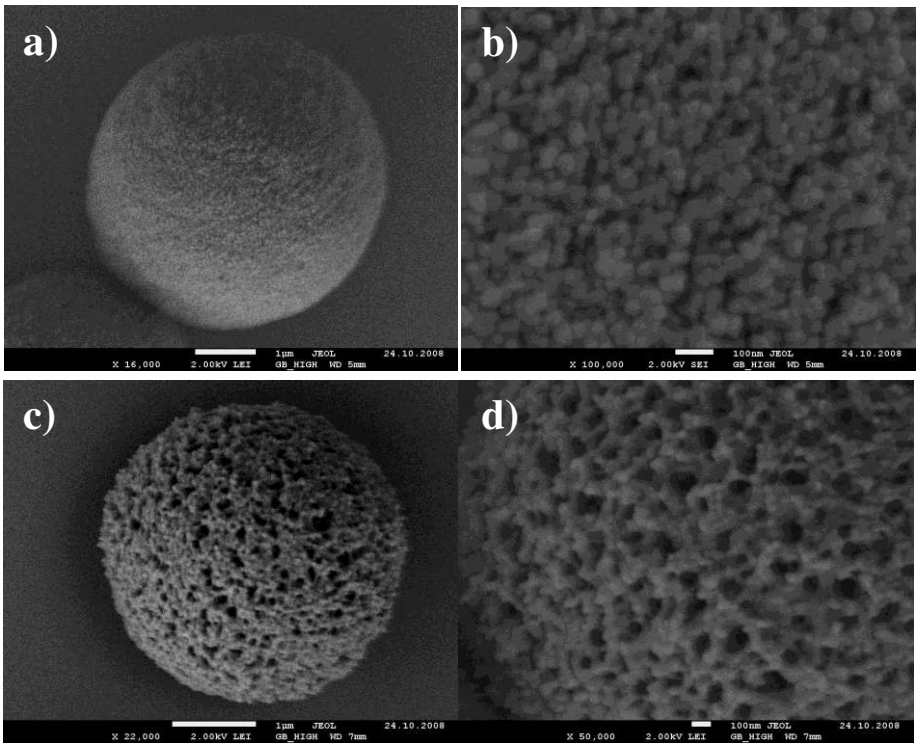

Figure 1: SEM images of $CaCO_3$ particles before (a + b) and after coating (c + d) with four bilayers of PSS/PAH. Resulting PE multilayer shell is porous and rough. Ions and small polymers can diffuse through these pores.

If the macromolecules that should be encapsulated are smaller than a certain threshold they cannot be retained stably inside the porous polymer shell. The cargo will leak out from the capsules and some molecules will stick to the polyelectrolyte walls due to electrostatic interaction. Such capsules suffer from the low filling rate of the cavity and cannot be used for fluorescence based sensing applications.

To encapsulate material that is still huge but suffers from the explained leakage problem, a post-loading method can be applied. To keep these materials stable inside the capsules one takes advantage of the heat dependent conformation changes of the polyelectrolyte shell materials. While dispersing the capsules (optionally pre-loaded with the desired filling) in a concentrated cargo solution, the mixture is heated up for 1-2 hours at around 65-70°C[37]. The small material desired to be encapsulated is interpenetrating the capsules and slowly being entrapped inside the capsule´s cavities as the polymer shell shrinks due to the heat. While polyelectrolytes fold and stick more tightly at a higher temperature, the pores in the polymer shell are getting smaller. This process is mostly irreversible (depending on the used polyelectrolytes) and therefore the resulting capsules are less penetrable and have a smaller diameter. Cargo molecules that are in the mentioned size fraction can be encapsulated safely in so-fabricated capsules without losing their penetrability for solvents, small molecules (<<10 kDa) or ions.

For encapsulating cargo that is much smaller than 10 kDa or even hydrophobic another approach can be used. Micelles consisting of amphiphilic block-copolymers are co-precipitated within the $CaCO_3$ instead of huge macromolecules described above[38]. For the presented work polystyrene-block-poly acrylic acid (PS-b-PAA) copolymers were used to

fabricate nanoscaled micelles inside the capsules. The block-copolymer powder is dissolved in a polar, organic solvent (here dimethylformamide) and then slowly dropped into a diluted Na_2CO_3 solution. The phase-change leads to the formation of spherical PS-PAA micelles that are later entrapped within the porous $CaCO_3$ particles similarly to the huge cargo molecules described above. After coating of the templates with several layers of polyelectrolytes the $CaCO_3$ is removed via EDTA treatment retaining capsules that are enriched with block-copolymer micelles. As long as so fabricated capsules are dispersed in aqueous solvents the hydrophilic ends (PAA) are showing outwards the micelles. If hydrophilic molecules that are small enough to penetrate the PE shell are exposed to the capsules they will stick to the hydrophilic PAA of the micelles. If otherwise the capsules are dispersed in an organic solvent containing hydrophobic cargo molecules, the phases of the copolymer micelles reverse and the loading material can stick to the hydrophobic polystyrene (PS) block. After phase transfer back to aqueous solvent, the cargo is safely entrapped within the micelles. Alternatively, a sequential loading of both types of cargo (small hydrophilic and hydrophobic molecules) can be applied to combine the different cargo properties.
Further details about the filling strategies of PEM capsules with various cargo materials of different sizes can be found in the following chapters.

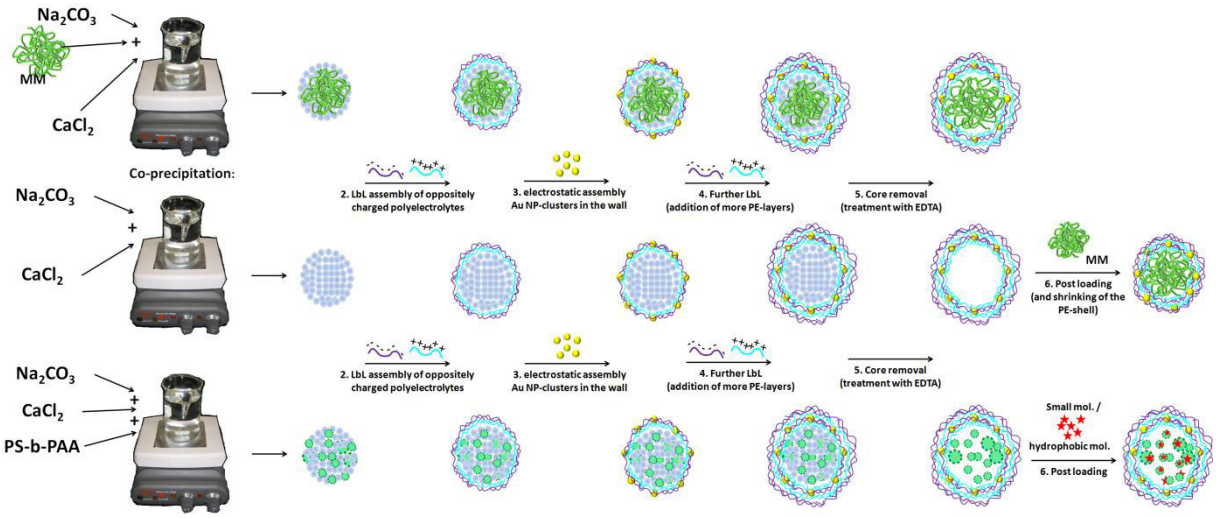

Figure 2: Schematic drawing of the three different fabrication/loading approaches applied in this work. Upper row represents the co-precipitation method for loading capsules with huge macromolecules (>> 10 kDa). Center row shows post-loading for encapsulation of macromolecules in the range of ~ 10 kDa. Lowest row shows the block-copolymer micelle-approach that can be applied for loading small molecules (<< 10 kDa) or hydrophobic cargo into the capsules.

2.2 Synthesis of pre-filled capsules via co-precipitation method

Solid $CaCO_3$ spheres filled with high molecular weight cargo material (like dextran-conjugated fluorophores, Proteins or nucleic acids) were fabricated using the following protocol (volumes can vary depending on application):
615 µL aqueous $CaCl_2$ (0,33 M) were mixed with 1 mL of a desired high molecular weight cargo solution. While stirring at 1000 rpm, 615 µL Na_2CO_3 (0,33 M) were added rapidly and mixed for 30 seconds. Afterwards the suspension was left for 3 minutes at room temperature to settle down. Resulting particles were dispersed in clean water (MilliQ). Then, the supernatant water was removed by centrifugation of the suspension at 1200 rpm for 2 minutes. This washing step was repeated 3 times.
Clean particles were then resuspended in 1 mL of PSS solution (5 mg/mL in 0,5 M NaCl; pH 6,5) and left in shaker for 15 minutes.
Supernatant PSS solution was then removed and suspension was washed 3 times with clean water. A positive layer of polyelectrolyte was deposited by resuspending the PSS coated, negatively charged particles in 1 mL of PAH solution (5 mg/mL in 0,5 M NaCl; pH 6,5). The coating procedure included shaking within PE solution, washing and resuspending. These steps were repeated until four to five PE-bilayers were achieved (depending on requirements of the application).
After final coating step particles were again washed 3 times with clean water and well suspended in EDTA solution (0,2 M; pH 5,5) to remove the $CaCO_3$ cores. Removal of the $CaCO_3$ can be observed due to slight formation of gas bubbles (leakage of CO_2). After suspension became clear supernatant EDTA solution was removed via slow centrifugation to avoid aggregation of PE microcapsules (1000 rpm, 10-12 minutes). Afterwards the capsules were washed for 3 times with clean water.
Final capsules were observed to be stable for months stored in aqueous solvent at 4-8°C.
Macromolecules that have been co-precipitated with the $CaCO_3$ were stably kept within the cavities of the capsules. The high molecular weight and the mostly branched structure of such macromolecules lead to highly and uniformly filled capsules. Dextrane-conjugated fluorophores that were entrapped within the capsules were mostly used as markers or as sensor materials for fluorescence based sensing applications.

2.3 PEM capsules enriched with small hydrophilic or hydrophobic cargo molecules

$CaCO_3$ templates for incorporation of small molecules within block-copolymer micelles were produced following a protocol explained by Tong et al.[38]. For this purpose 10 mg of PS-b-PAA block copolymer was dissolved in 1 mL of dimethylformamide and dropwise mixed with 10 mL of $NaCO_3$ solution (0,33 M) under vigorous stirring. After mixing for 30 minutes (to disperse the forming polymer micelles) 10 mL of $CaCl_2$ were rapidly added and the resulting suspension of $CaCO_3$ particles enriched with PS-b-PAA micelles was mixed for another 30 seconds. Particles were then left for 5 minutes of ripening and then washed 3 times with Ethanol to remove unbound PS-b-PAA polymer risiduals. Finally the particles were washed 3 times with clean water and redispersed in MiliQ water.

The coating procedure of these particles was similar to the ones filled via co-precipitation method with high molecular weight macromolecules (cf. section 2.2). Alternating dispersion of the particles in polyelectrolytes of opposite charge (LbL assembly) lead to the formation of multilayer shells. Final structure of the polymer shell was according to the one of other capsules made by four to five bilayers.

The removal of $CaCO_3$ from the template was performed via chelating process with EDTA solution (0,2 M; pH 5,5) for 30-60 minutes. The removal of the $CaCO_3$ for this kind of capsules turned out to be much slower than for other capsules. We assume that this results from the hydrophobic sub-structures (micelles) that are present in the pores of the $CaCO_3$ template. Slight hydrophobic interaction hinders the EDTA from entering the pores and slows down the chelating process. Nevertheless, the dissolution of the core finally leads to empty capsules that were enriched with nano-sized block-copolymer micelles. Resulting capsules were washed 3 times with clean water and supernatant was removed.

Capsules were then suspended in 200 µL of an aqueous solution containing the hydrophilic cargo molecules or in an organic solution containing the hydrophobic cargo material for three hours. As organic solvent ethanol, acetone and dimethylsulfoxide (DMSO) were successfully tested. Other organic solvents are most likely to work as well for filling the capsules with hydrophobic molecules. The concentration of the desired cargo was set as high as possible to obtain efficient filling rates of the capsules.

Finally capsules were washed 3 times with clean water to remove unbound cargo substrate and (if suspended in organic solvent) to reverse micelle phases towards hydrophilic exterior.

2.4 Modification of PEM capsules with nanoparticles for further functionalization

PEM capsules have been further modified with nanoparticles to gain functionality (fluorescence, magnetic susceptibility or energy conversion property) in the polymer shell.
To obtain fluorescently labeled capsules the polyelectrolyte shell was treated with fluorescent quantum dots (QDs). The ones used for this study were CdSe/ZnS core-shell particles with narrow fluorescence emission maxima at 577 nm, 596 nm, and 610 nm respectively. But also any other quantum dots could be embedded within the multilayer shell of the capsules. In this study, the quantum dots were used as markers to stain or trace the polymer capsules. Combinations of several different sizes of fluorescent particles (different colors) lead to a multitude of "bar-coded" capsules that could facilitate multiplexing applications.
To fabricate capsules with magnetic properties for targeted deposition or directed delivery, capsules were incubated in iron-oxide nanoparticles (fabricated with a protocol previously published[39, 40]). These particles show high magnetic susceptibility and therefore respond to external magnetic fields and provide finally magnetic properties to the microcapsules.
Capsules that should be opened via remote-controlled external triggers were modified with gold-nanoparticles (AuNPs). These metallic NPs show a strong surface plasmon resonance that is used to convert electromagnetic energy (from light) into heat. For this study usually 15 nm gold-nanoparticles (stabilized with sodium citrate) fabricated through the Turkevich method[37, 41].

Basis for the implementation of nanoparticles into the polymer multilayer shell is the surface charge of the nanoparticles. AuNPs are sodium citrate stabilized and show negative charge. The semiconductor QDs and the magnetic iron-oxide particles were previously stabilized with an amphiphilic polymer to make them water-soluble[42]. The surface coating of the nanoparticles also provides negative charge.
Therefore all nanoparticles for capsule modification were attached after a positive polyelectrolyte coating step. Usually, capsules were suspended within a nanoparticle containing solution after finishing the second (PSS/PAH)-bilayer. Capsules were left in the nanoparticle solution under slight shaking for ~15 minutes. Afterwards the NPs were sufficiently adsorbed to the surface of the microcapsules. To ensure the total charge saturation of the previously positive charged surfaces, capsules were afterwards incubated in negatively charged PSS solution followed by three washing steps with clean water.
Resulting $CaCO_3$ microparticles were washed and LbL treatment with PSS and PAH was continued similar to the protocol in section 2.2 until the desired number of polyelectrolyte bilayers was reached. A typical structure of the final multilayer shell corresponded to the following: **$(PSS/PAH)_2$-NPs-$(PSS/PAH)_2$**.

2.5 Fabrication of Ball-in-Ball capsules as versatile multi-ion sensor systems

So-called Ball-in-Ball multi-compartment capsules were fabricated based on completely coated (and filled) $CaCO_3$ microparticles. These were produced with the protocol described in the previous sections. Coated particles with four or more bilayers of polyelectrolytes were redispersed within a solution containing $CaCl_2$ (0,33 M) and stirred at 1000 rpm. An equal amount of Na_2CO_3 solution (0,33 M) was added dropwise to the suspension. After 30 seconds of additional stirring and 3 minutes ripening time, particles were washed several times with fresh water to remove small, unbound $CaCO_3$ microbeads. The arising calciumcarbonate layer assembled around the outer shell of the initial microparticle. The dropwise addition of the Na_2CO_3 was found out to be essential for the formation of uniform and spherical layer expansion. If the precursor was added rapidly to the suspension of microtemplates and $CaCl_2$, arising salt was not attached as a flat and uniform layer around the template but as huge Bucky balls and clusters resulting in non-spherical and aggregated particles. After the microparticles were enlarged by the addition of $CaCO_3$ layers, they were coated with polyelectrolyte multilayers until a desired thickness of the outermost shell was reached.
If the $CaCO_3$ layer that assembled around the PE shell did not reach sufficient thickness for desired applications, its layer thickness could be increased. This was done either by increasing the volume of precursor solution or by coating the arised $CaCO_3$ with a layer of PSS and subsequent repetition of salt attachment.
The so-fabricated Ball-in-Ball capsules provide a second cavity around the inner PEM shell. This facilitates the embedding of more functionality into the complex system (second cavity and second PE shell). The second cavity can also just act as spacer between the inner cavity and the outermost polyelectrolyte layers. This turned out to be crucial for the fabrication of bar-coded multiplexing sensor capsules[28].

2.6 Remote-controlled release of cargo material inside living cells

Polymer microcapsules modified with gold nanoparticles in the shell are known to perform as remote-controllable release-system for cargo material inside living cells[43-45]. AuNPs can easily being embedded into the polyelectrolyte multilayer shell of the capsules due to electrostatic interactions (see section 2.4)[46]. In our approach a laser system emitting near-infrared (NIR) light was decided to be used as the electromagnetic spectrum shows significantly lower absorbance in biological tissue [47, 48]. However, gold-nanoparticles of a certein size (here 15 nm) have an absorbance peak around 530 nm. This corresponds to the surface plasmon resonance of quasi-free electrons present in the metallic nanoparticle [49-52]. To modify the collective surface plasmon resonance (SPR) peak of the nanoparticles, they have to be agglomerated. By reducing the colloidal stability of the nanoparticles (screening the electrostatic repulsion), NPs come closer and finally attach to each other. This leads to the fusion of the surface electron states and an increased mean free path of the electrons in the nanoparticle. The SPR frequency shifts towards higher wavelengths and thus the absorbance maximum of final clusters. The fabrication and embedding of such AuNP aggregates is explained in section 2.4.

So-modified capsules show strong absorbance and energy conversion ability at the presented laser emission wavelength (830 nm; max. 130 mW output; CV-laser), whereas initial gold nanoparticles absorb light energy mainly around 540 nm (green light).

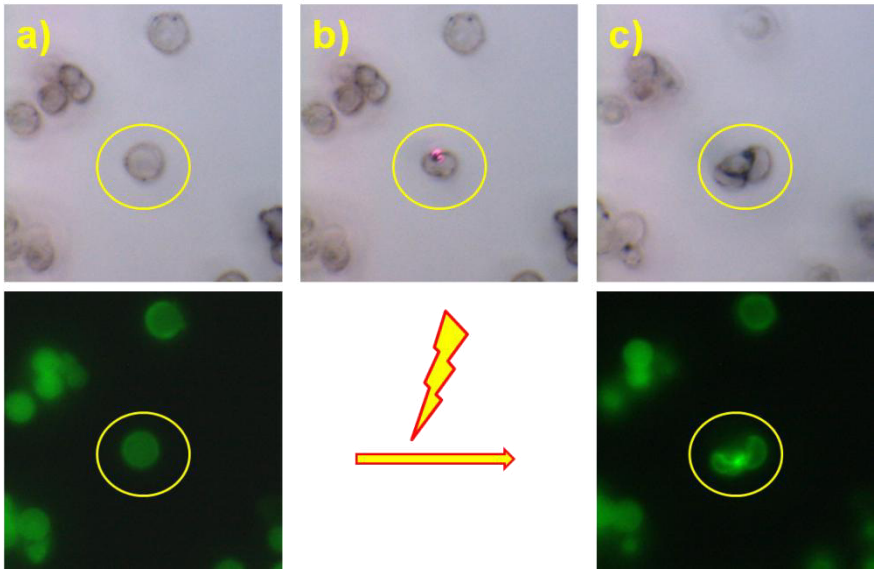

Figure 3: Microscopic imaging of light-controlled opening of gold-modified PEM microcapsules. Release strategy is demonstrated on one capsule that is filled with FITC-dextran a) before laser treatment. NIR-laser beam is focused on the gold-NP-cluster enriched PE multilayer shell of the microcapsule b) and induces deformation and cracking of the capsule. c) after opening the capsule is burst and has released a fraction of its cargo material.

The NIR light-beam was coupled into the optical pathway of the fluorescence microscope used for observation of the cargo release. By focusing the beam, its total area on the focal plane was only few μm^2 what means, the beam could be aimed on the edge of one single PEM capsule. By applying 50-70% of the total energy output of the laser (corresponds to ~15-20 mW on the focal plane), capsules could be opened efficiently with the laser system within few seconds of illumination. During the exposure of the capsules the occurring heat assembles within a small volume in and around the treated nanoparticle clusters and locally leads to very high temperatures. Consequently, the water in and around the particle clusters starts to evaporate and the upcoming pressure leads to the destruction of the multilayer structure of the polymer shell. As the effect is strongly localized on a small area within the shell (especially if the clusters are embedded within a multilayer structure), the occurring perforation is also small. Nevertheless, if the laser treatment is performed too long or the laser output is too high, the stronger heat accumulation leads to an "explosion" of the capsules. The reaction on the heating is not localized to a small volume within the PE shell but withtakes the whole capsule (cf. **Figure 3**).

The subsequent release of material from the capsules and its spreading over the cytosolic compartment of living cells was observed with the fluorescence microscope that was used to couple the laser. For the observation one has to consider, that released material was spread and diluted strongly within the cells. This leads to a very low fluorescence signal of the released fluorophore. To observe these low signals, the fluorescence within initial capsules often had to be overexposed. Furthermore, by using confocal microscopes, the emission contrast and therefore the observed signal could strongly be increased.

2.7 Targeted deposition of capsules via magnetic forces in flow-channel

Another goal of this study besides the demonstration of efficient release of reactive and functional cargo inside living cells was the targeted deposition of PEM capsules at a desired cellular growth area. For this purpose, capsules have been modified with magnetic iron-oxide nanoparticles (cf. section 2.4). This added magnetic susceptibility to the capsules and made them responding to magnetic field gradients.

To simulate the natural blood flow or intercellular medial movement, a flow channel experiment was prepared. With an adjustable peristaltic pump the transversal speed of the fluid in the flow-channel was set to ~8 cm/s which correspond to typical blood flow-rates in a human body. As basic flow device a "µ-slide-I" from Ibidi was used. Its flow channel had dimensions of 5 mm x 50 mm x 0.4 mm (width/length/height) resulting in 100 µL flow medium capacity. Two additional reservoirs were filled with 600 µL of flow medium each. Both reservoirs were connected to a polyethylene tube with 2 mm inner cross-section that passed the peristaltic pump. Within the channel of the device, adherent cells were growing. These were seeded at least one day before the experiment started to become a confluent layer and cover the whole ground of the flow channel. This was necessary as the confluent cells can be repelled from the surface of the device due to the high velocity of the pumped-through medium. The connection between the cells in a confluent layer keeps the cells on the ground.

Capsules modified with magnetic nanoparticles were mixed with the flow medium in the inlet reservoir. A strong permanent magnet was then placed underneath the flow channel. By starting the pump, due to the high flow velocity magnetic capsules were mainly floating through the channel without any interaction or contact with the adhering cells. Only at the sights where the magnet was placed underneath the channel, capsules were observed to settle down and stick to the cells on the ground.

With this method also sub-millimeter patterns could be prepared within the channel using three different capsules modified with diverse fluorescent dyes.

3. Results and Discussion

This thesis represents a cumulative work that should demonstrate the high versatility of the presented PEM microcapsules especially for cellular release of cargo material and intracellular sensing applications. The fundamental structure of multilayer polyelectrolyte shell around spherical, porous $CaCO_3$ microparticles turned out to be a highly advisable approach for the encapsulation of various cargo materials. The easy fabrication of the templates via simple chemical precipitation, its ability to be filled while core-production, the biological-friendly environmental conditions for core-removal and the wide range of material that can be embedded into so-fabricated capsules satisfy the requirements for such multifunctional systems.

The experimental progress shown in this work is resuming the basic investigation of fabrication and characterization of LbL-multilayer microcapsules shown in my diploma thesis. While the release of cargo molecules outside living cells and the ion-sensing potential of the capsules could be shown to some extent, especially the release of material inside living cells, sequential release from differently filled capsules and intracellular reactivity are very new approaches that are shown in this thesis. Furthermore, mathematical computations complete the proof of multiplexing capability of ion-selective sensor capsules. Intracellular release of such ion-sensitive fluorophore into the cytosol enable the first time for pH-determinations, unrestricted from endosomal compartments, inside cells. Release and reaction kinetics of biologically active messenger RNA and the comparison of the reactions triggered by laser-opening and passive release strategies finalizes the investigations that are presented in this thesis.

3.1 PEM microcapsules as ion-sensors for extra- and intracellular sensing

Microcapsules have already shown their potential to be filled with a high variety of different cargo materials. The enrichment of capsules with dextran-conjugated fluorophores of a high molecular weight (> 100 kDa) turned out to work well. Fluorophores can be co-precipitated with the core-forming $CaCO_3$. Furthermore, final capsules show a very homogeneous distribution of fluorophore in the cavity. The encapsulation of organic dyes that show pH-dependent fluorescence intensity change or sensitivity on other ions (here Na^+ and K^+ ions) can easily be entrapped within such capsules and be used as optical microsensors.
The first step, that represented the encapsulation of such ion-selective fluorophores, was already been done by several research groups[53-56].
Now, the capsules should act as multiplexing sensor tool for simultaneous determination of several ion concentrations. For this purpose three different types of capsules have been fabricated containing dextran-conjugated dyes sensitive for H^+, K^+ and Na^+ ions. To facilitate simultaneous detection of all three kinds of ions sensor capsules had to be modified with a unique QD-based bar-code tagging. Each type of capsule containing a different ion-sensitive dye was equipped with another composition of three different types of QDs. Yellow, orange and red QDs with a fluorescence emission maximum at 577 nm, 596 nm and 610 nm accordingly were used to produce the 3-bit encoded bar-code tagging (cf. **Figure 4**). Herein, the "concentration code" for the tagging could possibly be extended towards the fabrication of 7 different types of capsules ("100", "101", "110", "111", "001", "010" and "011") according to the QD-combination. Crucial for the identification of the different capsules was the selection of fluorescence filters set into the microscope. Their transmission windows had to be as narrow as possible and fitting to the maximum emission spectrum of the QDs. Nevertheless, spectral overlapping of the QD emission of one channel into the transmission window of another type of QD could not be prevented entirely (cross-talk). Especially cross-talk between the sensor dye in the cavity of the capsules and the outer shell turned out to be one mayor barrier for simultaneous fluorescence analysis in the cavity (sensing) and in the shell (identification). Therefore another layer of $CaCO_3$ was laminated onto the PE multilayer shell. Subsequent LbL-coating of the received core-shell particle and removal of the $CaCO_3$ resulted in a Ball-in-Ball structure (cf. section 2.5). Herein, the second cavity around the inner PE shell provided spatial distance between the inner cavity with the sensor dye and the outer shell including the staining nanoparticles. This prevented spectral overlapping of the bar-code signal and the emission of the sensor material and facilitated the successful multiplexing measurement (**Figure 4**).

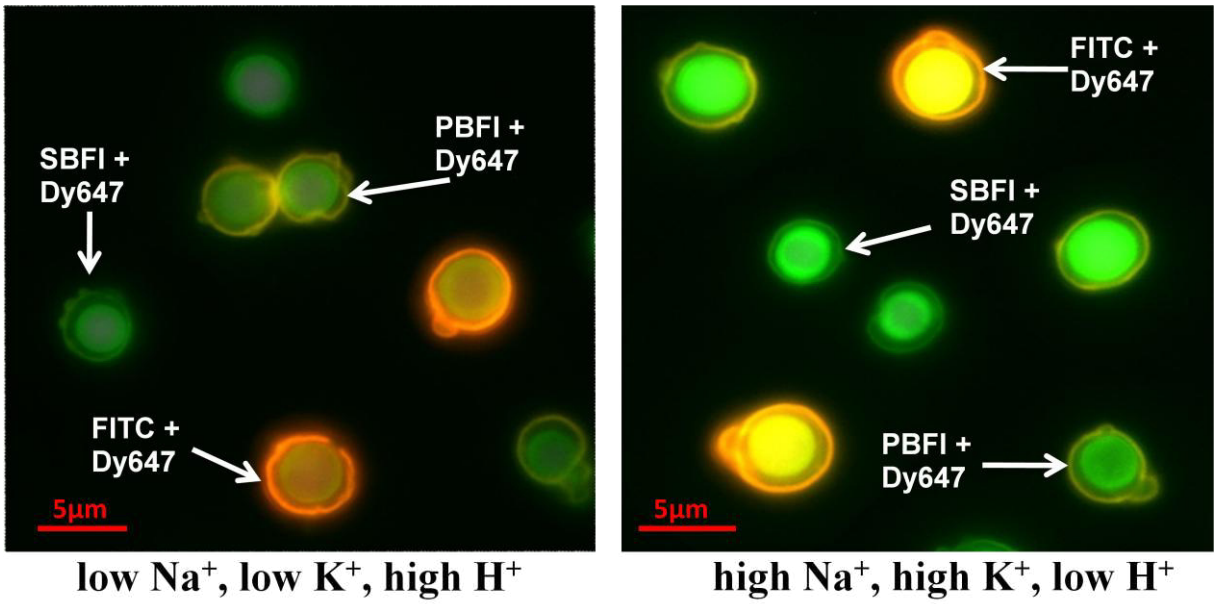

Figure 4: Fluorescence image of a mixture of the three different types of capsules in two solutions with different ion concentrations; via the fluorescent barcode the type of each capsule can be clearly identified. By changing from a low ion ($c(Na^+)$ = 5 mM, $c(K^+)$ = 5 mM, pH = 5) to a high ion condition ($c(Na^+)$ = 140 mM, $c(K^+)$ = 140 mM, pH = 9) the I_{SBFI}/I_{Dy647} ratio of the sodium responsive capsules is raised, and in the false color fluorescence image the capsule cavities appear more blue-green compared to the more reddish appearance at low sodium concentration.

Another complication of the multiplexing approach was the cross-sensitivity of the different sensor dyes. Changed pH-values for example are not only observed with the pH-sensitive dye in the corresponding capsules, but also strongly influences the emission intensity of the potassium and sodium sensor capsules. Furthermore, an increasing amount of sodium is also influencing the emission value of the potassium sensitive fluorophore (cf. **Figure 5**). To overcome these difficulties and facilitate the measurement of all three ion concentrations simultaneously, emission values have been determined firstly in test solutions to obtain calibration curves for each pair of cross-sensitive dye. Afterwards, intensity deconvolution had to be performed using the measured values and comparing them with the calibration curves.

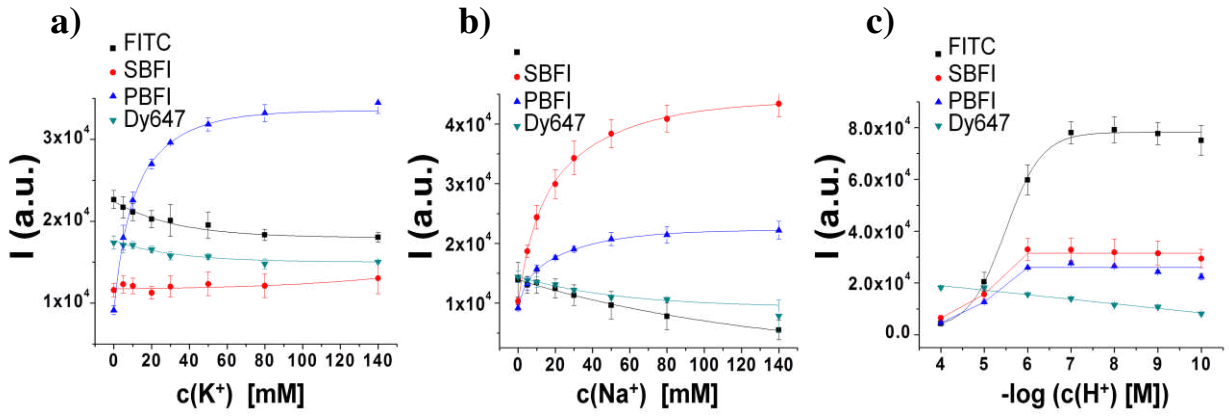

Figure 5: Fluorescence emission intensity of four different analyte sensitive fluorophores under different ion concentrations. The fluorescence intensity (I) of FITC, SBFI, PBFI, and Dy647 dyes is plotted versus pH (-log(c(H^+)), sodium ion concentration c(Na^+)), and potassium ion concentration (c(K^+)). Strong influence of changed pH value for the sensing of Na^+ and K^+ (c) as well as the cross-sensitivity of potassium sensitive dye for increasing sodium ion concentration can be observed (b).

For the purpose of intensity deconvolution the measured values have been ploted and fitted into 3D-surface curves (**Figure 6a**)) Afterwards, the intensity surface was projected onto the 2D-plane of the ion concentrations (here K^+ and Na^+) as a so-called contour plot (**Figure 6b**)). Here, each color corresponds to a certain intensity value. If now two contour plots have been overlaid and the border lines of the measured fluorescence values are followed towards the intersection, the true ion concentration could be determined (**Figure 6c**)). Additional to the cross-sensitive potassium- and sodium-capsules, the pH-dependence of the emission values determined via pH-sensor capsules was inset for finally measure all three ion concentrations simultaneously.

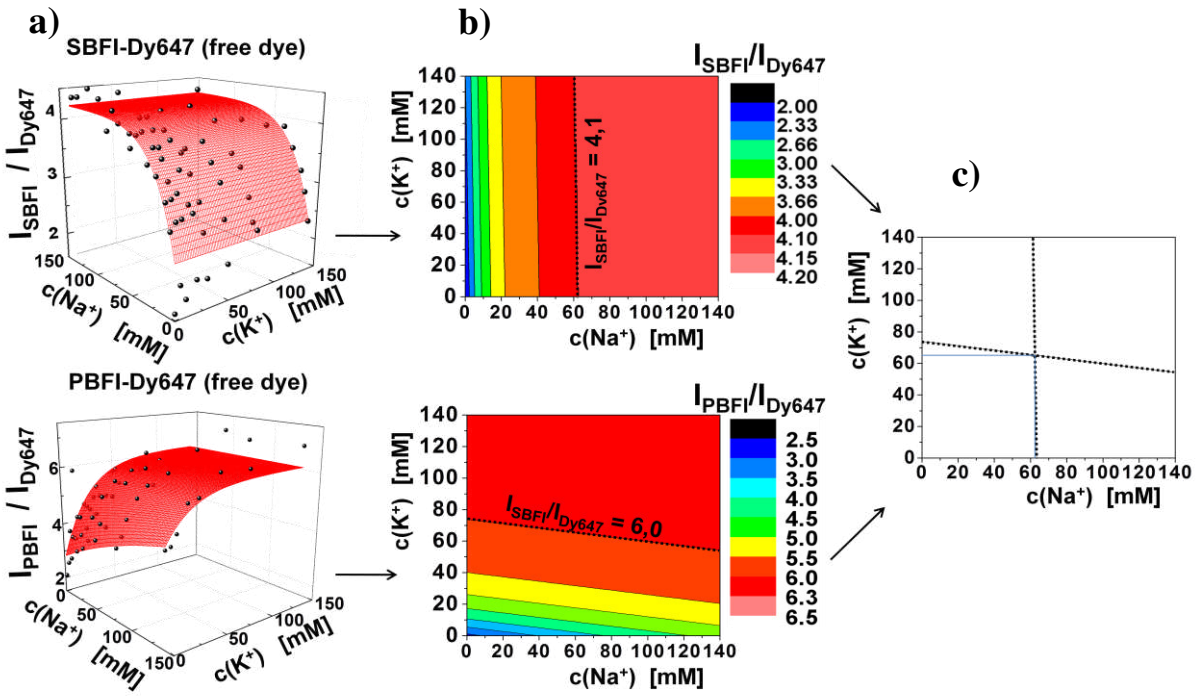

Figure 6: Cross-sensitivity between sodium and potassium sensitive fluorophores in solutions with different ion concentrations. (a) As potassium sensitive dye PBFI to Dy647 emission (I_{PBFI}/I_{Dy647}) was determined and plotted versus the Na^+ and K^+ concentration in a 3-dimensional representation. The sodium sensitive counterpart was the emission of SBFI to Dy647 (I_{SBFI}/I_{Dy647}) versus Na^+ and K^+ concentration. A contour plot of the same data is represented in (b), in which one looks toward the projection of I_{SBFI}/I_{Dy647} or I_{PBFI}/I_{Dy647}, accordingly in the c(Na^+) and c(K^+) plane. The intensity information is presented within the color steps. As following the lines of a measured intensity ratio in each dye/reference *combination one meets the intersection point that gives out the information of the "real"* ion concentration in the solution (c).

3.2 Statistical analysis of intracellular release success rate

To verify whether the release mechanism of cargo from the PEM microcapsules was reliable the success rate of intracellular laser treatment and subsequent release of cargo molecules was determined in the following experiment. Capsules filled with CascadeBlue-dextran (CB-dextran) (~10 kDa) were chosen for the experiment due to the high contrast of the fluorophore. To a confluent layer of HeLa cells in a round dish (containing ~100.000 cells) a number of ~500.000 CB- dextran filled capsules was added. After incorporation time of ~12 hours in 37°C at 5% CO_2 the cells were observed via fluorescence microscope. Certain areas covered with cells that contained at least one nicely filled capsule were photographed with the microscope. Afterwards, the according cells were treated with the laser beam. Note, that appropriate output energy, focusing of the beam on the focal plane and heating-technique were tested before the statistic analysis. Laser energy level of 60-70 % of the total power (corresponds to 18-21 mW on the focal plane) and a treatment time of around one second on the polymer shell were sufficient for effective release. The main attention during the treatment had to be on the lowest as possible mechanical and thermal stress delivered to the cells (cf. section 2.6). Hereby the required laser output varied not only from capsules to capsules (due to different NP-concentrations and cluster sizes in the entities) but also in the different spatial areas of the cell-culture-dishes. The surface of the dishes in which the cells were growing was not perfectly planar and thus the focal plane shifted slightly by moving along the x- and y-axes. This was one reason to photograph a whole number of cells at a certain area at once, treat the selected cells together with the laser, analyze the following release rate and then walk on to another area.

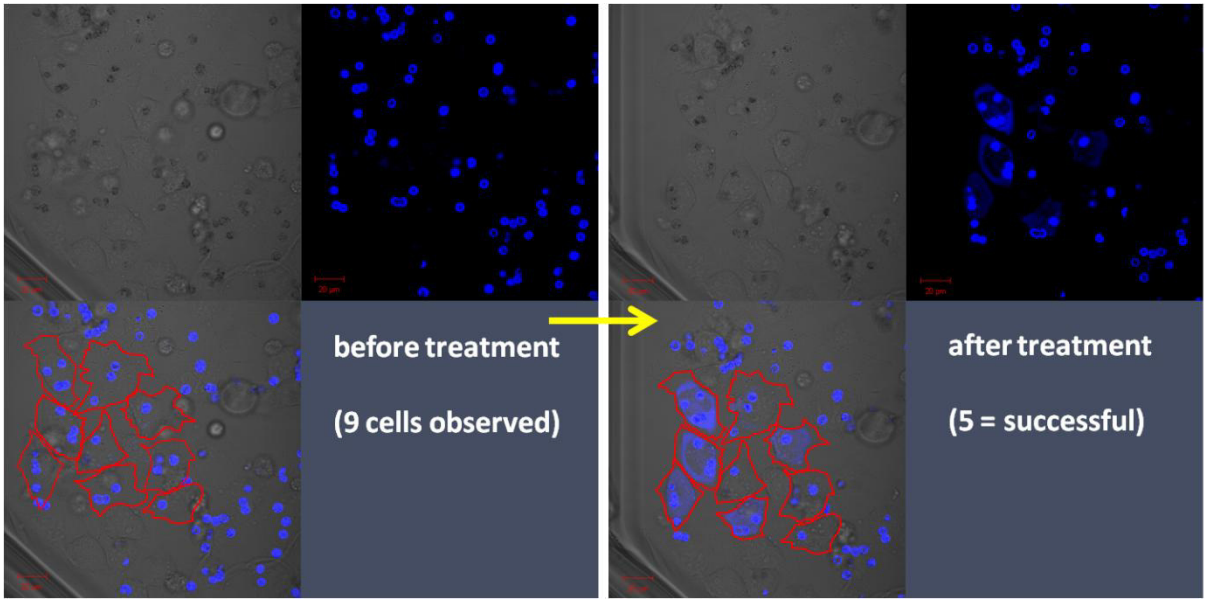

Figure 7: Microscopic photograph of a release-efficiency test. a) Before treatment an area with cells that incorporated at least one sufficiently filled capsule were selected and photographed. b) After laser treatment the selected cells were photographed again and the release efficiency was analyzed.

The analysis of the release rate and the accompanied success rate was based on the confocal fluorescence images taken of the chosen area after laser treatment. About 10 minutes after the heating procedure capsules were photographed with the microscope to select only appropriate success events. Capsules that were not efficiently incorporated by the cells or mistakenly lying on top of a cell were releasing their cargo to the extracellular medium. Fluorophore that was accidently staining the cell membrane or partially released into the cytosol was cleared within this time period. Cells that suffered from hypothermia or from physical stress due to overheated capsules were dying (or at least showing significant mortality signs) within the ten minutes.
Resulting images were afterwards analyzed towards the release success rate and accompanied the non-success rate of the heating procedure. The statistical results of the experiment are presented in **Figure 8**.

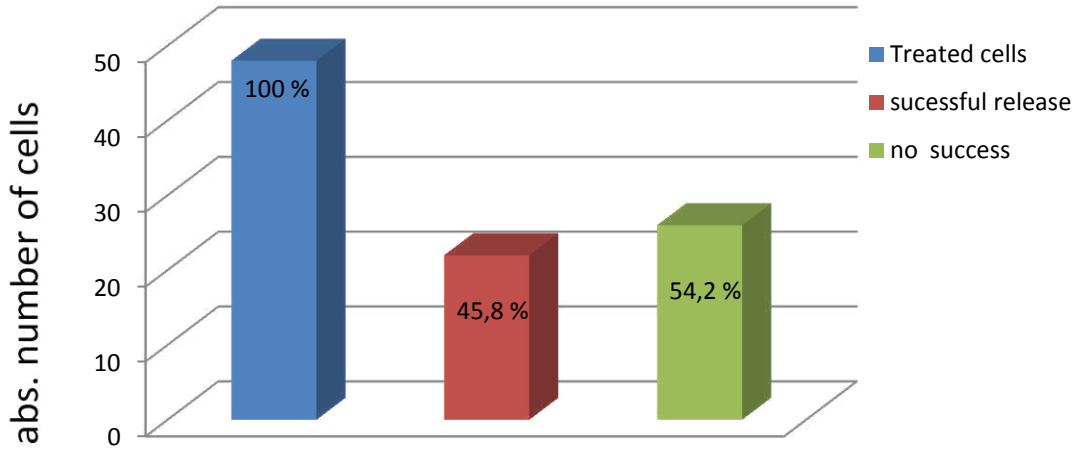

Figure 8: Statistical analysis of the release success rate from CascadeBlue-dextran filled PEM microcapsules in HeLa cells. From the 48 treated cells, 22 showed successful release without significant signs of mortality and 26 cells did not show cytosolic enrichment with the released fluorophore or were suffering from physio-thermal stress.

3.3 Intracellular release of pH-sensitive dye and in vitro measurement

Ion-selective capsules like the ones described in section 3.1 can easily be used as sensor systems for single or multiplexed analysis in buffer solutions (e.g. for flow-sensing devices or industrial applications) or for intracellular sensing. But one major problem is occurring for the intracellular use of these capsules: It is the uptake mechanism that underlies the entering of the capsules into the cells.

Microcapsules like the ones described above have a diameter of a few micrometers. Adherent cells that were used to investigate the functionality of the PEM capsules are able to incorporate several microcapsules at the same time. Nevertheless, the capsules enter the cells via an endocytotic pathway, that means that microcapsules are transferred into endosomes within the cytosol. These intracellular compartments are surrounded by a lipid membrane and have a totally different chemical composition of internal media than the cytosol. This means, that capsules internalized by the cells can only measure the endosomal ion-concentrations. For actual biologically interesting applications it would be desirable to determine the "real" composition of the cytosol.

Therefore, as a prototype for ion selective fluorophores, SNARF1 (a pH-sensor dye) was encapsulated within PEM capsules with the aim to be released into the cytosol of living cells.

Two major difficulties had to be overcome towards the release and successful intracellular pH-measurement. Firstly, a high amount of sensor dye had to be encapsulated within the cavities. Secondly, the fluorophore that was encapsulated had to efficiently escape the capsules and the endosomes. These two prerequisites were crucial, as they defined the amount of dye that was released into the cytosol. After releasing material from a relatively small capsule to a comparable huge cellular volume, its concentration decreases dramatically. Though, the final concentration of the released sensor fluorophore in the cytosol had to be high enough to perform ratiometric analysis via fluorescence microscopy.

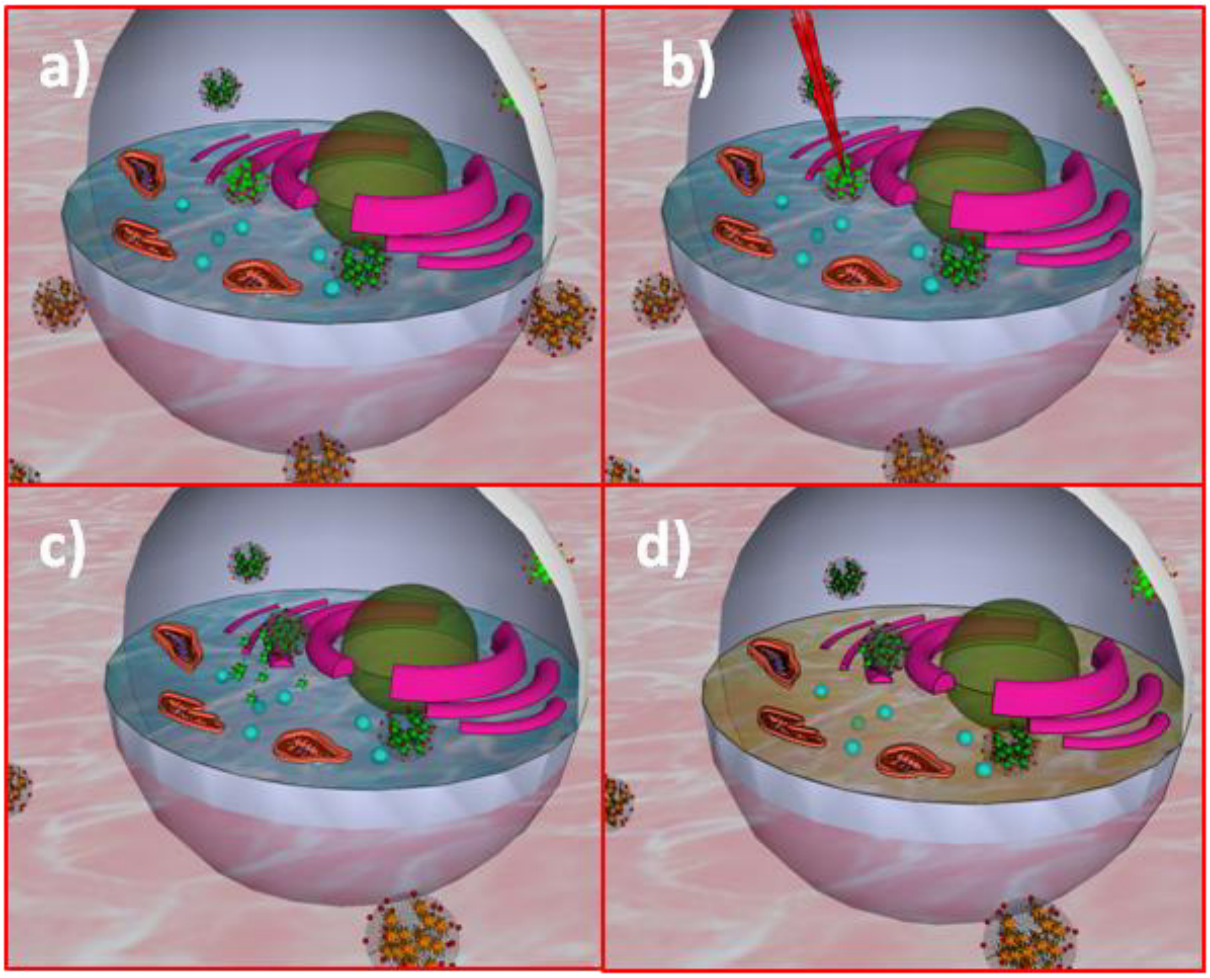

Figure 9: Schematic drawing of the release strategy and subsequent fluorometric pH determination due to intracellular opening of PEM microcapsules filled with SNARF1-dextran. a) After incorporation of SNARF1-filled capsules by cells they are present in acidic endosomal/lysosomal compartments what leads to greenish-yellow appearance of the capsules in contrast to the orange emission of capsules in the extracellular environment (neutral pH). b) Laser beam is focused on the gold-cluster modified PEM shell of one of the microcapsules and thus induces the opening of the shell within few seconds. c) Encapsulated material escapes through the crack in the PEM shell and spreads over the cytosol. d) pH-sesitive SNARF1 dye changes its emission color due to pH-change in the cytosol (neutral pH) and intracellular medium appears orange.

The encapsulation of many dye-molecules is no problem, as the conjugation of fluorophore to a huge dextran molecule (used as anchor molecule; ~500 kDa) can be tuned towards a high dye-per-dextran ratio. The principle of conjugation has been demonstrated elsewhere[28, 57]. Nevertheless, the use of a high molecular weight dextran turned out to be insufficient for releasing it. Due to the small effect of heating upon the PEM capsules (crucial to avoid harming the cells) the release of huge molecules was minimal. This emphasized the use of a much smaller dextran conjugates (~10 kDa) to facilitate the release from opened capsules. On the other hand, the smaller dextran conjugate did not sufficiently retain inside the PEM capsules by loading them with the co-precipitation method (pre-filling of the templates, cf.

section 2.2). Most of the dye that was entrapped within the $CaCO_3$ during the core formation was lost during the dissolution process after LbL coating.

Therefore, the post-loading approach had to be applied to enrich empty capsules with a high amount of sensor dye (-dextran conjugate) and close the pores of the capsules during a heat-treatment. This increased the amount of fluorophore that could be encapsulated and furthermore facilitated the escaping of the cargo after remote-controlled opening inside the cells. Besides the destruction of the polymer shell of the capsules, the laser treatment induced the local decomposition of the lysosomal membrane entrapping the capsule. Sensor material that was encapsulated could be released through opening the capsules and spread all over the cytosol (cf. **Figure 11 e)**).

Now, measurements of the encapsulated sensor dye (before opening) and another measurement of released sensor dye (after opening) clearly confirmed the lower pH value of intact endosomes compared to the surrounding cytosol (cf. **Figure 11 b)-d)**). For this purpose, calibration curves for the pH-dependent behavior of the SNARF1 dye-dextran conjugate were prepared in buffer solutions. Firstly, the capsules filled with the sensor-conjugate have been placed in buffer solutions with varying pH values. Intensity ratios have been determined with the same microscopic settings as used for the observations of capsules in the cell-release experiments. With different settings (increased sensitivity), the released fluorophore was observed in the cells after the opening of the capsules. These settings were applied to prepare the calibration curve for free dye in different pH-buffers. Furthermore, the concentration of the sensor dye was decreased until the final intensity values were comparable to the ones gained from intracellular observation. These measures ensured the correctness (with a certain tolerance) of the pH measurements in the cells.

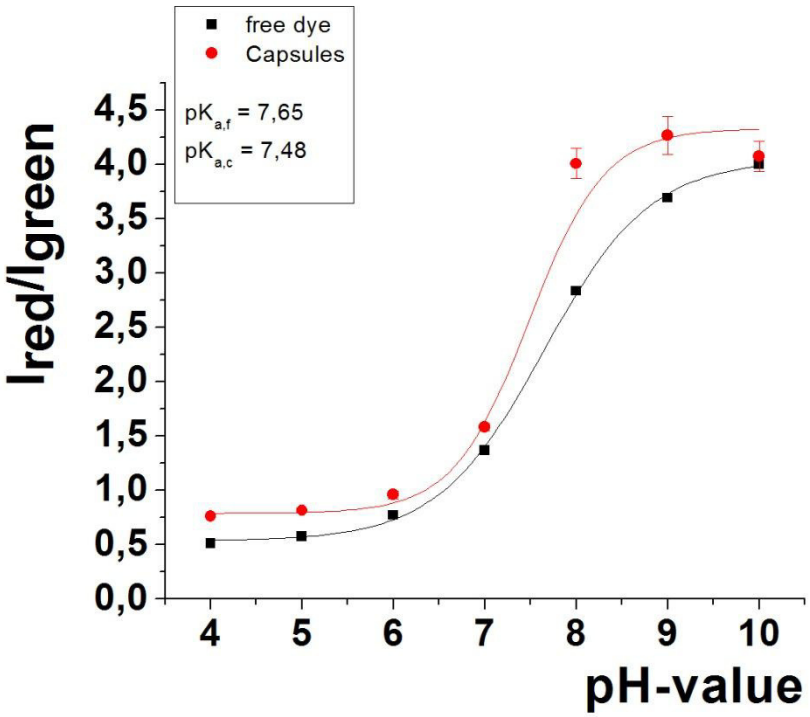

Figure 10: Calibration curves obtained from ratiometric pH-measurements within SNARF1-filled capsules and free dye in pH buffer solutions.

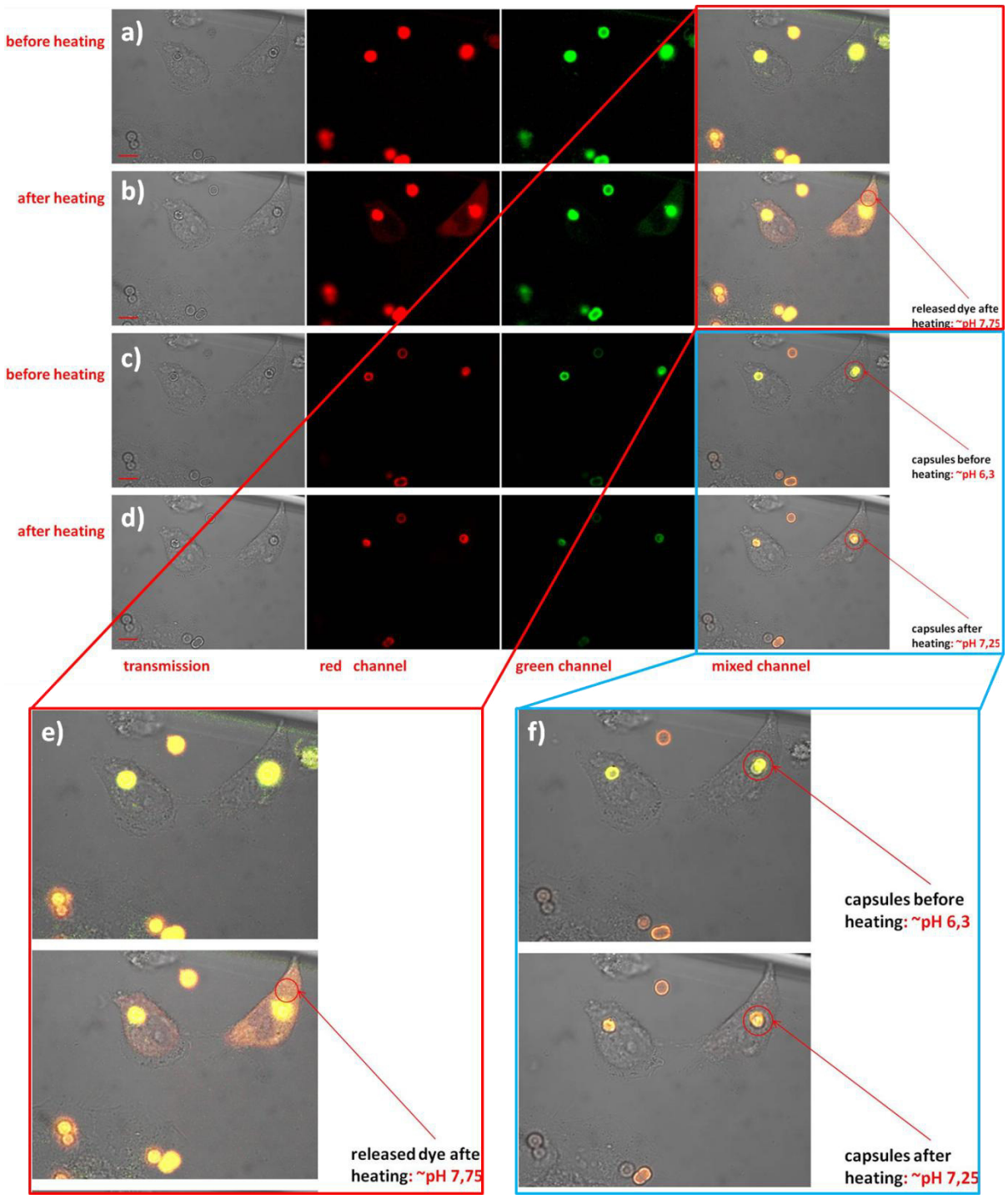

Figure 11: fluorescence microscopy image of SNARF1-dextran filled capsules incorporated by HeLa cells before (a+c) and after laser treatment (b+d). From left to right column transmission, red, green and overlay channel are presented. Photographs in a), b) and e) were overexposed to visualize fluorescence signal of the released material after laser treatment. Lines c), d) and f) show normal exposure of SNARF-filled capsules and subsequent enable for ratiometric pH-analysis of the encapsulated fluorophore c) before and d) after laser treatment. Enlarged overlay figures in e) and f) visualize the shift of the capsules from acidic environment in the endosomes before heating to a neutral environment in the cytosol (comparable to extracellular medium) after laser treatment. Scale bars correspond to 10 µm.

3.4 Sequential release of various probes into living cells

Previous applications of the presented microcapsules as sensor and delivery vehicle showed the general potential of the system. Especially the release of functional material (ion-selective fluorophores) into the cytosol presented the progress from pure release towards introduction of functionality. A further step towards liberation of functional material from micro-carriers like ours was the sequential release in cells. This approach would represent an important step towards the initiation of intracellular reactions from delivered material.
Therefore, two (or more) differently filled types of capsules had to be produced with cargo material that could easily be released into the cytosol. After internalization by the cells, a sequential opening of the two types of capsules had to be performed. The sufficient filling of the capsules and the ability of the cargo material to escape from the treated microcapsules into the cytosol was again crucial for the success of this application. After few dye-dextran combinations were tested, the final choice fell to CascadeBlue-dextran (CB-dextran; ~10 kDa) and Tetramethylrhodamine-dextran (TMR-dextran; ~10 kDa) for sequential release.

The experimental procedure started with the incubation of cell cultures with the two types of capsules in an equal quantity (between 2-5 capsules per cell each). After a sufficient incorporation time (e.g. overnight) the cells were observed on the microscope and a desired area with cells that incorporated both types of capsules was photographed (**Figure 12 a**)).
In a first release step only the blue capsules (containing CascadeBlue) were treated with the laser beam. Now all the successfully treated cells were again documented by taking fluorescence images (**Figure 12 b**)). It turned out, that about 50% of the selected cells were actually stained after this first treatment and showing no significant mortality signs. This success rate was similarly observed in the analysis of section 3.2. Afterwards, the second release step could be performed. Only the red capsules (TMR-dextran filled) were chosen for the second laser treatment, that were incorporated by the successfully stained (blue) cells. Statistically only ~20% of the treated red capsules showed finally release of dye and survival of the surrounding cell. This means that in total about 10% of all treated cells showed both color staining and no significant signs of mortality (**Figure 12 c**)).

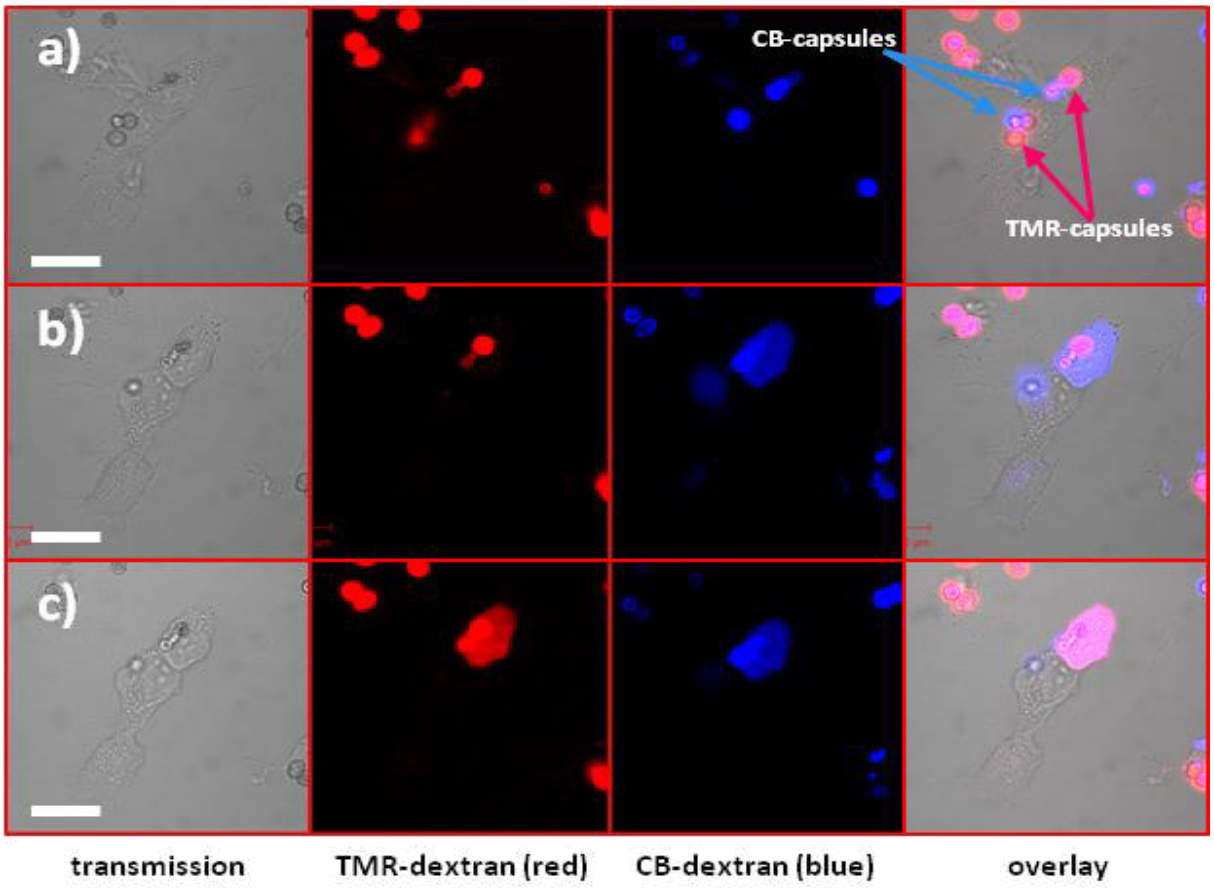

Figure 12: Sequential release of two dyes (red TMR-dextran and blue CB-dextran) from distinct capsules inside living cells. a) Cells that incorporated the two kinds of capsules before treatment. b) After treating the blue capsules CB-dextran is distributed over the cytosol of the cell. c) After release of TMR-dextran from another capsule, cells are filled with both dyes and appear violet in the overlay channel. Scale bars correspond to 20 µm.

Notwithstanding the fact, that only 1/10th of the originally selected cells could successfully be stained with both colors (sequential release of both dyes) the approach turned out to be a success and an important step towards remotely induced reactions of intracellular released chemicals. The propagation of abortive attempts lead to a low success rate of the sequential approach. But it shows the tolerance of the cells towards the application of physical stress by heating and even the possibility to open two or more capsules in one particular cell.
Nevertheless, it has to be mentioned that one has to be extremely careful by heating the capsules inside the cells due to their sensitivity. This fact gains even more in importance if the treatment is applied twice or more times in a cell.

3.5 Intracellular release of Proteins

The release of organic fluorophores (coupled to dextran) into the cytosol of living cells surely represents an interesting approach towards the goal of fabricating a multifunctional drug-delivery vehicle. Though, the carrier system should be able to transport more than only fluorescent probes into cells. A next step was it to encapsulate and release Proteins within the PEM capsules. This approach would present another step towards the delivery of biologically active substances to living cells. As the release of high molecular weight dextran conjugated fluorophores already showed, this approach would also be challenging. We chose green fluorescent protein (GFP) as model protein to be delivered to the cells. This molecule is commercialy available and the main functionality of the protein is its green fluorescence originating from the molecular fold structure. The fluorescence enables forobserving its distribution over the cell after being released, as well as the continuance of its fluorescence, which indicates an intact chemical structure of the protein.

Encapsulation of proteins cannot be performed with the post-loading method (like for the small dye-conjugates). This is because proteins undergo denaturation at temperatures over 40°C. Therefore, we utilized the co-precipitation approach to pre-load the $CaCO_3$ templates with the His-terminated GFP. Although, this loading method of the capsules seemed to work quite efficiently, release of protein to the cytosol was observed to be very rare. Two underlying effects were supposed for this observation: 1. The size (molecular weight) of the Protein is comparably big (~35 kDa), as compared to the dye-dextran conjugates released in the previously described experiments. 2. Due to the co-precipitation and the subsequent labeling of the template core enriched with GFP, the protein is forming a matrix-like structure within the PEM capsule and can hardly escape the polymer shell after heating it[36]. Interactions between the protein molecules or between the protein and the polyelectrolytes partly entering the template pores may cause this hindered escape.

Nevertheless, release and distribution of GFP molecules from the PEM microcapsules into the cytosol could be observed (cf. **Figure 13**). Enough protein was released (which was intact) to proof its distribution over the cell. It demonstrated the general feasibility of this approach and its simplicity. Furthermore, the survival of the main functional structure of the GFP showed that the heat formation in the capsules due to laser irradiation is local. The heat dissipation seems to be confined to a small volume around the spot of heating (a nanoparticle cluster) and does not affect the protein structure in the rest of the capsule. Otherwise, the fluorescence signal of the GFP would be significantly decreased in the capsules after laser treatment.

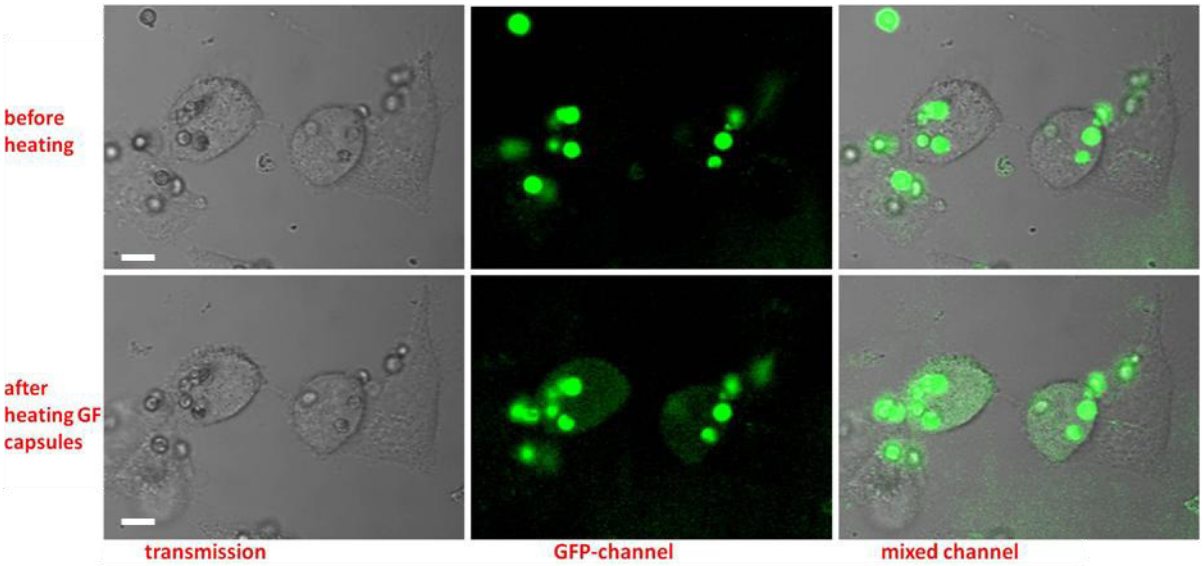

Figure 13: Remote-controlled release of green fluorescent protein (GFP) in living cells. The amount of released protein is due to the loading method and the huge structure of the protein rather low but sufficient for microscopic observation. Scale bars correspond to 10 µm.

3.6 Sequential delivery of reactive compounds for triggered intracellular reactions

The delivery of (biological) active compounds and the sequential release of various materials into cells have been demonstrated in the previous sections (**3.3 + 3.4**). Now, these two approaches should be combined to allow for unique intracellular reactions triggered by external stimulation of the capsules. More specifically, two compounds should be encapsulated in two distinct types of capsules. After cells had incorporated both kinds of capsules, they should be opened inside the cells and intracellular reaction should be observed between the two encapsulated compounds.

The compounds that should be encapsulated had to be chosen so that they fulfill all demands towards success of the approach. Depending on the chemicals (heat-sensible or not; high or low molecular weight; etc.), the proper encapsulation strategy had to be chosen to gain sufficient filling of the capsules, stable retention within the polymer shell and efficient release in the cells. The reaction between the two compounds had to work under difficult terms of condition (inside cell-medium) in the presence of various biochemical molecules. The desired reaction should not be induced by these molecules or changed environmental conditions in cellular compartments (changed pH in endosomes). Furthermore, the reaction should be easily observable under the microscope (fluorescence should appear, finally).

The final choice fell on a self-quenched, organic dye (substrate) that reacts with alkaline phosphatase to a green fluorescent product. Alkaline phosphatase is an enzyme that dephosphorylates phosphate tagged molecules. In our case the substrate (ELF97-phosphatase) is the phosphorylated molecule. The phosphate group quenches the fluorescence what results in a non-emitting dye. If both, the substrate and the enzyme come in contact, the dephosphorylation starts and the substrate is converted into ELF97-alcohol. This is a strongly greenish fluorescent material that precipitates directly on the spot of the reaction.

The encapsulation of the phosphatase was easy, as the enzyme is a branched molecule that does not penetrate the polymer shell and remains inside the PEM capsules. To load the capsules with this enzyme, the co-precipitation approach was used. Although this often costs problems in releasing the cargo from capsules, the results suggest a sufficient escape of the phosphatase and efficient enzyme activity within the cells.

The substrate (ELF97-phosphate) is a rather small molecule (~431 Da) which is challenging to be efficiently loaded and retained inside the capsules, neither with the co-precipitation, nor with a post-loading approach. For encapsulation of such small cargo we utilized a loading procedure that originally was developed for encapsulation of hydrophobic molecules. It is based on the embedding of small block-copolymer micelles into the $CaCO_3$ template (cf. section 2.3). By adding the copolymer dissolved in an organic solvent to the aqueous precursor solution, small micelles are forming with a hydrophobic polystyrene core and a hydrophilic shell of poly acrylic acid. These micelles are huge enough to retain within the PEM capsules after core-removal. Furthermore, by incubating the final capsules within a highly concentrated substrate solution, the small ELF97 interpenetrates the multilayer shell of the capsules, attaches to the hydrophilic PAA-chains of the micelles and is stably retained in the capsules. Results proofed, that also the ELF97 molecules attached to the micelles were released after opening of the capsules and were reacting with the enzyme (cf. **Figure 15** A)

within the cytosol. The following sketch illustrates the intracellular reaction that follows the sequential release of the two compounds in the cells (cf. **Figure 14**).

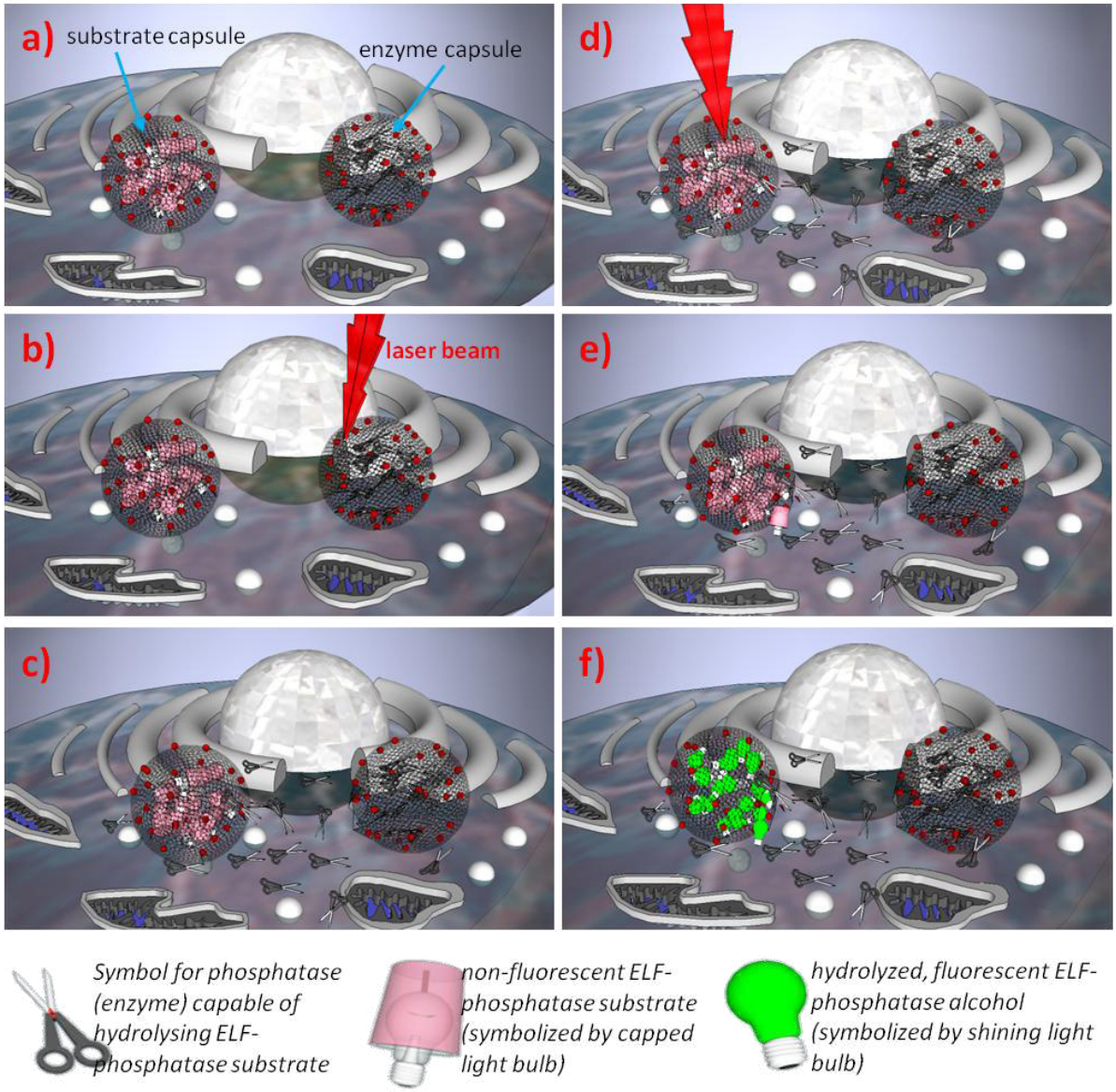

Figure 14: Sketch showing the principle of enzymatic reaction in living cells induced by light controlled release from PE microcapsules. After the uptake of two types of capsules a) (one filled with alkaline phosphatase and another one filled with ELF97 phosphatase substrate) one type of capsules (here the enzyme capsule) is opened via laser beam b). Its cargo is released into the cytosol c) and spreads all over the cell. In a second step d) the other capsule (filled with the substrate) is opened with the laser beam. The enzyme immediately enters this capsule e) and starts the hydrolysis of the substrate what leads to an upcoming fluorescence signal f) and precipitation of the substrate (ELF97 alcohol).

For easier distinction of the two types of capsules in the cell, both were labeled with a different dye staining (red and blue fluorophore). This was necessary as both, the enzyme and the substrate capsules were initially not fluorescent. Once incorporated, only cells containing at least one capsule of each type were used for experiments. After both capsules have been

opened, bright fluorescence signal appeared in one of the capsules. Further investigation of the reaction kinetics turned out that always the last capsule, which had been treated with the laser beam, exhibit the fluorescence signal in their cavity (cf. **Figure 15** B-D and E-G).

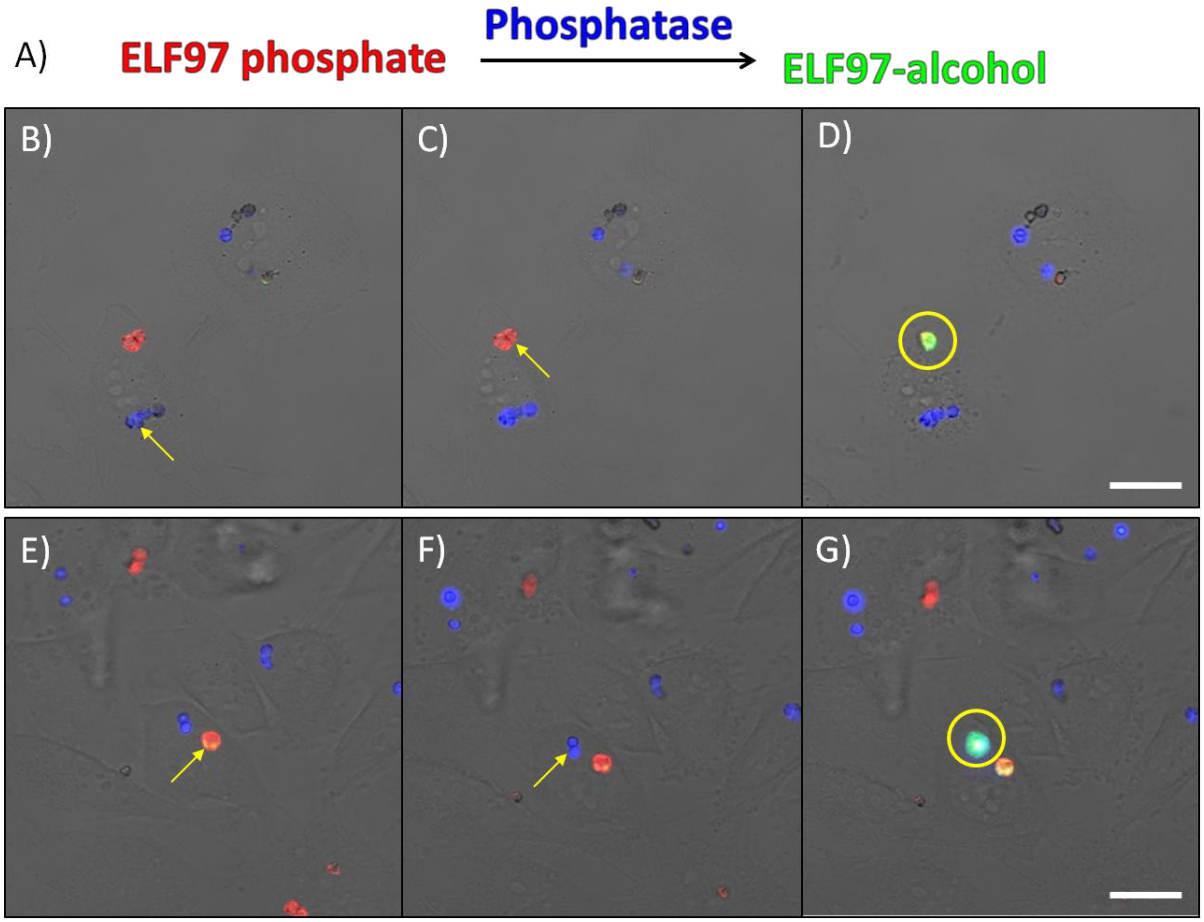

Figure 15: Sequential release of alkaline phosphatase and ELF97-phosphate via light-controlled heating. A) Capsules were filled with the enzyme alkaline phosphatase (AP, blue capsules) or the substrate ELF97-phosphate (red capsules). HeLa cells were incubated with both types of capsules. Capsules filled with alkaline phosphatase (B) or ELF97-phosphate (E) were first opened with a light pointer, as indicated by yellow arrows. In a next step the complementary capsules with ELF97-phosphate (C) or alkaline phosphatase (F) were opened, as indicated again by yellow arrows. Enzymatic processing of ELF97-phosphate by alkaline phosphatase led to the production of the green fluorescent product ELF97-alcohol (D, G). Note that cells with capsules which were not illuminated with the light pointer remained unaffected. The opening sequence determines the location of the emerging fluorescence of the product ELF97-alcohol. The scale bars correspo*nd to 25 µm.*

Our explanation for the observed behavior is based on the hydrophobic behavior of the dephosphorylated ELF97-alcohol. After cleavage of the phosphate group it forms a green fluorescent precipitate that settles down right at the place of enzymatic reaction. Presuming an efficient release and spreading of the cargo material from a first capsule (e.g. the substrate), the substrate is expected to be equally distributed over the cytosol. Now, after heating the second type of capsule in the cell, its content (the enzyme) is quite highly concentrated within

the capsule´s cavity and its surrounding. The substrate molecules that are distributed over the cytosol now rapidly enter the opened capsule and react with the enzyme. A comparably small amount of phosphatase is released into the cell medium and reacting with the free ELF97. Therefore, the amount of fluorescent precipitate forming in and around the capsule is quite high compared to the concentration in the cytosol. Facing the highly fluorescent spot in the last opened capsule, the emission signal around it can hardly be observed. If the sequence of release was reversed, again the last opened capsule (now the one containing the substrate) showed the bright fluorescence signal. In this case first the enzyme was released and distributed over the cytosol. After opening the second capsule (with ELF97) phosphatase entered the capsule and hydrolysed the substrate to form the fluorescent precipitate. Again, most of the precipitate was formed in and around the secondly opened capsule, as the amount of released substrate together with the amount of released phosphatase present in the cytosol only produced a low concentration of fluorophore (cf. **Figure 16**).

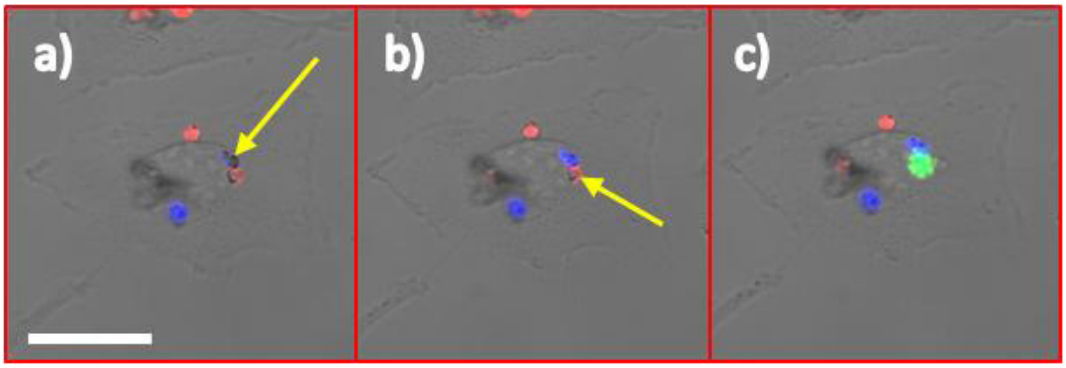

Figure 16: Detailed view on the ELF-phosphatase reaction induced via sequential release of: a)→b) the enzyme alkaline phosphatase into the cytosol and b)→c) the phosphorylated substrate. c) Inside and in the direct surrounding of the last opened capsule (ELF-capsule), the substrate concentration is high enough to produce a fluorescence signal after enzymatic reaction. Scale bar corresponds to 25 µm.

Concluding these results, the approach including the remote-controlled release of two distinct cargo materials in living cells and the clear observation of a reaction between them is a major step towards future drug delivery. It could allow for so-called prodrug delivery that is based on two non-reactive compounds that are released seperately and then form the actual reactive drug for intracellular therapy. The cargo release in two steps and easy encapsulation of various materials show the high versatility of the system. Furthermore, the number of encapsulated compounds could easily be increased. This could possibly trigger more reactions between different molecules or modifications of carried substances.

3.7 Statistical uptake of capsules and population analysis in living cells

The intracellular release of various compounds and the triggered reactions between the released materials (cf. sections 3.4 & 3.6) show high versatility of the PEM microcapsule system for biological applications. To continue this concept, potentially a greater number of compounds could be loaded within the capsules. After cells incorporated at least two types of the prepared capsules reactions between the corresponding cargo materials could be triggered by releasing them to the cytosol. Several reactions could be performed in this way. But a prerequisite for such multi-compound reactions would be the uptake capacity of the cells. They would have to incorporate a number of different capsules at once.
To investigate the uptake capacity of capsules into cells, their population was observed under changing conditions. Four different types of capsules were loaded with differently labeled dextran molecules emitting either blue, green, red or near infrared light (cf. **Figure 17**). It was demonstrated that a high number of capsules can be taken up by the cells without causing any acute cytotoxicity. Furthermore, the number of different capsules incorporated by one single cell increased with the number of added capsules.

The four different kinds of capsules were given to the cell-culture in a rate of two, four and six capsules (per kind) per cell. After a certain incubation time it was investigated, how many different capsules were taken up by single cells. The purpose of these observations was to estimate, whether release experiments and subsequent reactions in cells could be realized with a higher number of different capsules (different substances). E.g. if four different chemicals should be encapsulated and all four kinds of capsules could be used for intracellular interactions with each other, all four kinds of capsules have to be incorporated by one single cell simultaneously. Furthermore, if the reaction should be part of a medical treatment, most of the cells would have to incorporate all the different capsules.

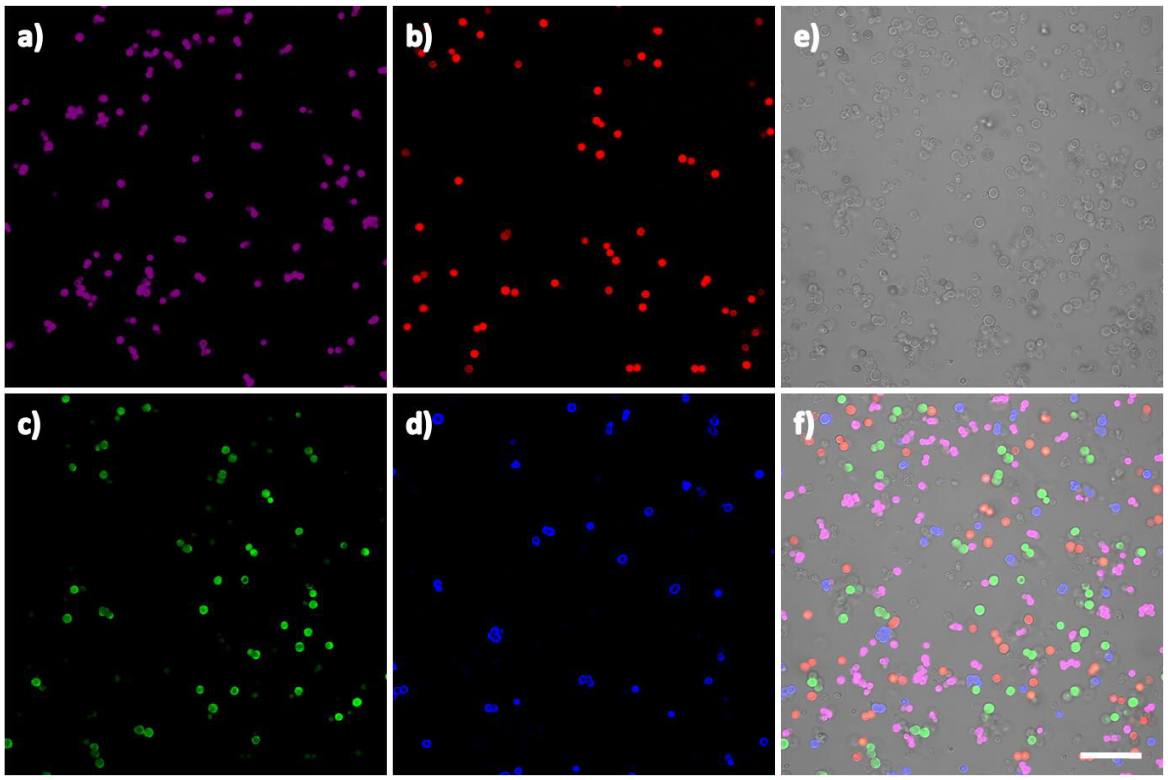

Figure 17: Fluorescence microscope image of the four different kinds of capsules used for the uptake studies. Channel a) shows capsules filled with Dy647 (violet), channel b) capsules with AlexaFluor594 (red), Fluorescein-enriched capsules (green) can be seen in channel c) and in channel d) capsules filled with Cascade-Blue. Channel e) and f) show the transmission channel and the overlay accordingly. Scale bar corresponds to 20 µm.

For the analysis, HeLa cells were cultured in Ibidi µ-dishes to reach confluence. Afterwards, they were incubated with amounts of capsules equivalent to 2, 4 or 6 capsules of each color per cell for 4 h. It is noticeable that even the incubation of 6 capsules of each color per cell (= 24 capsules/cell) did not cause any cytotoxic effect observably.
The number of different capsules taken up by each cell was determined by taking pictures with a fluorescence microscope. Analysis of a high number of cells (~100 cells/value) carried out the statistic population of capsules incorporated by the cells. **Figure 18 a) - c)** show exemplary pictures of the incorporated capsules in the cells and the principle of the statistical analysis.

The resulting values of incorporated capsules per cell are shown in **Figure 18 d)**. We specially emphasize the values for the addition of six different capsules per cell. Like mentioned before, about 50% of the analyzed cells were carrying all four types of capsules. These results support the thesis that a higher number of capsules mixed into the cell culture could enable for the incorporation of a high number of different cargo systems and could in this way facilitate intracellular reactions triggered by external laser treatment. The gained results are just based on statistical uptake processes. No further targeting or external delivery approach had to be applied.

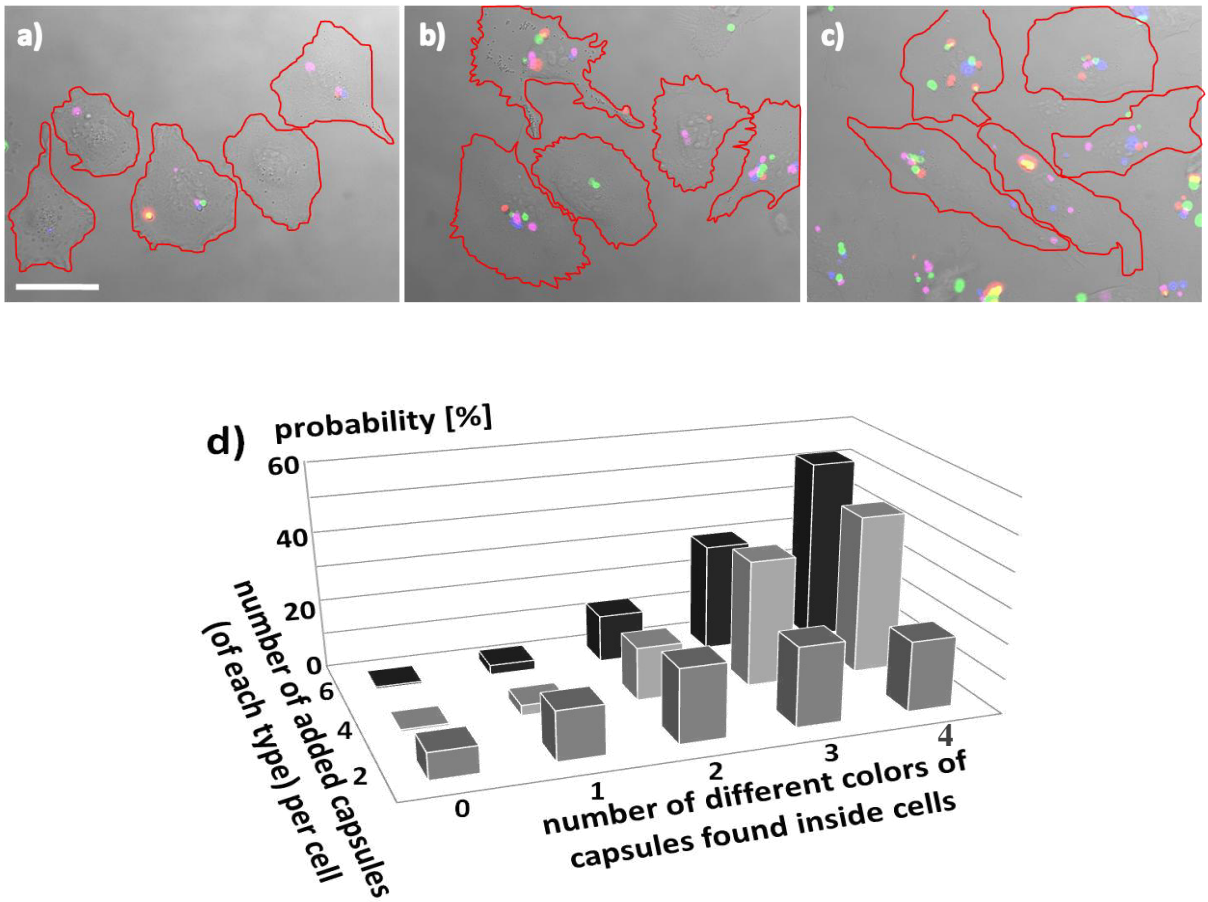

Figure 18: Hela cells were incubated with a homogeneous mixture of all 4 capsule types. a) Two, b) four or c) six capsules of each type were added per cell to the culture medium. The probability of observing in one cell 0, 1, 2, 3, and 4 capsules of different color is plotted in d). For the ratio of 6 capsules of each type per cell about 50% of all observed cells incorporated at least one capsule of each kind. Scale bar corresponds to 50 µm.

3.8 Magnetic targeting of microcapsules in flow device

One major point in controlling complex delivery or sensor systems like the presented capsules would be the supervision of movement. The microcapsules combine a high versatility of possible applications. Many of them have already been presented in the previous chapters. Nevertheless, a delivery system for therapeutic application should provide control over its location. If thinking of in vivo applications the capsules should accumulate in one desired compartment or even in a certain spot of a tissue. This is a very essential requirement for medical treatments or examinations. However, one does not need to step towards applications in complex organisms. The same applies for in vitro tests. A high efficiency of the system can only be achieved if as many capsules as possible accumulate at a certain spot in the cell culture. It would also prevent unspecific uptake of capsules. Furthermore, the fabrication of patterns by depositing capsules in desired arrangement would facilitate multi-functional tests with a high throughput. Different combinations of capsules could be directed towards certain points in the pattern and also changing concentrations could be tested in this way. Optical measurements could then be applied on a very small area for multiple testing conditions.

One approach towards the targeted deposition of capsules in cell culture is based on magnetic fields. Magnetic guidance is a very convenient access as the generation and the controlling or movement of magnetic fields is relatively easy. Even on a large scale (animal or human body) magnetic fields can be applied and focused throughout the whole organism.
By the implementation of magnetic properties into the presented microcapsules one would gain a very easy-to-control system. Our approach uses the high magnetic susceptibility of iron oxide nanoparticles. These materials proofed their properties towards magnetization and versatility in various applications[39, 58-60]. The used iron oxide particles were (due to their surface charge) embedded within the polyelectrolyte multilayer shell of the capsules. The embedding of a high number of such nanoparticles within the shell means a high magnetic coupling and therefore strong response of the capsules to applied magnetic fields.
Verification of the magnetic targeting properties was done in flow devices. Within a so-called flow-channel a confluent layer of adherent cells was seeded. Now, the device was connected to a peristaltic pump that applied a constant flow through the channel (comparable to the flow rate in human blood vessels). The magnetic capsules (modified with a violet dye) were mixed to the floating liquid (normally cell culture medium) and no significant deposition or adhesion of capsules to the cells was observed. Now a permanent magnet was placed underneath the channel to apply a high magnetic field. After few minutes the flow liquid was replaced with fresh medium that did not contain any magnetic capsules. Observation of the channel clearly showed efficient deposition of capsules at the spot of the magnet. Apart from this spot, the concentration of capsules was proofed to be very low.
In a second step, the magnet was moved along the flow device and another kind of capsules (carrying red fluorophore) was given to the flow medium. The deposition procedure and the following washing step were repeated. In a third step, blue capsules without any magnetic nanoparticles were mixed to the device and the flow was turned off.
The result was a huge pattern with three different types of capsules (red, violet and blue) deposited onto the cell-layer (cf. **Figure 19**). The red and violet capsules modified with

magnetic nanoparticles were attaching in a controlled manner to the cells with the help of the magnetic field. Between the two positions of magnetic deposition a gap was formed in which only few red or violet capsules could be found. The blue capsules, not modified with nanoparticles and not directed with a magnetic field, settled down all over the channel. The experiment was thought as a prototype for controlled reactivity of released material from three types of capsules. In the left part of the pattern a reaction could be triggered in cells where red and blue capsules were incorporated. In the right part another combination of cargo from violet and blue capsules could be released. In the gap between the two spots of magnetic targeting, the cargo of the blue capsules could be released singularly into the cells.
It should be noticed, that experiments presented in section 3.6 concerning intracellular reactions of two sequentially released compounds were repeated in flow device and by applying the presented targeting method. Red capsules were herein filled with the quenched substrate and the blue capsules were containing the enzyme.

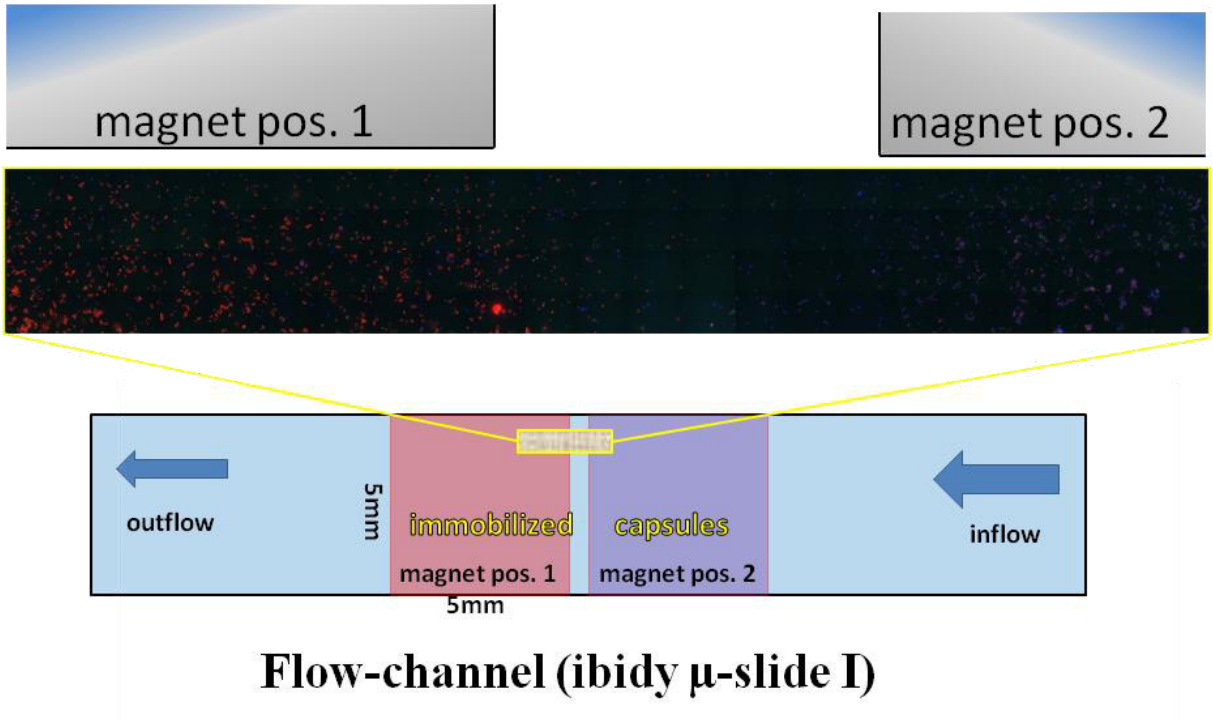

Figure 19: Schematic drawing of the flow-channel system and the resulting patterned deposition of magnetically modified microcapsules. A magnet (5mm x 5mm) was placed underneath the left position and the red capsules (filled with red AlexaFluor594-dextran) were deposed at the sight of magnetic field. After washing the magnet has been moved to the right position and the violet capsules (filled with violet Dy647-dextran) deposited on the cells. The flow rate was 8 cm/s. The image consists of 92 single frames (120 µm x 90 µm) which were merged afterwards to form the final picture.

In a second, more sophisticated experiment the size of the pattern should be decreased significantly. With the help of metallic plates the magnetic field was transferred to the bottom side of the channel. These metal plates were chosen to be thinner than 1 mm. By placing two

such plates on the permanent magnet (used for the experiment described above), the magnetic field is sharply focused on the two stripes on top of the metal plates (cf. magnet structure in **Figure 20**). Deposition of magnetic capsules labeled with a red dye now only took place above the two metal shields. After the common washing step, the magnet together with the metal plates was moved along the flow device (about 1 mm). The second step of the experiment achieved the deposition of blue labeled magnetic capsules along the new positions of the metal plates. Further washing of the device and movement of the magnet was followed by the deposition of a third kind of magnetic capsules (labeled in violet) along the metal shields.

A schematic drawing of the final structure of the deposition pattern can be seen in **Figure 20**. Six thin stripes consisting of magnetic capsules with different fluorescent labels developed along the flow channel. Each stripe showed a width of about 800 µm. Narrow gaps occurred between the stripes where no (or very few) capsules were deposited. For better visualization, the underlying cells were stained with a green fluorophore.

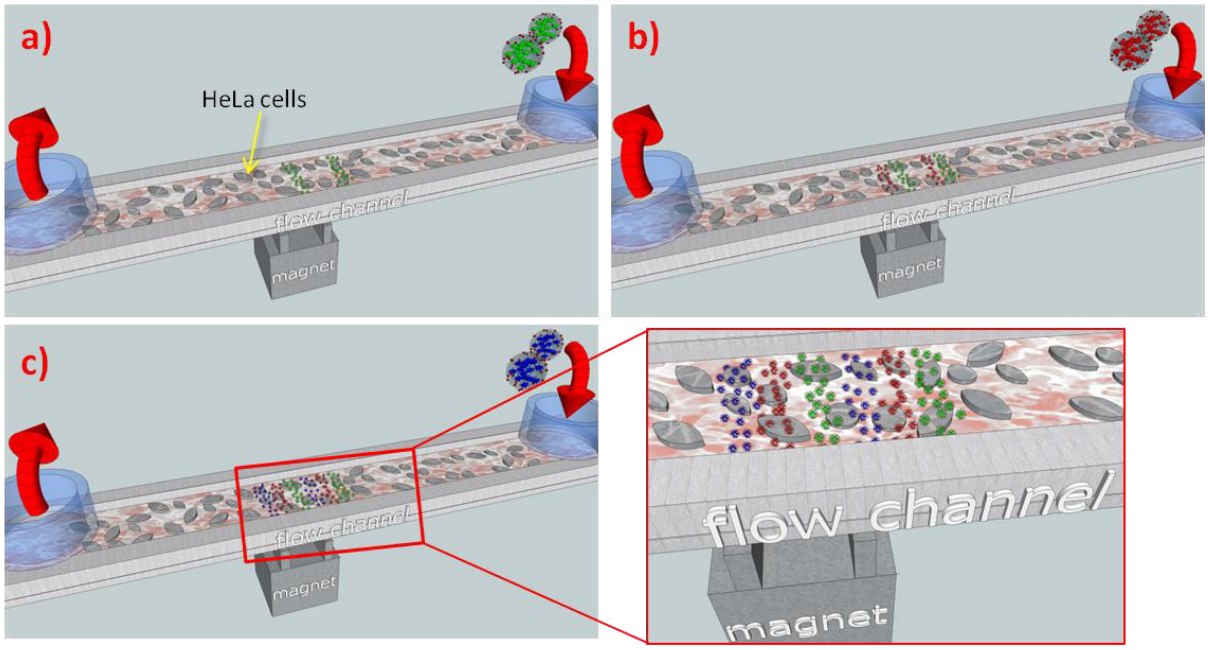

Figure 20: Sketch showing the principle of deposition of microcapsules via magnetic field in a flow channel. Magnetic field attracts the magnetically modified microcapsules of a certain kind (firstly green) at the desired place of the magnetic field. After moving the magnet, another type of capsules is added into the flow and deposited along the magnetic field (b and c). The procedure is repeated until three different kinds of capsules are deposited forming a sub-millimeter capsule pattern within the cell culture (c).

In the final microscopic fluorescence image, the three differently labeled capsules can clearly be distinguished from the green labeled cells. Fluorescence intensity was afterwards plotted against the position along the flow channel. The clear tendency of capsules to settle down at

the desired position over the magnetic metal plates and the sub-millimeter structure can be seen (cf. **Figure 21**).

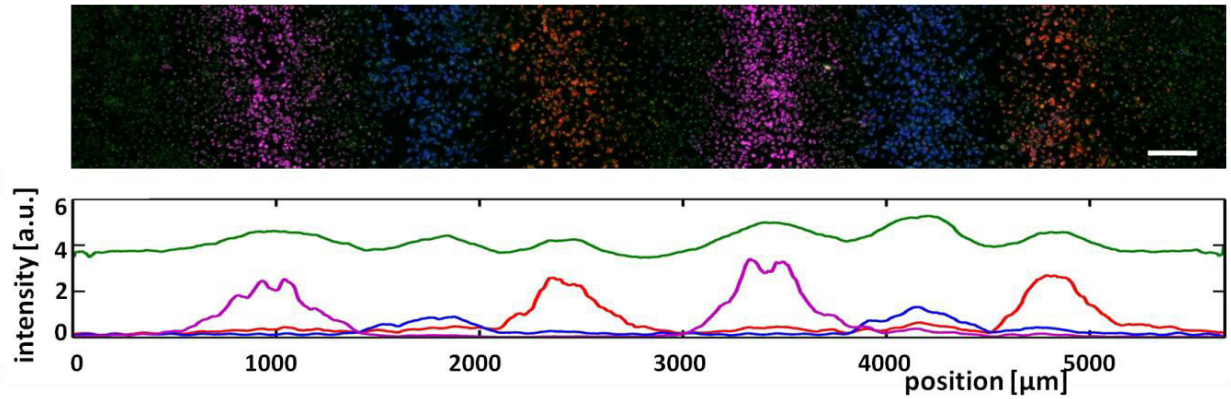

Figure 21: Microscopic photograph of the deposited microcapsules in the flow channel. Green fluorescence signal belongs to the membrane-staining of the underlying HeLa cells. Violet, blue and red signal belongs to the three types of magnetically modified microcapsules deposited along the magnetic field. Fluorescence intensity was analyzed by integration of the fluorescence signal at each x-position along the flow channel. Intensity values are plotted for each color signal over the position in the channel. Scale bar corresponds to 250 µm.

The experiment demonstrated the possibility to fabricate patterns of various different capsules with sub-millimeter sized structures. This deposition method could enable for easy and fast fluorescence analysis of sensor capsule systems or sequential release of various cargo compounds in vitro on a very small scale. It furthermore gives a hint towards future in vivo applications of micro- or nanocarriers for targeting in organisms.

3.9 Delivery of mRNA and observation of time kinetics

The Delivery of fluorescent probes or biological molecules into cells (cf. sections 3.3-3.6) was only the first step towards biological applications. The reactions performed within cells by releasing and mixing two reactive compounds intracellularly demonstrated the potential of the system towards "real" applications. One even more sophisticated approach in this direction was the delivery of nucleic acids as biologically active cargo into cells. Messenger RNA (mRNA) that encoded GFP was chosen for delivery as its release and subsequent translation into the fluorescent protein was easy to be monitored.

As mRNA strings are relatively huge molecules, the co-precipitation method (cf. section 2.2) was applied for embedding the compound in the capsules. The macromolecules are too huge to diffuse through the multilayer shell around the capsules. Nevertheless, a major demand on the system was that enough mRNA could escape the capsules after laser treatment in the cells – at least enough to observe the occurring fluorescence originating from the mRNA translation. Herein, not only the release of the nucleic acids and the proof of their functionality, but also the kinetics of the RNA translation should be investigated. Furthermore, the time scale and the control of the reaction were compared with a non-controlled delivery system. Complexes consisting of mRNA and the transfection reagent lipofectamine were chosen as alternative release system. After adding these complexes to the cells the fluorescence signal was observed over a long time scale (~ 24 hours). Observations showed an increase of green GFP signal after ~ 4 hours and a saturation of fluorescence intensity around 12 hours after addition. This high emission values were rather stable for at least 12 more hours. Observed signal behavior could be described by analysis of the uptake and release strategy that took place for the complexes. Firstly, the complexes were taken up by endocytotic pathways (active uptake processes) that were going on as long as complexes were present in the cell medium and come in contact with the cells. Complexes ending up in endosomes that are intracellular compartments enclosing incorporated material. In a second step, the transfection reagent lipofectamine fused with the endosomal membrane and sluiced the mRNA into the cytosol. Here the ribosomes translated the mRNA strings into the green fluorescent protein. The incorporation processes as well as the release of mRNA from the endosomes via lipofectamine are known to be continuous operations that induce the quasi-continuous increase of fluorescence signal and the remaining of the signal over long time scales. The results indicated for an overlapping of the two processes (incorporation and release) and showed that a controlled translation cannot be realized with this system.

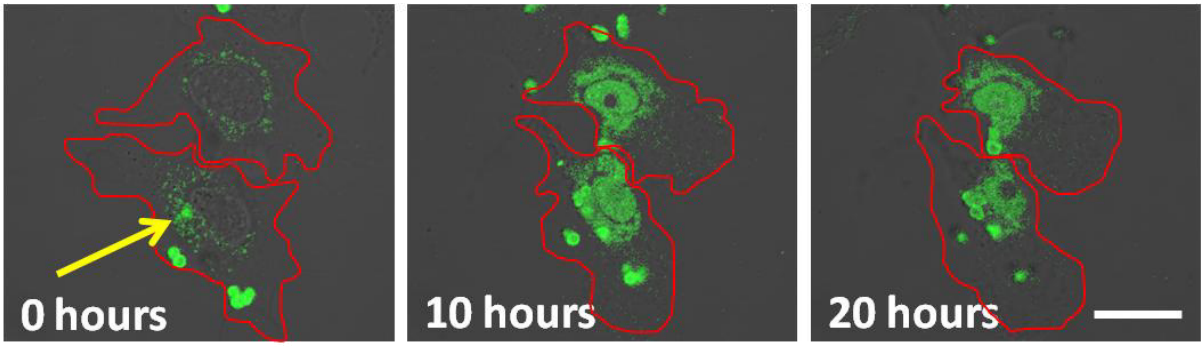

Figure 22: Demonstration of intracellular translation of delivered mRNA strings after release from microcapsules. Few hours after laser treatment of mRNA-enriched PEM capsules the surrounding HeLa cells showed increasing green fluorescence signal in the cytosol. It was assumed to be due to release of mRNA molecules from the capsules and subsequent ribosomal translation of the RNA sequence into green fluorescent protein (GFP). After >10 hours the signal was observed to decrease again. Background signal before and immediately after laser treatment was caused by autofluorescence emission collected due to very high exposure values.

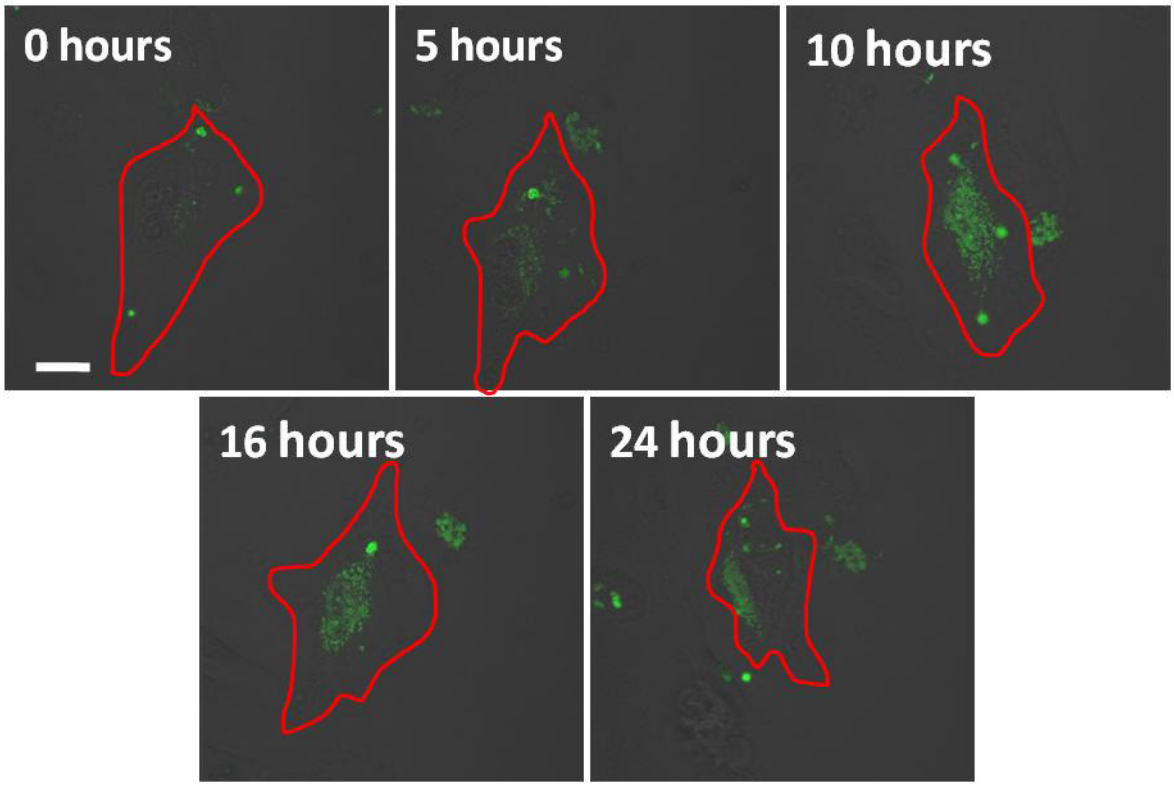

Figure 23: Time kinetics recorded of the GFP production following the release of mRNA from PEM microcapsules (less exposure than Figure 22). GFP induced fluorescence signal appears few hours after laser irradiation and increases until it reaches a maximum about 12-15 hours after treatment. Afterwards the total signal intensity drops down again and approaches its original value (almost no signal).

In contrast, the gold nanoparticle modified capsules filled with the mRNA molecules were given to the cells for about 6 hours. This time window turned out to be sufficient for capsule

incorporation by the cells. Now the capsules were also present in the endosomal compartments of the cytosol. By the external stimulus with the NIR laser beam, AuNPs converted enough light energy into heat to break up both, the PEM shell of the capsules as well as the endosomal membrane. Immediately after this opening process and subsequent release of mRNA into the cytosol, the ribosomes started to translate the nucleic acids into the green fluorescent protein. The emission signal rose until a saturation point about 10 hours after the laser treatment. Afterwards the majority of the mRNA seemed to be degraded by mRNAse and the fluorescence signal reduced to the starting value (about 18 hours after heating).

The results showed that externally triggered release of mRNA into the cytosol enables for controlled and temporal limited translation of the code sequence. A short and burst-like release was followed by a similar protein production. This demonstrated a huge benefit compared to the uncontrolled complex-based system. Together with the possibility of embedding magnetic nanoparticles in the PEM shell of the capsules, spatial direction and targeted deposition can be performed with the capsules.
Future medical applications could be performed by guided administration of the capsules to the organ or tissue of interest and subsequent opening of the drug-filled capsules after cellular uptake. This opening would be followed by a short-time release of drug or active substances and a temporally limited medical effect confined at the desired spot of interest. Opening strategy could assume a capsule-per-capsule approach or it could be extended to the irradiation of a bigger spot.

4. Conclusion

Biological and medical applications show very high demand on multifunctional but specifically deployable tools. Especially for delivery and sensing applications the needs for targeting and controlled release mechanisms as well as for additional functionality in the systems are significant. The presented PEM microcapsules show one very promising approach towards the fulfillment of several of these requirements. The possibility of embedding a high variety of different cargo materials into the cavities of the capsules makes them unique. Therefore the capsule based system shows a high versatility for both, delivery and sensing applications. Also the polymer shell prevents the cargo sufficiently from external threats like immuno clearance or degradation. The capsule structure with further functionalization provides for easy targeting methods as well as specified delivery. Shell staining or assembly of multiple compartments facilitate tracking of the capsules and the combination of multiple functional materials. Remote-controlled opening of single capsules enables for controlled release and delivery of cargo molecules. Intracellular heating combines furthermore the release of cargo from the capsules and from endosomal/lysosomal compartments which entrap the incorporated capsules. Therefore no additional transfection agent or release strategy from the endosomal compartments is required. Besides the delivery properties the sensing of different environmental conditions makes the capsules to a unique tool for real-time bio-analysis. Additional to sensor dyes (selective fluorophores) a high variety of sensor materials can potentially be embedded within the cavities of the capsules. In this way, sensor tools that lack of appropriate delivery or targeting strategies could be encapsulated and be transported to the spot of interest via the targeting functionality of the capsules. The combination of sensing and delivery potential in one capsule-based system could facilitate real-time control of metabolic changes upon release of cargo. Furthermore, multiplexing would be feasible as a high variety of sensor materials can be embedded and delivered simultaneously.

The presented data underline the fact that polyelectrolyte multilayer microcapsules are one promising approach towards becoming a very versatile delivery tool. The first point that is important for future applications is the easy fabrication. Precipitation of $CaCO_3$ can be realized in high and low amounts, depending on the demands of the application. It is simple and cost effective due to low costs of the precursors. Furthermore, macromolecules with a high molecular weight can easily be embedded within these $CaCO_3$ templates via co-precipitation. This method has been demonstrated to be non-harmful for the cargo and keeps its functionality. Examples for this very effective and fast method for filling the PEM capsules with desired cargo are the co-precipitation of the ion-sensitive fluorophores coupled to dextran. Final distribution of fluorophore within the cavities was homogenous enough to perform ratiometric measurements and determine ion-concentrations of all the three types in parallel. Another example was the encapsulation of the green fluorescent protein (GFP). Due to its size and structure co-precipitation of this protein in a high amount turned out to be challenging. Nevertheless, it was shown successfully that the protein can be embedded in an amount sufficient to monitor its intracellular release. This fact is also valid for the encapsulation of mRNA. Even if the release itself could not be observed within the cells, the

effect of releasing the mRNA to the cytosol, the fabrication of GFP, could clearly be demonstrated. Concluding the approach of precipitating $CaCO_3$ spherical templates for the fabrication of microcapsules can easily be applied for new applications. Nevertheless, the high variations of sphere, size and structure has to be taken into account. Depending on the cargo material that should be co-precipitated within the template its structure and especially its size can vary. But for established applications (e.g. regarding industrial fabrication) certain protocols for embedding one desired materials can easily be developed.

After fabrication of the core (filled or not filled) the polyelectrolyte multilayer shell has to be assembled around the template. This second step turned out to be not only very easy but also opened the possibility of embedding further functionality into the shell. The simple layer-by-layer adsorption of oppositely charged polymers onto the template surface is already used for many applications. The implementation of other charged materials into this multilayer structure opens a wide range of possibilities. In this study, the embedded materials are reduced to fluorophores and nanoparticles. Nevertheless, with these materials a high number of functionalities could be realized. Fluorophores and quantum dots that were embedded within the shell were successfully used for staining and differentiation of the capsules. The so-called bar-code approach in the sensor capsules demonstrated that with a low number of different QDs (here 3) already a high number of different capsules (here 8) could be labeled. But other nanoparticle materials turned out to be even more useful. Magnetic particles consisting of iron-oxide (also other ferrites available) provide a very high magnetization that can be used for moving and controlling the capsules. For targeting applications as well as for imaging (contrast agent) or future release mechanisms such magnetically modified capsules can be used. In the presented study the magnetic properties were applied for targeted deposition of capsules in a permanent liquid flow. This experiment illustrated how such systems could be directed and delivered to a certain spot of interest in an organism.
The gold nanoparticles that were embedded as clusters provided high energy conversion properties. Light power coming from the laser beam was efficiently transformed into heat and was used to open the PEM shell of the capsules and release the cargo. This approach demonstrated the easy implementation of such a release mechanism into the capsules. The laser wavelength applied in this study was in the near infrared (NIR) region what should enable for release of cargo in thin tissue or directly under the skin of organisms. Nevertheless, the NIR light can only penetrate tissue to a certain depth. For "real" applications in living organisms the strategy would have to be shifted towards magnetic opening. The easy implementation of various types of nanoparticles should provide a wide range of possible strategies for such usage. The actual approach that is based on gold clusters nevertheless shows some major drawbacks such as the inhomogeneous distribution of cluster sizes. We demonstrated that the formation of gold aggregates is very easy. Nevertheless, it lead to a wide size distribution of final aggregates and therefore to a wide range of plasmonic absorbance. Some aggregates will absorb the light of the used laser beam, whereas others will not absorb the applied wavelength. Some clusters may react very strongly to the light beam, others may only produce a little amount of heat. Furthermore, the cluster distribution within the polymer shell is not homogenous. This makes the opening of the capsules very challenging as too much stress is harmful for the cells. Alternative materials for heat

fabrication have already been demonstrated mainly with gold nanorods[29, 61, 62]. The aspect ratio of such particles can be tuned to specifically fit the used laser light. By using rods with a narrow size and aspect ratio distribution the absorbance of the capsule wall could be much more efficient in energy conversion. Nevertheless, the embedding of such particles into the multilayer shell did not succeed in a sufficient amount due to the missing surface charge of the rods.

The approach based on intracellular release of multiple cargo materials from distinct capsules to perform reactions was another step towards future medical applications. The possibility of delivering prodrugs or reactive compounds into biological matter via capsules would facilitate a wide range of therapeutic approaches. Side effects caused by the path of a drug/therapeutic through the body to the spot therapeutic interest could be significantly decreased. Also the administrated amount of drug could be decreased tremendously. This is because the compounds would targeted be delivered and unspecific uptake or clearence from the body would be suppressed. The same applies for undesired side effects as the compounds are protected and/or the prodrug only becomes reactive as two or more compounds are coming together. The triggered mixing of various molecules also opens the possibility for multiplexing or high-efficiency analysis applications in micro-patterns produced from the microcapsules deposited via magnetic targeting.

Finally the release of biologically active material was the most advanced approach demonstrated in this thesis. By encapsulating messenger RNA in the capsules and triggered release of the macromolecules into living cells, a whole new level of biological applications was introduced to the microcapsule approach. Releasing the mRNA with an external trigger not only presented the possibility of genetic manipulation of cells with such capsules but also presented a time-resolved control over intracellular reactions. Besides other approaches of introducing nucleic acids into living cells this methods provides real control over the point of time when the cargo is released. Also it abstains from any transfection substances that possibly manipulate the compound´s reactivity.

Nevertheless, the approach of laser induced heating and subsequent release of material inside cells also suffers from a crucial weakness. The application of heat and subsequent production of pressure and thermal stress to the cells is surely critical. Obviously many cells suffer from the thermal/physical stress that is induced during laser treatment. Furthermore, the whereabouts of the polymer remains and the nanoparticles released from the treatment is unsure. Possible cytotoxic effects and the effects of triggered destruction of endosomal compartments have to be investigated in future experiments. The high level of attention that has to be paid during the laser treatment also proofs the long distance of the approach from a real, clinical application. The still low success rate underlines this fact.

Notwithstanding these weaknesses, the approach shows great potential for future applications in medical treatment and biological analysis. With concentrated effort towards an improved energy conversion, better control of size and properties of the capsules and with investigations concerning possible cytotoxic effects such PEM microcapsules could become a useful tool for many bio-/ medical applications.

5. Publications

The presented cumulative thesis displays the results of scientific research assembled and published during the time of 2009 and 2012. These publications will be shortly summarized and the contributions to them, done by the author, will be outlined below. The released publication papers are attached to this thesis in the Appendix.

5.1 Reviews on Nano- and Microtechnology

Main focus of research presented in this thesis was lying in biological and medical applications of nano- and microtechnology. For this reason, several reviews have been prepared to provide an overview over past and actual status of research. Three main issues were investigated closer during these reviews: 1. Nanotechnology and nanoparticles for biological and medical sensing and delivery applications. 2. Microtechnology for delivery and sensing. Here, microcapsules were highlighted in particular. 3. Assembly of microcontainers and microclusters with incorporated nanoparticles. These systems combined the properties of nanotechnology and their physico-chemical advances with the high grade of control and packaging options of micro sized particles or capsules.

[A1][1] L. L. del_Mercato, P. Rivera-Gil, A. Z. Abbasi, M. Ochs, C. Ganas, I. Zins, C. Sönnichsen, W. J. Parak, "LbL multilayer capsules: recent progress and future outlook for their use in life sciences", Nanoscale **2010**, 2, 458

[A2][41] S. Carregal-Romero, M. Ochs, W. J. Parak, "Nanoparticle-functionalized microcapsules for in vitro delivery and sensing", Nanophotonics 2012, 0, 1

[A3][63] S. Carregal-Romero, E. Caballero-Diaz, A. M. Abdelmonem, M. Ochs, D. Hühn, B. S. Suao, M. Valcarcel, W.J. Parak, "Multiplexed Sensing and Imaging with Colloidal Nano- and Microparticles" Annual Review of Analytical Chemistry, **2013**, 6, accepted Nov. 2012

- The author´s contribution to the listed reviews mainly concentrated on the description and summarization of scientific facts and recent results on microsystems like beads, capsules or similar microcontainers. In particular the embedding of nanoparticles into such microsystems and the benefit of their properties to the assembled capsules was an important contribution to the reviews and strongly influenced the scientific research work presented in the following publications.

5.2 Polyelectrolyte microcapsules for sensing applications

Microcontainers like the presented microcapsules consisting of polyelectrolyte shell around solid, spherical templates are well known to be filled with fluorophores or sensitive molecules. By embedding ion-sensitive dyes into the cavities of the capsules, they can be used as versatile sensor tools. Ion concentrations can be detected in extra- and intracellular media. By tagging the capsules with fluorescent quantum dots they become ratiometric sensors for multiplexed measurements.

Capsules also act as spatial separators for fluorophores or fluorescent nanoparticles to provide for various sensing applications.

[A4][28] L. L. del_Mercato, A. Z. Abbasi, M. Ochs, W. J. Parak, "Multiplexed Sensing of Ions with Barcoded Polyelectrolyte Capsules", ACS Nano 2011, 5, 12, 9668

[A5][27] A. Z. Abbasi, F. Amin, T. Niebling, S. Friede, M. Ochs, S. Carregal-Romero, J. M. Montenegro Martos, P. Rivera-Gil, W. Heimbrodt, W. J. Parak, "How Colloidal Nanoparticles Could Facilitate Multiplexed Measurements of Different Analytes with Analyte-Sensitive Organic Fluorophores", ACS Nano 2011, 5, 21

- The author´s contribution to the presented publications was based on the fabrication and functionalization of the presented PEM microcapsules. Different fluorescent probes, as well as ion-sensitive fluorophores have been filled into the cavities. Herein the variety of different materials and molecular properties of the cargo required large effort. Additionally, the approach of "ball-in-ball" capsules with two or more cavities and shells has been adapted and tuned towards the fulfillment of the experimental requirements.

Besides the fabrication of the capsules, microscopic images have been prepared and ratiometric measurements were done. An automatic analysis software based on spreadsheet programming was developed and the mathematical data of the measurements were graphically analyzed.

5.3 Remote-controlled release and triggering of intracellular reactions

One major goal in the fabrication of microcapsules is the development of these containers to become a transport vehicle for pharmaceutical drugs or bio-active compounds. For this aim, capsules have to be filled with a variety of different materials. Furthermore, they have to possess a release-mechanism that enables for externally triggered opening of the capsules. Finally, the transport vehicles should be spatially controllable to deliver the capsules with their cargo only to a desired spot. The presented publications deal with the fulfillment of these three major requests on the presented PEM microcapsules. The methodology to fill the capsules with a broad band of different materials is presented. Furthermore, the embedding of metal nanoparticles into the PE shell to enable for laser-controlled, extra- and intracellular release of the cargo. Functionalization towards targeted delivery (with magnetic NPs) and the demonstration of reactivity of the released compounds are mainly presented in the second publication.

[A6][37] S. Carregal-Romero, M. Ochs, P. Rivera-Gil, C. Ganas, A. M. Pavlov, G. B. Sukhorukov, W. J. Parak, "NIR-light triggered delivery of macromolecules into the cytosol", Journal of Controlled Release **2012**, 159, 120

[A7][35] M. Ochs, S. Carregal-Romero, J. Rejman, K. Braeckmans, S. De Smedt, W. J. Parak, "Light-Adressable Capsules as Caged Compound Matrix for Controlled Triggering of Cytosolic Reactions", Angewandte Chemie (int. ed.) **2012**, accepted Nov. 2012

- The author did produce and develop the PEM microcapsules for the publications named above. The majority of the filling procedures and the light-controlled release experiments were done, as well as characterization and observation of the capsules. This included the intracellular release and the recording of reaction kinetics triggered by the opening of the capsules. Targeting experiments as well as uptake testing and mathematical analysis were also performed by the author.

These two publications present the main focus and efforts of the author´s thesis. The development of the capsules towards becoming a versatile delivery vehicle including controlled release, targeting and efficient filling mechanisms represents the aim of this work.

The author´s contribution presents the main results and essential role in the development of the publications. This is also reflected by the first author honor in one of the papers. The major developments and goals of the work (efficient filling strategies, intracellular release and reactivity of encapsulated chemicals) are achievements owing to the thesis and the work of the author.

References

[1] L. L. del_Mercato, P. Rivera_Gil, A. Z. Abbasi, M. Ochs, C. Ganas, I. Zins, C. Sönnichsen, W. J. Parak, Nanoscale **2010**, 2, 458.

[2] A. Merkoçi, Biosensing Using Nanomaterials, WILEY SERIES IN NANOSCIENCE AND NANOTECHNOLOGY, **2009**.

[3] R. Freeman, R. Gill, I. Shweky, M. Kotler, U. Banin, I. Willner, Angewandte Chemie-International Edition **2009**, 48, 309.

[4] A. J. Khopade, F. Caruso, Langmuir **2003**, 19, 6219.

[5] P. Rivera_Gil, S. D. Koker, B. G. De_Geest, W. J. Parak, Nano Letters **2009**, 9, 4398.

[6] G. B. Sukhorukov, A. Fery, M. Brumen, H. Mohwald, Physical Chemistry Chemical Physics **2004**, 6, 4078.

[7] G. Sukhorukov, A. Fery, H. Möhwald, Progress in Polymer Science **2005**, 30, 885.

[8] B. G. De_Geest, N. N. Sanders, G. B. Sukhorukov, J. Demeestera, S. C. D. Smedt, Chemical Society Reviews **2007**, 36, 636.

[9] G. Decher, J.-D. Hong, Macormol. Symp., Macormol. Symp. **1991**, 46, 321.

[10] G. B. Sukhorukov, A. L. Rogach, M. Garstka, S. Springer, W. J. Parak, A. Muñoz-Javier, Oliver Kreft, A. G. Skirtach, A. S. Susha, Y. Ramaye, R. Palankar, M. Winterhalter, SMALL **2007**, 3, 944.

[11] G. Decher, J. D. Hong, J. Schmitt, Thin Solid Films **1992**, 210, 831.

[12] G. B. Sukhorukov, E. Donath, S. Davis, H. Lichtenfeld, F. Caruso, V. I. Popov, H. Möhwald, Polymers for Advanced Technologies **1998**, 9, 759.

[13] B. G. De_Geest, S. De Koker, G. B. Sukhorukov, O. Kreft, W. J. Parak, A. G. Skirtach, J. Demeester, S. C. De Smedt, W. E. Hennink, Soft Matter **2009**, 5, 282.

[14] M. F. Bedard, A. Munoz-Javier, R. Mueller, P. del Pino, A. Fery, W. J. Parak, A. G. Skirtach, G. B. Sukhorukov, Soft Matter **2009**, 5, 148.

[15] G. Decher, Science **1997**, 277, 1232.

[16] E. Donath, G. B. Sukhorukov, F. Caruso, S. A. Davis, H. Möhwald, Angewandte Chemie International Edition **1998**, 37, 2202.

[17] A. P. R. Johnston, C. Cortez, A. S. Angelatos, F. Caruso, Current Opinion in Colloid & Interface Science **2006**, 11, 203.

[18] C. S. Peyratout, L. Dähne, Angewandte Chemie International Edition **2004**, 43, 3762.

[19] A. Fery, R. Weinkamer, Polymer **2007**, 48, 7221.

[20] A. Antipov, G. B. Sukhorukov, Advances in Colloid and Interface Science **2004**, 111, 49.

[21] M.-L. D. Temmerman, Ghent University (Ghent), **2012**.

[22] R. Georgieva, S. Moya, M. Hin, R. Mitlohner, E. Donath, H. Kiesewetter, H. Mohwald, H. Baumler, Biomacromolecules **2002**, 3, 517.

[23] W. Song, Q. He, H. Möhwald, Y. Yang, J. i. L., Journal of Controlled Release **2009**, 139, 160–166.

[24] F. Caruso, W. J. Yang, D. Trau, R. Renneberg, Langmuir **2000**, 16, 8932.

[25] F. Caruso, D. Trau, H. Möhwald, R. Renneberg, Langmuir **2000**, 16, 1485.

[26] A. M. Yu, Y. J. Wang, E. Barlow, F. Caruso, Advanced Materials **2005**, 17, 1737.

[27] A. Z. Abbasi, F. Amin, T. Niebling, S. Friede, M. Ochs, S. Carregal-Romero, J. M. M. Martos, P. Rivera_Gil, W. Heimbrodt, W. J. Parak, ACS Nano **2011**, 5, 21.

[28] L. L. del Mercato, A. Z. Abbasi, M. Ochs, W. J. Parak, ACS Nano **2011**, 5, 9668.

[29] H. Y. Koo, W. S. Choi, D. Y. Kim, Small **2008**.

[30] M. Bedard, B. De Geest, A. Skirtach, H. Mohwald, G. Sukhorukov, ADVANCES IN COLLOID AND INTERFACE SCIENCE **2010**, 158, 2.

[31] M. F. Bedard, D. Braun, G. B. Sukhorukov, A. G. Skirtach, Acs Nano **2008**, 2, 1807.

[32] B. Zebli, A. S. Susha, G. B. Sukhorukov, A. L. Rogach, W. J. Parak, Langmuir **2005**, 21, 4262.

[33] J. Rejman, G. Tavernier, N. Bavarsad, J. Demeester, S. C. De Smedt, Journal of Controlled Release **2010**, 147, 385.

[34] A. N. Zelikin, A. L. Becker, A. P. R. Johnston, K. L. Wark, F. Turatti, F. Caruso, ACS Nano **2007**, 1, 63–69.
[35] M. Ochs, S. Carregal-Romero, J. Rejman, K. Braeckmans, S. De Smedt, W. J. Parak, Angewandte Chemie (International ed. in English) **2012**.
[36] G. B. Sukhorukov, D. V. Volodkin, A. M. Günther, A. I. Petrov, D. B. Shenoy, H. Möhwald, Journal of Materials Chemistry **2004**, 14, 2073.
[37] S. Carregal-Romero, M. Ochs, P. Rivera_Gil, C. Gana, A. M. Pavlov, G. B. Sukhorukov, W. J. Parak, Journal Of Controlled Release **2012**, 159, 120.
[38] W. Tong, Y. Zhu, Z. Wang, C. Gao, H. Mohwald, Macromol Rapid Commun **2010**, 31, 1015.
[39] A. Z. Abbasi, L. Gutierrez, L. L. del Mercato, F. Herranz, O. Chubykalo-Fesenko, S. Veintemillas-Verdaguer, W. J. Parak, M. P. Morales, J. M. Gonzalez, A. Hernando, P. de la Presa, J. Phys. Chem. C **2011**, 115, 6257.
[40] T. Hyeon, S. S. Lee, J. Park, Y. Chung, H. B. Na, J. Am. Chem. Soc. **2001**, 123, 12798.
[41] S. Carregal-Romero, M. Ochs, W. J. Parak, Nanophotonics **2012**, 0, 1.
[42] C.-A. J. Lin, R. A. Sperling, J. K. Li, T.-Y. Yang, P.-Y. Li, M. Zanella, W. H. Chang, W. J. Parak, Small **2008**, 4, 334.
[43] A. P. Esser-Kahn, S. A. Odom, N. R. Sottos, S. R. White, J. S. Moore, Macromolecules **2011**, 44, 5539.
[44] A. Johnston, G. Such, F. Caruso, Angewandte Chemie International Edition **2010**, 49, 2664.
[45] S. De Koker, R. Hoogenboom, B. G. De Geest, Chemical Society Reviews **2012**, 41, 2867.
[46] N. A. Kotov, I. Dekany, J. H. Fendler, The Journal of Physical Chemistry **1995**, 99, 13065.
[47] R. Weissleder, Nat. Biotechnol. **2001**, 19, 316–317.
[48] N.-N. Dong, M. Pedroni, F. Piccinelli, G. Conti, A. Sbarbati, J. E. Ram¡rez-Hern·¡ndez, L. M. Maestro, M. C. Iglesias-de la Cruz, F. Sanz-Rodriguez, A. Juarranz, F. Chen, F. Vetrone, J. A. Capobianco, J. G. Sol¡©, M. Bettinelli, D. Jaque, A. Speghini, Acs Nano **2011**, 5, 8665.
[49] J. Davies, Nanobiology **1994**, 3, 5.
[50] T. Klar, M. Perner, S. Grosse, G. von Plessen, W. Spirkl, J. Feldmann, Physical Review Letters **1998**, 80, 4249.
[51] A. O. Govorov, H. H. Richardson, Nano Today **2007**, 2, 30.
[52] S. Eustis, M. A. El-Sayed, Chemical Society Reviews **2006**, 35, 209.
[53] O. Kreft, A. Muñoz_Javier, G. B. Sukhorukov, W. J. Parak, Journal Of Materials Chemistry **2007**, 17, 4471.
[54] M. J. Mc_Shane, J. Q. Brown, K. B. Guice, Y. M. Lvov, J Nanosci Nanotechnol **2002**, 2, 411.
[55] J. Q. Brown, M. J. McShane, Ieee Engineering in Medicine and Biology Magazine **2003**, 22, 118.
[56] T. A. Duchesne, J. Q. Brown, K. B. Guice, S. R. Nayak, Y. M. Lvov, M. J. McShane, in Optical Diagnostics and Sensing of Biological Fluids and Glucose and Cholesterol Monitoring II - Proceedings of SPIE, Vol. 4624 (Eds.: A. V. Priezzhev, G. L. Cote), SPIE, **2002**, pp. 66.
[57] L. L. del Mercato, A. Z. Abbasi, W. J. Parak, Small **2011**, 7, 351.
[58] R. Di Corato, D. Palumberi, R. Marotta, M. Scotto, S. Carregal-Romero, P. R. Gil, W. J. Parak, T. Pellegrino, Small **2012**, 8, 2731.
[59] L. Xiao, J. Li, D. F. Brougham, E. K. Fox, N. Feliu, A. Bushmelev, A. Schmidt, N. Mertens, F. Kiessling, M. Valldor, B. Fadeel, S. Mathur, Acs Nano **2011**, 5, 6315.
[60] M. Lewin, N. Carlesso, C. H. Tung, X. W. Tang, D. Corry, D. T. Scadden, R. Weissleder, Nature Biotechnolgy **2000**, 18, 410.
[61] M. Karg, I. Pastoriza-Santos, J. Perez-Juste, T. Hellweg, L. M. Liz-Marzan, Small **2007**, 3, 1222.
[62] M. Zanella, R. Gomes, M. Povia, C. Giannini, Y. Zhang, A. Riskin, M. Van Bael, Z. Hens, L. Manna, Advanced Materials **2011**, 23, 2205.
[63] S. Carregal-Romero, Caballero-Diaz, E., Beqa, L., Abdelmonem, A. M., Ochs, M., Hühn, D., Suao, B. S., Valcarcel, M., Parak, W. J., Annual Review of Analytical Chemistry **2013**, 6.

Abbreviations

QD(s)	quantumdot(s)
NP(s)	nanoparticle(s)
PE	polyelectrolyte
PEM	polyelectrolyte multilayer
PSS	poly (sodium 4-styrenesulfonate)
PAH	poly-(allylamine hydrochloride)
DNA	deoxyribonucleic acid
(m)RNA	(messenger) ribonucleic acid
FITC	fluorescein isothiocyanate
RITC	rhodamine isothiocyanate
rpm	revolutions per minute (centrifuge speed)
AU	airy unit (refers to the diameter of confocal pinhole)
pH	- decimal logarithm of H^+ concentration
EDTA	Ethylenediaminetetraacetic acid

Appendix

Official publications with the contributions of the author.

[A1][1] L. L. del_Mercato, P. Rivera-Gil, A. Z. Abbasi, M. Ochs, C. Ganas, I. Zins, C. Sönnichsen, W. J. Parak, "LbL multilayer capsules: recent progress and future outlook for their use in life sciences", Nanoscale **2010**, 2, 458

[A2][41] S. Carregal-Romero, M. Ochs, W. J. Parak, "Nanoparticle-functionalized microcapsules for in vitro delivery and sensing", Nanophotonics 2012, 0, 1

[A3][63] S. Carregal-Romero, E. Caballero-Diaz, A. M. Abdelmonem, M. Ochs, D. Hühn, B. S. Suao, M. Valcarcel, W.J. Parak, "Multiplexed Sensing and Imaging with Colloidal Nano- and Microparticles" Annual Review of Analytical Chemistry, **2013**, 6, accepted Nov. 2012

> Note, that this publication couldn´t be printed in its officially printed version, as the work was not published until the preparation of this work. The publication will be available until July 2013 on the publisher´s web page:
> - http://www.annualreviews.org/doi/abs/10.1146/annurev-anchem-062012-092621

[A4][28] L. L. del_Mercato, A. Z. Abbasi, M. Ochs, W. J. Parak, "Multiplexed Sensing of Ions with Barcoded Polyelectrolyte Capsules", ACS Nano 2011, 5, 12, 9668

[A5][27] A. Z. Abbasi, F. Amin, T. Niebling, S. Friede, M. Ochs, S. Carregal-Romero, J. M. Montenegro Martos, P. Rivera-Gil, W. Heimbrodt, W. J. Parak, "How Colloidal Nanoparticles Could Facilitate Multiplexed Measurements of Different Analytes with Analyte-Sensitive Organic Fluorophores", ACS Nano 2011, 5, 21

[A6][37] S. Carregal-Romero, M. Ochs, P. Rivera-Gil, C. Ganas, A. M. Pavlov, G. B. Sukhorukov, W. J. Parak, "NIR-light triggered delivery of macromolecules into the cytosol", Journal of Controlled Release **2012**, 159, 120

[A7][35] M. Ochs, S. Carregal-Romero, J. Rejman, K. Braeckmans, S. De Smedt, W. J. Parak, "Light-Adressable Capsules as Caged Compound Matrix for Controlled Triggering of Cytosolic Reactions", Angewandte Chemie (int. ed.) **2012**, accepted Nov. 2012

> Note, that the attached version does not contain the final page numbers and may differ slightly from the officially printed version as the attached paper corresponds to a preliminary online version.

Nanoscale

www.rsc.org/nanoscale

Volume 2 | Number 4 | April 2010 | Pages 445–624

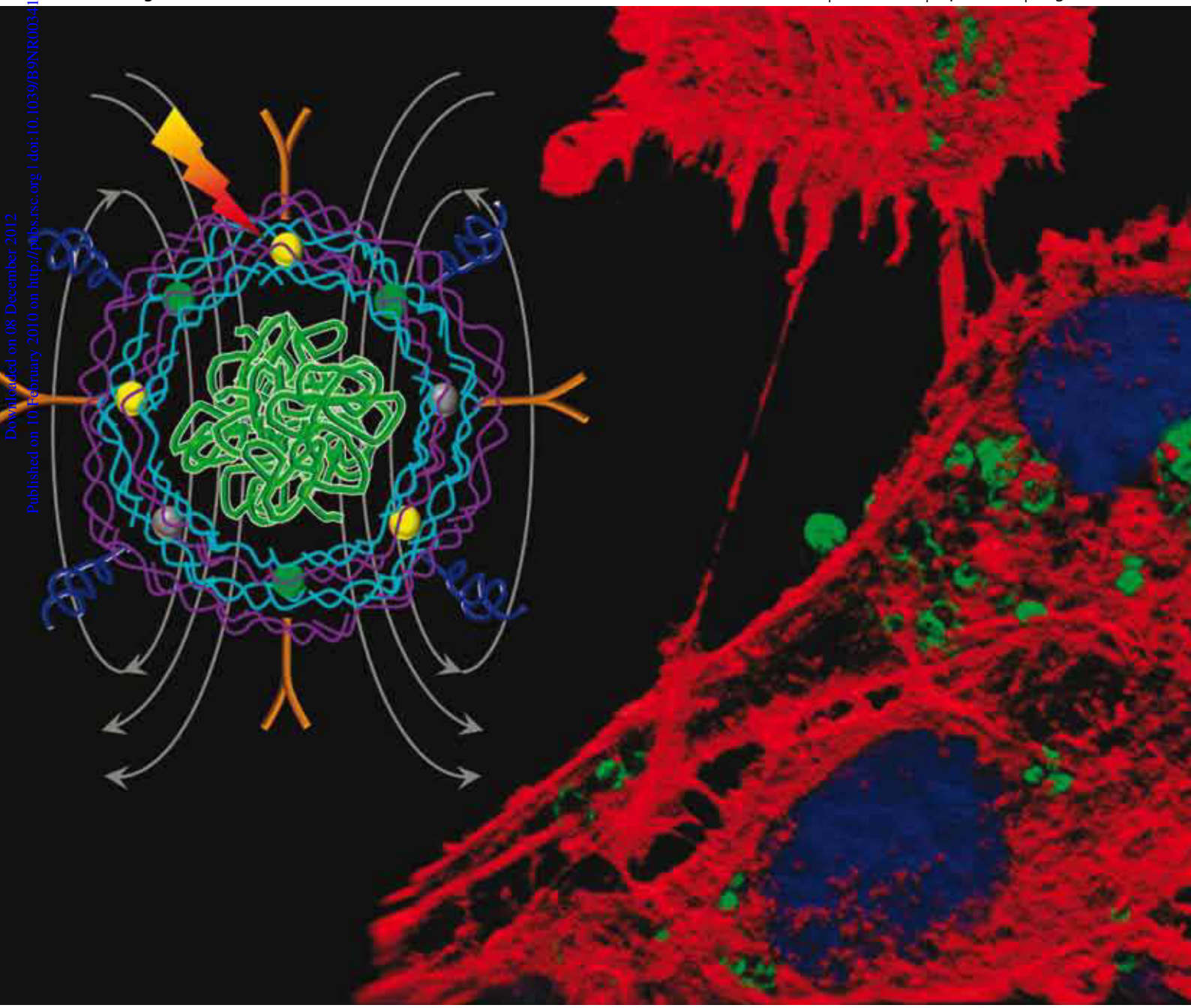

ISSN 2040-3364

RSC Publishing

LbL multilayer capsules: recent progress and future outlook for their use in life sciences

Loretta L. del Mercato,*[a] Pilar Rivera-Gil,[a] Azhar Z. Abbasi,[a] Markus Ochs,[a] Carolin Ganas,[a] Inga Zins,[b] Carsten Sönnichsen[b] and Wolfgang J. Parak[a]

Received (in Zürich, Switzerland) 6th November 2009, Accepted 28th December 2009
First published as an Advance Article on the web 10th February 2010
DOI: 10.1039/b9nr00341j

In this review we provide an overview of the recent progress in designing composite polymer capsules based on the Layer-by-Layer (LbL) technology demonstrated so far in material science, focusing on their potential applications in medicine, drug delivery and catalysis. The benefits and limits of current systems are discussed and the perspectives on emerging strategies for designing novel classes of therapeutic vehicles are highlighted.

Introduction

In the last three decades nanotechnology has attracted great interest in nanomedicine. Recent reviews describe the current impact and future prospects of nanotechnology with respect to drug/gene delivery and other fields of nanomedicine such as biosensing.[1–4] The main objectives in developing controlled release are avoidance of biological barriers, increase of the *in vivo* efficiency of drugs and targeted drug administration.[1,5] In addition the development of sensitive, specific and stable sensors, which allow for real-time measurements of physiological levels of important molecular species directly in the site of disease, is highly desirable.[6,7] For these purposes, a wide variety of carriers based on different methods of preparation have been developed ranging from nano-materials (such as carbon nanotubes,[8,9] nanoparticles,[10–13] and nanocomposites[14]) to biomaterials (such as dendrimers,[15] liposomes,[16,17] block co-polymer micelles,[18] biodegradable polymers[19]). These materials show some attractive properties such as small size (1 to 100 nm), chemically tailorable physical properties, tunable shape and structural robustness. Nonetheless, in the last years great attention has been focused on the development of novel "multifunctional" platforms[4,20–22] which combine a variety of properties allowing for the simultaneous or sequential performance of multiple functions in single cells, including enzymatic catalysis, controlled release, directed drug delivery and sensing. The most important requirements of a multifunctional system include (i) increased longevity and stability of the carrier in the circulation, (ii) targeting to the site of the disease *via* both non-specific and specific mechanisms, (iii) stimuli sensitivity to the local environment of the pathological site (such as pH or temperature) or to externally applied stimuli (such as magnetic field, ultrasound, laser irradiation), (iv) enhanced intracellular delivery of the cargo/drug, (v) contrast agents for both intra-cellular imaging of the carrier and real-time measurement of certain analytes in the body.[20] In this context polyelectrolyte multilayer capsules fabricated *via* the Layer-by-Layer (LbL) technique[23] have emerged as an interesting platform for the assembly of multifunctional carrier systems.[24] LbL-based hollow multilayer polyelectrolyte microcapsules consist of two distinct compartments: the multilayer shell and the cavity. The shell is built up through the consecutive adsorption of oppositely charged species around a charged spherical template and is held together due to the strong electrostatic forces that take place between each component layer.[23,25] The cavity, which is obtained after removal of the sacrificial template, represents the main volume of the capsules in which chemical reactions can be performed[26,27] and in which a range of materials from small molecules[28,29] to macromolecules[30–32] can be encapsulated, thus protecting unstable cargo from the surrounding hostile environment, beside increasing their biodistribution and solubility. Thanks to the high versatility of the LbL technique, the two compartments can be easily manipulated to create different types

[a]*Fachbereich Physik and Wissenschaftliches Zentrum für Materialwissenschaften, Philipps Universität Marburg, Renthof 7, 35037 Marburg, Germany. E-mail: loretta.delmercato@physik.uni-marburg.de*
[b]*Institut für Physikalische Chemie, Universität Mainz, Jakob-Welder-Weg 11, 55128 Mainz, Germany*

Loretta L. del Mercato

Dr Loretta Laureana del Mercato received her MSc in Biotechnology from the University "Federico II" of Naples (Italy) in 2004. In 2007 she obtained her Ph.D. in Innovative Materials and Technologies from the National Nanotechnology Laboratory (NNL) of CNR-INFM, Lecce (Italy) with a thesis on "Nanoscale characterization of synthetic polypeptides for nanobiotechnology applications". Since February 2008, she has been a postdoctoral researcher in the Biophotonics group of Professor Wolfgang J. Parak in the Physics Department of the Philipps Universität of Marburg (Germany). Her current research interests include the synthesis, functionalization and characterization of carrier systems based on polyelectrolyte capsules for applications in the biomedical field.

of active systems with respect to specific application requirements. The general properties of LbL microcapsules regarding their synthesis, loading and release,[33–36] physicochemical[36,37] and mechanical[38] properties as well as their permeability,[33,34,39] have been comprehensively reviewed by many articles in the past few years. Therefore, in this review, we first provide a short overview of the main steps involved in the preparation and functionalization of LbL-derived capsules, then we give an overview about some of the very recent progress achieved by several groups on the design of novel composite microcapsules, focusing on their use as drug delivery vehicles, intracellular sensors, and microreactor containers. Finally, we discuss the benefits and limits of current systems and we try to highlight the perspectives of the emerging strategies based on these systems for designing novel classes of therapeutics vehicles.

LbL-derived capsules: preparation and functionalization

LbL adsorption of oppositely charged species around submicrometre and micrometre-sized charged colloidal particles is a multi-step process which allows the fabrication of multilayer polyelectrolyte capsules for a wide range of applications. The technique is based on LbL adsorption of oppositely charged polymers on colloidal templates, followed by core dissolution.[23,25] Fig. 1 summarizes the main steps involved in the assembly of a multilayer polyelectrolyte capsule, based on a spherical porous template, in which more components with different functions have been combined at separate regions (cavity, wall and external surface of the capsule) to create a single object capable of performing multiple functions simultaneously.[40] As can be observed, the properties of the capsules can be varied at each step employing building blocks with different properties. For example, by using templates of different diameter (from 60 nm to 10 μm), the size of the resulting capsules can be tuned,[25,32,37,41] whereas by using different types of component layers, such as synthetic polyelectrolytes,[25,42] charged and not charged biopolymers,[43–47] the chemical properties of the multilayer shell can be tailored. Moreover the multilayer shell can be modified by simultaneously loading charged inorganic nanoparticles to yield capsules responsive to specific external stimuli.[48–51] Finally the surface of the capsules can be decorated to give low-fouling capsules by the adsorption of a poly(ethylene glycol)-based layer[52,53] or targeted capsules through the coupling of specific recognition elements (*e.g.*, antibodies).[54] In the following the range of materials used so far for each step of fabrication and their main properties are described.

The main classes of decomposable templates used for LbL assembly of capsules have been extensively reviewed in previous articles.[37,39,40] Briefly, capsules have been fabricated by using organic (*i.e.*, polystyrene latex,[55] melamine formaldehyde,[25] silicon dioxide[37]) or inorganic templates[41,56,57] (*i.e.*, $MnCO_3$, $CaCO_3$ $CdCO_3$) dissolvable in acidic or aqueous solvents, respectively. The choice of the initial core influences significantly the properties of the capsules such as their size distribution and the strategy used for loading the active molecules like dyes and drugs inside the cavities.[29,58,59] For instance, capsules based on organic cores are typically characterized by a good monodispersity and their cavities can be filled after the dissolution of the core by changing the permeability of the multilayer shell through variations in pH,[60–62] solvent polarity,[63] ionic strength[64,65] or temperature[59,64] (post-loading method). Instead

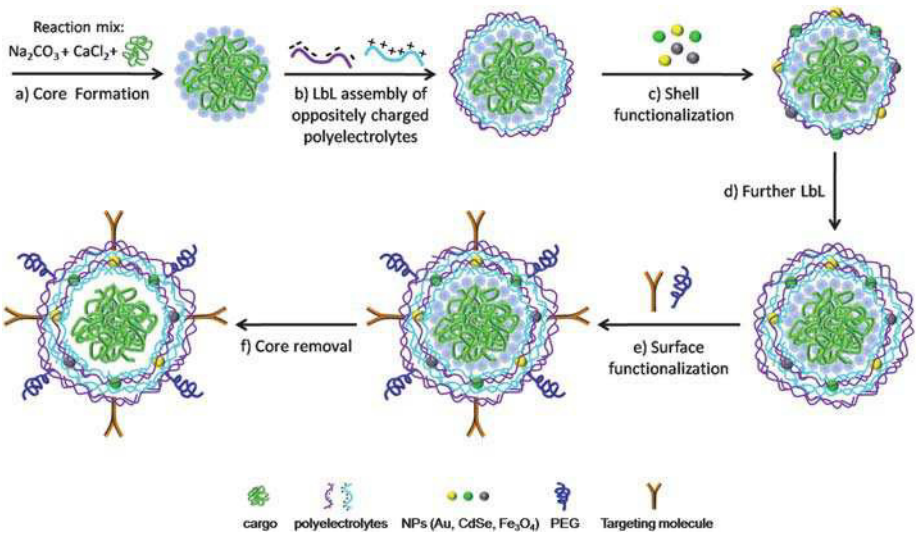

Fig. 1 Schematic illustration of the synthesis of a multifunctional polyelectrolyte capsule *via* LbL assembly. (a) A spherical $CaCO_3$ porous template is synthesized by mixing two solutions of Na_2CO_3 and $CaCl_2$ in presence of the cargo molecules (such as drugs, genes or proteins). The cargo molecules are embedded in the pores of the template. (b) The filled $CaCO_3$ particles are then coated *via* consecutive LbL deposition of oppositely charged polyelectrolytes to grow a multilayer polymer shell around the template. (c) The shell can be functionalized by loading charged NPs (such as metal, fluorescent and magnetic NPs) onto an oppositely charged layer during the LbL assembly. (d) LbL of polyelectrolytes is repeated to obtain a stable multilayer shell. (e) Additional surface functionalization to improve cellular uptake (*e.g.* targeting moieties) or *in vivo* longevity (*e.g.* conjugation of PEG) can be performed *via* electrostatic or covalent binding of molecules to the outer surface. (f) Finally the spherical template is removed to obtain a multilayer capsule with cargo molecules inside its cavity. Capsules are not drawn to scale. Only few layers of polyelectrolyte and of NPs are shown for sake of clarity.

capsules based on porous inorganic cores, such as carbonate crystals, can be directly loaded by mixing the cargo molecules with the porous templates, followed by the LbL coating with polyelectrolytes pairs (pre-loading method).[32,56] Because after the dissolution process some oligomers of the original core material can partially remain adsorbed within the shell,[66] capsules based on biocompatible templates, such as porous $CaCO_3$,[58] mesoporous silica[32] or polylactides microparticles (PLGA, PLA),[67] are typically preferred especially for biological applications.

Beside the choice of the cores, also the choice of the shell components plays a pivotal role in the LbL assembly since it directly influences the biocompatibility and degradability of the capsules inside living organisms. On one hand, capsules made of intracellular biodegradable shell components such as poly-aminoacids (*i.e.* poly-L-arginine), synthetic polymers (*i.e.* poly(hydroxypropyl)methacrylamide dimethylaminoethyl (p(HPMA-DMAE))[47] or chitosan[43,45,68] are very useful for biomedical applications related to the delivery of active compounds such as genes, proteins or drugs inside living organisms.[69] On the other hand, biocompatible but not "easily" degradable polyelectrolytes are necessary for other applications like sensing inside cells *i.e.* determination of the intracellular ion concentration of different organelles.[70] For such applications the synthetic bio-incompatible polylelectrolytes sodium poly(styrene sulfonate, sodium salt) (PSS), poly(allylamine hydrochloride) (PAH) and polydiallyl dimethyl ammonium chloride (PDAD-MAC) have been widely used up to now.[59,71] The challenge for these capsule-based systems might rely on the ability of synthesizing biocompatible capsules stable enough in the different environments inside the different organelles so that they can accurately inform about the local environment of the capsules.

The capsule wall can be functionalized to impart optical, magnetic and photothermal properties to microcapsules by introducing during the LbL process inorganic charged nanoparticles (NPs)[48–51] through the use of electrostatic interactions (Fig. 2). The shell modification with different types of nanoparticles allows for addressing important functions such as the labelling, the targeting and the controlled opening of the capsules which are essential for using these systems as carriers for drug delivery and sensing applications. For example, by modifying the walls of the capsules with fluorescent nanoparticles non invasive optical detection of the capsules inside living organisms can be performed.[72–74] By incorporating magnetic nanoparticles to fluorescent capsules (*e.g.*, functionalized with organic dye molecules or light-emitting quantum dots), capsules with dual-imaging functionalities, magnetic resonance (MR) imaging and luminescent properties, can be produced for their use as biomarkers *in vitro* and *in vivo*.[75–77] Additionally, magnetic NPs-modified capsules can be externally manipulated using magnetic fields for directing and accumulating capsules to the target region (*e.g.*, cancer cells) before delivering the chemotherapeutic drugs. For instance, by using Fe_3O_4-particle-modified capsules a specific accumulation and high local concentration of the NPs-modified capsules was observed along a magnetic field gradient and their internalization by breast cancer cells *in vitro*.[78] Finally by embedding gold, silver and magnetic NPs into the capsule walls, the release of encapsulated drug molecules from the cavities can be achieved upon exposure to an external physical trigger such as electromagnetic or sound waves.[49,50,79,80] In a recent work, the laser irradiation of gold-modified capsules has been used to locally heat the metal NPs and to perturb the integrity/permeability of the walls of the capsules inducing the release of cargo from the cavities of single capsules to the cytosol of the cells.[71] Gold nanorods (Au NRs)[81,82] have been also employed as absorbing elements of the capsule walls for light-controlled release of encapsulated material.[83] Like Au NPs, charged Au NRs can be embedded within the multilayer shell during the LbL deposition of oppositely charged layers around the sacrificial template[84] (Fig. 2b and Fig. 3b). The use of gold nanorods allows producing capsules with near-infrared absorbing properties whose opening can be induced by using laser wavelength which corresponds to the tissue transparency window (800–900 nm). Capsules with such properties might be very promising for biomedical applications. Fig. 3a shows the mechanism of photoactivated release of cargo from the cavity of a polyelectrolyte capsule containing Au NRs in the walls: laser irradiation leads to local heating of the metal nanorods and subsequent opening of small pores within the capsule wall. In Fig. 3c is reported the effect of the laser irradiation of a FITC-dextran loaded capsule with the following multilayer shell $(PSS/PAH)_3(PSS/AuNRs)(PAH/PSS)_2$. Before laser illumination, the intact capsule retains the green cargo inside the cavity (phase contrast and green channel images). During laser illumination the irradiated capsule is deformed because of the heating of the Au NRs. After switching-off the laser the capsule shell appears damaged, as it can be observed in the phase contrast image, and the partial release of the fluorescent cargo can be noticed in the corresponding fluorescent channel. Alternatively to laser irradiation

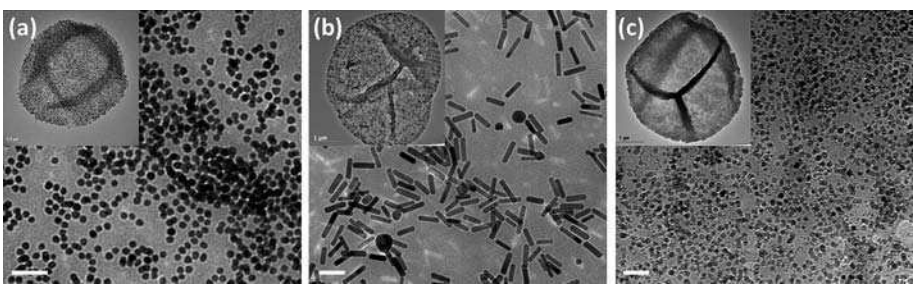

Fig. 2 Functionalization of polyelectrolyte capsules with inorganic nanoparticles incorporated in the multilayer shell. Typical TEM images of (a) Au NPs, (b) Au NRs and (c) Fe_3O_4 NPs embedded inside the multilayer shell of hollow $(PSS/PAH)_4$ capsules. Insets show the single nanoparticles-modified capsules. Scale bars represent 50 nm.

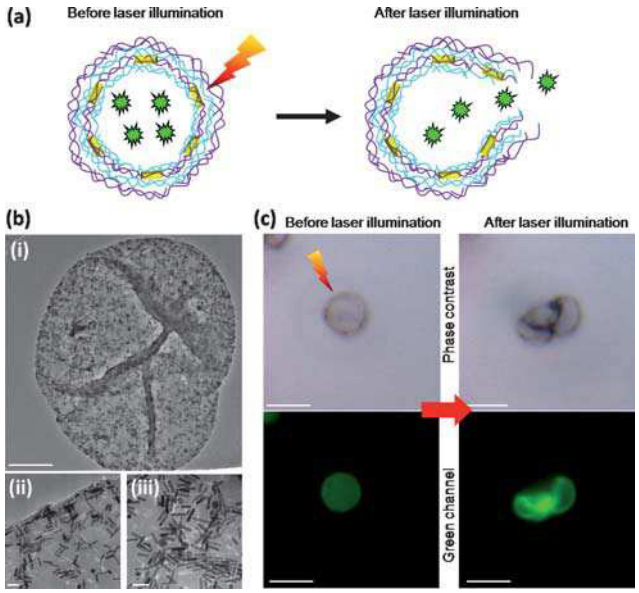

Fig. 3 Laser-opening of FITC-dextran loaded capsule with Au NRs embedded in the capsule wall. (a) Schematic representation of the geometry of a capsule with green dextran as cargo (green stars) encapsulated inside the cavity and Au NRs (yellow rods) embedded in the wall: laser irradiation of Au NRs-capsule (left) leads to local heating of the metal NRs and subsequent rupture of the capsule wall (right). (b) Representative TEM image of a single Au NRs-capsule (i) (scale bar 1 μm). (ii-iii) Two high-resolution images of the multilayer wall of the capsule shown in (i) (Scale bars 50 nm). (c) Effect of near-IR laser irradiation (830 nm) of a single Au NRs-capsule loaded with FITC-dextran. Before laser illumination: the capsule retains the green cargo inside the cavity. After laser illumination: the multilayer wall of the capsule is damaged (phase contrast) and the partial release of the green cargo throughout the small pores of the wall is observed (green channel) (scale bars 5 μm).

methods, ultrasound treatment of gold-doped capsules has been used to mechanically disintegrate the capsule walls.[85] In a different approach, high-frequency magnetic field (HFMF) has been proven to trigger the release of drugs from microcapsules prepared by loading Fe_3O_4 NPs into the walls.[86]

Capsules made of new components as layers

Besides conventional polyelectrolytes, a variety of substances have been investigated in the last years to construct capsules through LbL assembly. Generally these capsules display improved permeability properties and especially new features such as biocompatibility, degradability and controlled destructability, making them attractive for applications in the fields of pharmacology, medicine and cosmetics *etc*. In this section we describe some of the recent strategies exploited by several groups to fabricate LbL-derived capsules made of new combinations of building blocks (polymeric micelles, polysaccharides, proteins, liposome and oligonucleotides) as integral components of the capsules wall.

Hollow microcapsules containing polymeric micelles in their walls have been fabricated by alternating assembly of PAH and poly(styrene-b-acrylic acid) (PS-b-PAA) micelles on $MnCO_3$ microparticles.[87] In such a system, the micelles serve as hydrophobic reservoirs with a high loading capacity in the shells while the LbL shell provides the micelles with additional support and protection. Besides their potential use as a drug delivery vehicle, these capsules may also provide an alternative option to serve as bioreactors and biosensors.[87]

Iron-heparin hollow sub-micrometre capsules have been fabricated by alternating deposition of oppositely charged ferric ions(III) and heparin (a highly-sulfated glycosaminoglycan widely used as anticoagulant[88]) onto the surface of the polystyrene latex (PS) particles, followed by removal of the PS templates by dissolution.[89] The resulting capsules displayed longer anticoagulant activity in *in vitro* and *in vivo* assays compared with the same dose of an aqueous solution of heparin,[89] suggesting their potential use as injectable anticoagulant vehicles in the bloodstream.

Single-component degradable capsules based on poly(methacrylic acid) (PMA) cross-linked *via* disulfide linkages have been assembled and loaded with the protein transferrin[90] and oligonucleotides.[91] These capsules undergo a reversible swelling in response to changes in external pH, and degrade in the presence of a physiological concentration of a natural thiol-containing peptide (*i.e.*, glutathione)[92] releasing the cargo molecules in a reducing environment.

Disulfide bonds (S–S) have also been employed to cross-link the shell of protein-based microcapsules leading to capsules which are destroyable by organisms and cells. For example, bovine serum albumin (BSA) mono-component hollow microcapsules were fabricated by desolvation of BSA onto $MnCO_3$ microparticles followed by cross-linking with disulfide-containing dithiobis(succinimidylpropionate) (DSP) and subsequent core removal.[93] Destruction of the BSA microcapsules was achieved under the treatment with a reductive agent ($NaBH_4$) and with a further treatment of ultrasonication, indicating that these microcapsules are stabilized not only by S–S covalent bonds but also by other non-covalent forces (*i.e.*, hydrophobic forces and hydrogen bonds).[93] In another work, hemoglobin (Hb) microcapsules crosslinked by glutaraldehyde (GA) were fabricated through covalent LbL assembly onto $MnCO_3$ microparticles.[94] In this approach, the use of GA to crosslink proteins has been shown to lead to significant improvements in the permeability of Hb capsules in contrast to polyelectrolyte capsules.[94] In a further work, CF0F1-proteoliposomes, previously prepared by incorporating the chloroplastic F0F1-ATP synthase (CF0F1-ATP) into liposomes, were mixed with a suspension of Hb capsules leading to the adsorption of lipids on the capsule surface and the assembly of CF0F1-ATP synthase onto the capsule shells. The resulting lipid-coated Hb microcapsules were successfully used to synthesize ATP.[95]

Enzymatic proteins have been also used as layers to grow multilayer shells capable of performing specific reactions. Qi *et al.*, fabricated glucose-sensitive microcapsules from the LbL assembly of Hb and glucose oxidase (GOD) followed by cross-linking of the protein layers with GA.[96] The formation of hydrogen peroxide (H_2O_2) upon processing glucose, catalyzed by GOD and Hb, indicated that the proteins were still enzymatically active after their immobilization in the multilayer. In addition, the author observed a glucose-stimulated enhancement of the wall permeability probably due to the decrease in the local pH and the loosening of the multilayer structure. In a further work,

the author employed this pH dependent behaviour to control the release of insulin molecules encapsulated inside glucose-sensitive multilayer shells.[97] Briefly, GOD and catalase (CAT) were assembled onto insulin particles alternately *via* GA cross-linking. As expected, the release ratio of insulin from the protein multilayers was observed to linearly increase in response to addition of external glucose because of the increased permeability of the capsule wall[97] (Fig. 4). The described approach is interesting because it represents a proof of concept for potential applications of biocatalytic capsules sensitive to specific analytes for the controlled release of drugs.

Recently, the technologies of liposomes and LbL assembly have been combined to fabricate polyelectrolyte-coated magnetic liposomes with the aim of protecting the lipid bilayer with a polyelectrolyte multilayer shell, thus avoiding their fusion. Lately, superparamagnetic nanoparticles were encapsulated in liposomes and the resulting charged liposomes were used as templates for the stepwise LbL adsorption of the polyelectrolytes PAH and PSS. These polyelectrolyte-coated magnetic liposomes could be delivered to living cells and manipulated by applying an external magnetic field.[98] In a different approach, Caruso and co-workers combined liposomes and polyelectrolyte capsules to fabricate so-called capsosomes, a hybrid platform in which the properties/advantages of the two systems are merged. The capsosomes were formed through initial coating of silica cores with a precursor of PAH, followed by adsorption of 50 nm-sized DOPC liposomes and subsequent layering of PSS and PAH[99] (Fig. 5). However, since electrostatic interactions alone showed to provide insufficient affinity between liposomes and the underlying polymer surface, the authors developed a modified protocol in which cholesterol-modified polymers were used as noncovalent anchors for the loading of liposomes into the capsules. In this work the enzyme β-lactamase has been preloaded into the liposomes before their entrapment inside the polymer capsules and the presence of the active enzyme within the as-prepared capsosomes has been confirmed by quantitative enzymatic reaction.[100] The main novelty of the presented approach consists on the synthesis of a hybrid microreactor system which contains numerous liposome subcompartments (about 8×10^3) in which different enzymatic reactions might be carried out simultaneously.

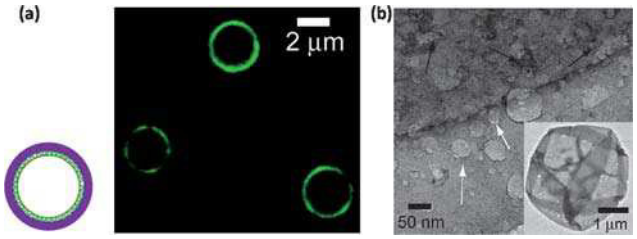

Fig. 5 Typical morphology of (PAH/liposomes$_{NBD}$/(PSS/PAH)$_4$/PSS) capsosome. (a) Scheme of the geometry of a capsosome with liposome embedded in its wall, CLSM image and (b) negative stained TEM image of capsosomes. The black arrows identify structurally intact liposomes, while the white arrows indicate areas where the liposomes have been displaced. The inset shows a complete capsosome. [Adapted from ref. 99.]

The use of DNA as shell component has also been demonstrated recently.[101] Multilayer DNA shells were formed by alternately depositing diblock oligonucleotides containing two different regions (one of which is complementary to the adsorbed single-stranded block in the film, whereas the second region is free for hybridization in the subsequent layer). In a related work the authors developed a method to encapsulate various nucleic acids inside degradable polyelectrolyte capsules.[91] Capsules entirely composed of DNA (as cargo and as shell constituents) could be of particular interest because they are biodegradable, biocompatible, and their physicochemical properties (*e.g.*, size, permeability, structure and shrinkage) can be finely controlled by base pairing of the nucleotides.

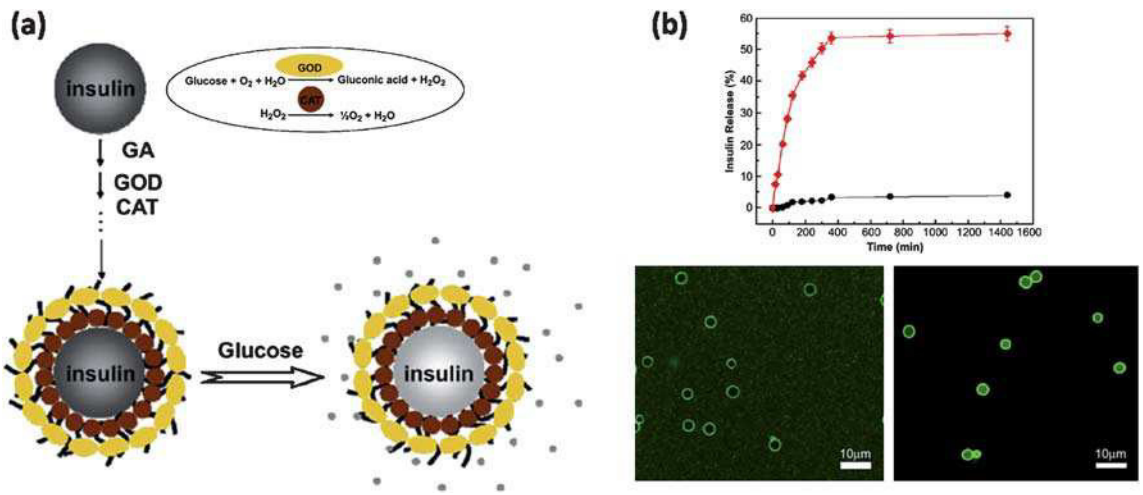

Fig. 4 Controlled release of insulin from glucose-sensitive enzyme multilayer shells. (a) Schematic representation of coupled reactions of glucose oxidase (GOD) and catalase (CAT) assembled onto insulin particles followed by the enhanced permeability of the capsule for release of insulin. (b) Top: Release profiles of coated insulin particles before (black line) and after (red line) external application of glucose solution, respectively. Bottom: CLSM images of (CAT/GOD)$_5$ microcapsules mixed with FITC–dextran (2000 kDa): (i) before and (ii) after adding glucose solution. [Adapted from ref. 97.]

Biostability in physiological environments

One of the main problems of charged systems is that they are easily cleared from the organism by serum protein adsorption (opsonization) and subsequent phagocytosis. Covalent linkage of PEG (poly(ethylene glycol)) or other hydrophilic polymers to the surface of several carrier systems have displayed to reduce their non-specific uptake by the cells (including cells from the mononuclear phagocyte system) due to their enhanced low-fouling properties.[20,102–104] Since the main stabilizing forces in polyelectrolyte capsules are electrostatic interactions, the efficient binding of a PEG corona to the surface of the capsule has to be carried out by previous linkage of PEG to highly charged substances like polyelectrolytes. In this way, modified PEG can be strongly and stably attached to charged surfaces by electrostatic interactions. Modifying the surface of the polyelectrolyte multilayer capsules by adding polyelectrolyte (*i.e.* poly(L-lysine))-*graft*-PEG molecules has been a successful strategy to resist protein adsorption and therefore opsonization.[52,105–107] As mentioned before, the main forces that stabilize LbL assembled systems are based on electrostatic interactions. This makes such systems very sensitive to environmental conditions such as changes in the ionic strength of the medium or in the temperature and thus susceptible to disassembly. Although systems assembled in this way can be tailored to take advantage of these properties, for some biomedical applications this can be an important limitation. Recent approaches have developed capsules whose synthesis combines the electrostatic forces *via* LbL assembly and covalent cross-linking *via* click chemistry.[108] This versatile approach has several advantages: (i) low charged polyelectrolytes can be now incorporated to the LbL (after incorporation of covalent bonds); (ii) linkage groups that remain unreacted can be easily post-functionalized; (iii) due to the mild, non-harmful conditions of the click chemistry, sensitive cargo (easy denaturizable active molecules like protein, nucleic acids) can be incorporated.[106] Nevertheless, post-functionalization of the capsule surface is still an important feature under investigation. With click chemistry, all reactions are catalyzed by copper, thus leading to cytotoxic effects,[106] although very recently a metal-catalyst-free approach has been developed to introduce functional groups to the multilayer of the capsules.[109]

Cytotoxicity

Regarding the cytotoxicity of the capsules, although not yet well studied, the main sources for toxicity come obviously from the polyelectrolytes composing the wall as well as from the functionalities embedded in the cavity and/or in the wall.[40] The magnitude of the cytotoxic effect of the capsules is primarily concentration- and time-dependent.[69,110] Additionally, the intrinsic chemical properties of the positively charged polyelectrolyte (polycation) turned out to make them effective triggers of mitochondrial-mediated cell death (apoptosis/necrosis).[111,112] Due to their positive charge, polycations cause cellular membrane damage with subsequent activation of signalling pathways that end up with mitochondrial depolarization and generation of reactive oxygen species resulting in cell death. In this regard, together with the molecular weights, the cationic charge density of the polycations are key parameters for the interaction with cell membrane and cell damage.[113,114] Furthermore, polycations containing (poly)amine functionalities may result in an increased interaction with anionic intracellular components that also lead to oxygen-independent cell death.[115] In this regard, a reduction of the cytotoxicity could be obtained by using materials that are already present in the cells *i.e.* lipids and proteins as natural polyions. Owing to their amphiphilic character, cellular lipids can aggregate in aqueous solution into spherically closed bilayer structures due to hydrophobic interactions. When the aqueous solution contains a charged protein, a self-assembly process that combines electrostatic interactions and hydrophobic forces occurs in the immiscible interface. The result is the adsorption of proteins and lipids onto the interface of emulsion droplets and the formation of a multilayer elastic shell.[116] Despite the compatibility of these biomimetic capsules and the potential to incorporate molecular functionalities like channels or receptors, the main approach of this technique still relies in controlling the size of the capsules and the unwanted degradation of the system.

Applications in medicine

One of the possible contributions of LbL-derived multilayer capsules to medicine is their use as biocompatible multifunctional composite carrier systems that are sensitive to remote guidance and activation for local release of cargo molecules (*i.e.* drugs) inside target cells/tissues.[40] Due to the high versatility of the LbL technique, not only hydrophilic molecules can be loaded but also hydrophobic molecules (*i.e.* many therapeutical drugs) have been efficiently encapsulated and released thus overcoming the obstacles of hydrophobicity.[117] To date it is a fact that polyelectrolyte multilayer capsules of different sizes (from nanometre to micrometre) are taken up by living cells.[69,118] The incorporation of the capsules occurs spontaneously and is non-cell specific. Therefore the addition of low-fouling polymers which posses protein-repellent qualities is required besides targeting features toward the design of novel vehicles for targeted drug delivery *in vivo*. For instance, microcapsules coated with a layer of PEG-grafted polyelectrolytes have been shown to escape clearance by the mononuclear phagocytic system.[52,105,106] As previously described, the release of the transported cargo molecules can occur under exposure to external stimuli (*e.g.*, light- or ultrasound-treatment of nanoparticles modified capsules) or more challenging, by using the conditions of the local environment of the capsules (*i.e.* intracellularly).[68,97] Recent publications have proven the use of biodegradable capsules for the delivery of pro-drugs inside the cells.[47,119] Pro-drugs are the non-active form of a medicament that needs to be enzymatically hydrolysed to release the active form of the drug. Fig. 6 shows a capsule-based system sensitive to enzymatic degradation at two distinct positions.[119] Both the capsule wall and the encapsulated cargo (in this case a pro-drug) are easily degraded by proteases located inside the cells. The intracellular degradation of the capsule wall leads to the release of the pro-drug and enables activation of the drug through enzymatic cleavage. Furthermore, sustained release of the cargo molecules is obtained by the continuous enzymatic digestion of the capsule membrane.[119] In this way, several main requirements for drug delivery are achieved. The incorporation of highly environmental-sensitive

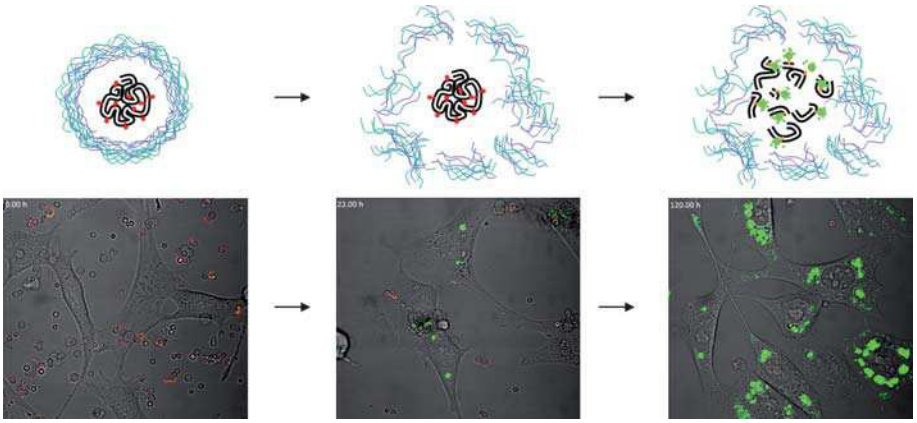

Fig. 6 Cargo release and activation mediated by intracellular degradation of capsules. Capsule walls are of DEXS/pARG and the cavity is filled with a fluorogenic substrate for proteases (DQ-OVA™). Upon cellular internalization, the capsule wall is actively degraded enzymatically, this lead specific enzymes to reach the cargo proteins (ovalbumine, OVA). When OVA is structurally intact, the fluorescence of the dyes conjugated to ovalbumine are quenched. On the contrary, when OVA is enzymatically cleavaged the quenching effect is relieved and a bright green fluorescence appears. As a result of the cleavage of OVA, single dye-labeled peptides are released out of the capsule. [Adapted from ref. 119.]

cargos (*i.e.* pro-drug or proteins) inside the capsule protects both the cargo from unwanted degradation and healthy cells from the action of the drug. Since less concentration of the drug could be administered in order to reach therapeutic concentrations, the side effects would be reduced. Thus, the intracellular degradation would enable the controlled release of cargo over a long period of time locally.

Anticancer drugs such as doxorubicin (DOX) have been demonstrated to be released upon changes in the pH of a solution.[120] Since the location of the capsules seems to be in acidic compartments,[70] by choosing the right materials that provide a good compromise between swelling and stiffness, drugs can be released from the capsules over time in a controlled manner self-regulated by the intracellular conditions. The low pH of the acidic vesicles where the capsules are transported causes swelling of the multilayer[121] with an initial rapid release of the drug due to high differences in the drug concentration between the bulk and the capsule cavity and followed by a plateau. The release can continue over a period of time until degradation of the capsule has been finalized or the entire amount of drug has been released. *In vivo* studies have demonstrated that this might be possible by using DOX-loaded biodegradable polyelectrolytes alternatively attached to doped $CaCO_3$-carboxylmethyl cellulose (CMS) templates. After chemical removal of the $CaCO_3$, CMS forms a complex with DOX and is stabilized in the capsule cavity. Direct injection of the loaded-capsules to the tumor of a mouse, led to a sustained release of DOX for 4 weeks, probably due to a non-favorable thermodynamic process at low pH, and resulted in a reduction of the tumor.[45]

The LbL approach appears to be a helpful technique not only for anticancer therapy but also for vaccination. One of the main challenges in vaccination is the efficient delivery of effective doses and the co-delivery of adjuvants with the antigen in order to generate sufficient immune response. Self-exploding microcapsules made of a semi-permeable polyelectrolyte multilayer around a sugar-based hydrophilic microgel core (size around 10 μm) have emerged as a "single shot" delivery system for the release of antigens in multiple pulses.[122] Due to the large size of the core, smaller carriers can be incorporated in the gel. Because of the semi-permeable conditions of the wall, water can penetrate causing a strong swelling of the gel that finally leads to the rupture of the microcontainer followed by the "shooting" of the smaller carriers that are able to propagate in water faster than if they were in solution. This is of special importance when the species has to be released in viscous medium. By tuning the density of the microgel, the resistance to disruption can be modulated and the microcontainers are able to release cargo (*i.e.* vaccines) at different times.

Conclusion/outlook

In this review we have highlighted some of the recent progresses of designing and utilizing novel types of multifunctional LbL-based multilayer capsules. LbL-assembled capsules are very versatile platforms which can be used to encapsulate, to store and to delivery cargo molecules. Their selective permeability allows to load not only different types of molecules, ranging from ions to macromolecules, but also to perform chemical reactions inside the interior. In addition, they can be easily functionalized with various natural molecules or inorganic nanoparticles to create multifunctional materials with hybrid properties.

Nowadays several *in vitro*[45,118,123–125] and *in vivo* studies[45,89] have established the use of these capsules as carriers in living systems. Notably, capsules with different physicochemical properties have been produced for different applications ranging from simultaneous imaging and delivery of biologically active molecules,[72–74] to intracellular sensing and bio-reactors.[26,27,70,96,126,127] Capsules modified by metal nanoparticles capable of protecting molecules in their cavities and release them by light irradiation, have been fabricated and characterized.[71,80] As an alternative to active release mechanisms, biocompatible controlled-release by using capsules made of biodegradable polymer shells which are gradually decomposed within the cellular environment, have been demonstrated.[47,119]

Nevertheless, there are still some challenges left to be overcome for further development of LbL capsules systems for drug

delivery and therapeutic purposes. In particular, the preparations of capsules need to be improved in terms of particles dispersion and aggregation as well as new efficient methods for the large-scale production have to be developed since production of capsules is often time-consuming and at the laboratory scale. In addition there is a need for more generally applicable strategies to efficiently encapsulate water-soluble low molecular weight drugs, in fact most capsule shells show pores size around 10 nm which are often the reason of fast diffusion of the cargo out of the cavities. Regarding this issue, the recent data obtained by Song and colleagues are promising: the authors showed the efficient entrapment of a small drug procainamide hydrochloride (PrH), molecular weight 271.79, inside (PDADMAC/PSS) capsules by heat treatment and shrinking of the capsules.[28]

The cellular uptake pathway and the degradation/release kinetics have to be intensively investigated for optimization of these systems in biological applications. The cytotoxicity and immune response of capsules need to be evaluated in more detail for clinical application. Also future improvements in developing new molecules and in studying new active targeting and controlled release mechanisms are essential in order to assemble new complex functional systems transferrable to the clinic. For example, the development of capsules with multiple compartments able to simultaneously transport multiple therapeutics agents in pathological sites would be very promising for tumors/cancer therapies. Such systems could then co-deliver anticancer drugs and small interfering RNA (siRNA) to inhibit genetic components of the tumors. It is expected that the cooperation between different scientific communities (bioengineers, chemists, physicists, biologists, bio-nanotechnologists) might be the best approach to overcome the limits of the available current systems by designing novel materials capable of fulfilling the needs of different communities.

Acknowledgements

This work was supported by the BMBF within the ERANET Neuron framework.

References

1 R. Langer and D. A. Tirrell, *Nature*, 2004, **428**, 487–492.
2 O. C. Farokhzad and R. Langer, *ACS Nano*, 2009, **3**, 16–20.
3 M. Ferrari, *Nat. Rev. Cancer*, 2005, **5**, 161–171.
4 J. Peteiro-Cartelle, M. Rodríguez-Pedreira, F. Zhang, P. Rivera Gil, L. L. del Mercato and W. J. Parak, *Nanomedicine*, 2009, **4**, 967–979.
5 D. Peer, J. M. Karp, S. Hong, O. C. FaroKHzad, R. Margalit and R. Langer, *Nat. Nanotechnol.*, 2007, **2**, 751–760.
6 A. Merkoçi, Biosensing Using Nanomaterials, *Wiley Series In Nanoscience and Nanotechnology*, 2009.
7 R. Freeman, R. Gill, I. Shweky, M. Kotler, U. Banin and I. Willner, *Angew. Chem., Int. Ed.*, 2009, **48**, 309–313.
8 S. J. Son, X. Bai and S. Lee, *Drug Discovery Today*, 2007, **12**, 657–663.
9 S. J. Son, X. Bai and S. B. Lee, *Drug Discovery Today*, 2007, **12**, 650–656.
10 E. Boisselier and D. Astruc, *Chem. Soc. Rev.*, 2009, **38**, 1759–1782.
11 M. Arruebo, R. Fernandez-Pacheco, M. R. Ibarra and J. Santamaria, *Nano Today*, 2007, **2**, 22–32.
12 L. Zhang, F. X. Gu, J. M. Chan, A. Z. Wang, R. S. Langer and O. C. Farokhzad, *Clin. Pharmacol. Ther.*, 2008, **83**, 761–769.
13 R. A. Sperling, P. Rivera_Gil, F. Zhang, M. Zanella and W. J. Parak, *Chem. Soc. Rev.*, 2008, **37**, 1896–1908.
14 J. H. Adair, T. Li, T. Kido, K. Havey, J. Moon, J. Mecholsky, A. Morrone, D. R. Talham, M. H. Ludwig and L. Wang, *Mater. Sci. Eng., R*, 1998, **23**, 139–242.
15 H. L. Crampton and E. E. Simanek, *Polym. Int.*, 2007, **56**, 489–496.
16 Y. Malam, M. Loizidou and A. M. Seifalian, *Trends Pharmacol. Sci.*, 2009, **30**, 592–599.
17 A. Samad, Y. Sultana and M. Aqil, *Curr. Drug Delivery*, 2007, **4**, 297–305.
18 K. Kataoka, A. Harada and Y. Nagasaki, *Adv. Drug Delivery Rev.*, 2001, **47**, 113–131.
19 Y. Yang, W. Jia, X. Qi, C. Yang, L. Liu, Z. Zhang, J. Ma, S. Zhou and X. Li, *Macromol. Biosci.*, 2004, **4**, 1113–1117.
20 V. Torchilin, *Eur. J. Pharm. Biopharm.*, 2009, **71**, 431–444.
21 S. A. Corr, Y. P. Rakovich and Y. K. Gun'ko, *Nanoscale Res. Lett.*, 2008, **3**, 87–104.
22 E. Tasciotti, X. W. Liu, R. Bhavane, K. Plant, A. D. Leonard, B. K. Price, M. M. C. Cheng, P. Decuzzi, J. M. Tour, F. Robertson and M. Ferrari, *Nat. Nanotechnol.*, 2008, **3**, 151–157.
23 G. Decher, *Science*, 1997, **277**, 1232–1237.
24 G. B. Sukhorukov, A. L. Rogach, M. Garstka, S. Springer, W. J. Parak, A. Muñoz-Javier, Oliver Kreft, A. G. Skirtach, A. S. Susha, Y. Ramaye, R. Palankar and M. Winterhalter, *Small*, 2007, **3**, 944–955.
25 E. Donath, G. B. Sukhorukov, F. Caruso, S. A. Davis and H. Möhwald, *Angew. Chem., Int. Ed.*, 1998, **37**, 2201–2205.
26 L. Dähne, S. Leporatti, E. Donath and H. Mohwald, *J. Am. Chem. Soc.*, 2001, **123**, 5431–5436.
27 D. G. Shchukin and G. B. Sukhorukov, *Adv. Mater.*, 2004, **16**, 671–682.
28 W. Song, Q. He, H. Möhwald, Y. Yang and J. i. L, *J. Controlled Release*, 2009, **139**, 160–166.
29 F. Caruso, W. J. Yang, D. Trau and R. Renneberg, *Langmuir*, 2000, **16**, 8932–8936.
30 R. Georgieva, S. Moya, M. Hin, R. Mitlohner, E. Donath, H. Kiesewetter, H. Mohwald and H. Baumler, *Biomacromolecules*, 2002, **3**, 517–524.
31 F. Caruso, D. Trau, H. Möhwald and R. Renneberg, *Langmuir*, 2000, **16**, 1485–1488.
32 A. M. Yu, Y. J. Wang, E. Barlow and F. Caruso, *Adv. Mater.*, 2005, **17**, 1737.
33 G. B. Sukhorukov, A. Fery, M. Brumen and H. Mohwald, *Phys. Chem. Chem. Phys.*, 2004, **6**, 4078–4089.
34 G. Sukhorukov, A. Fery and H. Möhwald, *Prog. Polym. Sci.*, 2005, **30**, 885–897.
35 Bruno G. De Geest, Niek N. Sanders, Gleb B. Sukhorukov, Joseph Demeestera and S. C. D. Smedt, *Chem. Soc. Rev.*, 2007, **36**, 636–649.
36 A. P. R. Johnston, C. Cortez, A. S. Angelatos and F. Caruso, *Curr. Opin. Colloid Interface Sci.*, 2006, **11**, 203–209.
37 C. S. Peyratout and L. Dähne, *Angew. Chem., Int. Ed.*, 2004, **43**, 3762–3783.
38 A. Fery and R. Weinkamer, *Polymer*, 2007, **48**, 7221–7235.
39 A. Antipov and G. B. Sukhorukov, *Adv. Colloid Interface Sci.*, 2004, **111**, 49–61.
40 P. Rivera Gil, L. L. del Mercato, P. del Pino, A. Munoz Javier and W. J. Parak, *Nano Today*, 2008, **3**, 12–21.
41 G. B. Sukhorukov, D. V. Volodkin, A. M. Günther, A. I. Petrov, D. B. Shenoy and H. Möhwald, *J. Mater. Chem.*, 2004, **14**, 2073–2081.
42 W. J. Tong and C. Y. Gao, *Polym. Adv. Technol.*, 2005, **16**, 827–833.
43 G. Berth, A. Voigt, H. Dautzenberg, E. Donath and H. Mohwald, *Biomacromolecules*, 2002, **3**, 579–590.
44 X. P. Qiu, S. Leporatti, E. Donath and H. Mohwald, *Langmuir*, 2001, **17**, 5375–5380.
45 Q. Zhao, B. Han, Z. Wang, C. Gao, C. Peng and J. Shen, *Nanomedicine*, 2007, **3**, 63–74.
46 A. M. Yu, I. R. Gentle and G. Q. Lu, *J. Colloid Interface Sci.*, 2009, **333**, 341–345.
47 B. G. De Geest, R. E. Vandenbroucke, A. M. Guenther, G. B. Sukhorukov, W. E. Hennink, N. N. Sanders, J. Demeester and S. C. d. Smedt, *Adv. Mater.*, 2006, **18**, 1005–1009.
48 F. Caruso, A. S. Susha, M. Giersig and H. Möhwald, *Adv. Mater.*, 1999, **11**, 950–953.
49 A. G. Skirtach, A. A. Antipov, D. G. Shchukin and G. B. Sukhorukov, *Langmuir*, 2004, **20**, 6988–6992.

50 A. S. Angelatos, B. Radt and F. Caruso, *J. Phys. Chem. B*, 2005, **109**, 3071–3076.
51 Z. Lu, M. D. Prouty, Z. Guo, V. O. Golub, C. S. Kumar and Y. M. Lvov, *Langmuir*, 2005, **21**, 2042–2050.
52 R. Heuberger, G. Sukhorukov, J. Vörös, M. Textor and H. Möhwald, *Adv. Funct. Mater.*, 2005, **15**, 357–366.
53 C. R. Kinnane, K. Wark, G. K. Such, A. P. R. Johnston and F. Caruso, *Small*, 2009, **5**, 444–448.
54 C. Cortez, E. Tomaskovic-Crook, A. P. R. Johnston, B. Radt, S. H. Cody, A. M. Scott, E. C. Nice, J. K. Heath and F. Caruso, *Adv. Mater.*, 2006, **18**, 1998–2003.
55 F. Caruso, *Chem.–Eur. J.*, 2000, **6**, 413–419.
56 D. V. Volodkin, N. I. Larionova and G. B. Sukhorukov, *Biomacromolecules*, 2004, **5**, 1962–1972.
57 A. A. Antipov, G. B. Sukhorukov, S. Leporatti, I. L. Radtchenko, E. Donath and H. Möhwald, *Colloids Surf., A*, 2002, **198–200**, 535–541.
58 D. V. Volodkin, A. I. Petrov, M. Prevot and G. B. Sukhorukov, *Langmuir*, 2004, **20**, 3398–3406.
59 K. Köhler and G. B. Sukhorukov, *Adv. Funct. Mater.*, 2007, **17**, 2053–2061.
60 T. Mauser, C. Dejugnat and G. B. Sukhorukov, *Macromol. Rapid Commun.*, 2004, **25**, 1781–1785.
61 Z. An, H. Möhwald and J. Li, *Biomacromolecules*, 2006, **7**, 580–585.
62 G. B. Sukhorukov, A. A. Antipov, A. Voigt, E. Donath and H. Mohwald, *Macromol. Rapid Commun.*, 2001, **22**, 44–46.
63 Y. Lvov, A. A. Antipov, A. Mamedov, H. Möhwald and G. B. Sukhorukov, *Nano Lett.*, 2001, **1**, 125–128.
64 C. Y. Gao, S. Leporatti, S. Moya, E. Donath and H. Mohwald, *Chem.–Eur. J.*, 2003, **9**, 915–920.
65 A. A. Antipov, G. B. Sukhorukov and H. Mohwald, *Langmuir*, 2003, **19**, 2444–2448.
66 C. Y. Gao, S. Moya, H. Lichtenfeld, A. Casoli, H. Fiedler, E. Donath and H. Möhwald, *Macromol. Mater. Eng.*, 2001, **286**, 355–361.
67 D. B. Shenoy, A. A. Antipov, G. B. Sukhorukov and H. Mohwald, *Biomacromolecules*, 2003, **4**, 265–272.
68 Y. Itoh, M. Matsusaki, T. Kida and M. Akashi, *Biomacromolecules*, 2008, **9**, 2202–2206.
69 S. De Koker, B. G. De Geest, C. Cuvelier, L. Ferdinande, W. Deckers, W. E. Hennink, S. De Smedt and N. Mertens, *Adv. Funct. Mater.*, 2007, **17**, 3754–3763.
70 O. Kreft, A. Muñoz_Javier, G. B. Sukhorukov and W. J. Parak, *J. Mater. Chem.*, 2007, **17**, 4471–4476.
71 A. Muñoz Javier, P. d. Pino, M. Bedard, A. G. Skirtach, D. Ho, G. Sukhorukov, C. Plank and W. J. Parak, *Langmuir*, 2008, **24**, 12517–12520.
72 A. Rogach, A. Susha, F. Caruso, G. Sukhorukov, A. Kornowski, S. Kershaw, H. Möhwald, A. Eychmüller and H. Weller, *Adv. Mater.*, 2000, **12**, 333–337.
73 N. Gaponik, I. L. Radtchenko, M. R. Gerstenberger, Y. A. Fedutik, G. B. Sukhorukov and A. L. Rogach, *Nano Lett.*, 2003, **3**, 369–372.
74 N. Gaponik, I. L. Radtchenko, G. B. Sukhorukov, H. Weller and A. L. Rogach, *Adv. Mater.*, 2002, **14**, 879–882.
75 S. Mornet, S. Vasseur, F. Grasset and E. Duguet, *J. Mater. Chem.*, 2004, **14**, 2161–2175.
76 C. Corot, P. Robert, J. M. Idee and M. Port, *Adv. Drug Delivery Rev.*, 2006, **58**, 1471–1504.
77 V. I. Shubayev, T. R. Pisanic and S. H. Jin, *Adv. Drug Delivery Rev.*, 2009, **61**, 467–477.
78 B. Zebli, A. S. Susha, G. B. Sukhorukov, A. L. Rogach and W. J. Parak, *Langmuir*, 2005, **21**, 4262–4265.
79 A. G. Skirtach, C. Dejugnat, D. Braun, A. S. Susha, W. J. Parak, H. Möhwald and G. B. Sukhorukov, *Nano Lett.*, 2005, **5**, 1371–1377.
80 M. F. Bédard, D. Braun, G. B. Sukhorukov and A. G. Skirtach, *ACS Nano*, 2008, **2**, 1807–1816.
81 C. Sönnichsen, T. Franzl, T. Wilk, G. von Plessen, J. Feldmann, O. Wilson and P. Mulvaney, *Phys. Rev. Lett.*, 2002, **88**, 077402.
82 A. Henkel, A. Jakab, G. Brunklaus and C. Sonnichsen, *J. Phys. Chem. C*, 2009, **113**, 2200–2204.
83 A. G. Skirtach, P. Karageorgiev, B. G. De_Geest, N. Pazos-Perez, D. Braun and G. B. Sukhorukov, *Adv. Mater.*, 2008, **20**, 506–510.
84 T. V. Bukreeva, B. V. Parakhonskiy, I. V. Marchenko, B. N. Khlebtsov, N. G. Khlebtsov, O. V. Dementieva, M. N. Savvateev, L. A. Feigin and a. M. V. Kovalchuk, *Nanotechnol. Russ.*, 2008, **3**, 85–93.
85 A. G. Skirtach, B. G. De_Geest, A. Mamedov, A. A. Antipov, N. A. Kotov and G. B. Sukhorukov, *J. Mater. Chem.*, 2007, **17**, 1050–1054.
86 S. H. Hu, C. H. Tsai, C. F. Liao, D. M. Liu and S. Y. Chen, *Langmuir*, 2008, **24**, 11811–11818.
87 Y. Zhu, W. J. Tong, C. Y. Gao and H. Mohwald, *Langmuir*, 2008, **24**, 7810–7816.
88 R. Lever and C. P. Page, *Nat. Rev. Drug Discovery*, 2002, **1**, 140–148.
89 L. Yu, Y. G. Gao, X. L. Yue, S. Q. Liu and Z. F. Dai, *Langmuir*, 2008, **24**, 13723–13729.
90 A. N. Zelikin, J. F. Quinn and F. Caruso, *Biomacromolecules*, 2006, **7**, 27–30.
91 A. N. Zelikin, Q. Li and F. Caruso, *Angew. Chem., Int. Ed.*, 2006, **45**, 7743–7745.
92 A. N. Zelikin, Q. Li and F. Caruso, *Chem. Mater.*, 2008, **20**, 2655–2661.
93 Y. Zhu, W. J. Tong, C. Y. Gao and H. Mohwald, *J. Mater. Chem.*, 2008, **18**, 1153–1158.
94 L. Duan, Q. He, X. H. Yan, Y. Cui, K. W. Wang and J. B. Li, *Biochem. Biophys. Res. Commun.*, 2007, **354**, 357–362.
95 W. Qi, L. Duan, K. W. Wang, X. H. Yan, Y. Citi, Q. He and J. B. Li, *Adv. Mater.*, 2008, **20**, 601–605.
96 W. Qi, X. Yan, L. Duan, Y. Cui, Y. Yang and J. Li, *Biomacromolecules*, 2009, **10**, 1212–1216.
97 W. Qi, X. H. Yan, J. B. Fei, A. H. Wang, Y. Cui and J. B. Li, *Biomaterials*, 2009, **30**, 2799–2806.
98 J. F. Pereira da Silva Gomes, A. Rank, A. Kronenberger, J. Fritz, M. Winterhalter and Y. Ramaye, *Langmuir*, 2009, **25**, 6793–6799.
99 B. Städler, R. Chandrawati, K. Goldie and F. Caruso, *Langmuir*, 2009, **25**, 6725–6732.
100 B. Städler, R. Chandrawati, A. D. Price, S. F. Chong, K. Breheney, A. Postma, L. A. Connal, A. N. Zelikin and F. Caruso, *Angew. Chem., Int. Ed.*, 2009, **48**, 4359–4362.
101 A. P. R. Johnston, E. S. Read and F. Caruso, *Nano Lett.*, 2005, **5**, 953–956.
102 L. van Vlerken, T. Vyas and M. Amiji, *Pharm. Res.*, 2007, **24**, 1405.
103 G. Prencipe, S. M. Tabakman, K. Welsher, Z. Liu, A. P. Goodwin, L. Zhang, J. Henry and H. J. Dai, *J. Am. Chem. Soc.*, 2009, **131**, 4783–4787.
104 V. C. F. Mosqueira, P. Legrand, A. Gulik, O. Bourdon, R. Gref, D. Labarre and G. Barratt, *Biomaterials*, 2001, **22**, 2967–2979.
105 U. Wattendorf, O. Kreft, M. Textor, G. B. Sukhorukov and H. P. Merkle, *Biomacromolecules*, 2008, **9**, 100–108.
106 C. J. Ochs, G. K. Such, B. Stadler and F. Caruso, *Biomacromolecules*, 2008, **9**, 3389–3396.
107 A. J. Khopade and F. Caruso, *Langmuir*, 2003, **19**, 6219–6225.
108 B. G. De Geest, W. Van Camp, F. E. Du Prez, S. C. De Smedt, J. Demeester and W. E. Hennink, *Chem. Commun.*, 2008, 190–192.
109 L. A. Connal, C. R. Kinnane, A. N. Zelikin and F. Caruso, *Chem. Mater.*, 2009, **21**, 576–578.
110 C. Kirchner, A. M. Javier, A. S. Susha, A. L. Rogach, O. Kreft, G. B. Sukhorukov and W. J. Parak, *Talanta*, 2005, **67**, 486–491.
111 A. C. Hunter, *Adv. Drug Delivery Rev.*, 2006, **58**, 1523–1531.
112 D. Fischer, Y. X. Li, B. Ahlemeyer, J. Krieglstein and T. Kissel, *Biomaterials*, 2003, **24**, 1121–1131.
113 T. Bieber, W. Meissner, S. Kostin, A. Niemann and H. P. Elsasser, *J. Controlled Release*, 2002, **82**, 441–454.
114 W. T. Godbey, K. K. Wu and A. G. Mikos, *J. Biomed. Mater. Res.*, 1999, **45**, 268–275.
115 N. Seiler and F. Raul, *J. Cell. Mol. Med.*, 2005, **9**, 623–642.
116 J. B. Li, H. Mohwald, Z. H. An and G. Lu, *Soft Matter*, 2005, **1**, 259–264.
117 K. Wang, Q. He, X. Yan, Y. Cui, W. Qi, L. Duana and J. Li, *J. Mater. Chem.*, 2007, **17**, 4018–4021.
118 A. Muñoz Javier, O. Kreft, M. Semmling, S. Kempter, A. G. Skirtach, O. Bruns, P. del Pino, M. F. Bedard, J. Rädler, J. Käs, C. Plank, G. Sukhorukov and W. J. Parak, *Adv. Mater.*, 2008, **20**, 4281–4287.
119 P. Rivera-Gil, S. De Koker, B. G. De Geest and W. J. Parak, *Nano Lett.*, 2009, **9**, 4398–4402.

120 X. L. Yang, X. Han and Y. H. Zhu, *Colloids Surf., A*, 2005, **264**, 49–54.
121 C. Déjugnat and G. B. Sukhorukov, *Langmuir*, 2004, **20**, 7265–7269.
122 B. G. De Geest, M. J. McShane, J. Demeester, S. C. De Smedt and W. E. Hennink, *J. Am. Chem. Soc.*, 2008, **130**, 14480–14482.
123 Y. J. Wang, V. Bansal, A. N. Zelikin and F. Caruso, *Nano Lett.*, 2008, **8**, 1741–1745.
124 Z. H. An, K. Kavanoor, M. L. Choy and L. J. Kaufman, *Colloids Surf., B*, 2009, **70**, 114–123.
125 M. Semmling, O. Kreft, A. Muñoz Javier, G. B. Sukhorukov, J. Käs and W. J. Parak, *Small*, 2008, **4**, 1763–1768.
126 M. J. McShane, J. Q. Brown, K. B. Guice and Y. M. Lvov, *J. Nanosci. Nanotechnol.*, 2002, **2**, 411–416.
127 U. Reibetanz, D. Haloan, M. Brumen and E. Donath, *Biomacromolecules*, 2007, **8**, 1927–1933.

Nanophotonics 1 (2012): 171–180 © 2012 Science Wise Publishing & De Gruyter • Berlin • Boston. DOI 10.1515/nanoph-2012-0014

Review

Nanoparticle-functionalized microcapsules for *in vitro* delivery and sensing

Susana Carregal-Romero, Markus Ochs and Wolfgang J. Parak*

Fachbereich Physik and WZMW, Philipps Universität Marburg, Marburg, Germany,
e-mail: wolfgang.parak@physik.uni-marburg.de

*Corresponding author

Abstract

Inorganic nanoparticles such as magnetic nanoparticles, fluorescent quantum dots, and plasmonic nanoparticles can be used as building blocks for designing multifunctional systems based on polymeric capsules. The properties of the inorganic nanoparticles hereby are harnessed to provide additional functionality to the polymer capsules. Biological applications towards *in vitro* sensing and delivery are discussed. Examples will be given in which magnetic nanoparticles are used to direct capsules with magnetic field gradients, colloidal quantum dots are used to identify capsules *via* the formation of optical barcodes, and gold nanoparticles are used as light-controlled heat-sources for opening capsules and releasing macromolecules from their cavity upon optical excitation. This demonstrates that combination of inorganic nanoparticles and organic/polymeric molecules as carrier matrices allow for tailoring multifunctional hybrid particles for practical applications.

Keywords: polyelectrolyte capsules; colloidal nanoparticles; quantum dots; magnetic nanoparticles; plasmonic nanoparticles; multifunctionality; delivery system; sensors; hybrid particles.

1. Introduction

Progress in biology is often influenced by the development of new assays or tools. They even can allow for monitoring cellular processes which have not been experimentally accessible before, be it due to previous limits in sensitivity, long-term stability, biocompatibility, or experimental complexity. Particle-based systems are helpful tools in this direction and have been used as contrast agents for imaging, as sensors for the detection of analytes, or as delivery vehicles *in vitro* and *in vivo* [1–4]. Inorganic nanoparticles (NPs) for example can contribute different properties based on their material composition. Fluorescent quantum dots (QDs) such as CdSe/ZnS or InP NPs can be used as tags for cellular imaging. Magnetic NPs such as Fe_2O_3 or Fe_3O_4 NPs can be used as contrast agents for magnetic resonance imaging (MRI) or can be guided in magnetic field gradients. Plasmonic NPs such as Au or Ag NPs can be used for optical sensing or for converting light into heat. To produce heat efficiently the nanoparticles have to be irradiated with light in the same wavelength range of the plasmon band absorption. The plasmon band of such NPs can be tuned easily by changing size or shape. Plasmonic NPs absorbing in the near-infrared region of the electromagnetic spectrum of the light are more suitable for biological applications since the absorption of light by tissue is minimal. Therefore, Au nanoshells, small Au aggregates or Au nanorods are convenient platforms to be used as nanoheaters [5–7]. By integrating different inorganic NPs into bigger carrier systems their properties can be combined, which thus allows for creating multifunctional objects. Polymeric polyelectrolyte capsules are one example of such a carrier system [8], which is on first order held together by electrostatic attraction and thus easily allows for integrating charged NPs of different materials [9–11]. In this review we will show three examples on how incorporation of magnetic, fluorescent, and plasmonic NPs into capsules provide them particular properties useful for *in vitro* delivery and sensing.

2. Polyelectrolyte capsules as universal carrier systems

Polyelectrolyte multilayer (PEM) capsules are fabricated following a bottom-up approach *via* Layer-by-Layer (LbL) self-assembly [12] of differently charged polyelectrolytes on top of a template particle [13, 14]. Hereby the onion-shaped LbL geometry is held together predominantly by electrostatic force. Subsequent dissolution of the template particle leads to PEM capsules, *cf.* Figure 1. PEM capsules have several distinct features: (i) They can carry a cargo in their cavity and other functionalities can be integrated in their PEM walls. Cargo can comprise macromolecules [16], hydrophobic drugs [17], micelles [18], or NPs [19]. In addition, walls can be modified with biological ligands or NPs. As pointed out before NPs can be fluorescent, magnetic, light mediated heaters, etc. Loading the cavity and the walls independently with several of the aforementioned entities allows for multifunctionality. (ii) The cargo inside the capsule cavity is protected within the polyelectrolyte walls and does not participate in the control over pharmacokinetics and biodistribution. Cells which have incorporated capsules are also protected from direct contact with the containing cargo. (iii) Size and charge of the PEM capsules can be easily tuned [14, 20]. Size and charge are important parameters which affect interaction with cells. Neutral or slightly negative charge helps to reduce non-

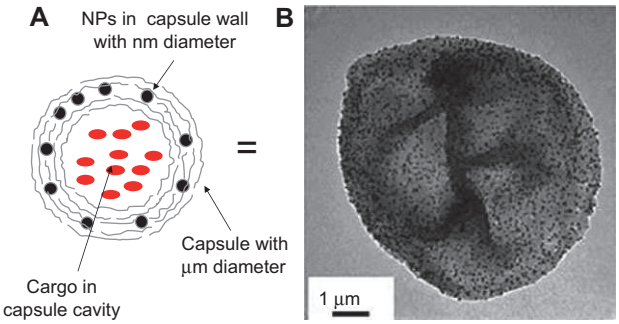

Figure 1 (A) Scheme of a multifunctional PEM capsule (not drawn to scale). (B) Transmission electron microscope (TEM) image of a PEM capsule with incorporated NPs in their wall (5 double layers of polystyrene sulfonate M_w≈70 kDa)/poly (allylamine hydrochloride) (M_w≈56 kDa); Au NPs with core diameter of 20 nm). The scale bar corresponds to 1 µm. Image taken from del Mercato et al. [15].

specific uptake by living cells *in vivo* and positive charged systems favored non-specific uptake [21]. (iv) The PEM wall can be biodegradable or non-degradable and its porosity can be tuned by the number of polyelectrolyte layers and by the PEM materials. Due to this tunable porosity small molecules can diffuse in and out the cavity to bulk solution, but bigger molecules as cargo are trapped inside the cavity. The porosity of the capsules depends strongly on the number of polyelectrolyte layers and on the presence of other entities such as nanoparticles. Dong et al. studied, for example, the diffusion of different fluorophores with different hydrodynamic sizes (from 0.8 to 9 nm) for capsules made with a different number or polyelectrolyte layers [22] but changes in the LbL process such ionic strength, the polyelectrolyte composition and the addition of NPs or the pH of the environment are known to change the diffusion of analytes through the polymeric shell [22, 23]. Nevertheless, the PEM capsule shell is in general permeable for small ions such as H^+ or Na^+.

In Figure 1 the idealized scheme of a PEM capsule is shown. It is important to point out the different size of the NPs (hydrodynamic diameters around 10 nm) and the PEM capsules (diameters around 3–5 µm) which will be discussed in the following. The PEM wall of the capsules is remarkably thin, wherein each layer contributes between 1 and 10 nm to the thickness depending on the PE nature and on the ionic strength during the LbL process [22]. Thus typically the size of NPs incorporated in the capsule wall is bigger than the actual thickness of the plain wall. Even at diameters of a few microns PEM capsules are non-specifically incorporated by most cell lines [24, 25]. Though the actual mechanism for internalization is still not fully unraveled, most studies agree that the internalized capsules are finally located in the lysosome. For most *in vitro* applications there is no acute cytotoxicity [26, 27]. Even *in vivo* administration generates only a moderate immune reaction upon subcutaneous and mucosal administration similar to some of natural and synthetic polymer-based particles such as polylactide-co-glycolide (PLGA) [26, 28]. PEM capsules are generally stable in cell medium but there is anyway absorption of proteins due to their charged surface. Nevertheless, it can be minimized by functionalizing the surface with poly(L-lysine)-g-poly(ethylene glycol) [29]. Thus, in the case of *in vitro* applications capsules have sufficient biocompatibility for performing experiments over the time range of weeks. In the present review now three applications of multifunctional capsules with inorganic nanoparticles will be introduced and discussed. These examples will demonstrate how (i) magnetic NPs, (ii) fluorescent NPs, and (iii) plasmonic NPs can be harnessed to add functionality to the PEM capsules and facilitate applications for *in vitro* delivery and sensing.

3. Magnetic NPs for targeted local uptake and release

The idea of exploiting magnetic guidance, which uses an implanted permanent magnet or an externally applied field, to increase the accumulation of drugs at diseased sites dates back to the late 1970s. Objects possessing a magnetic moment experience a force in magnetic field gradients. In this way it is possible to direct and accumulate those objects at a designated target site. This concept has been successfully used for example for *in vivo* targeting of drug-loaded magnetic NPs to tumor tissue [30, 31]. As pointed out NPs can be easily incorporated in the wall of PEM capsules. In this way the existing concept of magnetic targeting could be easily transferred to capsules. As many magnetic NPs can be loaded to each capsule the resulting magnetic moment is rather high. Thus even gradients generated by magnets from a toy store are sufficient to trap capsules at desired positions of cell cultures in a model flow channel system [32]. The magnetic field gradient itself does not stimulate internalization of the capsules, but it accumulates capsules by locally trapping them. As the uptake of capsules by cells depends on their local concentration consequently at the target region cells have a higher number of internalized capsules. This can be used for active delivery of cargo to the target region. One very interesting type of "cargo" is small interference RNA (siRNA). RNA interference (RNAi) has gained increasing attention due to its remarkable potential to regulate gene expression of virtually any identifiable molecular target. In particular, gene silencing can be induced by siRNA [33]. However, this molecule can be degraded *in vivo* by serum or tissue nucleases and due to its small size it suffers as well from a rapid renal clearance [34]. Encapsulation might help to circumvent some of these drawbacks. The concept of magnetic targeting is very universal, and magnetic NPs can be introduced into a large variety of carrier systems, as demonstrated above for PEM capsules. Lipospheres (stabilized with a mixture of cationic lipids) are conceptually similar to capsules and can also be modified with magnetic NPs in their walls and can carry a cargo such as siRNA in their cavity. For example magnetic targeting of lipospheres was demonstrated with HeLa cells which were expressing green fluorescent protein (GFP). Lipospheres with magnetic NPs and siRNA against GFP expression were added in a flow channel system above HeLa eGFP cells in which a little magnet was

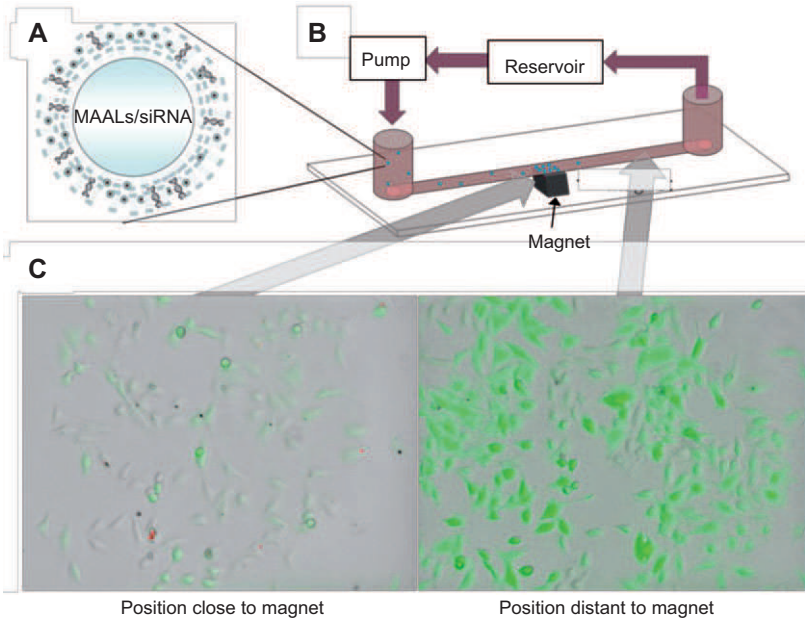

Figure 2 (A) Sketch of a liposphere containing magnetic NPs in their walls and siRNA against GFP expression as cargo. Lipospheres are added to a flow channel above a cell culture of GFP expressing HeLa cells. A magnet is placed in the middle of the flow channel to define the target region for magnetically targeted delivery. (B) Optical microscopy images taken 72 h after addition of lipospheres (overlay of phase contrast and green fluorescence channel). Expression of GFP in cells close to the magnet is quenched due to the delivery of siRNA, whereas cells further away from the magnet are unaffected. Image taken from del Pino et al. [35].

placed at the target region [35], *cf.* Figure 2. As mentioned above, the magnetic field gradient accumulated lipospheres close to the magnet, and due to their enhanced concentration more lipospheres entered cells and thus delivered siRNA. The siRNA interacted with a target mRNA leading to suppression of GFP expression in the cells close to the magnet. SiRNA delivery could be observed by quenching of GFP fluorescence in the cells nearby the magnetic field, *cf.* Figure 2. Similar delivery of active compounds should be possible also with PEM capsules. Recently, the release of a fluorophore from PEM capsules loaded with magnetite upon the action of an alternating magnetic field has been achieved in water [36]. Thus, *in vitro* applications of magnetically triggered release from PEM capsules are expected in the future. At any rate this example demonstrates that addition of magnetic NPs to carrier systems provides them with new properties, in this case with a magnetic moment, which can be used for magnetic targeting and delivery.

Magnetic NPs embedded into PEM capsules could also act as contrast agents for MRI imaging due to their magnetic properties that can be tuned by changing the packing of the NPs within the polymeric shell. They could be useful for *in vivo* imaging or as theranostic agents (therapy and diagnosis) [37]. The use of PEM capsules for *in vivo* applications is still a matter of discussion but there is a general agreement about the importance of the wall composition to avoid toxicity effects. The use of polypeptides homopolymers or polyssacharides as polyelectrolytes and non toxic nanoparticles such as magnetite NPs will, in principal, decrease the potential toxic effects. Moreover, the size of the capsules could limit their applications. Drug delivery and vaccination applications of PEM capsules have been recently discussed by De Geest et al. [8, 38].

4. Fluorescent NPs for barcoding of capsules enabling spatially resolved sensing

Sensing of ions is important for a large variation of cell biological applications. One common detection technique is fluorescence detection of analyte-sensitive fluorophores. Such analyte-sensitive fluorophores are (often organic) fluorescence dyes, of which (in general) the fluorescence emission intensity selectively depends on the presence of a specific type of ion, such as H^+, K^+, Na^+, Ca^{2+}, Cl^-, etc. Presence of ions can either enhance or quench the fluorescence, depending on the chemical nature of the fluorophore. There are many fluorophores available to determine the concentration of different ions such as H^+ [39], K^+ [40], Na^+ [41], and Cl^- ions [42], etc. The response of different fluorophores can (upon simultaneous excitation) only be distinguished if they emit at sufficiently different wavelengths. Although a few fluorophores can be independently detected, the number of fluorophores that can be spectrally distinguished is clearly limited by their spectral width of emission, which ultimately results in emission crosstalk and thus hinders multiplexing (Figure 3).

One suggested possibility of circumventing this problem is based on spatial discrimination instead of spectral resolution [43]. The concept of spatial discrimination of different ion-sensitive fluorophores is straightforward. In case each

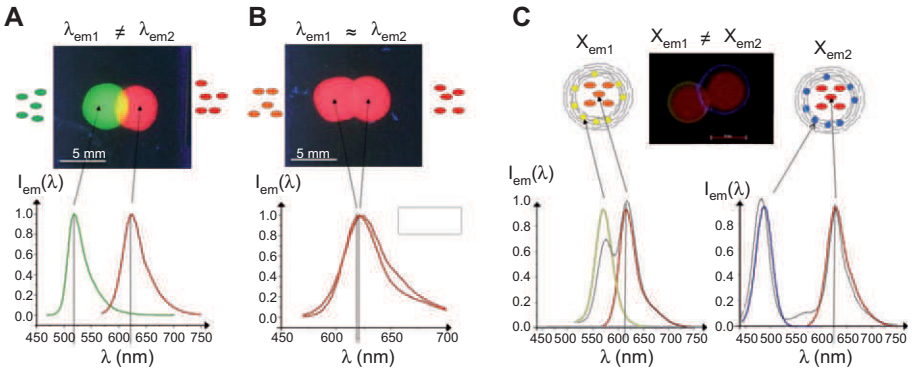

Figure 3 (A) Two fluorophores can be spectrally distinguished in case their wavelengths λ of emission are sufficiently different. (B) In case two fluorophores emit at similar wavelength they cannot be spectrally resolved. (C) In case the fluorophores are located at different positions x they can be resolved, even in case their spectra overlap. Fluorophores can be spatially separated by placing them in containers such as PEM capsules. In order to distinguish between different capsules they can be tagged with a fluorescent barcode on their surface. Data adopted from Abbasi et al. [43].

different ion-sensitive fluorophore can be provided with a unique tag (which might be a fluorophore or inorganic NPs), and in case the average distance between different fluorophores is higher than the optical resolution limit, individual fluorophores can be separately addressed and read-out. PEM capsules are promising systems in this direction due to the porosity of their wall and the possibility of loading different parts of their geometry with fluorophores. The inner cavity can be loaded with the ion-sensitive fluorophores, and the wall of the capsules with a fluorescent barcode. Micrometer sized PEM capsules can be clearly individually resolved, and thus fluorescence of the ion-sensitive fluorophores of each capsule can be individually recorded. The fluorescent barcode within the PEM walls allows for differentiation of the individual capsules and subsequent identification of the different sensor fluorophores.

In order to sense ions they must be able to traverse the capsule walls and reach the ion-sensitive fluorophores in the capsule cavity. As the wall of PEM capsules is porous [44] this is generally no problem. Porosity depends for example on the used polyelectrolyte materials and the number of polyelectrolyte layers [22, 45]. A bigger problem is keeping the ion-sensitive fluorophores inside the capsules. In order to prevent their diffusion through the pores of the PEM walls they can be linked to macromolecules such as dextran. In addition, the number of deposited layers influences the permeability of the PEM walls. Besides the analyte sensitive fluorophore, which emits e.g., in the green an additional reference fluorophore, whose fluorescence does not depend on the ion concentration and which emits in a different spectral field e.g., in the red can be introduced into the same capsule. This allows for radiometric measurements, i.e., ion concentrations are not measured in terms of absolute fluorescence intensities but via analyzing emission intensity ratios of the ion sensitive fluorophores to the reference fluorophores [16]. Taking advantage of their fluorescence stability against photobleaching and their sharp emission band, mixtures of different quantum dots (QDs) can be used as barcode for every type of capsule. QDs in general have been proven as versatile barcodes allowing for many different combinations [46–48]. However, the principle of spatial discrimination between different types of capsules only works if the fluorescent barcodes (for distinguishing the capsules) do not interfere with the fluorescence for the ion-sensitive fluorophores inside the capsule cavity (for determining the ion-concentration). As mentioned above, fluorophores inside the capsule cavity tend to diffuse through the pores of the PEM walls. Though this can be reduced by attachment to macromolecules the fluorophore distribution inside the capsules is not homogeneous and fluorophores tend to stick to the inner wall [16]. Thus they would interfere with the barcode. In order to circumvent this problem double wall capsules [49] can be used, in which the ion-sensitive fluorophores are retained in the inner cavity, and the barcode is situated in the outer PEM wall, *cf.* Figure 4 [50]. In Figure 5 a mixture of three different types of such PEM capsules, loaded with ion-sensitive fluorophores against H^+, Na^+, and K^+ with orange, green, and yellow barcode, respectively, are shown. Due to the barcode the different types of capsules can be clearly distinguished. This also applies for the fluorescence read-out of the distinct fluorophores depending on their respective analyte concentration [43]. Thus the principle of multiplexed ion detection could be demonstrated.

Non-specific response of several ion-sensitive fluorophores (e.g., the fluorophores SBFI and PBFI for the detection of Na^+ and K^+ interfere with pH) imposes a technical complication for determining specific ion concentrations [43]. However, multiplexed detection as demonstrated above can help to circumvent this problem. Let us assume a situation in which concentrations of 3 ions in solution is to be detected using 3 different ion-sensitive fluorophores. Though each fluorophore predominantly will respond only to one type of ion, it still also will slightly respond to changes in concentration of the other ion species. For example fluorophores specific to Na^+ typically also respond slightly to K^+, and *vice versa*. However, as the ion-sensitive fluorophores are confined in different capsules all three types of fluorophores can be read-out in parallel. Thus there are 3 unknowns (ion concentrations), but also 3 read-outs (due to the multiplexed

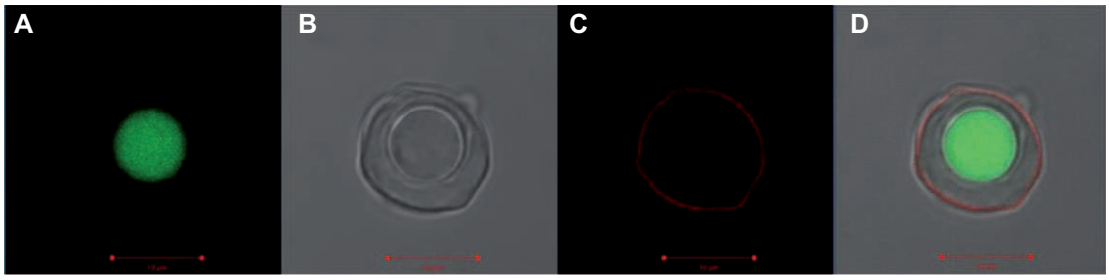

Figure 4 Double wall PEM capsule with a first inner capsule which is filled with a green fluorophore linked to dextran, and an outer wall which is labeled with red fluorescent QDs. (A) green fluorescence, (B) transmission, and (C) red fluorescence channel. (D) overlay of all channels. Scale bars correspond to 10 μm.

detection), which allows for determining all 3 unknowns via a calibration curve [43].

In order to demonstrate potential applications of capsule-based ion-sensing *in vitro* in the following an example based on pH-sensitive capsules, which are loaded with the pH-sensitive fluorophore SNARF in their cavity, is given. SNARF fluoresces in the green-yellow and red at acidic and alkaline pH, respectively. Thus capsules in the slightly alkaline extracellular medium show red fluorescence, whereas capsules which have been incorporated by cells and are located in the acidic lysosome are fluorescent in yellow [25], as can be seen in Figure 6. Internalized capsules reside in the lysosome over time. This automatically involves the fact that intracellular sensing as shown here is actually sensing of the environment of the lysosome, and not of the cytosol. At any rate, addition of certain pharmaceutical agents, such as Monensin, Chloroquine, and Bafilomycin changes the lysosomal pH. By time-resolved recording the fluorescence of the internalized capsules changes in pH upon stimulating cells with pharmaceutical agents can be observed. In particular this allows for recording of kinetics, i.e., to determine how fast the pH in the lysosome changes upon addition and removal of pharmaceutical agents [51].

In the future similar assays may offer a convenient tool for recording changes in the ion composition inside the lysosome, in case cells are fed not only with one type of capsules (as the pH-sensitive ones as shown above), but with several barcoded capsules which are sensitive for different types of ions. Clearly one limitation of this technique is the fact that capsules inside cells are confined to the lysosome and not freely mobile in the cytosol. Pharmaceutical research offers several approaches for transferring molecules from the lysosome to the cytosol, such as the proton sponge effect of polyethyleneimine (PEI) [52], which also might be used for translocation of capsules. We on the other hand want to point out that also in this case inorganic NPs might offer and interesting solution, as will be explained in the next paragraph.

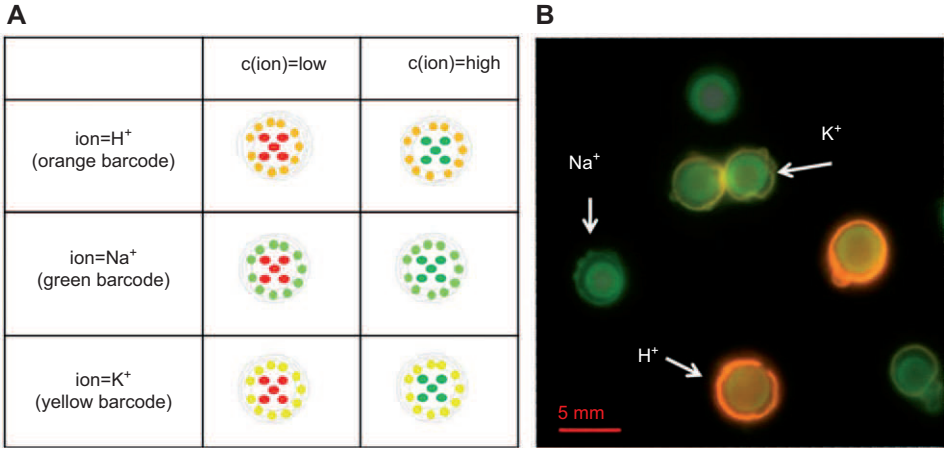

Figure 5 Multiplexed measurements of ions with barcoded PEM capsules. (A) Three different types of capsules have been synthesized. Capsules were co-loaded in their cavities with the dextran-modified ion sensitive fluorophores FITC, SBFI, and PBFI, and with dextran-modified reference fluorophore Dy647 [50]. Thus fluorescence originating from the cavity is sensitive to pH, Na^+, and K^+, respectively. The capsules were labeled with a quantum dot based fluorescent barcode (orange, green, and yellow) on their outermost surface, (B) Fluorescence image of a mixture of the three different types of capsules. Due to the barcodes all types of capsules can be read-out independently, which allows for multiplexed ion detection. The scale bar corresponds to 5 μm. Figure adopted from Abbasi et al. [43].

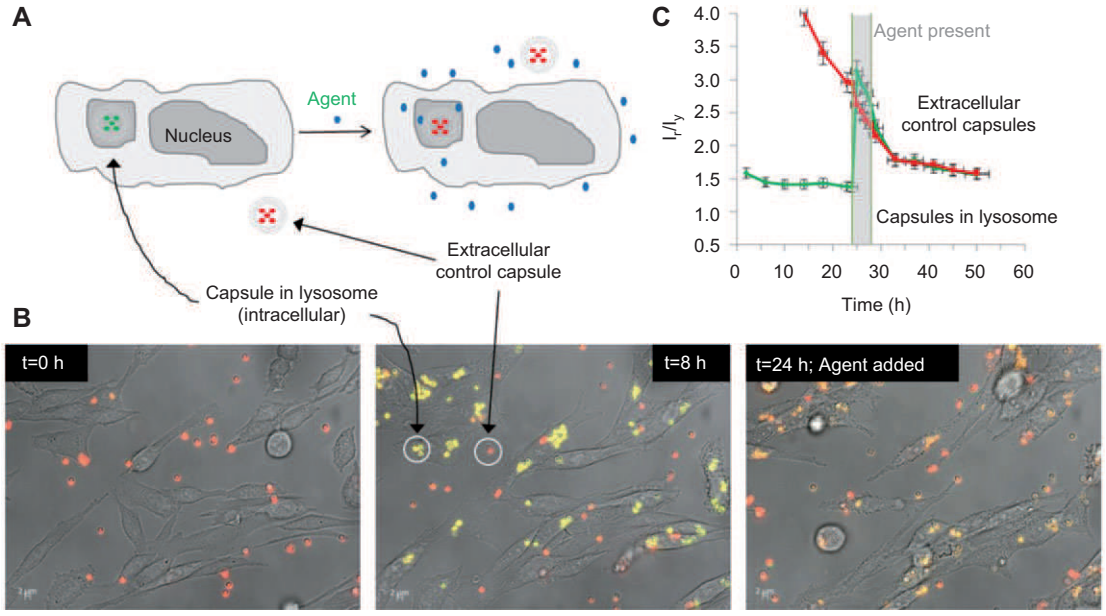

Figure 6 (A) Cells have been incubated with pH-sensitive PEM capsules, which have green-yellow/red fluorescence in acidic/alkaline environment. Some of the capsules are spontaneously incorporated by the cells and are transported to the acidic lysosome and thus are fluorescent in the green-yellow, whereas capsules remaining in the slightly alkaline cell medium fluoresce in red. pH changes in the lysosome upon stimulation of cells with pharmaceutical agents can be traced by monitoring the color of fluorescence of the internalized capsules. (B) Overlay of microscopy images (phase contrast, yellow fluorescence, red fluorescence) before and after addition of an agent (in this case Chloroquine), which increases the pH inside the lysosome. (C) The ratio of red to yellow fluorescence (I_r/I_y) of the capsules depends on the surrounding pH. Reference capsules in the slightly alkaline extracellular medium act as control to compensate for photobleaching. Upon stimulation with a pharmaceutical agent the pH inside the lysosome may change, as can be seen by changes in the I_r/I_y-ratio of internalized capsules. Image adopted from Rivera Gil et al. [51].

5. Plasmonic nanoparticles – light-triggered release

Macromolecules or particles (such as PEM capsules) internalized *via* the endocytic pathway are subsequently routed to lysosomes for enzymatic degradation [53]. Thus, disruption or timely permeabilization of the endosomal membrane is a prerequisite for their cytosolic translocation. Strategies in this direction involve cell penetrating peptides [54], pH-sensitive carriers [55], or the proton sponge effect of PEI [56]. Recently, several groups have also proposed release by local heating. Plasmonic NPs, in particular Au NPs, can be optically excited to a resonance in which a collective motion of free electrons occurs, the so-called surface plasmon [57]. Energy is transferred ultrafast from the electrons to the crystal lattice in the form of phonons and the occurring heat dissipates to the local environment. In other words, plasmonic NPs can efficiently convert light into local heat. This effect has been for example used to locally destroy tissue [58, 59]. Other groups have used this strategy for opening containers, such as PEM capsules [10, 60]. For this purpose Au NPs are integrated in the PEM wall of the capsules. Illumination at the surface plasmon resonance frequency causes heating of the NPs, which in turn locally disintegrates the PEM wall and also perforates the membrane of the surrounding lysosome in which the capsules are located [61–63], resulting in release of the molecules from the capsule cavity to the cytosol. Release to the cytosol is indicated by the fact that the released cargo is homogeneously distributed over the whole body of the cells (excluding the nucleus), and that released pH indicators (*cf.* pH detection with SNARF in the paragraph above) demonstrate transfer from an acidic compartment (lysosome) to a neutral compartment (cytosol) [64]. Before discussing obvious limitations of this technique we first point out its potentials. Light-mediated release of macromolecules from capsules can be seen as an extension of the concept of caged-calcium [65, 66], where Ca^{2+} ions are released from chelators upon a light trigger. Caged compounds have been proven to be a very valuable tool for *in vitro* investigations, where onset of a biological action can be externally triggered by light-mediated release of a specific compound. Typically caged compounds are rather available from small molecules. PEM capsules modified with plasmonic NPs in their walls and macromolecular cargo in their cavity can extend this concept for the light-triggered release (*in vitro*) of macromolecules. Opening of capsules works on the basis of individual capsules. In case both the capsules and the light-pointer have micrometer size, the capsules can be opened one by one (with complete control) and the whole process of irradiation and release can be observed with optical microscopy. If cells are loaded with capsules bearing different macromolecules in their cavities subsequent opening causes controlled mixing of the released macromolecules in the cytosol, *cf.* Figure 7 [64].

Obviously there are also clear limitations for this technology. First, the power of the light-pointer has to be controlled

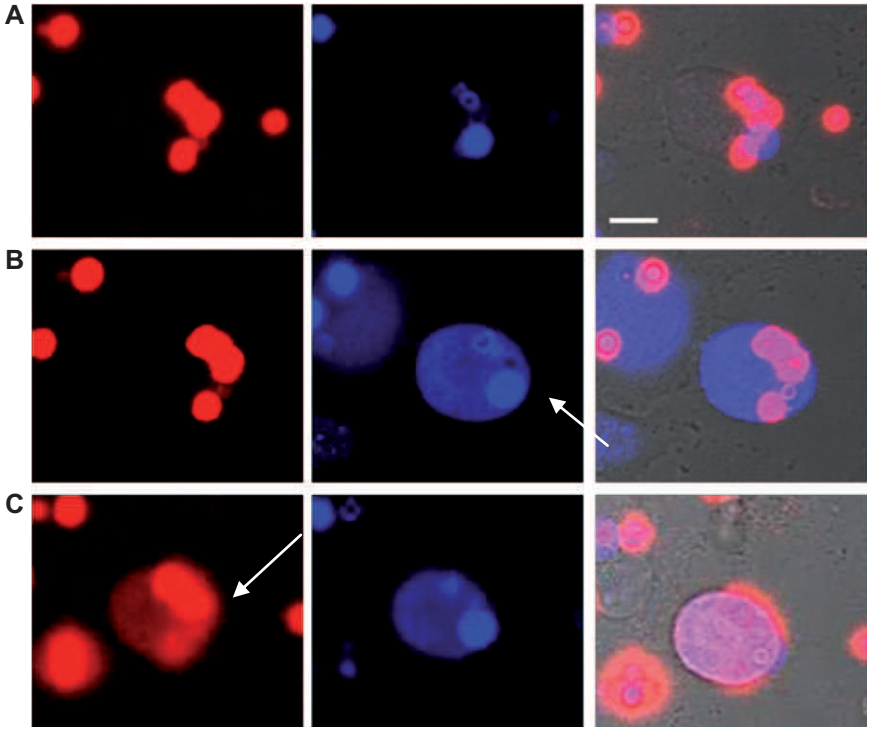

Figure 7 (A) Cells were incubated with a mix of Au NP modified capsules which were loaded either with blue or with a red fluorescence labeled dextran. The shown microscopy images are the red and blue fluorescence channel and an overlay of both with the transmission channel. (B) First the blue capsules inside cells were opened with the light pointer and subsequent release of blue fluorescent dextran to the cytosol can be observed. Red fluorescent dextran is still confined to the capsules. (C) In a second step also the red capsules were opened with the light pointer and thus red fluorescent dextran was released to the cytosol, where it mixed with the blue fluorescent dextran. The scale bars represent 10 μm. Arrows pointed at the irradiated and thus opened capsules. Image adapted from Carregal-Romero et al. [64].

very well. Simply speaking heating is trivial, but controlled heating is more complicated. In case too much power is applied water is evaporated and the resulting gas bubbles destroy cells. Fortunately the complex cellular environment reduces bubble formation [6], but nevertheless overheating remains the main risk. The mode of laser-tissue interactions depends on how the light energy is applied. At low laser energy flow and long exposure, exposure can lead to photochemical or photothermal interactions. Confining the laser into short pulses can cause intense heating followed by water phase change in biological systems, i.e., bubble formation and photoablation and further increase of the laser energy or shorter pulses eventually may lead to plasma-induced ablation and photodisruption [67]. In this context, for capsules modified with plasmonic NPs the simultaneous opening of many capsules via homogeneous illumination is technically challenging due to the shifts of the laser power. Moreover, the cargo molecules in the cavity of the capsule could be damaged upon light-mediated heating. Bioactive molecules should keep their functionally upon laser irradiation. However, localized heating could lead to the destruction of the active part of the molecules to be released. In order to study the possible laser damage of the capsule payload, green fluorescent protein (GFP) has been released into the cytosol [64]. As fluorescence of released GFP could be observed one can conclude that at least part of the released GFP and its function remained intact. The local heating produced after light absorption of the gold NPs in the capsule walls can be thus tuned in a way that it is enough to disrupt the PEM walls of the capsules (and the surrounding lysosomal membrane), but does not damage the whole amount of released protein. Clearly quantitative release as the current state-of-the-art is not possible, due to inhomogeneous loading of the capsules with cargo in their cavity, variations in Au NP concentrations in the PEM walls, and possible partial destruction of the cargo molecules by heat. Thus PEM capsules are best suited for the release of molecules which can make an all-or-nothing response, which does not quantitatively depend on the exact amount of released functional molecules. Kinetics of drug release by light responsive capsules is as well difficult to perform since the increase of fluorescence in the cytosol when cargo molecules are released (if they were not quenched or needed the action of enzymes) is immediate. Only molecules that develop fluorescence with the time once they are located into the cytosol are suitable to perform kinetic studies due to the limitation of the optical microscopes themselves.

6. Outlook

In these perspectives we tried to point out how inorganic NPs can be useful building blocks for modifying

organic/polymeric carrier matrices with additional functionalities. This helps for creating new multifunctional hybrid materials, which have a clear potential as tools for *in vitro* sensing and delivery. On purpose this perspective is limited on *in vitro* applications, as any *in vivo* applications would involve problematic points such as cytotoxicity issues, biodistribution, etc. to a much higher extent. On the other hand, three examples have been given on how these hybrid capsules could serve as interesting tools for cell culture experiments.

Acknowledgements

This work has been supported by BMBF Germany (ERANET grant Nanosyn to WJP). SCR is grateful to the Junta Andalucía for a fellowship.

References

[1] Cheon J, Lee JH. Synergistically integrated nanoparticles as multimodal probes for nanobiotechnology. Acc Chem Res 2008;41:1630–40.
[2] Xia F, Zuo X, Yang R, Xiao Y, Kang D, Vallée-Bélisle A, Gong X, Yuen JD, Hsu BBY, Heeger AJ, Plaxco KW. Colorimetric detection of DNA, small molecules, proteins, and ions using unmodified gold nanoparticles and conjugated polyelectrolytes. Proc Natl Acad Sci USA 2010;107:10837–41.
[3] Thomas CR, Ferris DP, Lee JH, Choi E, Cho MH, Kim ES, Stoddart JF, Shin JS, Cheon J, Zink JI. Noninvasive remote-controlled release of drug molecules in vitro using magnetic actuation of mechanized nanoparticles. J Am Chem Soc 2010;132:10623–5.
[4] Parveen S, Misra R, Sahoo SK. Nanoparticles: a boon to drug delivery, therapeutics, diagnostics and imaging. Nanomedicine 2012;8:147–66.
[5] Gobin AM, Lee MH, Halas NJ, James WD, Drezek RA, West JL, Near-infrared resonant nanoshells for combined optical imaging and photothermal cancer therapy. Nano Letters 2007;7:1929–34.
[6] Hühn D, Govorov A, Rivera Gil P, Parak WJ. Photostimulated Au nanoheaters in polymer and biological media: characterization of mechanical destruction and boiling. Adv Funct Mater 2012;22:294–303.
[7] Skirtach AG, Karageorgiev P, De Geest BG, Pazos-Perez N, Braun D, Sukhorukov GB. Nanorods as wavelength-selective absorption centers in the visible and near-infrared regions of the electromagnetic spectrum. Adv Mater 2008;20:506–10.
[8] De Koker S, Hoogenboom R, De Geest BG. Polymeric multilayer capsules for drug delivery. Chem Soc Rev 2012;41:2867–84.
[9] Shchukin DG, Sukhorukov GB. Nanoparticle synthesis in engineered organic nanoscale reactors. Adv Mater 2004;16:671–82.
[10] Bedard MF, Braun D, Sukhorukov GB, Skirtach AG. Toward self-assembly of nanoparticles on polymeric microshells: near-IR release and permeability. Acs Nano 2008;2:1807–16.
[11] Dubreuil F, Shchukin DG, Sukhorukov GB, Fery A. Polyelectrolyte capsules modified with YF_3 nanoparticles: an AFM study. Macromol Rapid Commun 2004;25:1078–81.
[12] Decher G. Fuzzy nanoassemblies: toward layered polymeric multicomposites. Science 1997;277:1232–7.
[13] Sukhorukov GB, Dähne L, Hartmann J, Donath E, Möhwald H. Controlled precipitation of dyes into hollow polyelectrolyte capsules based on colloids and biocolloids. Adv Mater 2000;12:112–5.
[14] Sukhorukov GB, Rogach AL, Zebli B, Liedl T, Skirtach AG, Köhler K, Antipov AA, Gaponik N, Susha AS, Winterhalter M, Parak WJ. Nanoengineered polymer capsules: tools for detection, controlled delivery and site specific manipulation. Small 2005;1:194–200.
[15] del Mercato LL, Gonzalez E, Abbasi AZ, Parak WJ, Puntes V. Synthesis and evaluation of gold nanoparticle-modified polyelectrolyte capsules under microwave irradiation for remotely controlled release for cargo. J Mater Chem 2011;21:11468–71.
[16] del Mercato LL, Abbasi AZ, Parak WJ. Synthesis and characterization of ratiometric ion-sensitive polyelectrolyte capsules. Small 2011;7:351–63.
[17] Cui J, Wang Y, Postma A, Hao J, Hosta-Rigau L, Caruso F. Monodisperse polymer capsules: tailoring size, shell thickness, and hydrophobic cargo loading via emulsion templating. Adv Funct Mater 2010;20:1625–31.
[18] Tong W, Zhu Y, Wang Z, Gao C. Möhwald H. Micelles-encapsulated microcapsules for sequential loading of hydrophobic and water-soluble drugs. Macromol Rapid Commun 2010;31:1015–19.
[19] Rivera_Gil P, del Mercato LL, del Pino P, Muñoz-Javier A, Parak WJ. Nanoparticle-modified polyelectrolyte capsules. Nano Today 2008;3:12–21.
[20] Bazylinska U, Skrzela R, Szczepanowicz K, Warszynski P, Wilk K. Novel approach to long sustained multilayer nanocapsules: influence of surfactant head groups and polyelectrolyte layer number on the release of hydrophobic compounds. Soft Matter 2011;7:6113–24.
[21] Heidel JD, Davis ME. Clinical developments in nanotechnology for cancer therapy. Pharmaceut Res 2011;28:187–99.
[22] Dong WF, Ferri JK, Adalsteinsson T, Schonhoff M, Sukhorukov GB, Möhwald H. Influence of shell structure on stability, integrity, and mesh size of polyelectrolyte capsules: mechanism and strategy for improved preparation. Chem Mater 2005;17:2603–11.
[23] Biesheuvel PM, Mauser T, Sukhorukov GB, Möhwald H. Micromechanical theory for pH-dependent polyelectrolyte multilayer capsule swelling. Macromolecules 2006;39:8480–86.
[24] Muñoz Javier A, Kreft O, Piera Alberola A, Kirchner C, Zebli B, Susha AS, Horn E, Kempter S, Skirtach AG, Rogach AL, Rädler J, Sukhorukov GB, Benoit M, Parak WJ. Combined atomic force microscopy and optical microscopy measurements as a method to investigate particle uptake by cells. Small 2006;2:394–400.
[25] Muñoz Javier A, Kreft O, Semmling M, Kempter S, Skirtach AG, Bruns OT, del Pino P, Bedard MF, Rädler J, Käs J, Plank C, Sukhorukov GB, Parak WJ. Uptake of colloidal polyelectrolyte coated particles and polyelectrolyte multilayer capsules by living cells. Adv Mater 2008;20:4281–7.
[26] De Koker S, De Geest BG, Cuvelier C, Ferdinande L, Deckers W, Hennink WE, De Smedt SC, Mertens N. In vivo cellular uptake, degradation, and biocompatibility of polyelectrolyte microcapsules. Adv Funct Mater 2007;17:3754–63.
[27] Kirchner C, Muñoz Javier A, Susha AS, Rogach AL, Kreft O, Sukhorukov GB, Parak WJ. Cytotoxicity of nanoparticle-loaded polymer capsules. Talanta 2005;67:486–91.
[28] De Cock LJ, Lenoir J, De Koker S, Vermeersch V, Skirtach AG, Dubruel P, Adriaens E, Vervaet C, Remon JP, De Geest BG. Mucosal irritation potential of polyelectrolyte multilayer capsules. Biomaterials 2011;32:1967–77.
[29] Heuberger R, Sukhorukov GB, Vörös J, Textor M, Möhwald H. Biofunctional polyelectrolyte multilayers and microcapsules:

control of non-specific and bio-specific protein adsorption. Adv Funct Mater 2005;15:357–66.
[30] Widder KJ, Senyei AE, Ranney DF. Magnetically responsive microspheres and other carriers for the biophysical targeting of antitumor agents. Adv Pharmacol Chemother 1979;16:213–71.
[31] Hirsch LR, Stafford RJ, Bankson JA, Sershen SR, Rivera B, Price RE, Hazle JD, Halas NJ, West JL. Nanoshell-mediated near-infrared thermal therapy of tumors under magnetic resonance guidance. Proc Natl Acad USA 2003;100:13549–54.
[32] Zebli B, Susha AS, Sukhorukov GB, Rogach AL, Parak WJ. Magnetic targeting and cellular uptake of polymer microcapsules simultaneously functionalized with magnetic and luminescent nanocrystals. Langmuir 2005;21:4262–5.
[33] Zintchenko A, Philipp A, Dehshahri A, Wagner E. Simple modifications of branched PEI lead to highly efficient siRNA carriers with low toxicity. Bioconjug Chem 2008;19:1448–55.
[34] Buyens K, Meyer M, Wagner E, Demeester J, de Smedt SC, Sanders NN. Monitoring the disassembly of siRNA polyplexes in serum is crucial for predicting their biological efficacy. J Controlled Release 2010;141:38.
[35] del Pino P, Muñoz Javier A, Vlaskou D, Rivera Gil P, Plank C, Parak WJ. Gene silencing mediated by magnetic lipospheres tagged with small interfering RNA. Nano Lett 2010;10:3914–21.
[36] Katagiri K, Nakamura M, Koumoto K. Magneto responsive smart capsules formed with polyelectrolytes, lipid bilayers and magnetic nanoparticles. ACS Appl Mater Interfaces 2010;2:768–73.
[37] Abbasi AZ, Gutiérrez L, del Mercato LL, Herranz F, Chubykalo-Fesenko O, Veintemillas-Verdaguer S, Parak WJ, Morales MP, González JM, Hernando A, de la Presa P. Magnetic capsules for NMR imaging: effect of magnetic nanoparticles spatial distribution and aggregation. J Phys Chem C 2011;115:6257–64.
[38] De Geest BG, Willart MA, Lambrecht BN, Pollard C, Vervaet C, Remon JP, Grooten J, De Koker S. Surface-engineered polyelectrolyte multilayer capsules-synthetic vaccines mimicking microbial structure and function. Angew Chem, Int Ed 2012;51:3862–6.
[39] Buckler KJ, Vaughanjones RD. Application of a new pH-sensitive fluoroprobe (carboxy-SNARF1) for intracellular pH measurement in small, isolated cells. Eur J Physiol 1990;417:234–9.
[40] Kasner SE, Ganz MB. Regulation of intracellular potassium in mesangial cells-a fluorescence analysis using the dye, PBFI. Am J Physiol 1992;262:F462–7.
[41] Nath S, Jezek P, Garlid KD. Reconstitution of the Na^+-Selective Na^+/H^+ antiporter from beef-heart mitochondria – quantitation of Na^+ transport with the novel fluorescent-probe, SBFI. Biophys J 1990;57:A477–A477.
[42] Engblom AC, Akerman KEO. Determination of the intracellular free chloride concentration in rat-brain synaptoneurosomes using a chloride-sensitive fluorescent indicator. Biochim Biophys Acta 1993;1153:262–6.
[43] Abbasi AZ, Amin F, Niebling T, Friede S, Ochs M, Carregal-Romero S, Montenegro JM, Rivera_Gil P, Heimbrodt W, Parak WJ. How colloidal nanoparticles could facilitate multiplexed measurements of different analytes with analyte-sensitive organic fluorophores. ACS Nano 2011;5:21–5.
[44] McShane M, Ritter D. Microcapsules as optical biosensors. J Mater Chem 2010;20:8189–93.
[45] Kolbe A, del Mercato LL, Abbasi AZ, Rivera_Gil P, Gorzini SJ, Huibers WHC, Poolman B, Parak WJ, Herrmann A. De novo design of supercharged, unfolded protein polymers, and their assembly into supramolecular aggregates. Macromol Rapid Commun 2011;32:186–90.
[46] Chan WC, Nie S. Quantum dot bioconjugates for ultrasensitive nonisotopic detection. Science 1998;281:2016–8.
[47] Gao X, Chan WCW, Nie S. Quantum-dot nanocrystals for ultrasensitive biological labeling and multicolor optical encoding. J Biomed Optics 2002;7:532–7.
[48] Fournier-Bidoz S, Jennings TL, Klostranec JM, Fung W, Rhee A, Li D, Chan WCW. Facile and rapid one-step mass preparation of quantum-dot barcodes. Angew Chem Int Ed 2008;47:5577–81.
[49] Kreft O, Prevot M, Möhwald H, Sukhorukov GB. Shell-in-shell microcapsules: a novel tool for integrated, spatially confined enzymatic reactions. Angew Chem Int Ed 2007;46:5605–8.
[50] del Mercato LL, Abbasi AZ, Ochs M, Parak WJ. Multiplexed sensing of ions with barcoded polyelectrolyte capsules. ACS Nano 2011;5:9668–74.
[51] Rivera-Gil P, Nazarenus M, Ashraf S, Parak WJ. pH sensitive capsules as intracellular optical reporters for monitoring lysosomal pH changes upon stimulation. Small 2012;8:943–8.
[52] Rejman J, Tavernier G, Bavarsad N, Demeester J, de Smedt SC. mRNA transfection of cervical carcinoma and mesenchymal stem cells mediated by cationic carriers. J Controlled Release 2010;147:385–91.
[53] Dierendonck M, de Koker S, Vervaet C, Remon JP, de Geest BG. Interaction between polymeric multilayer capsules and immune cells. J Controlled Release doi: 10.1016/j.jconrel.2012.03.001 (2012).
[54] Delehanty JB, Bradburne CE, Boeneman K, Susumu K, Farrell D, Mei BC, Blanco-Canosa JB, Dawson G, Dawson PE, Mattoussi H, Medintz IL. Delivering quantum dot-peptide bioconjugates to the cellular cytosol: escaping from the endolysosomal system. Integrative Biology 2010;2:265–77.
[55] Anandhakumar S, Nagaraja V, Raichur AM. Reversible polyelectrolyte capsules as carriers for protein delivery. Colloids Surf B 2010;78:266–74.
[56] Akinc A, Thomas M, Klibanov AM, Langer R. Exploring polyethylenimine-mediated DNA transfection and the proton sponge hypothesis. J Gene Med 2005;7:657–63.
[57] Salgueirino-Maceira V, Caruso F, Liz-Marzan LM. Coated colloids with tailored optical properties. J Phys Chem B 2003;107:10990–4.
[58] O'Neal DP, Hirsch LR, Halas NJ, Payne JD, West JL. Photothermal tumor ablation in mice using near infrared-absorbing nanoparticles. Cancer Lett 2004;209:171–6.
[59] Huang X, El-Sayed IH, Qian W, El-Sayed MA. Cancer cell imaging and photothermal therapy in the near-infrared region by using gold nanorods. J Am Chem Soc 2006;128:2115–20.
[60] Radt B, Smith TA, Caruso F. Optically addressable nanostructured capsules. Adv Mater 2004;16:2184–9.
[61] Skirtach AG, Muñoz Javier A, Kreft O, Köhler K, Piera Alberola A, Möhwald H, Parak WJ, Sukhorukov GB. Laser-induced release of encapsulated materials inside living cells. Angew Chem Int Ed 2006;45:4612–7.
[62] Muñoz Javier A, del Pino P, Bedard MF, Ho D, Skirtach AG, Sukhorukov GB, Plank C, Parak WJ. Photoactivated release of cargo from the cavity of polyelectrolye capsules to the cytosol of cells. Langmuir 2009;24:12517–20.
[63] Palankar R, Skirtach AG, Kreft O, Bédard M, Garstka M, Gould K, Möhwald H, Sukhorukov GB, Winterhalter M, Springer S.

Controlled intracellular release of peptides from microcapsules enhances antigen presentation on MHC class I molecules. Small 2009;5:2168–76.

[64] Carregal-Romero S, Ochs M, Rivera_Gil P, Ganas C, Pavlov AM, Sukhorukov GB, Parak WJ. NIR-light triggered delivery of macromolecules into the cytosol. J Control Rel 2012;159: 120–7.

[65] Gilroy S, Read ND, Trewavas AJ. Elevation of cytoplasmic calcium by caged calcium or caged inositol trisphosphate initiates stomatal closure. Nature 1990;346:769–71.

[66] Adams SR, Lev-Ram V, Tsien RY. A new caged Ca^{2+}, azid-1, is far more photosensitive than nitrobenzyl-based chelators. Chem Biol 1997;4:867–78.

[67] Qin Z, Bischof JC. Thermophysical and biological responses of gold nanoparticle laser heating. Chem Soc Rev 2011;41: 1191–217.

Received March 21, 2012; accepted May 22, 2012

Multiplexed Sensing of Ions with Barcoded Polyelectrolyte Capsules

Loretta L. del Mercato,[†,‡,⊥] Azhar Z. Abbasi,[†,§,⊥] Markus Ochs,[†] and Wolfgang J. Parak[†,*]

[†]Fachbereich Physik and WZMW, Philipps Universität Marburg, Marburg, Germany [‡]Current address: National Nanotechnology Laboratory, Institute Nanoscience-CNR, Lecce, Italy. [§]Current address: Leslie Dan Faculty of Pharmacy, University of Toronto, Toronto ON, Canada. [⊥]These authors contributed equally to this work.

ABSTRACT

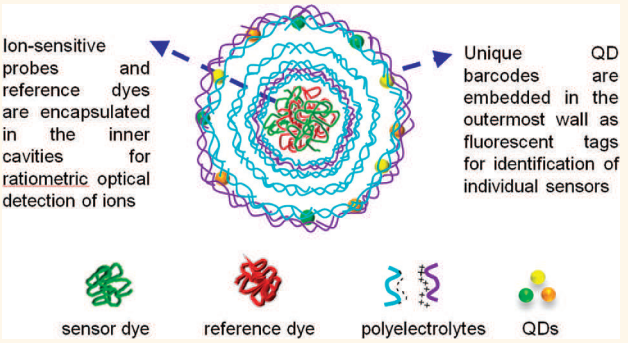

Multiplexed detection of analytes is a challenge for numerous medical and biochemical applications. Many fluorescent particulate devices are being developed as ratiometric optical sensors to measure the concentration of intracellular analytes. The response of these sensors is based on changes of the emission intensity of analyte-sensitive probes, entrapped into the carrier system, which depends on the concentration of a specific analyte. However, there are a series of technical limits that prevent their use for quantitative detection of several analytes in parallel (*e.g.*, emission crosstalk between different sensor molecules). Here we demonstrate that double-wall barcoded sensor capsules can be used for multiplexed analysis of proton, sodium, and potassium ions. The sensor detection methodology is based on porous microcapsules which carry ion-sensitive probes in their inner cavity for ion detection and a unique QD barcode in their outermost wall as tag for identification of individual sensors. The engineering of QD barcodes to capsules walls represents a promising strategy for optical multianalyte determination.

KEYWORDS: polyelectrolyte capsules · quantum dots · barcode · ion sensing · fluorescence

One technical desire in the sensing of ions is the quantitative detection of as many ionic species as possible in parallel. Depending on the applied method (*i.e.*, electrochemical or optical sensing) different problems for such multiplexed detection exist.[1−5] In the case of ion-sensitive fluorophores the major problem is spectral overlap between the emission spectra of the different fluorophores (*i.e.*, emission crosstalk).[6,7] Though a few fluorophores can be well distinguished there is a fundamental problem associated with the finite spectral width of wavelengths of fluorescent light where nearly all fluorescent dyes emit (from blue(violet) to NIR), which ultimately results in emission crosstalk. One suggested possibility of circumventing this problem is basing discrimination on spatial or temporal instead of spectral resolution.[8] The concept of spatial discrimination of different ion-sensitive fluorophores is straightforward. In case each different ion-sensitive fluorophore can be provided with a unique tag (which might be a fluorophore), and in case the average distance between different fluorophores is higher than the optical resolution limit, individual fluorophores can be separately addressed and read-out. Microcapsules built by layer-by-layer assembly are a promising system in this direction.[9,10] Such capsules (which basically have the geometry of a ping pong ball with porous walls) comprise a cavity, which can be loaded with ion-sensitive fluorophores, and a semipermeable wall formed out of several layers of polyelectrolytes, which can be tagged with a label to identify individual capsules.[11] By offering two separate spatial entities (cavity and wall) two different fluorescence sources (ion-sensitive fluorophore, fluorescence tag) can be integrated into one carrier system. Ion sensing with ion-sensitive probes integrated into particulate carrier systems has been demonstrated before.[3,12,13] Such integration of organic ion-sensitive fluorophores into particulate carrier systems offers several advantages. First, as several fluorophores are integrated *per* particle the absolute fluorescence intensity raises. Second, due to the particulate nature, individual particles (even at high concentration) can be identified in case their size is above the optical resolution limit. To assemble microcapsules for multiplexed ion-sensing we intended to make capsules filled with different ion-sensitive fluorophores in their cavities[14] which possess individual fluorescence tags

* Address correspondence to wolfgang.parak@physik.uni-marburg.

Received for review August 15, 2011 and accepted November 4, 2011.

Published online November 04, 2011
10.1021/nn203344w

in their walls as tag for identification. High quantity tagging with fluorescent barcodes has been recently demonstrated with DNA-mediated assembly strategies of fluorophores[5,15] or quantum dots (QDs).[16−19] In our work, we fabricated microcapsules sensitive for H^+, Na^+, and K^+ (embedded with dextran conjugated with the ion-sensitive fluorophores FITC (fluorescein 5(6)-isothiocyanate), SBFI (sodium-binding benzofuran isophthalate), and PBFI (potassium-binding benzofuran isophthalate), respectively) (see Supporting Information, sections I, II). As tag we employed a simple digital QD barcode in the wall of the capsules ("0" or "1") formed by the combination of three different QD colors (emission at 577, 596, and 610 nm), providing the principle capability for encoding seven different types of ion-sensitive microcapsules ("001", "010", "011", "100", "101", "110", "111") (see Supporting Information, section IV). QDs were preferred to conventional organic fluorophores commonly used for fluorescence imaging for several reasons. First, they are characterized by a broad excitation spectrum and a narrow and more sharply defined emission peak.[20] Thus, a single light source can be used to excite multicolor QDs simultaneously without signal overlap.[20,21] Second, the fluorescence decay time for QDs is about 10−40 ns, which is longer than the fluorescence decay time of a few nanoseconds of typical organic fluorophores.[20−22] Third, QDs as prepared in our study, are charged and thus can be easily embedded within the charged shell of double-wall sensor capsules by employing the electrostatic forces that guide the LbL assembly of polyelectrolytes.[11] Lastly, QDs show minimal sensitivity to ions which is a crucial requirement for their use as fluorescent tags of the double-wall sensor capsules presented in this study. For tagging H^+, Na^+, and K^+ sensitive capsules the codes 001, 100, and 010 leading to orange, green, and yellow false-color, respectively, were employed. However, partial diffusion of dextran conjugated to the ion-sensitive fluorophores from the cavity to the wall of the capsules was observed.[14] Such phenomenon turned out to be a major problem when using capsules with QD barcode integrated in the walls. Indeed, the spatial separation of the fluorescence originating from the ion-sensitive fluorophores and the fluorescent QD barcode was hindered by the partial diffusion of labeled dextran to the walls. To circumvent this problem, capsules with two different walls were assembled by using a modified synthesis protocol previously reported by Kreft *et al.* (Scheme 1).[23] Such microcapsules comprise a cavity which can be filled with ion-sensitive fluorophores, which is surrounded by a first wall formed by multiple polyelectrolyte layers. A second polyelectrolyte wall with the integrated QD barcode is formed around the first one, whereby both walls are clearly spaced.[23] In this way ion-sensitive fluorophores in the cavity (and partly in the first wall) and QD barcodes in the second wall are spatially separated (Scheme 1). As a result, capsules sensitive for H^+, Na^+, and K^+ can be identified by their fluorescent barcode in the outer walls and the H^+, Na^+, and K^+ concentrations can be determined by reading out the fluorescence intensity of the respective ion-sensitive fluorophores embedded in the capsule cavities.

RESULTS AND DISCUSSION

In our work we employed the four different fluorophores FITC, SBFI, PBFI, and Dy647 (see Supporting Information, section II). While the blue-green fluorescence of FITC, SBFI, and PBFI is intentionally responsive to the concentration of H^+, Na^+, and K^+ ions in solution, Dy647 was chosen, as its red fluorescence in first order does not depend on the concentration of these ions. Consequently, in the case where FITC, SBFI, and PBFI are mixed with Dy647, ratiometric measurements of H^+, Na^+, and K^+ are possible, in which the ratio of the ion sensitive blue-green fluorescence is related to the constant red fluorescence. The fluorescence emission intensity of the four dyes under different H^+, Na^+, and K^+ ion concentrations is shown in Figure 1A. Data clearly indicate limited selectivity of the fluorophores used in this work. Besides Na^+ and K^+, SBFI and PBFI also respond to H^+ and PBFI also to Na^+, respectively, though with low sensitivity. However, sensitivity of the fluorophores was retained after their conjugation to dextran, as well as after encapsulation of the dye−dextran conjugates (Figure 1B) (see also Supporting Information, section III). As previously reported,[14] in the case of SBFI and PBFI sensor capsules, a charge effect of the amino-dextran on the fluorescence response of the indicators dyes occurs after their conjugation to charged dextran. It has been observed that positively charged amino-dextran affects the sensing properties of SBFI and PBFI by repelling sodium and potassium ions in the local environment. Consequently, the intensity of the fluorescence signal of dye−dextran conjugates is reduced compared to the one of free dyes. Nevertheless, an increase of the fluorescence signal of both the encapsulated SBFI−dextran and PBFI−dextran was detected at high Na^+ and K^+ concentrations (Figure 1B), thus indicating the ability of the capsules to sense low, medium, and high concentrations of these ions in the surrounding bulk solution.

To demonstrate multiplexed measurements, capsules loaded with dextran conjugated to FITC, SBFI, and PBFI (in addition to dextran conjugated to Dy647) in their cavity, and with orange, green, and yellow QD barcodes in their outer walls, respectively, were mixed and added to eight different solutions (Figure 2A) (see also Supporting Information, section V). The solutions were permutations of low/high H^+ ($c(H^+)$ = pH 9/pH 5), low/high Na^+ ($c(Na^+)$ = 5 mM/140 mM), and low/high K^+ ($c(K^+)$ = 5 mM/140 mM). Fluorescence images were obtained by recording the fluorescence signals of the fluorophores loaded into the inner cavities

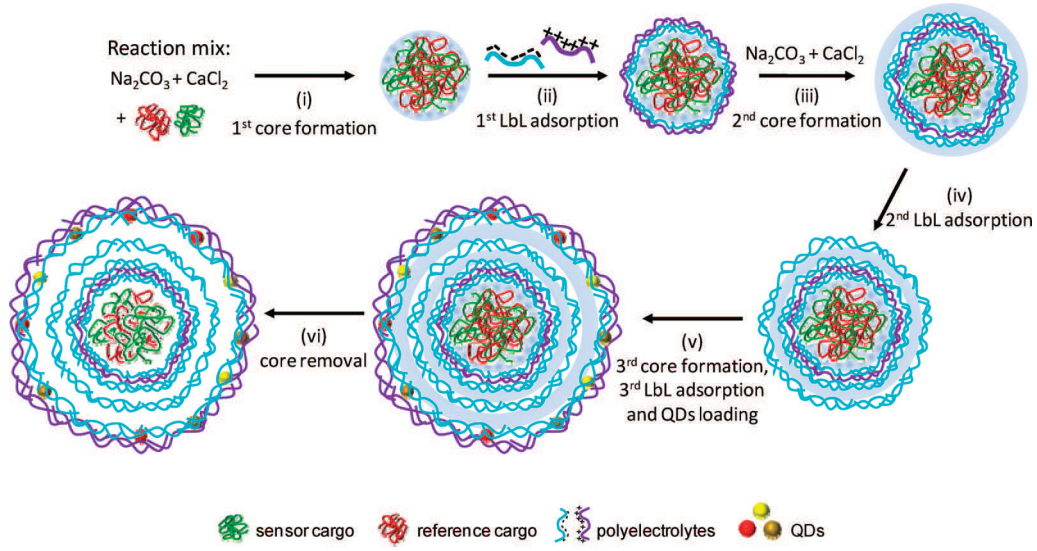

Scheme 1. LbL assembly of a multilayer polyelectrolyte double-wall sensor capsule. (i) $CaCO_3$ microparticles are fabricated by coprecipitation from supersaturated $CaCl_2$ and Na_2CO_3 solutions mixed in the presence of the fluorescent analyte-indicator and the reference fluorophore covalently linked onto individual dextran polymers. (ii) Five bilayers of oppositely charged polyelectrolytes are consecutively adsorbed around the spherical templates by electrostatic attractions. (iii) The resulting core−shell particles are subjected to a second coprecipitation step leading to the formation of a second $CaCO_3$ compartment. (iv) One layer of negatively charged polyelectrolyte is adsorbed around the resulting particles. Step v includes the synthesis of a third $CaCO_3$ compartment accompanied by LbL absorption of five additional bilayers of (PSS/PAH) and one layer of QDs. Finally, a terminal polyelectrolyte PSS/PAH bilayer is added to terminate the LbL coating. The resulting particles are characterized by the following architecture: $CaCO_3$-dextran-fluorophores$(PSS/PAH)_5(CaCO_3/PSS/CaCO_3)(PSS/PAH)_4$(QDs/PSS/PAH). (vi) All $CaCO_3$ compartments are removed by dissolution with EDTA in order to obtain multilayer capsules with double cavities and double shells. In such a configuration, the sensor and reference fluorophores conjugated to dextran molecules are encapsulated within the inner cavity, whereas the QDs tags are embedded in the outermost shell. The two empty cavities serve as spacers which physically and optically separate the fluorescence signals of the sensor and reference fluorophores from the fluorescence signal of the QDs. This region avoids overlay of fluorescence signals and therefore the cross-talk between them.

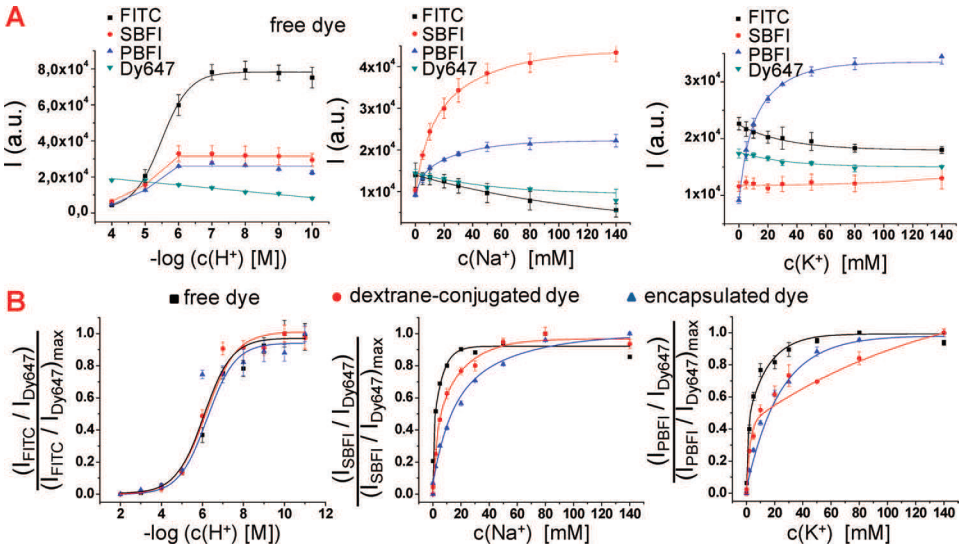

Figure 1. Fluorescence emission intensity of four different analyte sensitive fluorophores under different ion concentrations. (A) The fluorescence intensity (I) of FITC, SBFI, PBFI, and Dy647 dyes is plotted *versus* pH (−log($c(H^+)$), sodium ion concentration ($c(Na^+)$), and potassium ion concentration ($c(K^+)$). (B) The fluorescence response to ions is compared between the free organic dyes, the dyes conjugated to dextran, and dyes conjugates to dextran followed by encapsulation in a polyelectrolyte cavity. For ratiometric detection the ratios of fluorescence read-out of the ion-sensitive fluorophores FITC, SBFI, and PBFI (I_{FITC}, I_{SBFI}, I_{PBFI})) and the nonsensitive reference fluorophore Dy647 (I_{Dy647}) are determined and are normalized to the maximum ratios. These graphs represent the response curves of the ratiometric read-out to the presence of ions.

and the QDs embedded into the outermost shell. To achieve this accomplishment we used three distinct excitation wavelengths ranges for the QDs barcodes, red reference dye, and ion-sensitive dyes. In particular,

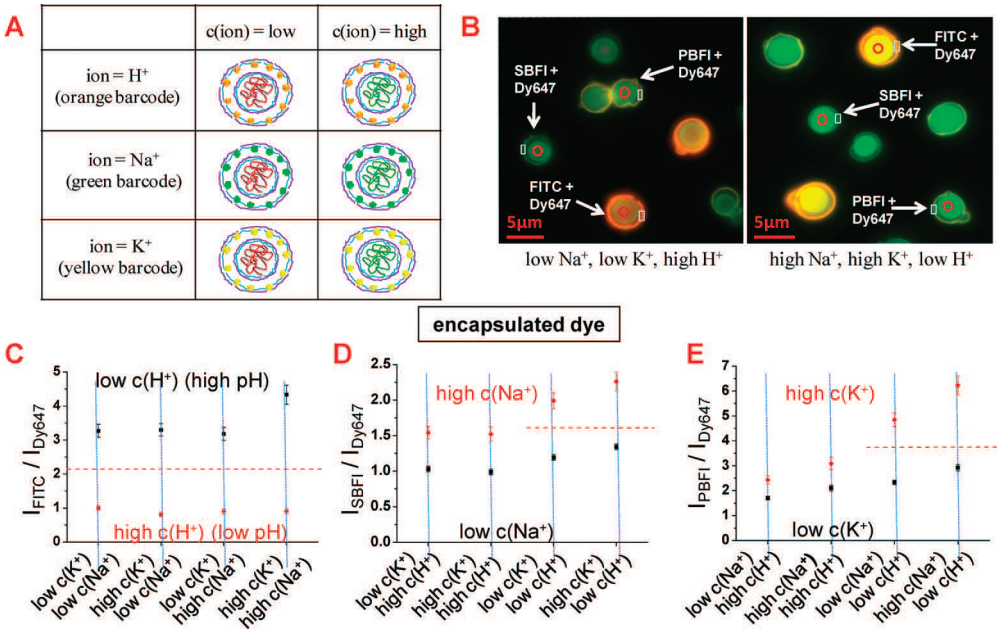

Figure 2. Multiplexed measurements of ions with barcoded polyelectrolyte sensor capsules. (A) Three different types of capsules have been synthesized. Capsules coloaded in their cavities with dextran modified FITC, SBFI, and PBFI and with dextran modified Dy647, which are thus sensitive to pH, Na^+, and K^+, respectively. These capsules were labeled with a quantum dot based orange, green, and yellow fluorescent barcode on their outermost surface, respectively. (B) Fluorescence image of a mixture of the three different types of capsules in two solutions with different ion concentrations; *via* the fluorescent barcode the type of each capsule can be clearly identified. By changing from a low Na^+ ($c(Na^+)$ = 5 mM, $c(K^+)$ = 5 mM, pH = 5) to a high Na^+ condition ($c(Na^+)$ = 140 mM, $c(K^+)$ = 140 mM, pH = 9) the I_{SBFI}/I_{Dy647} ratio of the sodium responsive capsules is raised, and in the false color fluorescence image the capsule cavities appear more blue-green compared to the more reddish appearance at low sodium concentration. (C−E) By variation of the pH from low (5) to high (9), the sodium concentration from low (5 mM) to high (140 mM), and the potassium concentration from low (5 mM) to high (140 mM) eight different combinations of ion concentrations with defined ion mixtures were generated. From left to right: The I_{FITC}/I_{Dy647}, I_{SBFI}/I_{Dy647}, and I_{PBFI}/I_{Dy647} read-outs of the different capsules in these buffers were determined and are plotted here (data points represent mean values as determined from 30 capsules and standard deviations). The I_{FITC}/I_{Dy647} read-out of the pH-sensitive capsules clearly allows for distinguishing between low and high pH in all solutions, regardless the Na^+ and K^+ concentration. The red dotted line shows the threshold for the I_{FITC}/I_{Dy647} read-out distinguishing between low and high pH. The I_{SBFI}/I_{Dy647} and I_{PBFI}/I_{Dy647} read-outs of Na^+ and K^+ sensitive capsules allowed for distinguishing between low and high Na^+ and K^+ concentrations at high pH, and a threshold (red dotted line) can be given. At low pH SBFI as well as PBFI interfere with pH.

the ion-sensitive dyes were excited by using a excitation filter starting from 314 up to 366 nm, the yellow ($\lambda_{max,em}$ = 577 nm), orange ($\lambda_{max,em}$ = 595 nm) and red ($\lambda_{max,em}$ = 615 nm) QDs were excited by using a single excitation filter starting from 485 up to 545 nm, and the red reference dye was excited by using a excitation filter starting from 620 up to 690 nm. A detailed description of the filter sets used for fluorescence imaging is provided in the Supporting Information (see section III.2). As can be seen from Figure 2B, the three different types of capsules can be clearly distinguished by their QD barcode in the outer wall (Figure 2B shows the overlay of all five channels). FITC-sensors are tagged with red barcode (001, shown in orange false colors), SBFI-sensors with green barcode (100, shown in green false colors) and PBFI-sensors with yellow barcode (010, shown in yellow false colors). Capsules are marked with small rectangular regions of interest (ROIs) in the QDs labeled walls and with spherical ROIs in the inner cavities. The calculated mean intensity values are yielded by the program for both kinds of ROIs and are entered into a calculation table (a detailed description of the ratiometric analysis is provided in the Supporting Information, section IV). Since the capsules with orange, green, and yellow barcodes are filled with FITC, SBFI, and PBFI, plus Dy647, the blue-green to red ratio of the fluorescence originating from the capsules cavity is a measure for the surrounding H^+, Na^+, and K^+ concentration, respectively. Figure 2 panels B and C indicate that FITC filled capsules allow for clearly distinguishing with high precision between low and high H^+ concentrations (pH = 5, pH = 9), regardless of the Na^+ and K^+ concentration. In the case of SBFI and PBFI filled capsules there is crosstalk with pH. In the case of high pH (pH = 9) SBFI and PBFI loaded capsules can distinguish between low and high Na^+ and K^+ concentration (5 mM/140 mM), despite the respective K^+ and Na^+ concentration (Figure 2D,E). In other words, errors due to crosstalk between Na^+ and K^+ are significantly lower than the signal to be detected, which allows for discrimination of Na^+ and K^+ in parallel. This clearly demonstrated the possibility of multiplexed measurements. At high pH H^+, Na^+, and K^+ can be detected in parallel. In case the FITC read-out

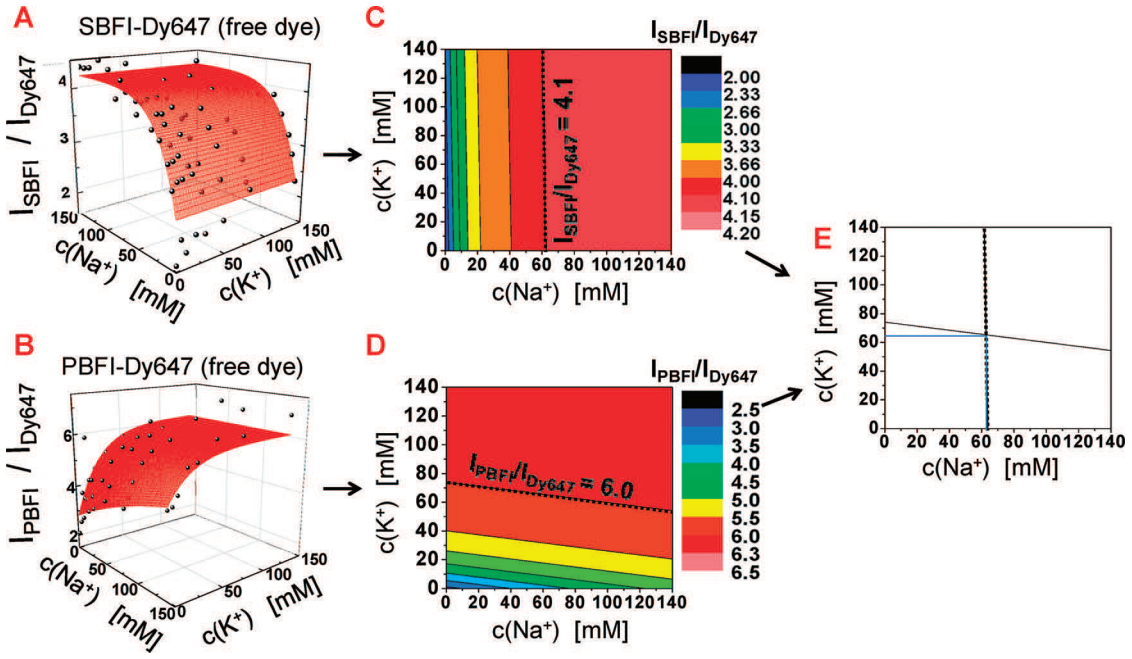

Figure 3. Cross-talk between sodium and potassium sensitive fluorophores in solutions with different ion concentrations. (A, B) Solutions with different sodium and potassium concentrations ($c(Na^+)$, $c(K^+)$) were prepared, and each one was split in two fractions. To one fraction a combination of SBFI and Dy647, to the other a combination of PBFI and Dy647 was given, always in the form of free dye molecules. The intensity of fluorescence of each dye was determined. (A) For the first fraction of each sample the ratio of SBFI to Dy647 emission (I_{SBFI}/I_{Dy647}) was determined; (B) for the second fraction the ratio of PBFI to Dy647 emission (I_{PBFI}/I_{Dy647}) was determined and plotted *versus* the Na^+ and K^+ concentration in a 3-dimensional representation. (C,D) A contour plot of the same data is represented, in which one looks toward the plane spanned by the $c(Na^+)$ and $c(K^+)$ axes and in which the intensity information (I_{SBFI}/I_{Dy647} and I_{PBFI}/I_{Dy647}) is color coded. Lines and areas of equal color here correspond to concentration combinations of $c(Na^+)$ and $c(K^+)$ which have the same fluorescence read-out. If SBFI and PBFI emission corresponded only to changes in sodium and potassium concentration the lines of equal color in the I_{SBFI} and I_{PBFI} plots should be perpendicular to the $c(Na^+)$ axis and to the $c(K^+)$ axis, respectively. However, as the lines are slightly declined the SBFI and PBFI dye emission also responds to K^+ and Na^+ concentration, respectively. A situation is indicated in which the read-out of I_{SBFI}/I_{Dy647} was 4.1 and the read-out of I_{PBFI}/I_{Dy647} was 6.0. This represents two read-outs (I_{SBFI}/I_{Dy647} and I_{PBFI}/I_{Dy647}) and two unknowns ($c(Na^+)$, $c(K^+)$). (E) By combining both read-outs in one graph the cross-section of the lines of equal I_{SBFI}/I_{Dy647} and equal I_{PBFI}/I_{Dy647} ratios lead to the concentration of sodium and potassium of the solution in which these read-outs have been determined.

indicates high pH the read-outs of SBFI and PFBI can be correlated to the Na^+ and K^+ concentration. In the case of low pH (pH = 5) the read-out of SBFI and PBFI is corrupted by H^+ (Figure 2D,E), which however is rather a problem of the used fluorophores and not an intrinsic problem of our detection scheme.

The proposed capsule sensor system should even help to reduce consequence of the cross-talk between different analyte sensitive fluorophores. Fluorescence of SBFI and PBFI primarily depends on Na^+ and K^+, though there is crosstalk to K^+ and Na^+, respectively.[24] In Figure 3 panels A and B, the response of both dyes in solutions with different Na^+ and K^+ concentrations is plotted. With the plain fluorophores one solution can either contain SBFI, or PBFI as ion-sensitive indicator, due to the high spectral overlap of both fluorophores. This is demonstrated in Figure 3 panels C and D. The blue-green to red ratio of the SBFI read-out provides one value, which however does not only depend on Na^+-concentration but also on K^+-concentration. In this way this value does not correspond to one point of concentration, $c(Na^+)$, $c(K^+)$, but to a line. Small changes in the Na^+ concentration can have for example the same effect as big changes in the K^+ concentration. If in case of SBFI the read-out corresponded only to Na^+, the line of equal SBFI read-out should be parallel to the $c(K^+)$ axis (Figure 3C). The same is true for PBFI, which however is stronger influenced by crosstalk with Na^+ then SBFI is influenced by crosstalk with K^+ (Figure 3D). At any rate, read-out of only one fluorophore does not lead to unequivocally determined Na^+ or K^+ concentrations. However, by taking advantage of the geometry of the proposed capsule-based sensor system, both of SBFI and PBFI containing capsules can be placed in the same solution (as they can be spatially distinguished by their barcodes) for parallel detection of Na^+ or K^+ ions. Indeed, one can obtain two read-outs (SBFI and PBFI sensitive capsules) for two unknowns (Na^+, K^+ concentration). From each readout one obtains one line in the $c(Na^+)$–$c(K^+)$ plane, which corresponds to regions which fit to the determined blue-green-to-red ratio. However, as there are two lines their crossing point can be determined, which corresponds to one Na^+ and one K^+ concentration (Figure 3E) (see also Supporting Information, section VI). In this way, a

combination of several read-outs of cross talking fluorophores still allows for the determination of individual ion concentrations. It is important to point out that the key advantage of the capsule-based system is that it allows for reading out several analyte-sensitive fluorophores in parallel in the same solution. Clearly the performance of this system could be further improved in the future by using optimized analyte-sensitive fluorophores.

CONCLUSIONS

The results show the possibility of measuring the concentration of several ions in parallel, indicating the feasibility of the proposed sensors and the potential for their successful use in cells. Though fluorescence based sensing with particle based carriers has been described in the past,[3,12] we believe that the introduction of a QD barcode to capsules with two walls adds an important feature which allows for multiplexed measurements and thus for detecting several ions in parallel. Intracellular sensing in the lysosome for H^+ has been demonstrated with capsules.[13] Delivery of different types of capsules to the cytosol of cells and their multiplexed detection remains a challenge for the future.

EXPERIMENTAL SECTION

Fabrication of Double-Wall Barcoded Polyelectrolyte Capsules. Calcium carbonate ($CaCO_3$) porous microparticles with size distribution around 3.5−4 μm were obtained by mixing aqueous solutions of calcium chloride ($CaCl_2$) (0.33 M) and sodium carbonate (Na_2CO_3) (0.33 M) in the presence of the fluorescent analyte-indicator (~50 μM) and the reference fluorophore (~50 μM) previously linked onto individual dextran polymers. Five bilayers of oppositely charged polystyrene sulfonate (PSS) and polyallylamine hydrochloride (PAH) polyelectrolytes were then consecutively adsorbed around the spherical templates by electrostatic attractions. The resulting core−shell particles were subjected to a second coprecipitation step. Then, one layer of PSS was adsorbed around the particle and a third coprecipitation step was performed before starting the third LbL assembly of four bilayers of (PSS/PAH). Subsequently, the coated particles were incubated in solutions of yellow ($\lambda_{max,em}$ = 577 nm), orange ($\lambda_{max,em}$ = 595 nm), and red ($\lambda_{max,em}$ = 615 nm) CdSe/ZnS quantum dots (QDs) with different concentrations. All QDs were coated with a amphiphilic polymer consisting of a polymer backbone [poly(isobutylene-alt-maleic anhydride)] to which alkylamine chains were linked *via* direct amidation between maleic anhydride and amino-ligands.[25] Finally, a terminal polyelectrolyte bilayer of (PSS/PAH) was added to complete the shell formation. The final structure of the double-wall sensor capsules was $(PSS/PAH)_5(CaCO_3/PSS/CaCO_3)(PSS/PAH)_4$(QDs/PSS/PAH). Finally, all $CaCO_3$ compartments were removed by dissolution with EDTA in order to obtain multilayer capsules with double cavities and double walls containing the fluorescent indicator and reference fluorophore within the inner cavity and QD barcode in the outermost wall. A detailed description of the synthesis is provided in the Supporting Information (see section I).

QD Barcodes for Proton, Sodium, and Potassium Sensor Capsules. The outermost wall of sensitive capsules for H^+, Na^+, and K^+-ions was tagged with three different QD barcodes: 001, 100, and 010, leading to orange, green, and yellow false-colors, respectively. In particular, H^+-sensitive capsules were tagged with code 001 obtained by mixing equal volumes of 0.01 μM yellow ($\lambda_{max,em}$ = 577 nm), 0.01 μM orange ($\lambda_{max,em}$ = 595 nm), and 0.1 μM red ($\lambda_{max,em}$ = 615 nm) QDs. Na^+-sensitive capsules were tagged with code 100 obtained by mixing equal volumes of 0.1 μM yellow, 0.01 μM orange, and 0.01 μM red QDs. K^+-sensitive capsules were tagged with code 010 obtained by mixing equal volumes of 0.01 μM yellow, 0.1 μM orange and 0.01 μM red QDs. The detailed description of the sample preparation and labeling methods are provided in the Supporting Information (see section IV).

Multiplexed Measurements of Proton, Sodium, and Potassium Sensor Capsules. The fluorescence behavior of double-wall sensor capsules sensitive for H^+, Na^+ and K^+-ions was investigated by mixing the three types of sensor capsules altogether in buffer solutions containing different ions in low or high concentration. The samples were analyzed *via* fluorescence microscopy after 5 min of equilibration time of the capsules in the aqueous ion solutions. In total, five channels were scanned independently to register all fluorescence signals: two channels for detecting the sensor and reference fluorophores loaded into the inner cavities and three channels for detecting the three QDs embedded into the outermost shell. The obtained fluorescent images were processed using the ImageJ v1.42 m software (http://rsb.info.nih.gov/ij/) in order to perform ratiometric analysis. Capsules were marked with ROIs of the same size and shape in the outer shell and in the inner cavity to read-out the fluorescence tag in the outermost shell as well as the fluorescence changes of the cavity. The program calculates for every marked capsule the barcode tag and thereby the type of capsule. Furthermore it shows the type of ion for which the fluorescence of the corresponding sphere is sensitive. Using the data from the cavities, the program calculates the average concentration (low or medium) of the corresponding ions in solution. The detailed description of sample preparation, fluorescence imaging, and data analysis are given in the Supporting Information (see sections III, IV, and V).

Acknowledgment. This work was supported by in part by BMBF/ERANET Nanosyn and EU Nandiatream (grants to W.J.P.). AZA is thankful to HEC (Pakistan)/DAAD for the fellowship.

Supporting Information Available: Description of capsule synthesis procedure and characterization *via* electron microscopy (SEM and TEM); description of the optical properties of ion-sensitive fluorophores and fluorescence measurements of their crosstalk; studies of the effect of encapsulation on the fluorophore signals *via* fluorescence spectrometer and fluorescence microscopy measurements; description of the barcode labeling approach; description of the multiplexed measurements and parallel determination of ions *via* fluorescence microscopy analysis. This material is available free of charge *via* the Internet at http://pubs.acs.org.

REFERENCES AND NOTES

1. Goodey, A.; Lavigne, J. J.; Savoy, S. M.; Rodriguez, M. D.; Curey, T.; Tsao, A.; Simmons, G.; Wright, J.; Yoo, S.-J.; Sohn, Y.; *et al.* Development of Multianalyte Sensor Arrays Composed of Chemically Derivatized Polymeric Microspheres Localized in Micromachined Cavities. *J. Am. Chem. Soc.* **2001**, *123*, 2559–2570.
2. Bakker, E.; Bhakthavatsalam, V.; Gemene, K. L. Beyond Potentiometry: Robust Electrochemical Ion Sensor Concepts in View of Remote Chemical Sensing. *Talanta* **2008**, *75*, 629–635.
3. Lee, Y. E. K.; Smith, R.; Kopelman, R. Nanoparticle Pebble Sensors in Live Cells and *in Vivo*. *Annu. Rev. Anal. Chem.* **2009**, *2*, 57–76.
4. Medintz, I. L.; Uyeda, H. T.; Goldman, E. R.; Mattoussi, H. Quantum Dot Bioconjugates for Imaging, Labelling and Sensing. *Nat. Mater.* **2005**, *4*, 435–446.

5. Li, Y. G.; Cu, Y. T. H.; Luo, D. Multiplexed Detection of Pathogen DNA with DNA-Based Fluorescence Nanobarcodes. *Nat. Biotechnol.* **2005**, *23*, 885–889.
6. Ruedas-Rama, M. J.; Wang, X.; Hall, E. A. A Multi-ion Particle Sensor. *Chem. Commun. (Cambridge)* **2007**, 1544–1546.
7. Choi, Y.; Park, Y.; Kang, T.; Lee, L. P. Selective and Sensitive Detection of Metal Ions by Plasmonic Resonance Energy Transfer-based Nanospectroscopy. *Nat. Nanotechnol.* **2009**, *4*, 742–746.
8. Abbasi, A. Z.; Amin, F.; Niebling, T.; Friede, S.; Ochs, M.; Romero, S. C.; Martos, J. M. M.; Rivera Gil, P.; Heimbrodt, W.; Parak, W. J. How Colloidal Nanoparticles Could Facilitate Multiplexed Measurements of Different Analytes with Analyte-Sensitive Organic Fluorophores. *ACS Nano* **2011**, *5*, 21–25.
9. Decher, G. Fuzzy Nanoassemblies: Toward Layered Polymeric Multicomposites. *Science* **1997**, *277*, 1232–1237.
10. Donath, E.; Sukhorukov, G. B.; Caruso, F.; Davis, S. A.; Möhwald, H. Novel Hollow Polymer Shells by Colloid-Templated Assembly of Polyelectrolytes. *Angew.Chem., Int. Ed.* **1998**, *37*, 2202–2205.
11. Rivera Gil, P.; del Mercato, L. L.; del Pino, P.; Muñoz Javier, A.; Parak, W. J. Nanoparticle-Modified Polyelectrolyte Capsules. *Nano Today* **2008**, *3*, 12–21.
12. Buck, S. M.; Koo, Y. L.; Park, E.; Xu, H.; Philbert, M. A.; Brausel, M. A.; Kopelman, R. Optochemical Nanosensor Pebbles: Photonic Explorers for Bioanalysis with Biologically Localized Embedding. *Curr. Opin. Chem. Biol.* **2004**, *8*, 540–546.
13. Kreft, O.; Muñoz Javier, A.; Sukhorukov, G. B.; Parak, W. J. Polymer Microcapsules as Mobile Local pH-Sensors. *J. Mater. Chem.* **2007**, *17*, 4471–4476.
14. del Mercato, L. L.; Abbasi, A. Z.; Parak, W. J. Synthesis and Characterization of Ratiometric Ion-Sensitive Polyelectrolyte Capsules. *Small* **2011**, *7*, 351–363.
15. Um, S. H.; Lee, J. B.; Kwon, S. Y.; Li, Y.; Luo, D. Dendrimer-like DNA-Based Fluorescence Nanobarcodes. *Nat. Protoc.* **2006**, *1*, 995–1000.
16. Han, M.; Gao, X.; Su, J. Z.; Nie, S. Quantum-Dot-Tagged Microbeads for Multiplexed Optical Coding of Biomolecules. *Nat. Biotechnol.* **2001**, *19*, 631–635.
17. Sheng, W.; Kim, S.; Lee, J.; Kim, S. W.; Jensen, K.; Bawendi, M. G. *In-Situ* Encapsulation of Quantum Dots into Polymer Microspheres. *Langmuir* **2006**, *22*, 3782–3790.
18. Lee, J. A.; Mardyani, S.; Hung, A.; Rhee, A.; Klostranec, J.; Mu, Y.; Li, D.; Chan, W. C. W. Toward the Accurate Read-out of Quantum Dot Barcodes: Design of Deconvolution Algorithms and Assessment of Fluorescence Signals in Buffer. *Adv. Mater.* **2007**, *19*, 3113–3118.
19. Fournier-Bidoz, S.; Jennings, Travis L.; Klostranec, Jesse M.; Fung, W.; Rhee, A.; Li, D.; Chan, Warren C. W. Facile and Rapid One-Step Mass Preparation of Quantum-Dot Barcodes. *Angew. Chem., Int. Ed.* **2008**, *47*, 5577–5581.
20. Alivisatos, A.; Gu, W.; Larabell, C. Quantum Dots as Cellular Probes. *Annu. Rev. Biomed. Eng.* **2005**, *7*, 55–76.
21. Chan, W. C. W.; Maxwell, D. J.; Gao, X.; Bailey, R. E.; Han, M.; Nie, S. Luminescent Quantum Dots for Multiplexed Biological Detection and Imaging. *Curr. Opin. Biotechnol.* **2002**, *13*, 40–46.
22. Michalet, X.; Pinaud, F. F.; Bentolila, L. A.; Tsay, J. M.; Doose, S.; Li, J. J.; Sundaresan, G.; Wu, A. M.; Gambhir, S. S.; Weiss, S. Quantum Dots for Live Cells, *in Vivo* Imaging, and Diagnostics. *Science* **2005**, *307*, 538–544.
23. Kreft, O.; Prevot, M.; Mohwald, H.; Sukhorukov, G. B. Shell-in-Shell Microcapsules: A Novel Tool for Integrated, Spatially Confined Enzymatic Reactions. *Angew. Chem., Int. Ed.* **2007**, *46*, 5605–5608.
24. Meuwis, K.; Boens, N.; De Schryver, F. C.; Gallay, J.; Vincent, M. Photophysics of the Fluorescent K^+ Indicator PBFI. *Biophys. J.* **1995**, *68*, 2469–2473.
25. Lin, C.-A. J.; Sperling, R. A.; Li, J. K.; Yang, T.-Y.; Li, P.-Y.; Zanella, M.; Chang, W. H.; Parak, W. J. Design of an Amphiphilic Polymer for Nanoparticle Coating and Functionalization. *Small* **2008**, *4*, 334–341.

PERSPECTIVE

How Colloidal Nanoparticles Could Facilitate Multiplexed Measurements of Different Analytes with Analyte-Sensitive Organic Fluorophores

Azhar Zahoor Abbasi, Faheem Amin, Tobias Niebling, Sebastian Friede, Markus Ochs, Susana Carregal-Romero, Jose-Maria Montenegro, Pilar Rivera Gil, Wolfram Heimbrodt, and Wolfgang J. Parak*

Fachbereich Physik and WZMW, Philipps Universität Marburg, Renthof 7, 35037 Marburg, Germany

ABSTRACT Multiplexed measurements of several analytes in parallel using analyte-sensitive organic fluorophores can be hampered by spectral overlap of the different fluorophores. The authors discuss how nanoparticles can help to overcome this problem. First, different organic fluorophores can be separated spatially by confining them to separate containers, each bearing a nanoparticle-based barcode. Second, by coupling different fluorophores to nanoparticles with different fluorescence lifetimes that serve as donors for excitation transfer, the effective fluorescence lifetime of the organic fluorophores as acceptors can be tuned by fluorescence resonance energy transfer (FRET). Thus, the fluorophores can be distinguished by their effective lifetimes. This is an example of how the modification of classical functional materials has already yielded improved and even new functionalities by the integration of nanoparticles with hybrid materials. We outline future opportunities in this area.

Sensing of analytes is important for a large variation of applications. One common detection technique is fluorescence detection of analyte-sensitive fluorophores. Such analyte-sensitive fluorophores are (often organic) fluorescence dyes, of which (in general) the fluorescence emission intensity selectively depends on the presence of a specific analyte. The presence of an analyte can either enhance or quench the fluorescence, depending on the chemical nature of the fluorescence dye. Such fluorophores are available for many different analytes, such as H^+,[1] K^+,[2,3] Na^+,[4,5] and Cl^- ions,[6,7] *etc*. Naturally, one would like to use several of these fluorophores in parallel in order to determine simultaneously the concentration of different analytes.[8] Leaving aside the fact that the selectivity of many fluorophores to the target ligand is sometimes not as high as required, there is one fundamental problem for such multiplexed detection. The response of different fluorophores can (at simultaneous excitation) only be distinguished in the case where they emit at different wavelengths (λ). Although a few fluorophores can be independently detected, the number of fluorophores that can be spectrally distinguished in the optical regime is clearly limited and thus hinders multiplexing (Figure 1).

RESOLVING FLUOROPHORE EMISSIONS WITH HYBRID MATERIALS

Nanotechnology, which enables the design and assembly of new materials,[9] offers an exciting toolkit for this purpose. In the case of sensing, we argue that colloidal nanoparticles, as an integral building block of nanotechnology, have the potential to improve existing materials—classic analyte-sensitive fluorophores—leading to new advanced hybrid material. Hereby the functional part, the emission intensity, which depends on the concentration of a specific analyte, would be provided by traditional analyte-sensitive fluorophores. Organic macromolecules/biological molecules would form the glue with which to assemble colloidal nanoparticles as recognition/transducer elements with analyte-sensitive fluorophores.

For such an improved hybrid material, different resolution mechanisms (besides spectral resolution) could be employed. In fact, emission of different fluorophores cannot only be distinguished spectrally (*i.e.*, in dependence of the wavelength λ_{em}) but also spatially (*i.e.*, in dependence of the location x_{em}). The emission of two fluorophores can be distinguished, even if the emission spectra completely overlap. This could be achieved when the two fluorophores are not at the same position, that is, the distance is bigger than the optical resolution limit. However, in order to distinguish between different fluorophores, each of them would have to be provided with a recognition element. Fluorescent nanoparticles in the form of colloidal quantum dots have been demonstrated to form suitable fluorescent barcodes as recognition elements.[10−12] To combine quantum-dot-based barcodes and analyte-sensitive fluorophores, the fluorophores could be integrated in a carrier matrix[13−18] with the quantum-dot barcode on the surface of the carrier.[19] Polyelectrolyte capsules[20] have proven to be a versatile system for this

*Address correspondence to wolfgang.parak@physik.uni-marburg.de.

Published online January 25, 2011.
10.1021/nn1034026

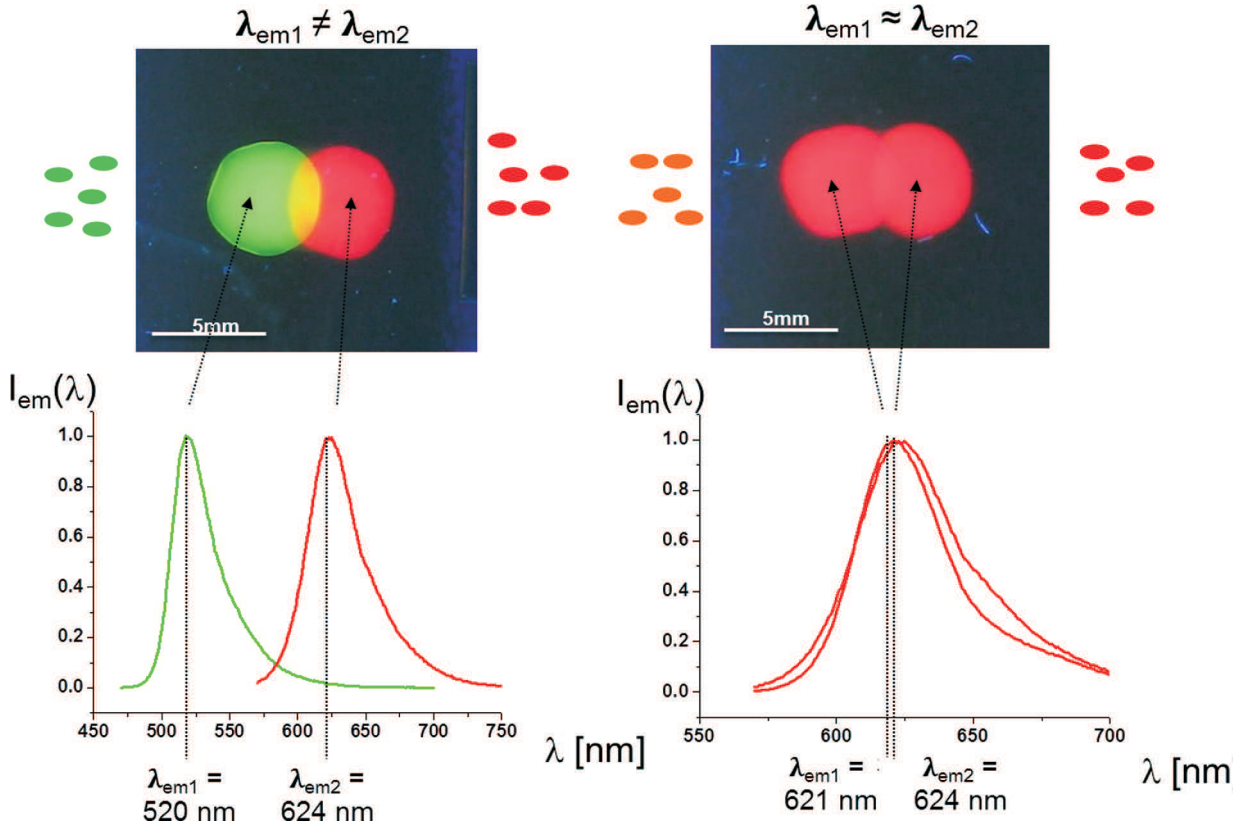

Figure 1. Spectral separation of two different fluorophores. (Left side) Two drops of water mixed with either fluorescein isothiocyanate (FITC) or cresyl violet perchlorate (CV) have been put on two glass coverslips placed on top of each other. The glass coverslips were put onto an UV illumination table and the fluorescence of the drops was imaged with a digital camera. Corresponding normalized fluorescence emission spectra $I_{em}(\lambda)$ have been recorded with a fluorescence spectrometer. As both fluorophores emit at different wavelengths (FITC, λ_{em} = 520 nm; CV, λ_{em} = 623 nm) they both can be distinguished by their color, as can be seen in the regime where the drops overlap with each other. (Right side) The same experiment was performed, but now with two drops containing either CV or ATTO-590 NHS-ester (ATTO-590). As both dyes emit at very similar wavelengths (CV, λ_{em} = 621 nm; ATTO-590, λ_{em} = 624 nm) they cannot be optically resolved. In the contact zone of the two drops, the contribution of both dyes cannot be spectrally distinguished as $\lambda_{em1} \approx \lambda_{em2}$.

purpose[17,18] (Figure 2). If such capsules have diameters ≥0.5 μm, which are larger than the optical resolution limit, fluorescence from their walls can be distinguished by the fluorescence from their cavity. In this way, individual capsules could be read out in a single-particle manner. First, observation of the barcode would provide information about which analyte-sensitive fluorophore is embedded in the cavity of the respective capsule. Second, evaluation of the fluorescence emission originating from the capsule cavity would lead to the concentration of the analyte to which this capsule is sensitive. These carriers could be spatially resolved and simultaneously read out on a single-particle basis. Thus, by confining different analyte-sensitive fluorophores to different carriers, multiplexed measurements of several analytes would be possible, even if the emission spectra of the different analyte-sensitive fluorophores overlap. A drawback is that this method would be limited to particles larger than the optical resolution limit.

Fluorescence emission of different fluorophores can also be resolved in time. If the decay times τ_{em} of different fluorophores are distinct, the contribution of the respective fluorophores could, in principle, be determined from time-resolved fluorescence measurements.[21,22] This is the basis of time-gated/fluorescence lifetime imaging (FLIM).[23,24] High-quality core−shell quantum dots typically have decay times longer than those of organic fluorophores and thus can be resolved in time-gated measurements.[25] However, to find analyte-sensitive fluorophores where all possess different emission lifetimes, τ_{em}, is unlikely. Here again, nanoparticles in the form of quantum dots could help. If the emission of a quantum dot overlaps with the absorption of an adjacent fluorophore, the excitation of the quantum dot (donor) can lead to a transfer of energy to the fluorophore (acceptor). The resulting effect is the emission of the fluorophore,[26] a phenomenon called fluorescence resonance energy transfer (FRET).[27] One method of creating such an assembly is embedding fluorophores in a polymer shell around quantum dots.[28,29] Importantly, the effective lifetime of the acceptor will be determined by the lifetime of the donor[30] (Figure 3). Donor lifetimes can even be

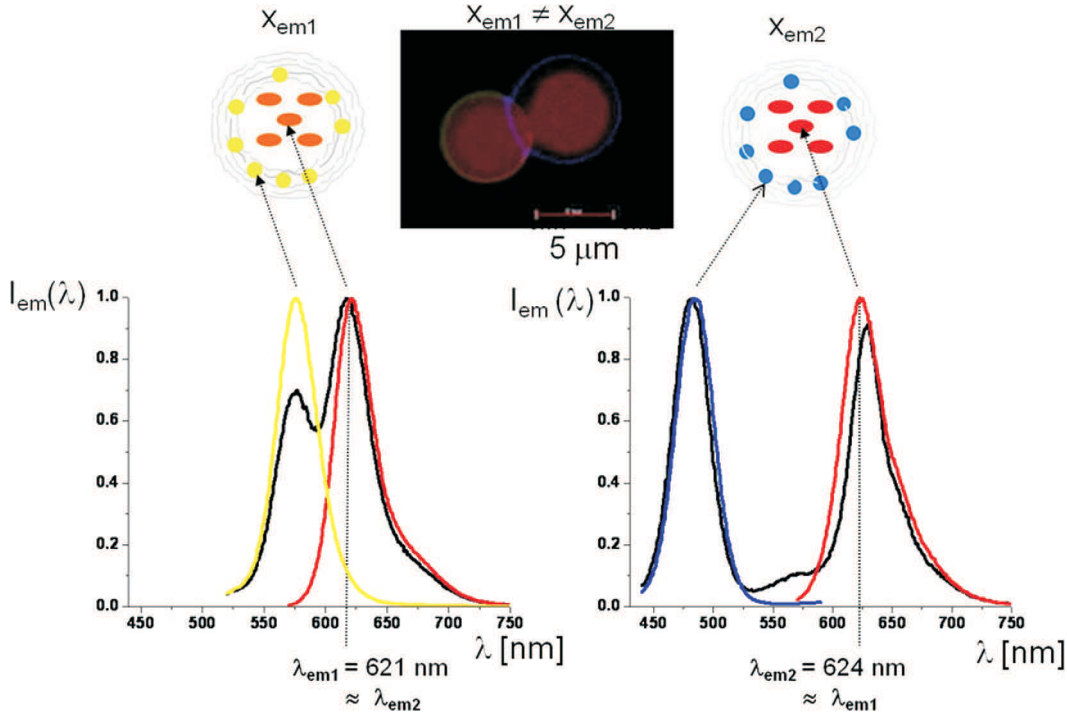

Figure 2. Polyelectrolyte capsules were assembled with layer-by-layer deposition around $CaCO_3$ template cores that had been loaded either with CV conjugated to dextran or ATTO590 conjugated to dextran, followed by dissolution of the template cores, according to previously published protocols.[17,18] Yellow and blue polymer-coated CdSe/ZnS quantum dots[29] were integrated in the polyelectrolyte walls according to earlier reports.[19] This led to two different types of capsules. The first type had CV fluorophore conjugated to dextran in their cavity, and their wall was labeled with yellow fluorescent quantum dots. The second type had ATTO590 fluorophore conjugated to dextran in their cavity, and their wall was labeled with blue fluorescent quantum dots. The capsule walls were permeable to ions.[18] The image shows an overlay of fluorescence images recorded with a blue, yellow, and red filter-set. Though CV and ATTO590 cannot be well resolved spectrally ($\lambda_{em1} \approx \lambda_{em2}$) the respective types of each capsule can be recognized on a single capsule level by the color of fluorescence of the wall when the capsules are located at different positions ($x_{em1} \neq x_{em2}$). Because the type of each capsule can be identified, it is known which fluorophore is inside each capsule and thus one can spatially distinguish the emission of the different fluorophores.

further increased by doping of the quantum dots with transition metal elements, such as Mn^{2+}.[31−33] Effective donor lifetimes lasting hundreds of microseconds can be achieved because the internal Mn^{2+} $3d^5$ transitions are dipole-forbidden by spin and parity selection rules. The selection rules are partly relaxed by spin−orbit coupling and p−d hybridization.[34−36] In this way, the effective lifetimes τ_{em} of different analyte-sensitive fluorophores could be tuned by linking them to different donor nanoparticles, each of which possess significantly different lifetimes.

CONCLUSIONS AND PROSPECTS

In this way, the functionality of traditional analyte-sensitive fluorophores could be improved with the help of nanotechnology. We have outlined the perspective of making hybrid materials of analyte-sensitive fluorophores and colloidal quantum dots, and of making use of the fact that fluorescence emission $I_{em} = I_{em}(\lambda_{em}, x_{em}, \tau_{em})$ can be resolved spectrally (λ_{em}), spatially (x_{em}), and temporally (τ_{em}). This demonstrates that combining nanotechnological compounds such as colloidal nanoparticles with classical molecular compounds could make novel hybrid materials with advanced properties. Naturally, the given example covers only one small area of research and development. Indeed, we believe that by adding nanotechnologically created compounds to traditional materials, hybrid materials with improved properties in a wide context can be created in the future.

> The effective lifetimes τ_{em} of different analyte-sensitive fluorophores could be tuned by linking them to different donor nanoparticles, each of which possess significantly different lifetimes.

Acknowledgment. This work was supported by the German Research Foundation (DFG, Grant PA794/11-1). A.Z.A. and F.A. are grateful to Higher Education Commission of Pakistan (HEC) and the

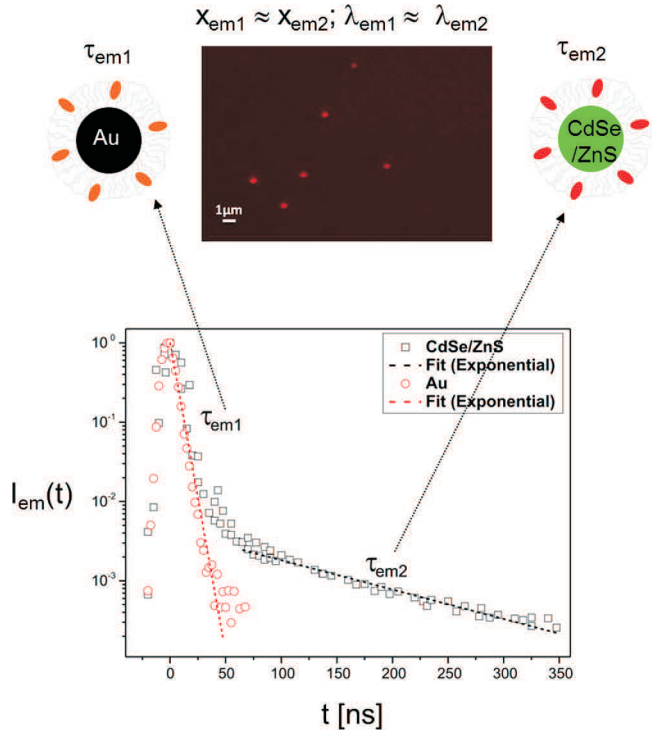

Figure 3. The time-dependent fluorescence emission $I_{em}(t)$ is shown for two different fluorophores: CV and ATTO590, which have similar fluorescence lifetimes. CV fluorophores and ATTO590 fluorophores were integrated in the polymer shell of colloidal Au and CdSe/ZnS nanoparticles, respectively, following previously published protocols.[28,29] Coupling CV to the surface of Au nanoparticles did not significantly affect the fluorescence lifetime τ_{em1} of CV (red circles).[30] On the contrary, the effective lifetime τ_{em2} of ATTO590 (black squares) was increased by FRET with the underlying CdSe/ZnS nanoparticle. In this way, the effective lifetimes of two fluorophores have been put in a different regime by coupling them to different types of nanoparticles.

German Academic Exchange Service (DAAD) for a fellowship. J.M.M.M. and S.C.R. are grateful to the Junta Andalucia for a fellowship.

REFERENCES AND NOTES

1. Buckler, K. J.; Vaughanjones, R. D. Application of a New pH-Sensitive Fluoroprobe (Carboxy-Snarf-1) for Intracellular pH Measurement in Small, Isolated Cells. *Pflug. Arch. Eur. J. Phys.* **1990**, *417*, 234–239.
2. Kasner, S. E.; Ganz, M. B. Regulation of Intracellular Potassium in Mesangial Cells—A Fluorescence Analysis Using the Dye, PBFI. *Am. J. Physiol.* **1992**, *262*, F462–F467.
3. Jezek, P.; Mahdi, F.; Garlid, K. D. Reconstitution of the Beef-Heart and Rat-Liver Mitochondrial K^+/H^+ (Na^+/H^+) Antiporter—Quantitation of K^+ Transport with the Novel Fluorescent-Probe, PBFI. *J. Biol. Chem.* **1990**, *265*, 10522–10526.
4. Nath, S.; Jezek, P.; Garlid, K. D. Reconstitution of the Na^+-Selective Na^+/H^+ Antiporter from Beef-Heart Mitochondria—Quantitation of Na^+ Transport With The Novel Fluorescent-Probe, SBFI. *Biophys. J.* **1990**, *57*, A477.
5. Naftalin, R. J.; Pedley, K. C. Video Enhanced Imaging of the Fluorescent Na^+ Probe SBFI Indicates that Colonic Crypts Absorb Fluid by Generating a Hypertonic Interstitial Fluid. *FEBS Lett.* **1990**, *260*, 187–194.
6. Graefe, A.; Stanca, S. E.; Nietzsche, S.; Kubicova, L.; Beckert, R.; Biskup, C.; Mohr, G. J. Development and Critical Evaluation of Fluorescent Chloride Nanosensors. *Anal. Chem.* **2008**, *80*, 6526–6531.
7. Engblom, A. C.; Akerman, K. E. O. Determination of the Intracellular Free Chloride Concentration in Rat-Brain Synaptoneurosomes Using a Chloride-Sensitive Fluorescent Indicator. *Biochim. Biophys. Acta* **1993**, *1153*, 262–266.
8. Nagl, S.; Wolfbeis, O. S. Optical Multiple Chemical Sensing: Status and Current Challenges. *Analyst* **2007**, *132*, 507–511.
9. Whitesides, G. M. Nanoscience, Nanotechnology, and Chemistry. *Small* **2005**, *1*, 172–179.
10. Han, M.; Gao, X.; Su, J. Z.; Nie, S. Quantum-Dot-Tagged Microbeads for Multiplexed Optical Coding of Biomolecules. *Nat. Biotechnol.* **2001**, *19*, 631–635.
11. Gao, X.; Nie, S. Quantum Dot-Encoded Beads. In *NanoBiotechnology Protocols*; Rosenthal, S. J., Wright, D. W., Eds.; Humana Press: Totowa, NJ, 2005; pp 61−71.
12. Fournier-Bidoz, S.; Jennings, T. L.; Klostranec, J. M.; Fung, W.; Rhee, A.; Li, D.; Chan, W. C. W. Facile and Rapid One-Step Mass Preparation of Quantum-Dot Barcodes. *Angew. Chem., Int. Ed.* **2008**, *47*, 5577–5581.
13. Clark, H. A.; Hoyer, M.; Philbert, M. A.; Kopelman, R. Optical Nanosensors for Chemical Analysis inside Single Living Cells. 1. Fabrication, Characterization, and Methods for Intracellular Delivery of PEBBLE Sensors. *Anal. Chem.* **1999**, *71*, 4831–4836.
14. Clark, H. A.; Kopelman, R.; Tjalkens, R.; Philbert, M. A. Optical Nanosensors for Chemical Analysis inside Single Living Cells. 2. Sensors for pH and Calcium and the Intracellular Application of PEBBLE Sensors. *Anal. Chem.* **1999**, *71*, 4837–4843.
15. Volodkin, D. V.; Larionova, N. I.; Sukhorukov, G. B. Protein Encapsulation *via* Porous $CaCO_3$ Microparticles Templating. *Biomacromolecules* **2004**, *5*, 1962–1972.
16. Duchesne, T. A.; Brown, J. Q.; Guice, K. B.; Nayak, S. R.; Lvov, Y. M.; McShane, M. J.; Priezzhev, A. V.; Cote, G. L. Nanoassembled Fluorescent Microshells as Biochemical Sensors. *Proc. SPIE* **2002**, *4624*, 66–75.
17. Kreft, O.; Muñoz-Javier, A.; Sukhorukov, G. B.; Parak, W. J. Polymer Microcapsules as Mobile Local pH-Sensors. *J. Mater. Chem.* **2007**, *17*, 4471–4476.
18. del-Mercato, L. L.; Abbasi, A. Z.; Parak, W. J. Synthesis and Characterization of Ratiometric Ion-Sensitive Polyelectrolyte Capsules. *Small* 2010, DOI: 10.1002/smll.201001144.
19. Sukhorukov, G. B.; Rogach, A. L.; Zebli, B.; Liedl, T.; Skirtach, A. G.; Köhler, K.; Antipov, A. A.; Gaponik, N.; Susha, A. S.; Winterhalter, M.; *et al.* Nanoengineered Polymer Capsules: Tools for Detection, Controlled Delivery, and Site-Specific Manipulation. *Small* **2005**, *1*, 194–200.
20. Sukhorukov, G. B.; Donath, E.; Davis, S.; Lichtenfeld, H.; Caruso, F.; Popov, V. I.; Möhwald, H. Stepwise Polyelectrolyte Assembly on Particle Surfaces: A Novel Approach to Colloid Design. *Polym. Adv. Technol.* **1998**, *9*, 759–767.
21. Borisov, S. M.; Neurauter, G.; Schroeder, C.; Klimant, I.; Wolfbeis, O. S. Modified Dual Lifetime Referencing Method for Simultaneous Optical Determination and Sensing of Two Analytes. *Appl. Spectrosc.* **2006**, *60*, 1167–1173.
22. Nagl, S.; Stich, M. I. J.; Schaferling, M.; Wolfbeis, O. S. Method for Simultaneous Luminescence

Sensing of Two Species Using Optical Probes of Different Decay Time, and its Application to an Enzymatic Reaction at Varying Temperature. *Anal. Bioanal. Chem.* **2009**, *393*, 1199–1207.
23. Tinnefeld, P.; Buschmann, V.; Herten, D.-P.; Han, K.-T.; Sauer, M. Confocal Fluorescence Lifetime Imaging Microscopy (FLIM) at the Single Molecule Level. *Single Mol.* **2000**, *1*, 215–223.
24. Emiliani, V.; Sanvitto, D.; Tramier, M.; Piolot, T.; Petrasek, Z.; Kemnitz, K.; Durieux, C.; Coppey-Moisan, M. Low-Intensity Two-Dimensional Imaging of Fluorescence Lifetimes in Living Cells. *Appl. Phys. Lett.* **2003**, *83*, 2471–2473.
25. Dahan, M.; Laurence, T.; Pinaud, F.; Chemla, D. S.; Alivisatos, A. P.; Sauer, M.; Weiss, S. Time-Gated Biological Imaging by use of Colloidal Quantum Dots. *Opt. Lett.* **2001**, *26*, 825–827.
26. Goldman, E. R.; Clapp, A. R.; Anderson, G. P.; Uyeda, H. T.; Mauro, J. M.; Medintz, I. L.; Mattoussi, H. Multiplexed Toxin Analysis Using Four Colors of Quantum Dot Fluororeagents. *Anal. Chem.* **2004**, *76*, 684–688.
27. Förster, T. Zwischenmolekulare Energiewanderung und Fluoreszenz. *Ann. Phys., Berlin* **1948**, *437*, 55–75.
28. Fernández-Argüelles, M. T.; Yakovlev, A.; Sperling, R. A.; Luccardini, C.; Gaillard, S.; Medel, A. S.; Mallet, J.-M.; Brochon, J.-C.; Feltz, A.; Oheim, M.; *et al*. Synthesis and Characterization of Polymer-Coated Quantum Dots with Integrated Acceptor Dyes as FRET-Based Nanoprobes. *Nano Lett.* **2007**, *7*, 2613–2617.
29. Lin, C.-A. J.; Sperling, R. A.; Li, J. K.; Yang, T.-Y.; Li, P.-Y.; Zanella, M.; Chang, W. H.; Parak, W. J. Design of an Amphiphilic Polymer for Nanoparticle Coating and Functionalization. *Small* **2008**, *4*, 334–341.
30. Niebling, T.; Zhang, F.; Ali, Z.; Parak, W. J.; Heimbrodt, W. Excitation Dynamics in Polymer-Coated Semiconductor Quantum Dots with Integrated Dye Molecules: The Role of Reabsorption. *J. Appl. Phys.* **2009**, *106*, 104701.
31. Erwin, S. C.; Zu, L. J.; Haftel, M. I.; Efros, A. L.; Kennedy, T. A.; Norris, D. J. Doping Semiconductor Nanocrystals. *Nature* **2005**, *436*, 91–94.
32. Mikulec, F. V.; Kuno, M.; Bennati, M.; Hall, A. D.; Griffin, R. G.; Bawendi, M. G. Organometallic Synthesis and Spectroscopic Characterization of Manganese-Doped CdSe Nanocrystals. *J. Am. Chem. Soc.* **2000**, *122*, 2532–2540.
33. Pradhan, N.; Battaglia, D. M.; Liu, Y. C.; Peng, X. G. Efficient, Stable, Small, and Water-Soluble Doped ZnSe Nanocrystal Emitters as Non-cadmium Biomedical Labels. *Nano Lett.* **2007**, *7*, 312–317.
34. Furdyna, J. K. Diluted Magnetic Semiconductors. *J. Appl. Phys.* **1988**, *64*, R29–R64.
35. Goede, O.; Heimbrodt, W. Optical Properties of (Zn, Mn) and (Cd, Mn) Chalcogenide Mixed-Crystals and Superlattices. *Phys. Status Solidi B* **1988**, *146*, 11–62.
36. Archer, P. I.; Santangelo, S. A.; Gamelin, D. R. Direct Observation of sp−d Exchange Interactions in Colloidal Mn^{2+}- and Co^{2+}-Doped CdSe Quantum Dots. *Nano Lett.* **2007**, *7*, 1037–1043.

Journal of Controlled Release 159 (2012) 120–127

Contents lists available at SciVerse ScienceDirect

Journal of Controlled Release

journal homepage: www.elsevier.com/locate/jconrel

NIR-light triggered delivery of macromolecules into the cytosol

Susana Carregal-Romero [a], Markus Ochs [a], Pilar Rivera-Gil [a], Carolin Ganas [a], Anton M. Pavlov [b], Gleb B. Sukhorukov [b], Wolfgang J. Parak [a,*]

[a] Department of Physics and WZMW, Philipps Universität Marburg, D-35037, Marburg, Germany
[b] School of Engineering & Materials Science Queen Mary University of London Mile End Road, L E1 4NS, London, United Kingdom

ARTICLE INFO

Article history:
Received 16 November 2011
Accepted 17 December 2011
Available online 29 December 2011

Keywords:
Light stimuli-responsive
Polyelectrolyte capsules
Controlled release
pH sensor
Protein
Enzymatic degradation

ABSTRACT

Light-responsive microcapsules constructed by layer-by-layer self-assembly are used as microcarriers to deliver different macromolecules inside cells. The microcapsules carry the macromolecules as cargo in their cavity, while their walls are modified with agglomerated gold nanoparticles. Microcapsules are incorporated by living cells and are then located in lysosomal compartments. Controlled release of the encapsulated material from the interior of the capsule to the cytosol is possible upon NIR-light irradiation. This is based on local heating of the gold nanoparticles upon NIR light and disruption of the capsule wall, what results on release of encapsulated materials. We illustrate several key advances in controlled release induced by light. First, we demonstrate that capsules can be opened individually, which allows for sequentially releasing cargo from different capsules within one single cell. Second, by using a pH-indicator as cargo the claim of release from the acidic lysosomal compartments to the neutral cytosol is experimentally evident which until now has been only speculated. Third, green fluorescent protein (GFP) is released to the cytosol while retaining its functionality. This demonstrates that proteins can be released without destruction by the local heating. Fourth, GFP is also administered in biodegradable capsules, which leads to a different release mechanism compared to externally triggering for light-responsive microcapsules.

1. Introduction

The design of new materials with improved properties is in continuous evolution. In the last years colloidal chemistry and nanoscience have made big steps forward due to the huge improvement in the controlled synthesis of nanostructures, in their assembly with other structures, and in the creation/improvement of the technology necessary for their characterization. To give some examples about applications in life sciences, gold nanoparticles with different shapes are nowadays being used for hyperthermia applications *in vivo* [1,2], polymer based nanostructures are currently in clinical research studies [3], and fast detection of prions has been possible in serum and blood with supercrystals of Au nanorods as surface enhancers of Raman scattering spectroscopy [4]. In this context, polyelectrolyte multilayer (PEM) microcapsules can be regarded as materials for potential applications in diagnosis and drug delivery [5–8]. PEM capsules loaded with different ion sensors have for example already demonstrated feasibility for quantitative estimation of ion concentrations in the capsule's surrounding medium [9]. Their broad range of different options to load the capsule in different parts of the material (wall or inner cavity) and with different molecules, nanoparticles, vesicles, etc. and the posibility to tune the size of the capsule itself, make PEM capsules promising drug delivery vehicles [10–14]. Drug delivery systems have to fulfill some basic physicochemical requirements. They have to protect the drug from degradation *in vivo*. For targeted release the drug must not leak out from the carrier system before it is at the designated target region. These conditions involve big challenges for colloidal engineering. The micro/nanocarriers must be stable in *in vivo* conditions, able to entrap efficiently different molecules with different sizes which can be hydrophobic or hydrophilic, have the capability to be targeted, and the process of release must keep the activity of the drug intact. There are many examples of colloidal nano/micro carrier systems, such as gold nanoparticles, protein based nanoparticles, liposomes, polymersomes, etc [15–18]. PEM capsules are interesting in this context, as they are simple, stable, potentially biocompatible, and very versatile [19,20]. This manuscript focuses on the controlled release from light responsive capsules upon NIR irradiation. Hereby the capsules carry a cargo in their cavity and gold nanoparticles in their walls. Gold nanorods and nanoparticle agglomerates have been used to efficiently open the wall of the capsules through plasmon-assisted photothermal processes [21,22]. In this contex, there are many biological applications of gold nanoparticles that take advantage of the possibility to produce optothermal effects such as cancer therapy (hyperthermia) [2,23–25], cytosolic release of gold nanoparticles [26] and drug delivery [27,28]. Capsules were irradiated with a 830 nm laser. The light

* Corresponding author at: Philipps University of Marburg, FB Physics, Biophotonics, Renthof 7, 35037 Marburg, Germany. Tel.: +49 64212824102; fax: +49 64212827034.
E-mail address: wolfgang.parak@physik.uni-marburg.de (W.J. Parak).

0168-3659/$ – see front matter © 2011 Elsevier B.V. All rights reserved.
doi:10.1016/j.jconrel.2011.12.013

absorption and heat dissipation are competing mechanisms that rule the temperature in the metallic nanostructures and consequently the capsule opening and the cargo release [29]. The capsules themselves do not cause acute toxicity *in vitro*[30] and they can be opened without killing the cell in which they are located [31,32]. In this study we investigated important properties of this process: can individual capsules be opened sequentially in one cell? Can the cargo be released to the cytosol? Does the cargo retain their active properties and trigger intracellular processes? So far release to the cytosol from light reponsive capsules has been only speculated and the high precision of the opening of individual capsules in a controlled way hasn't been demonstrated yet.

2. Materials and methods

2.1. Materials

Poly(sodium 4-styrenesulfonate) (PSS, $M_w \approx 70$ kDa, #243051), poly(allylamine hydrochloride) (PAH, $M_w \approx 56$ kDa, #283223), calcium chloride dehydrate ($CaCl_2$, #223506), sodium carbonate (Na_2CO_3, #S7795), ethylenediaminetetraacetic acid disodium salt dihydrate (EDTA disodium salt, #E5134), dextran sulfate sodium salt (DEXS, $M_w \approx 10$ kDa, #D4911), dextran ($M_w \approx 2000$ kDa, #95771) and poly-L-arginine hydrochloride (PARG, $M_w \approx 70$ kDa, #P3892) were purchased from Sigma-Aldrich. Tetramethylrhodamine-dextran (TMR-dextran, $M_w \approx 10$ kDa, #D-1817), Cascade Blue-dextran (CB-dextran, $M_w \approx 10$ kDa, #D-1976), SNARF–dextran ($M_w \approx 10$ kDa, #D-3303), and Fluorescein-dextran (FITC-dextran, $M_w \approx 10$ kDa, #D-1821) were obtained from Invitrogen. His-tagged Green Fluorescent Protein (GFP, $M_w \approx 35$ kDa) was purchased from Biomedal. All chemicals were used as received. Ultrapure water with a resistance greater than 18.2 MΩ cm^{-1} was used for all experiments.

2.2. Synthesis of light responsive capsules

Four different types of light responsive capsules were produced: red and blue capsules based on TMR and CB, pH-sensitive capsules based on SNARF, and protein loaded capsules based on GFP. The capsules were loaded using different approaches. The incorporation of the macromolecule inside the PEM capsule is highly dependent from the size and nature of the cargo. TMR-, CB-, and SNARF–dextran capsules were postloaded due to the small size and the thermal stability of these molecules. Contrary, GFP capsules were produced by coprecipitation, i.e. the protein was incorporated during the $CaCO_3$ core formation. The synthesis of GFP capsules was carried out as follows: Firstly $CaCO_3$ microparticles were synthesized from solutions of $CaCl_2$ and Na_2CO_3 under vigorous stirring [33]. In a glass vial equal volumes (615 μL) of aqueous $CaCl_2$ and Na_2CO_3 solutions (0.33 M) were mixed under the presence of 750 μL of GFP (1 mg mL^{-1}). The solution was thoroughly mixed on a magnetic stirrer (1000 rpm) for 30 s and afterwards the mixture was left without stirring for 3 minutes. All steps were performed at room temperature (RT). During this time spherical and porous $CaCO_3$ loaded with GFP microparticles were formed. After tree washing steps with Milli-Q water the resulting particles were used directly for the LbL assembly of polyelectrolytes. The isoelectric point of the GFP is 6.6. Hence, the cores should be slightly negative at neutral pH and positive below the isoelectric point [34,35]. The zeta potential of the GFP loaded cores (in Milli-Q water) was measured to be -14.5 ± 0.3 mV, whereas cores without GFP had a zetapotential of $+3.1 \pm 0.2$ mV. After the coating with the first and negative monolayer of PSS it changed to -22.8 ± 0.8 mV and -2.2 ± 0.2 mV respectivaly which indicates that the first adsorption step is not predominantly through charge. The calcium carbonate cores that were used as templates for the TMR, CB and SNARF capsules were prepared following the same protocol but without introducing the protein and instead adding 2000 kDa dextran in the porous matrix of $CaCO_3$. The presence of dextran in the cores helps the core dissolution at the end of the synthesis. In all the cases the average diameter of the microparticles ranged from 2.5 to 3.5 μm. It was measured from confocal images with the software ImageTool. Core shell structures were prepared by alternating incubation of $CaCO_3$ cores in PSS and PAH solutions (2 mg mL^{-1}) within 0.5 M NaCl. The pH of the polyelectrolyte solution was adjusted to 6.5 by adding HCl/NaOH. Each adsorption cycle (2 min in a sonication bath and 10 min shaking) was completed after three washing steps with 1 mL of Milli-Q water to remove unbound polymer before the next polyelectrolyte addition. After self-assembly of two bilayers of polyelectrolytes $(PSS/PAH)_2$, gold nanoparticle agglomerates were deposited on the core shell microstructure through electrostatic interactions. Gold nanoparticle agglomerates were formed after increasing the ionic strength of a solution with sodium citrate stabilized Au nanoparticles (1 mL, $[Au] = 5 \times 10^{-4}$ M) with NaCl (0.2 mL, 0.5 M). The initial Au nanoparticles were 15 nm particles synthesized through the Turkevich method [36]. The agglomerates were mixed with the positively coated $CaCO_3$ after 5 min of their formation. Three washing steps followed the Au deposition and two more bilayers of polyelectrolytes were then added. The resulting architecture consisted of a core of $CaCO_3$ coated with four bilayers of polyelectrolytes embedding gold nanoparticle agglomerates in the middle of the capsule walls. The dissolution of the cores was carried out by Ca^{2+} ion complexation with EDTA. For this purpose the core-shell microparticles were shaken for 2 min in a solution of EDTA (1 mL, 0.2 M at pH 5.5) and finally washed four times at 1100 rpm for 8 min with Milli-Q water. In Fig. 1a one can see the broad absorption band of gold nanoparticles after agglomeration, before to take part of the PEM wall. The position of the plasmon band and the further red

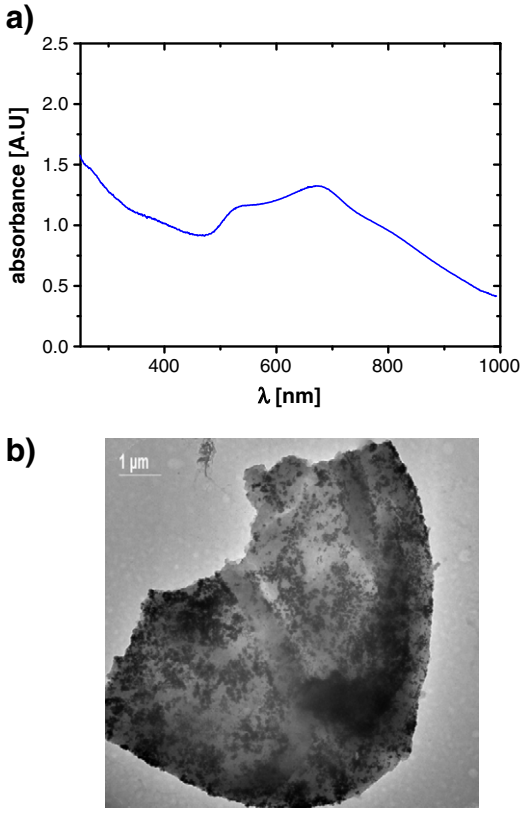

Fig. 1. Absorbance spectra of Au agglomerates before incorporation in the PEM capsule wall (a). Transmission electronic microscopy (TEM) image of a PEM capsule loaded with Au agglomerates with composition $(PSS/PAH)_2$ Au_{agg} $(PSS/PAH)_2$ after laser irradiation exposure (laser intensity of 14 mW/μm^2 during few seconds) in water. For *in vitro* experiments lower intensity was used to avoid cell death.

shift after self-assembly of gold agglomerates on the positevely coated surface of CaCO3 make the capsules high sensitive to the 830 nm laser. In Fig. 1b a transmission electron microscopy (TEM) image of a fully broken capsule after laser irradiation in water is shown. TMR–, CB– and SNARF–dextran capsules were prepared by post-loading of solutions of dextran (1 mg mL^{-1}) conjugated to red (Tetramethylrhodamine), blue (Cascade Blue) and pH sensitive (SNARF) fluorophores. Encapsulation of fluorescence labeled dextran was accomplished by first incubating the prepared PEM microcapsules for 30 min in a highly concentrated solution of labeled dextran. Second, by heating the solution to 65 °C for 2 h [37]. Exchanging the supernatant with water by careful centrifugation (1100 rpm, 8 min) and further three washing steps with Milli-Q water yielded filled capsules. Hereby the fluorescence labeled dextran remained inside the cavity of the capsules. All the light responsive capsules had the same $(PSS/PAH)_2$ Au_{agg} $(PSS/PAH)_2$ structure but different cargo.

2.3. Synthesis of biodegradable capsules

GFP loaded calcium carbonate microparticles were synthesized as it has been described above. The same cores of $CaCO_3$ were used for the LbL assembly of biodegradable polyelectrolytes. Four bilayers of dextran sulfate and poly-L-arginine $(DEXS/PARG)_4$ were deposited on the $GFP/CaCO_3$ core. The polyelectrolyte solutions were (1 mg mL^{-1}) and (2 mg mL^{-1}) for PARG and DEXS, both with 0.5 M of NaCl and pH 6.5. The dissolution and the washing steps were carried out following the same protocol used for light responsive capsules.

2.4. Capsule internalization by living cells

A total of 1×10^5 human carcinoma A459 cells and SH-SY5Y human neurons were seeded on culture 35 mm diameter dishes and were incubated with capsules (20 capsules per cell) for about 12 h. The size of the capsules allows us to measure the concentration of the capsule solution (always around 1×10^8 capsule mL^{-1}) with a hemocytometer. After a washing step to remove free capsules, the culture dish was attached to the *x-y-z* stage of the microscope. Two different microscopes were used for release observation. Therefore, the bottom of the cell culture dishes had to be marked to relocate the same cell position.

2.5. Microscopy set-up

For capsule opening a 100 mW laser (830 nm CW diode) was coupled to an upright microscope (Axitotech, Zeiss, 63× objective) leading to a focused light spot of 2.6 ± 0.1 μm^2 in the image plane. The laser power was measured at the well surface. By changing the operation voltage of the laser, the resulting power of the focused light spot could be tuned in the range of 0–31 mW. Note that this range corresponds to intensities measured in the image plane after coupling the laser to the microscope and therefore, because of the optics used for the coupling, these values are attenuated in respect to the intensities measured directly after the diode laser. Fluorescence images of cells were taken with a LSM 510 META confocal microscope from Zeiss. Images comprised phase contrast and blue, green / yellow and red fluorescence channels. A typical series of images before and after capsule opening was obtained in the following sequence. Firstly, in the confocal microscope 10 different positions where cell have incorporated capsules were selected. For these 10 positions images in phase contrast and fluorescence channels were taken. Afterwards, the culture dish was placed in the sample holder of the microscope coupled with the laser. Then, capsules were opened upon laser irradiation only in the cells that were previously selected. The culture dish was again transferred to the confocal microscope and phase contrast images and images of all channels of fluorescence were recorded in between some minutes and 2–3 h after laser irradiation. No differences were observed concerning the time of observation. No changes in acquisition and scanning mode were performed in between taking pictures before and after laser irradiation. The confocal microscope was chosen to image the cytosolic release because of the higher resolution and quality of the images. In the case of the study of GFP release *via* enzimatic degradation of PEM capsules, only LSM 510 META confocal microscope was used for imaging. Several times series were carried out. Particular care was taken to maintain the same settings in the microscope during the comparison experiments before and after irradiation and with the biodegradable DEXS/PARG and non-degradable PSS/PAH capsules without gold nanoparticles. One key point is to verify where the fluorescence comes from, since not all the capsules within one cells are in the same focal plane. Therefore fluorescence scans along the *z*-axis were performed for every experiment.

3. Results and discussion

Inorganic nanoparticle modified capsules can be used to externally trigger delivery of macromolecular cargo from their cavities under different stimuli such as light, oscillating magnetic fields, ultrasound or microwaves (MW), depending on the nature of the nanoparticles [21,38–43]. In the present study near-IR light (750–1100 nm) has been used to stimulate capsules opening, because it covers the optical transparency window of biological tissues. The lower boundary of the range is determined by strong scattering of short-wavelength radiation in biological tissues and absorption of light by melanin and blood, while the upper limit is determined by absorption of light in water. Capsules can be fabricated with metal oxides or metallic nanostructures, that have strong absorption in the NIR spectra, in between the polyelectrolyte layers which form their walls [44]. In the present case we chose gold nanoparticle agglomerates made from 15 nm spherical gold colloids as local heat source under NIR illumination for the following reasons: i) the plasmon band position is in the NIR due to plasmon coupling effects, ii) the total optothermal energy deposited in the agglomerates is higher than in single particles and iii) the bigger size of the agglomerates leads to bigger pore sizes upon laser irradiation than for single particles [44,45]. PEM capsules allow for the incorporation of different cargos in the nanometer thick wall and the microsized inner cavity. The macromolecules as cargo (which could be bioactives) can be loaded inside the PEM capsule following two different protocols: co-precipitation or preloading and postloading [8,46,47]. We synthesized the capsules via the layer-by-layer technique as it has been published elsewhere [47,48]. As dextran-based cargo we used Cascade Blue-dextran (CB-dextran), Tetramethylrhodamine-dextran (TMR-dextran), and SNARF–dextran. Cargo was introduced to the capsules by post-loading and further thermal shirking [49]. The light responsive capsules loaded with protein cargo, in the present case green fluorescent protein (GFP) have been prepared by co-precipitation of the protein during the $CaCO_3$ core synthesis to avoid possible damage of the protein during the shriking of the capsule which involve high temperatures.

3.1. Sequential controlled release of different macromolecules inside cells

PEM capsules loaded with different macromolecules likely undergo a similar uptake by living cells. Internalization can be assumed to be similar because of the similar surface composition, size and shape of capsules. These three factors are key aspects in cellular uptake. In this paragraph we show the possibility to deliver two different macromolecules sequentially which has not been demostrated so far and can help in the study *in vitro* of cell response upon highly controlled release of different molecules. For this purpose two different types of $(PSS/PAH)_2$ Au_{agg} $(PSS/PAH)_2$ capsules, loaded each with one type of macromolecule need to be present in the same cell. Sequential NIR illumination of individual capsules allows for subsequent release of cargo.

Non-degradable capsules prepared with PSS and PAH as polyelectrolytes were loaded with Au nanoparticle agglomerates in their wall and with one of two different fluorophores conjugated with dextran (Mol. w ≈ 10 kDa) in their cavity: TMR-dextran (fluorescent in red) and CB-dextran (fluorescent in blue). The Au nanoparticles agglomerates were produced by increasing the ionic strength of a solution of 15 nm Au nanoparticles coated with citrate ions. The gold plasmon band was shifted (cf. Fig. 1) from 520 nm to the NIR and thus made the capsules responsive to excitation at 830 nm. Individual capsules were excited for release of their cargo. Light spots of 3.8 mW/μm^2 intensity (10 mW laser power in the focus of the objective, 2.6 μm^2 laser spot area) and less than 2 s of exposure time were used to produce the rupture of the capsules and thus cargo release. Fig. 2 shows the sequential release inside human lung carcinoma A549 cells of first CB-dextran and subsequently TMR-dextran. In the images one can see that first only the Cascade Blue-dextran was released (as only these capsules were illuminated). TMR-dextran capsules inside the same cell (which were not illuminated) did not show any red dextran leaking. One hour after the blue capsules had been opened, the red capsules were irradiated with NIR light of the same intensity. Again no obvious damaging in the cell structure was visible as it was expected from a previous work [31].

The fluorescence labeled dextran was distributed more or less homogeneously inside cells, which can indicate release to the cytosol. In case cells had engulfed both capsules, the two different cargos can be released in the same intracellular space. This is supposed to provide controlled mixing of cargo inside cells followed, by triggering of intracellular biochemical reactions. Sequentially controlled release has been studied for different cell lines (see Supporting Information, Figures SI-5 and SI-6), such as with SH-SY5Y human neurons, MDA-MB-231 cells, and 3 T3 fibroblasts. In all the cases the release was not complete. It is possible to still see residual fluorescence inside the capsule cavity. We speculate that the cargo was not fully released partially because the PEM capsules produced using $CaCO_3$ as template own an internal matrix of polyelectrolytes. This matrix is formed due to the porosity of the $CaCO_3$ during the layer-by-layer adsorption process [50]. In addition, in previous work a less evident incomplete release of cargo from PEM capsules made using SiO_2 beads as templates was also observed. Silica cores lack the polyelectrolyte matrix, thus the charged polyelectrolytes of the capsule wall should be also responsible of the storage of cargo besides the capsule wall opening. However, for triggering of reactions inside cells complete release is not crucial, as most of the time a few released molecules (which could be for example siRNA) might be sufficient to induce a cell response. In this way the sequential release demonstrates high control and selectivity in light triggered delivery. The demonstration of addressing individual capsules and such cargos with NIR triggered delivery may open the possibility of analyzing the cellular response after producing reactions or interactions in the cellular cytosol upon laser irradiation of microcapsules loaded with different functional macromolecules.

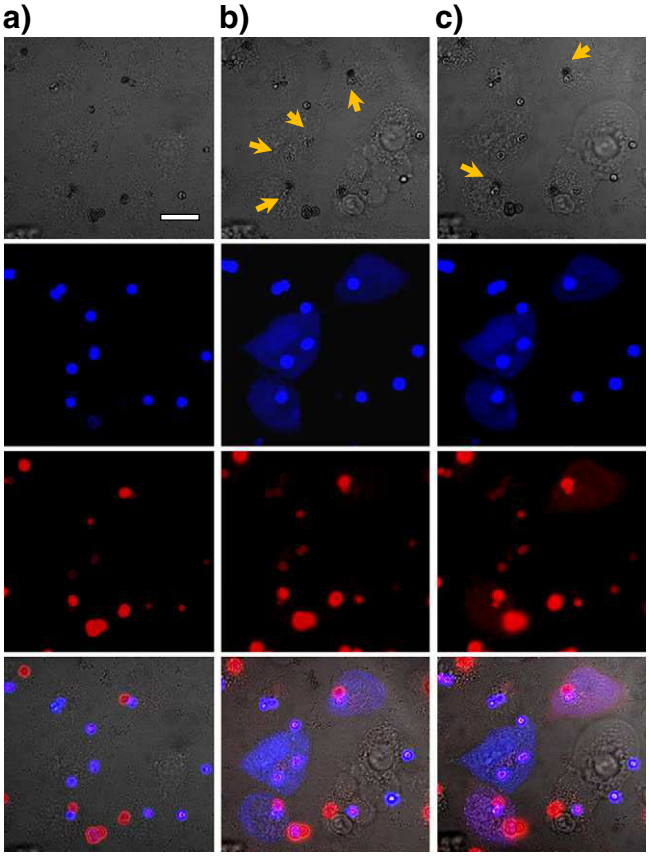

Fig. 2. Phase contrast, fluorescence and overlay images (from the top to the bottom) of A549 cells (a) before, (b) after the opening of $(PSS/PAH)_2$ Au_{agg} $(PSS/PAH)_2$ capsules loaded with 10 kDa Cascade Blue-dextran, and (c) after the opening of capsules loaded with dextran-Tetramethylrhodamine. Capsules had Au nanoparticle agglomerates embedded within their walls. They were illuminated with a laser intensity of 3.8 mW/μm^2 during few seconds. Both cargo molecules (blue and red fluorescence modified dextran) were released in the cytosol. The scale bars represent 20 μm. Arrows pointed at the irradiated and thus opened capsules.

3.2. Release of a pH sensor: demonstration of cytosolic release

Incorporated capsules are located in lysosomal compartments within cells [51]. After opening of capsules the macromolecules are quasi homogeneously distributed around cells, which indicates that they have been released to the cytoplasm [31], cf. Fig. 1. In this way macromolecules should experience a change in pH upon release from capsules inside acidic lysosomal compartments to the neutral cytoplasm. To experimentally demonstrate this cytosolic release, SNARF-modified dextran had been loaded into the cavity of $(PSS/PAH)_2$ Au_{agg} $(PSS/PAH)_2$ capsules. SNARF is a widely used pH indicator because of its unique dual emission. Its emission intensity at two different wavelengths depends on the pH value of the environment. The acidic form emits at 583 nm and the basic one at 627 nm. In this way SNARF offers the advantage of being able to perform ratiometric measurements without the requirement of a reference dye. The pH can be simply calculated from the ratio of the emission intensities [52]. After cell uptake, capsules are incorporated inside lysosomal compartments and therefore the emission of the capsules is yellow [51]. After opening of the capsules via NIR exposure the SNARF–dextran was released, distributed quasi homogeneously in the cells, and emission shifted more to the red, cf. Fig. 3. As red emission indicates neutral pH these data prove release to the neutral cytosol. One can also see that the pH in the capsule remaining changes to basic. This means that the lysosomal membrane did not close. For quantitative evaluation a more sophisticated data evaluation was performed.

Firstly, calibration curves relating the ratiometric fluorescence read-out (i.e. the ratio of red to yellow fluorescence intensity) had to be recorded. Such ratiometric image analysis on region-of-interest (ROI) of individual SNARF–dextran loaded capsules and free SNARF–dextran at low concentration was performed at different pH values. Two calibration curves were obtained as spectral parameters of SNARF–dextran are different for SNARF–dextran free in solution or being encapsulated in PEM capsules. Free SNARF–dextran calibration curve was relevant to released SNARF–dextran in cytosol, while encapsulated SNARF–dextran required a separate calibration curve [51,53]. In fact it was observed that the pK_a of the SNARF–dextran changed slightly once it has been encapsulated in a PEM capsule [9] and had an additional slight shift depending on the concentration (cf. the SI for more details). Images of the cell culture were taken

before and after the opening of the capsules at two different imaging settings. PEM capsules have SNARF–dextran in a high concentration in their inner cavity and therefore the exposure time that is required for observation is shorter than the exposure time necessary to observe the diluted SNARF–dextran dispersed in the cytosol, cf. Fig. 3. The color of capsules changed from yellow (before irradiation) to orange (after NIR exposure). Also red fluorescence appeared in the cytosol after laser irradiation.

Ratiometric image analysis was performed for ten capsules and the cytosol of ten different cells: By using the calibration curves this yielded the pH of the capsules before and after opening, as well as the pH around the released SNARF–dextran. The pH values for internalized capsules before opening, after irradiation and the cytosol were determined to be 6.4, 7.1, and 7.4, respectively. The calculated pH values are consistent with the values calculated through flow cytometry for the lysosome [54] or using a pH-sensitive GFP derivate [55]. They clearly indicate that upon capsule opening cargo does not stay in the acidic lysosomal compartment but is released to the neutral cytosol. Consequently, laser opening of capsules must also locally perforate the membrane of the lysosomal compartment in which the capsule resides or be opened due to the fast increase of foreign molecules in its interior. The release of SNARF–dextran and image analysis on ROIs was also performed for SH-SY5Y human neurons obtaining similar values of pH (cf. SI). This demonstrates that release of cargo to the cytosol is not limited to one particular type of cell.

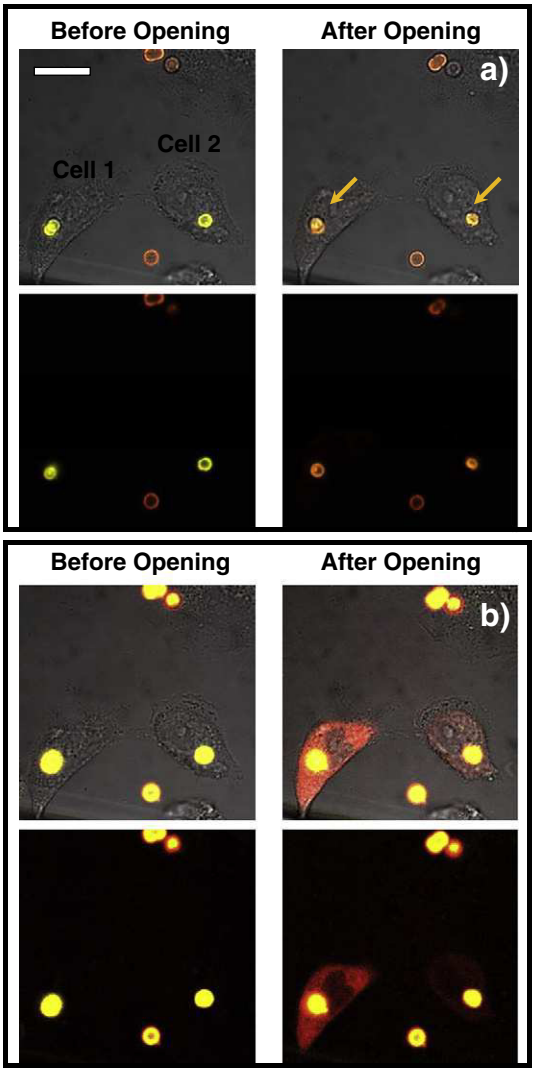

Before irradiation	After irradiation	
Capsule pH	**Capsule pH**	**Cytosol pH**
6.4 ± 0.3	7.1 ± 0.4	7.4 ± 0.4

Fig. 3. Opening of $(PSS/PAH)_2$ Au_{agg} $(PSS/PAH)_2$ loaded with 10 kDa SNARF–dextran. The release of pH-sensitive SNARF–dextran in A549 cells was analyzed through ratiometric image analysis performed on ROIs of individual SNARF–dextran loaded capsules and SNARF–dextran in the cytosol after release. Images at low (A) and high (B) exposure time had to be taken and two different calibration curves were used to quantify the pH values before and after the opening in the capsules and in the cytosol. Capsules were illuminated with laser intensity of 3.8 mW/μm^2 for few seconds. The scale bar represents 20 μm. Arrows point at the opened capsules. Fluorescence is displayed in false colors.

3.3. Controlled release of GFP

Different strategies have been developed to release proteins inside cells from nano/microcontainers [56–58]. Most of these strategies are based in the leakage of the protein through the wall of the container [59] or the enzymatic degradation of the protein carrier once it is incorporated inside the cell [11,60,61]. Here we show that light responsive capsules can be also used to release proteins to the cytosol by keeping their activity (cf. Fig. 4). We also compare this delivery method to the release of proteins with biodegradable capsules. Firstly, it has to be pointed out that capsules had to be loaded by co-precipitation in order to not damage the protein, which might be the case by using post-loading of the capsules followed by heat-shrinking. We took this precaution, though for SIINFEKL peptides it has been demonstrated that heat-shrinking doesn´t damage the molecule [62]. Cores of calcium carbonate were synthesized in the presence of GFP in aqueous solution and therefore, the protein was entrapped inside the pores. The GFP loaded cores were afterwards coated with different polyelectrolytes producing two different capsules: light responsive $(PSS/PAH)_2$ Au_{agg} $(PSS/PAH)_2$ capsules composed by non degradable polyelectrolytes, (poly(sodium 4-styrenesulfonate) and poly(allylamine hydrochloride), and biodegradable $(PARG/DEXS)_4$ capsules composed by biodegradable polyelectrolytes (dextran sulfate and poly-L-arginine). The number of polyelectrolyte bilayers was the same, four in each case. The biodegradable capsules did not have gold agglomerates in their wall. It is well known that the size of the encapsulated macromolecule is a key factor towards successful loading. Molecules of around 10 kDa are small enough when using our capsule geometry (by means number of layers, nature of polyelectrolyte, etc.) to diffuse out of the PEM capsules by leaking, if the capsule has not been heat-shrunken after loading. Contrary, if the size of the macromolecule is too big (around 70 kDa), it may be hard to release them via NIR triggered disruption of the capsules. The GFP protein used in the present study had a molecular weight of 35 kDa. In Fig. 4 the release of GFP upon laser irradiation of the capsules can be observed.

The protein has been released in the cytosol successfully without losing activity (fluorescence). The GFP is quasi homogeneously distributed within the cell. This result demonstrates that active proteins can be released with light responsive capsules. The local heating produced after light absorption of the gold nanoparticle agglomerates in the capsule walls is enough to disrupt the polyelectrolyte network of the capsule but not to damage the whole amount of released protein. The fluorescence of GFP is the result of an internal chromophore formed by the autocatalytic post-translational cyclization of three amino acids, Ser65-Tyr66-Gly67. GFP retains its fluorescence capability upon exposure to mild denaturants, heat, detergents, and proteases because of the protected location of the chromophore inside the β-barrel of the protein but the color, the intesity and the photostability of the protein can be anyway affected by changes in the hydrogen-bonding network and the electron-stacking interactions. The fluorescence of GFP can be lost if the ternary structure is destructed [63,64].

As it can be observed in Fig. 4 and in the SI, the amount of released GFP seems to be lower. There are mainly two possible reasons: 1) the size of the protein is bigger than dextran and thusthe quantity of

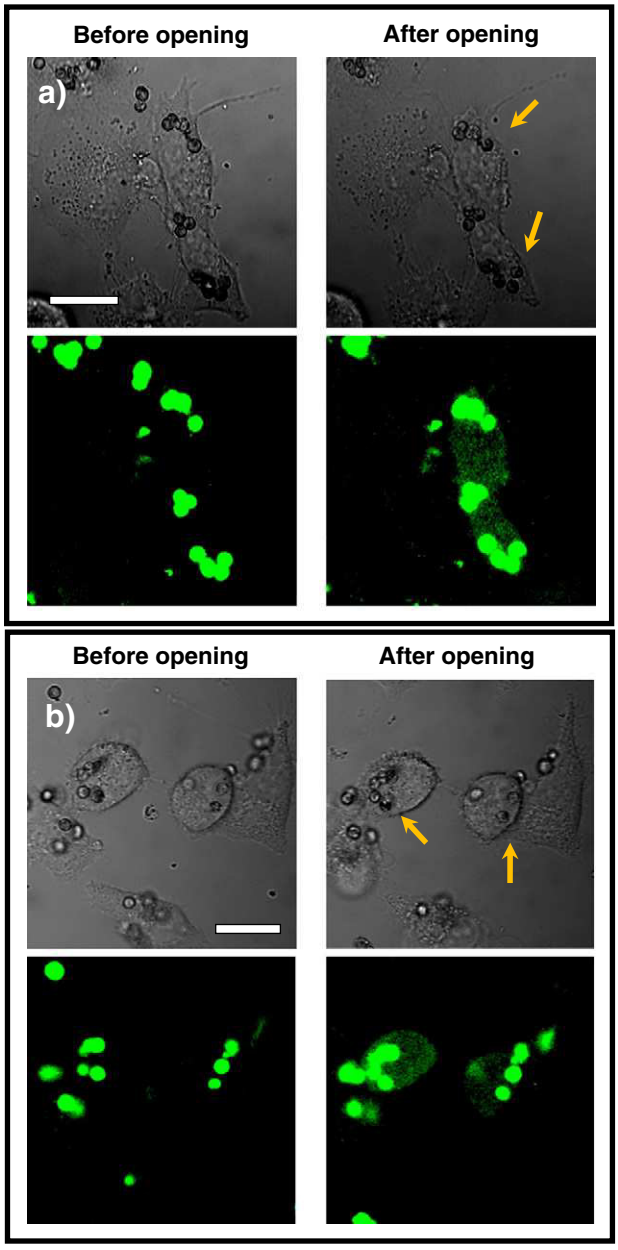

Fig. 4. IR-light triggered remote controlled release of green fluorescent protein in A549 cells (a) and SH-SY5Y neurons (b) $(PSS/PAH)_2$ Au_{agg} $(PSS/PAH)_2$ capsules loaded with GFP were illuminated with an intensity of 3.8 mW/μm^2 for a few seconds. The protein was successfully released in the cytosol, while preserving its fluorescence. The scale bar represents 20 μm. Arrows point at the opened capsules.

delivered cargo is lower or 2) the protein structure of some of the released macromolecules was affecte the presence of fluorescence demonstrates that some GFP remains active. Thus PEM capsules are suited for release of molecules which make all-or-nothing answer, such as siRNA, where the most important point is the presence of the released molecule but not how much. This is, to the best of our knowledge, the first time that a protein has been released from a light responsive container to the cytosolic space in a controlled manner. GFP release triggered by NIR irradiation was also carried out within SH-SY5Y neurons to verify again that the procedure does not depend on a specific cell line (cf. Fig. 4b and SI-21).

In order to demonstrate the particular features of NIR stimulated delivery, GFP was also delivered using biodegrade PEM capsules as microcarriers. Such capsules can be degraded *in vitro* or *in vivo*, *via* various mechanisms depending on the capsule wall [6,65]. Proteins and drugs such as the cancer therapeutic doxorubicin hydrochloride (DOX) have been released from polymeric capsules *via* enzymatic cleavage [11,66]. In our case, dextran sulfate/poly-L-arginine capsules were used as biodegradable carriers as it was mentioned. To verify that the release is not due to protein leakage from the capsule cavity to the cytosol, a third kind of PEM capsule was prepared; non-degradable capsules (made by PSS and PAH) with four bilayers but this time without gold in the wall. This third type of capsules $(PSS/PAH)_4$ have been used in control experiments since the porosity of the wall is affected by the presence/absence of nanoparticles and it is necessary to verify that the release is only due to the biodegradable nature of the (DEXS/PARG) wall. $(DEXS/PARG)_4$ and $(PSS/PAH)_4$ capsules loaded with GFP were incubated in cell medium with human lung carcinoma cells A549. Images were taken every hour. Both types of capsules were incorporated by cells. In Fig. 5 one can see that no release of GFP was observed for the non-degradable capsules $(PSS/PAH)_4$ after 26 h, as it was expected. Contrary, after 3 h cells that had incorporated biodegradable capsules started showing small GFP-

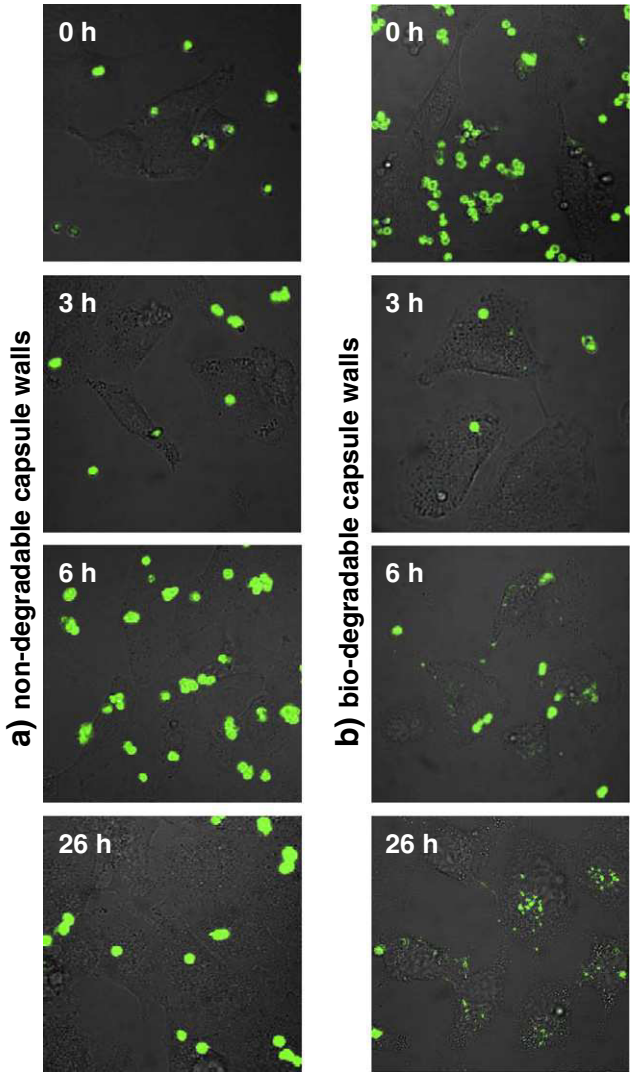

Fig. 5. Delivery of protein cargo with capsules without Au nanoparticles. Human carcinoma A549 cells were incubated with (a) non-degradable $(PSS/PAH)_4$ or (b) degradable $(DEXS/PARG)_4$ capsules filled with GFP as cargo. Images were taken immediately after addition of the capsules ($t = 0$ h) over time up to 26 h with a confocal microscope in different channels, green and transmission (for a detailed description we refer readers to the Supporting Information). An overlay of the different channels is presented in the figures.

containing exocytotic vesicles. After 6 h the release of GFP to small vesicles becomes more evident.

It has to be mentioned that the observation of these vesicles was not easy since the exocytotic vesicles are small compared with the optical resolution and they are distributed at different depths inside the cytosol. Only when the number of exocytotic vesicles per cell was high (after 6 h), the GFP delivery was clearly evident. As an example, in Figure SI-22 images at different positions along the *z* axis are shown. The images correspond to the *z* scan of Fig. 5b after 26 h. In this image it can be also observed that cells proliferated and passed the capsules or GFP vesicles to their respective daughter cells. In this context, cells with GFP vesicles that didn't have internalized GFP capsules can be observed. Results with GFP biodegradable capsules confirmed our previous data in which another protein was used as cargo [11]. GFP released from biodegradable capsules is supposedly located in small intracellular vesicles, which can be deduced from the inhomogeneous localized distribution of GFP fluorescence. On the other hand, GFP released from light responsive capsules via NIR illumination is quasi homogeneously distributed within the cytosol as it has been observed also for peptides [62].

4. Conclusions

Light mediated heating of capsules offers a controlled way for time specific delivering macromolecular cargo to the cytosol. Upon light irradiation capsules decorated with Au nanoparticles are able to release their cargo and deliver encapsulated material directly into the cytosol. Thus, illumination of capsules that have been phagocyted by cells, can trigger intracellular process with externally delivered bioactive compound. Individual optical addressing of the internalized capsules offers the possibility to sequentially release cargo from different capsules inside the same cell. This is in contrast to delivery of cargo with biodegradable capsules where there is no trigger mechanism and delivery time is a factor of capsule wall composition and thickness. Also in case of biodegradability the capsules are likely degraded inside lysosomal compartments while dislocation of cargo by light to cytosol prevents the cargo from undesirable digestion in lysosomal and introduce it for further intracellular processes.

Acknowledgements

This work was supported by the BMBF (Eranet project Nanosyn to WJP). SCR is grateful to the Junta Andalucía for a fellowship. Supporting Information is available online from Wiley InterScience.

Appendix A. Supplementary data

Supplementary data to this article can be found online at doi:10.1016/j.jconrel.2011.12.013.

References

[1] S.N. Bhatia, G. von Maltzahn, J.H. Park, A. Agrawal, N.K. Bandaru, S.K. Das, M.J. Sailor, Computationally guided photothermal tumor therapy using long-circulating gold nanorod antennas, Cancer Res. 69 (9) (2009) 3892–3900.
[2] D.P. O'Neal, L.R. Hirsch, N.J. Halas, J.D. Payne, J.L. West, Photo-thermal tumor ablation in mice using near infrared-absorbing nanoparticles, Cancer Lett. 209 (2) (2004) 171–176.
[3] J.M. McKiernan, L.J. Barlow, M.A. Laudano, M.J. Mann, D.P. Petrylak, M.C. Benson, A phase I trial of intravesical nanoparticle albumin-bound paclitaxel in the treatment of bacillus calmette-guerin refractory nonmuscle invasive bladder cancer. J. Urology 186 (2) (2011) 448–451.
[4] R.A. Alvarez-Puebla, A. Agarwal, P. Manna, B.P. Khanal, P. Aldeanueva-Potel, E. Carbo-Argibay, N. Pazos-Perez, L. Vigderman, E.R. Zubarev, N.A. Kotov, L.M. Liz-Marzan, Gold nanorods 3D-supercrystals as surface enhanced Raman scattering spectroscopy substrates for the rapid detection of scrambled prions, Proc. Natl. Acad. Sci. U. S. A. 108 (20) (2011) 8157–8161.
[5] A.Z. Abbasi, L. Gutierrez, L.L. del Mercato, F. Herranz, O. Chubykalo-Fesenko, S. Veintemillas-Verdaguer, W.J. Parak, M.P. Morales, J.M. Gonzalez, A. Hernando, P. de la Presa, Magnetic capsules for NMR imaging: effect of magnetic nanoparticles spatial distribution and aggregation, J. Phys. Chem. C 115 (14) (2011) 6257–6264.
[6] T. Borodina, E. Markvicheva, S. Kunizhev, H. Möhwald, G.B. Sukhorukov, O. Kreft, Controlled release of DNA from self-degrading microcapsules, Macromol. Rapid Commun. 28 (18–19) (2007) 1894–1899.
[7] X. Zhang, M. Oulad-Abdelghani, A.N. Zelkin, Y.J. Wang, Y. Haikel, D. Mainard, J.C. Voegel, F. Caruso, N. Benkirane-Jessel, Poly(L-lysine) nanostructured particles for gene delivery and hormone stimulation, Biomaterials 31 (7) (2010) 1699–1706.
[8] A.L. Becker, A.P.R. Johnston, F. Caruso, Layer-by-layer-assembled capsules and films for therapeutic delivery, Small 6 (17) (2010) 1836–1852.
[9] L.L. del Mercato, A.Z. Abbasi, W.J. Parak, Synthesis and characterization of ratiometric ion-sensitive polyelectrolyte capsules, Small 7 (2011) 351–363.
[10] A.G. Skirtach, C. Dejugnat, D. Braun, A.S. Susha, W.J. Parak, H. Möhwald, G.B. Sukhorukov, The role of metal nanoparticles in remote release of encapsulated materials, Nano Lett. 5 (7) (2005) 1371–1377.
[11] P. Rivera_Gil, S. de Koker, B.G. de Geest, W.J. Parak, Intracellular processing of proteins mediated by biodegradable polyelectrolyte capsules, Nano Lett. 9 (12) (2009) 4398–4402.
[12] J. Cui, Y. Wang, A. Postma, J. Hao, L. Hosta-Rigau, F. Caruso, Monodisperse polymer capsules: tailoring size, shell thickness, and hydrophobic cargo loading via emulsion templating. Adv. Funct. Mater. 20 (10) (2010) 1625–1631.
[13] U. Bazylinska, R. Skrzela, K. Szczepanowicz, P. Warszynski, K.A. Wilk, Novel approach to long sustained multilayer nanocapsules: influence of surfactant head groups and polyelectrolyte layer number on the release of hydrophobic compounds. Soft Matter 7 (13) (2011) 6113–6124.
[14] W. Tong, Y. Zhu, Z. Wang, C. Gao, H. Möhwald, Micelles-encapsulated microcapsules for sequential loading of hydrophobic and water-soluble drugs. Macromol. Rapid Commun. 31 (11) (2010) 1015–1019.
[15] G. Han, P. Ghosh, V.M. Rotello, Multi-functional gold nanoparticles for drug delivery, Adv. Exp. Med. Biol. 620 (2007) 48–56.
[16] H.K. Valo, P.H. Laaksonen, L.J. Peltonen, M.B. Linder, J.T. Hirvonen, T.J. Laaksonen, Multifunctional hydrophobin: toward functional coatings for drug nanoparticles, ACS Nano 4 (3) (2010) 1750–1758.
[17] N.O. Dhoot, M.A. Wheatley, Microencapsulated liposomes in controlled drug delivery: strategies to modulate drug release and eliminate the burst effect, J. Pharm. Sci. 92 (3) (2003) 679–689.
[18] K.T. Kim, S.A. Meeuwissen, R.J. Nolte, J.C. van Hest, Smart nanocontainers and nanoreactors, Nanoscale 2 (6) (2010) 844–858.
[19] S. de Koker, L.J. de Cock, P. Rivera-Gil, W.J. Parak, R. Auzely Velty, C. Vervaet, J.P. Remon, J. Grooten, B.G. de Geest, Polymeric multilayer capsules delivering biotherapeutics, Adv. Drug Deliv. Rev. 63 (9) (2011) 748–761.
[20] S. de Koker, B.G. de Geest, C. Cuvelier, L. Ferdinande, W. Deckers, W.E. Hennink, S. de Smedt, N. Mertens, In vivo cellular uptake, degradation, and biocompatibility of polyelectrolyte microcapsules, Adv. Funct. Mater. 17 (18) (2007) 3754–3763.
[21] M. Bedard, B. de Geest, A. Skirtach, H. Möhwald, G. Sukhorukov, Polymeric microcapsules with light responsive properties for encapsulation and release, Adv. Colloid Interface Sci. 158 (1–2) (2010) 2–14.
[22] A.G. Skirtach, P. Karageorgiev, B. de Geest, N. Pazos-Perez, D. Braun, G.B. Sukhorukov, Nanorods as wavelength-selective absorption centers in the visible and Nnear-infrared regions of the electromagnetic spectrum, Adv. Mater. 20 (2008) 506–510.
[23] A.R. Lowery, A.M. Gobin, E.S. Day, N.J. Halas, J.L. West, Immunonanoshell laser-assisted therapy targets and ablates tumor cells, Breast Cancer Res. Treat. 100 (2006) S289–S.
[24] E.B. Dickerson, E.C. Dreaden, X. Huang, I.H. El-Sayed, H. Chu, S. Pushpanketh, J.F. McDonald, M.A. El-Sayed, Gold nanorod assisted near-infrared plasmonic photothermal therapy (PPTT) of squamous cell carcinoma in mice, Cancer Lett. 269 (1) (2008) 57–66.
[25] R. Bardhan, S. Lal, A. Joshi, N.J. Halas, Theranostic nanoshells: from probe design to imaging and treatment of cancer, Acc. Chem. Res. 44 (10) (2011) 936–946.
[26] Z. Krpetic, P. Nativo, V. See, I.A. Prior, M. Brust, M. Volk, Inflicting controlled nonthermal damage to subcellular structures by laser-activated gold nanoparticles, Nano Lett. 10 (11) (2010) 4549–4554.
[27] A. Agarwal, M.A. MacKey, M.A. El-Sayed, R.V. Bellamkonda, Remote triggered release of doxorubicin in tumors by synergistic application of thermosensitive liposomes and gold nanorods, ACS Nano 5 (6) (2011) 4919–4926.
[28] R. Huschka, J. Zuloaga, M.W. Knight, L.V. Brown, P. Nordlander, N.J. Halas, Light-induced release of DNA from gold nanoparticles: nanoshells and nanorods, J. Am. Chem. Soc. 133 (31) (2011) 12247–12255.
[29] G. Baffou, R. Quidant, F.J. Garcia de Abajo, Nanoscale control of optical heating in complex plasmonic systems, ACS Nano 4 (2) (2010) 709–716.
[30] C. Kirchner, A.M. Javier, A.S. Susha, A.L. Rogach, O. Kreft, G.B. Sukhorukov, W.J. Parak, Cytotoxicity of nanoparticle-loaded polymer capsules, Talanta 67 (2005) 486–491.
[31] A. Muñoz_Javier, P. del Pino, M. Bedard, A.G. Skirtach, D. Ho, G. Sukhorukov, C. Plank, W.J. Parak, Photoactivated release of cargo from the cavity of polyelectrolye capsules to the cytosol of cells, Langmuir 24 (2009) 12517–12520.
[32] A.M. Pavlov, A.V. Sapelkin, X. Huang, K.M.Y. P'ng, A.J. Bushby, G.B. Sukhorukov, A.G. Skirtach, Neuron cells uptake of polymeric microcapsules and subsequent intracellular release, Macromol. Biosci. 11 (6) (2011) 848–854.
[33] G.B. Sukhorukov, D.V. Volodkin, A.M. Günther, A.I. Petrov, D.B. Shenoy, H. Möhwald, Porous calcium carbonate microparticles as templates for encapsulation of bioactive compounds, J. Mater. Chem. 14 (2004) 2073–2081.
[34] P. Moulin, H. Roques, Zeta potential measurement of calcium carbonate, J. Colloid Interface Sci. 261 (1) (2003) 115–126.

[35] K. Velikov, P. Versluis, A. Popp, Interaction between biopolyelectrolytes and sparingly soluble mineral particles, Langmuir 27 (1) (2011) 83–90.
[36] B.V. Enustun, J. Turkevich, Coagulation of colloidal gold, J. Am. Chem. Soc. 85 (21) (1963) 3317–3328.
[37] L. Dähne, S. Leporatti, E. Donath, H. Möhwald, Fabrication of micro reaction cages with tailored properties, J. Am. Chem. Soc. 123 (23) (2001) 5431–5436.
[38] A.S. Angelatos, B. Radt, F. Caruso, Light-responsive polyelectrolyte/gold nanoparticle microcapsules, J. Phys. Chem. B 109 (2005) 3071–3076.
[39] Z. Lu, M.D. Prouty, Z. Guo, V.O. Golub, C.S. Kumar, Y.M. Lvov, Magnetic switch of permeability for polyelectrolyte microcapsules embedded with Co–Au nanoparticles, Langmuir 21 (5) (2005) 2042–2050.
[40] A.M. Pavlov, V. Saez, A. Cobley, J. Graves, G.B. Sukhorukov, T.J. Mason, Controlled protein release from microcapsules with composite shells using high frequency ultrasound-potential for in vivo medical use, Soft Matter 7 (9) (2011) 4341–4347.
[41] L.L. del Mercato, E. Gonzalez, A.Z. Abbasi, W.J. Parak, V. Puntes, Synthesis and evaluation of gold nanoparticle-modified polyelectrolyte capsules under microwave irradiation for remotely controlled release for cargo, J. Mater. Chem. 21 (31) (2011) 11468–11471.
[42] N. Antipina Maria, G.B. Sukhorukov, Remote control over guidance and release properties of composite polyelectrolyte based capsules, Adv. Drug Deliv. Rev. 63 (9) (2011) 716–729.
[43] B. Radt, T.A. Smith, F. Caruso, Optically addressable annostructured capsules, Adv. Mater. 16 (23–24) (2004) 2184–2189.
[44] M. Bedard, D. Braun, G.B. Sukhorukov, A.G. Skirtach, Toward self-assembly of nanoparticles on polymeric microshells: near-IR release and permeability, ACS Nano 2 (9) (2008) 1807–1816.
[45] S.K. Dondapati, T.K. Sau, C. Hrelescu, T.A. Klar, F.D. Stefani, J. Feldmann, Label-free biosensing based on single gold nanostars as plasmonic transducers, ACS Nano 4 (11) (2010) 6318–6322.
[46] L.L. del Mercato, P. Rivera_Gil, A.Z. Abbasi, M. Ochs, C. Ganas, I. Zins, C. Sönnichsen, W.J. Parak, LbL multilayer capsules: recent progress and future outlook for their use in life sciences, Nanoscale 2 (4) (2010) 458–467.
[47] Z. She, M.N. Antipina, J. Li, G.B. Sukhorukov, Mechanism of protein release from polyelectrolyte multilayer microcapsules, Biomacromolecules 11 (5) (2010) 1241–1247.
[48] P. Rivera_Gil, L.L. del Mercato, P. del Pino, A. Muñoz_Javier, W.J. Parak, Nanoparticle-modified polyelectrolyte capsules, Nano Today 3 (3–4) (2008) 12–21.
[49] K. Köhler, G.B. Sukhorukov, Heat treatment of polyelectrolyte multilayer capsules: a versatile method for encapsulation, Adv. Funct. Mater. 17 (13) (2007) 2053–2061.
[50] D.V. Volodkin, A.I. Petrov, M. Prevot, G.B. Sukhorukov, Matrix polyelectrolyte microcapsules: new system for macromolecule encapsulation, Langmuir 20 (8) (2004) 3398–3406.
[51] O. Kreft, A. Muñoz_Javier, G.B. Sukhorukov, W.J. Parak, Polymer microcapsules as mobile local pH-sensors, J. Mater. Chem. 17 (2007) 4471–4476.
[52] J. Han, A. Loudet, R. Barhoumi, R.C. Burghardt, K. Burgess, A ratiometric pH reporter for imaging protein-dye conjugates in living cells, J. Am. Chem. Soc. 131 (5) (2009) 1642–1643.
[53] L.I. Kazakova, L.I. Shabarchina, G.B. Sukhorukov, Co-encapsulation of enzyme and sensitive dye as a tool for fabrication of microcapsule based sensor for urea measuring, Phys. Chem. Chem. Phys. 13 (23) (2011) 11110.
[54] R.F. Murphy, S. Powers, C.R. Cantor, endosome pH measured in single cells by dual fluorescence flow cytometry: rapid acidification of insulin to pH 6, J. Cell Biol. 98 (5) (1984) 1757–1762.
[55] R. Orij, J. Postmus, A. Ter Beek, S. Brul, G.J. Smits, In vivo measurement of cytosolic and mitochondrial pH using a pH-sensitive GFP derivative in *Saccharomyces cerevisiae* reveals a relation between intracellular pH and growth, Microbiology 155 (1) (2009) 268–278.
[56] W.R. Gombotz, D.K. Pettit, Biodegradable polymers for protein and peptide drug delivery, Bioconjug. Chem. 6 (4) (1995) 332–351.
[57] N.W. Kam, H. Dai, Carbon nanotubes as intracellular protein transporters: generality and biological functionality, J. Am. Chem. Soc. 127 (16) (2005) 6021–6026.
[58] L.E. Bromberg, E.S. Ron, Temperature-responsive gels and thermogelling polymer matrixes for protein and peptide delivery, Adv. Drug Deliv. Rev. 31 (3) (1998) 197–221.
[59] N.G. Balabushevitch, G.B. Sukhorukov, N.A. Moroz, D.V. Volodkin, N.I. Larionova, E. Donath, H. Möhwald, Encapsulation of proteins by layer-by-layer adsorption of polyelectrolytes onto protein aggregates: factors regulating the protein release, Biotechnol. Bioeng. 76 (3) (2001) 207–213.
[60] V.R. Sinha, A. Trehan, Biodegradable microspheres for protein delivery, J. Control. Release 90 (3) (2003) 261–280.
[61] I.M. Abdulagatov, U.B. Magomedov, Thermal conductivity of aqueous solutions of Nacl and Kcl at high pressures, Int. J. Thermophys. 15 (3) (1994) 401–413.
[62] R. Palankar, A.G. Skirtach, O. Kreft, M. Bedard, M. Garstka, K. Gould, H. Möhwald, G.B. Sukhorukov, M. Winterhalter, S. Springer, Controlled intracellular release of peptides from microcapsules enhances antigen presentation on MHC class I molecules, Small 5 (19) (2009) 2168–2176.
[63] L.C.d.L. Novaes, P.G. Mazzola, A. Pessoa, Jr., T.C.V. Penna, Citrate and phosphate influence on green fluorescent protein thermal stability. Biotechnol. Prog. 27 (1) (2010) 269–272.
[64] J.-R. Huang, T.D. Craggs, J. Christodoulou, S.E. Jackson, Stable intermediate states and high energy barriers in the unfolding of GFP, J. Mol. Biol. 370 (2) (2007) 356–371.
[65] C. Priest, A. Quinn, A. Postma, A.N. Zelikin, J. Ralston, F. Caruso, Microfluidic polymer multilayer adsorption on liquid crystal droplets for microcapsule synthesis, Lab Chip 8 (12) (2008) 2182–2187.
[66] C.J. Ochs, G.K. Such, Y. Yan, M.P. van Koeverden, F. Caruso, Biodegradable click capsules with engineered drug-loaded multilayers, ACS Nano 4 (3) (2010) 1653–1663.

Intracellular Release

DOI: 10.1002/anie.201206696

Light-Addressable Capsules as Caged Compound Matrix for Controlled Triggering of Cytosolic Reactions**

*Markus Ochs, Susana Carregal-Romero, Joanna Rejman, Kevin Braeckmans, Stefaan C. De Smedt, and Wolfgang J. Parak**

Layer-by-layer assembly was introduced almost two decades ago as a versatile technique for the construction of thin multiple-layer films composed out of polyelectrolytes.[1,2] Shortly after, the concept was extended from planar to spherical geometry, resulting in polyelectrolyte multilayer capsules.[3–5] The semipermeable wall of the capsules (with a thickness of a few nanometers)[6,7] and the cavity can be further loaded with inorganic colloidal nanoparticles (NPs) made of different materials and with multiple cargos,[8–10] respectively (Figure 1). The resulting multifunctional capsules are well-suited for in vitro delivery of cargo inside cells.[11,12] This concept has been highlighted in several recent reviews.[13–15] Meanwhile technology has advanced to a point at which these capsules could be a helpful tool for controlled multifunctional in vitro delivery. Nowadays the cavity of capsules can be loaded with a large variety of cargo. While large molecules such as proteins will be readily kept inside the cavity, small molecules need to be either linked to macromolecules such as dextran,[16] or be embedded inside micelles.[17] The micelle approach even allows for encapsulation of small hydrophobic molecules. The materials forming the polyelectrolyte wall can be chosen such that capsules internalized by cells are not degraded and preserve their cargo over weeks. Leakage of the cargo molecule is reduced and controlled release of cargo upon external stimuli can be performed.

A large number of capsules can be taken up by cells in vitro without causing acute cytotoxicity, even for capsules with large sizes of around 5 μm.[18–20] It is conceivable that if cells are exposed simultaneously to different types of capsules with similar layer composition, they will internalize them with a statistical distribution. To demonstrate this we exposed cells to a mixture of four types of capsules loaded with different fluorescently labeled dextrans emitting blue, green, red, or near-infrared light (Figure 2A) corresponding to Cascade Blue, fluorescein isothiocyanate, AlexaFluor594, and Dy647, respectively. HeLa cells were incubated with amounts of capsules equivalent to two, four, or six capsules of each color per cell for four hours. Figure 2B presents the number of capsules of each color internalized per cell. When six capsules of each color (i.e. 24 capsules in total) were added per cell, 50% of the cells had internalized at least one capsule of each color. Contrary, when only two capsules per cell of the four kinds were added the percentage dropped to less than 20%. These findings demonstrate the feasibility to simultaneously load cells with a variety of encapsulated cargos.

The loading of cells can be specifically directed by incorporating magnetic NPs in the wall of the capsules. This is possible since magnetic field gradients, which are created by positioning a magnet in a flow channel system, trap the capsules close to the magnet.[21] This method can ultimately be used to achieve specific capsule distribution patterns in the cell culture or in vivo for certain applications. Figure 2C,D shows the results of an experiment demonstrating the targeted deposition of differently colored capsules in a submillimeter pattern. A magnet with an edge length of 5 mm (ca. 1,3 T) was modified with two iron slips on top (width ca. 800 μm) that apply the magnetic field in the shape of two stripes underneath a flow channel, which simulates blood

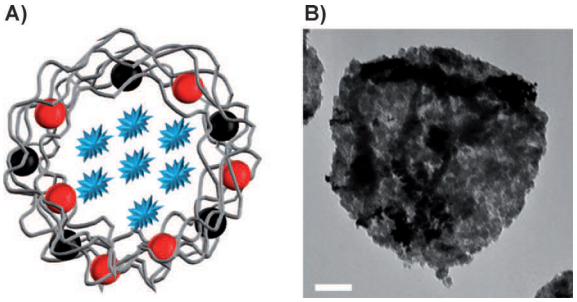

Figure 1. A) Schematic representation of a capsule with walls produced via layer-by-layer assembly (gray). The cavity of the capsule is loaded with a cargo (blue). The wall of the capsule contains magnetic (black) and plasmonic (red) NPs. B) A representative transmission electron microscopy (TEM) image of a capsule with a large amount of magnetic Fe_2O_3 and plasmonic Au NPs in its walls. The scale bar corresponds to 1 μm.

[*] M. Ochs,[+] Dr. S. Carregal-Romero,[+] Prof. W. J. Parak
Fachbereich Physik and WZWM, Philipps Universität Marburg
Renthof 7, 35037 Marburg (Germany)
E-mail: wolfgang.parak@physik.uni-marburg.de
Dr. S. Carregal-Romero[+]
Bionand. Severo Ochoa 35, 29590 Málaga (Spain)
Dr. J. Rejman, Prof. K. Braeckmans, Prof. S. C. De Smedt
Laboratory of General Biochemistry and Physical Pharmacy
Ghent University
Harelbekestraat 72, Ghent (Belgium)
Prof. K. Braeckmans
Center for Nano and Biophotonics, Ghent University
Harelbekestraat 72, Ghent (Belgium)

[+] These authors contributed equally to this work.

[**] This work was supported by BMBF/ERANET (project Nanosyn) and the DFG (project PA794/11.1). We acknowledge technical discussions with Drs. Rafael Fernandez Chacón, Loretta del Mercato, Arnold Grünweller, Roland Hartmann, Pilar Riveral Gil and Gleb B. Sukhorukov.

Supporting information for this article is available on the WWW under http://dx.doi.org/10.1002/anie.201206696.

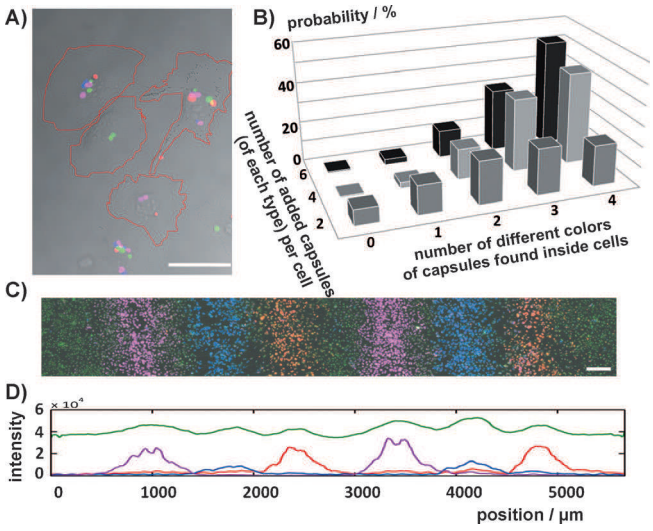

Figure 2. A) HeLa cells were incubated with a homogeneous mixture of fluorescent capsules in blue, green, red, and violet. An overlay of phase contrast and different fluorescence images is shown. The scale bar corresponds to 50 µm. Cell borders are indicated by red lines. B) Two, four, or six capsules of each type per cell were added to the culture medium. The probability of observing in one cell 0, 1, 2, 3, and 4 capsules of different color is plotted. C) Lateral arrangement of fluorescent capsules within a cell culture owing to magnetic guidance in a flow chamber. The scale bar corresponds to 250 µm. D) Corresponding fluorescence intensity of each color along the flow channel shown in (C). The green fluorescence signal belongs to cell staining with AlexaFluor488 useful to colocalize the fluorescent signals from capsules and cells.

stream, in which the cells were cultured. Capsules loaded with a fluorescent dye linked to dextran and magnetic NPs were added and allowed to circulate in the flow medium above the cells for ten minutes. Then the magnet was moved along the channel, and a new type of capsules loaded with another fluorophore was added to the flow medium for ten minutes. This procedure was repeated, and the magnet was moved along the channel in distance steps of 800 µm. The respective capsules were trapped close to the position of the magnet, locally concentrated, and subsequently internalized by the cells. This procedure allowed for obtaining a submillimeter resolution level of the patterns. In summary, capsules with different cargo can be directed by magnetic field gradients to specific regions of a cell culture.

Most cell types internalize capsules in a nonspecific way through different endocytotic pathways, whereby most of the capsules ultimately are located inside lysosomes.[18] Capsules modified with plasmonic NPs allow for releasing cargo from lysosomes to the cytosol by photothermal heating.[22–25] This is similar to the classical concept of light-controlled release of caged compounds (such as caged calcium) inside cells.[26] Our approach, however, allows light-controlled release of a much larger class of molecules and also subsequent release of different molecules. Moreover, the technique to open the capsules is applied on individual capsules, thereby permitting sequential opening of different capsules within one cell.[27] Local disruption of the capsule walls also leads to (transient) permeability of the membrane of the lysosomes in which the illuminated capsules are located. Release however can be triggered in a controlled way with keeping the biological activity of the cargo molecule and with tolerable effects on cellular viability.[22,27] The appropriate intensity of the infrared laser pointer was studied previously.[22] Au NPs were loaded at high density to the capsule walls, as photothermally deposited heat increases for larger clusters.[28] Here, we demonstrate that this approach can be employed to orchestrate intracellular reactions. We have studied the triggering of an enzymatic reaction upon consecutive opening of capsules containing either the enzyme or the substrate (Figure 3). Alkaline phosphatase (enzyme) converts ELF97 phosphate (substrate) into green fluorescent ELF97 alcohol (Figure 3A). These two cargos were loaded separately in two different types of capsules and delivered into the same cell. Both capsules, which had Au NPs in their walls, were independently opened with a light pointer (intensity 3 mW µm^{-2} for 1 s), which had been focused on the respective capsule. As a result the contents of the capsules (the enzyme or the substrate) were released into the cytosol (Figure 3). The substrate in its original state is a phosphorylated (and thus quenched) fluorophore. When only the substrate or the enzyme was released into the cytosol by light-controlled opening of one of the capsules no effect was observed (Figure 3C,F). However, after the opening of the second capsule with the complementary cargo, that is, the capsule with ELF97 phosphate or enzyme, by a second illumination, both cargos were colocated. Interaction between the substrate and the enzyme resulted in the formation of the fluorescent product, ELF97 alcohol, which precipitated at the site of the enzymatic reaction (Figure 3D,G). Production of the fluorescent product was either observed when first the substrate and second the enzyme were released or vice versa (Figure 3E–G). It is important to stress that reactions (as observed by onset of fluorescence) only occurred after successful opening of both types of capsules in the same cell.

The opening sequence mattered in the sense that the fluorescent compound formed after cleavage of the phosphate group settled down as a nonsoluble precipitate at the site where the second capsule was opened, irrespective of its content being the enzyme or the substrate. The reason for this observation is the much higher concentration of released material inside/around the last opened capsule compared to the surrounding cytosol. The efficiency of cytosolic release was around 50% (see the Supporting Information). To demonstrate that triggering of enzymatic reactions is not cell-phenotype dependent, the same experiments were performed on two more cell lines (MCF-7 and MDA-MB-231, see the Supporting Information). Finally, all these experiments demonstrate that sequential release of encapsulated materials can trigger reactions with not only one but also multiple reactive compounds inside cells.

Moreover, reaction kinetics can be recorded. The potentially strongest asset of light-mediated release lies in the possibility to employ it to follow processes in time. We demonstrate the feasibility of that approach by employing mRNA encoding green fluorescent protein (GFP). Conventionally, mRNA can be delivered to cells in the form of lipoplexes or polyplexes. These complexes are taken up by the

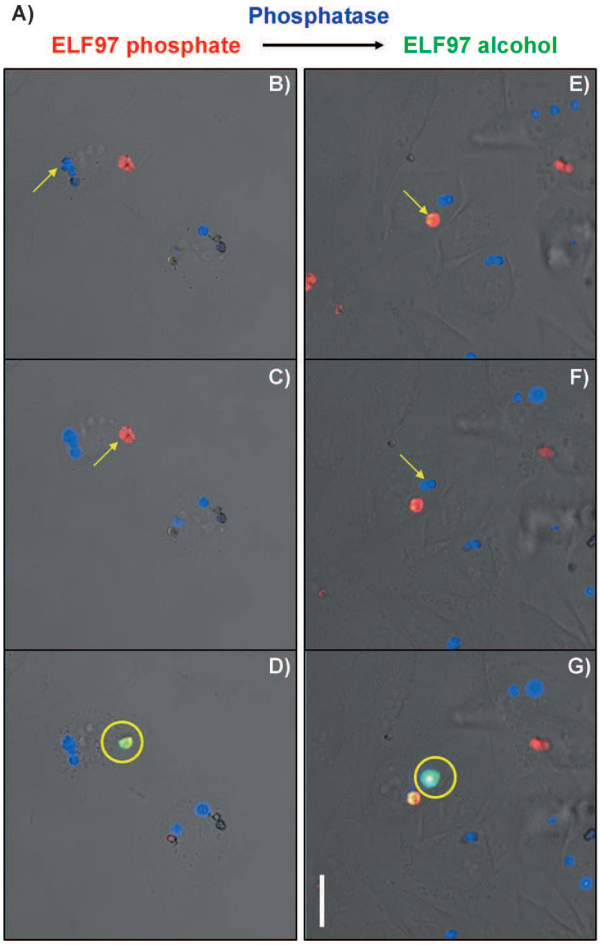

Figure 3. Alkaline phosphatase and ELF97 phosphate are sequentially released by light-controlled heating from capsules modified with Au NPs. A) Capsules were filled with Cascade Blue–dextran and the enzyme alkaline phosphatase (AP, blue capsules) or AlexaFluor594–dextran and the substrate ELF97 phosphate (red capsules). Fluorescently labeled dextran derivatives were co-encapsulated, because both the enzyme and the substrate are nonfluorescent by themselves. When the enzyme and the substrate interact with each other, alkaline phosphatase cleaves the phosphate group of ELF97 phosphate, thereby producing ELF97 alcohol, which is a yellow-green fluorescent precipitate. HeLa cells were incubated with both types of capsules. Only cells that contained at least one capsule of each type were selected. Capsules filled with alkaline phosphatase (B) or ELF97 phosphate (E) were first opened with a light pointer, as indicated by yellow arrows. In a next step the complementary capsules with ELF97 phosphate (C) or alkaline phosphatase (F) were opened, as indicated again by yellow arrows. Enzymatic processing of ELF97 phosphate by alkaline phosphatase led to the production of the green fluorescent product ELF97 alcohol (D, G). The scale bar corresponds to 25 μm.

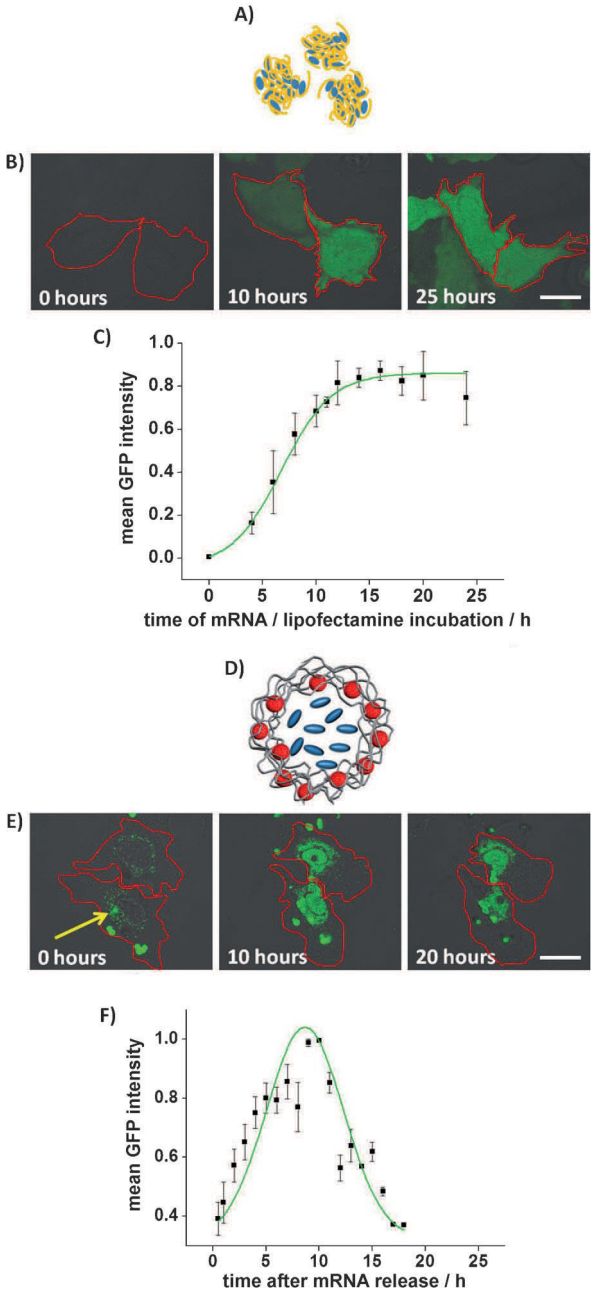

Figure 4. A) Lipoplexes or polyplexes (yellow) as carrier systems of mRNA encoding GFP (drawn in blue). B) Confocal images of the expression of GFP in HeLa cells using the transfection agent lipofectamine as carrier system. C) The mean fluorescence intensity per cell is plotted versus the incubation time. D) Light-responsive capsules as carrier systems of mRNA encoding GFP. Polyelectrolytes (gray), Au NPs (red), and mRNA (blue). E) Confocal images of capsules internalized by HeLa cells. Capsules were irradiated with a light pointer, as indicated by the yellow arrow. At time $t = 0$ mRNA is released into the cytosol where GFP expression started. F) The mean fluorescence intensity per cell in which one capsule was opened is plotted versus the time after capsule opening. Cell borders are indicated by red lines. Scale bars correspond to 20 μm.

cells by means of endocytosis. To ensure protein production the complexes need to escape from the lysosome and mRNA needs to be released into the cytosol to produce the encoded protein (Figure 4). The process can be monitored by plotting GFP fluorescence versus time. If mRNA is conventionally delivered by cationic lipids or polymers, the observed protein production kinetics are a convolution of three distinct processes: the uptake of the polyplexes/lipoplexes, their release from the lysosome to the cytosol, and translation of mRNA in the cytosol (Figure 4 A–C). Since uptake of polyplexes/lipoplexes by cells is a statistical process over the time period of hours one cannot give the "time point zero" at

which the mRNA is actually present in the cytosol. To overcome this shortcoming, we encapsulated mRNA by using a coprecipitation method in capsules with Au NPs in their walls. The size of mRNAs is in the range of hundreds of kDa, and therefore leakage is avoided owing to steric hindrance. After internalization by cells these capsules resided in lysosomes without releasing any mRNA. Release of mRNA was triggered only by light-mediated opening of the capsules. In this way the starting point at which mRNA is first present in the cytosol can be precisely defined by the externally controlled opening process. Kinetics of protein production are thus no longer convoluted with kinetics of polyplex/lipoplex delivery and thus can be recorded independently (Figure 4 D–F). Furthermore, as the release of mRNA is triggered in a "burst-like" way, there is only one distinct event in which the encapsulated mRNA is released. This event results in fluorescence intensity curves of GFP that have a Gaussian distribution with an intensity maximum around ten hours after induced release. In contrast, as shown in Figure 4 C, mRNA delivered by cationic lipids is available for translation over an extended period of time. Therefore, the amount of produced GFP and subsequent fluorescence intensity is growing to a rather constant value and is stable for long time.[29] In summary, light-mediated release of encapsulated cargo can be used to directly record kinetics of reactions that are triggered by the cargo in the cytosol.

We think that one of the major advantages of the proposed method is the possibility to record kinetics of intracellular processes independently from cellular uptake processes and carrier system degradation. This method could be used for in vitro screening of the effects of molecular cargo released in a controlled way into the cytosol. The possibility to deliver capsules with different cargos to different parts of a cell population by using magnetic field gradients (Figure 2), combined with the ability to release the cargo of capsules individually (Figure 3), could allow for screening of the effects of several cargos and their combinations. It should be kept in mind, however, that upon light-mediated release, the membrane of the intracellular compartment in which the treated capsule is confined is locally perforated, as otherwise no release into the cytosol could occur. The applied mechanical and thermal stress can clearly lead to acute cell death. If the light energy transferred to the gold NPs and herein the resulting temperature increase is too high, treated cells die immediately. Nevertheless, if the correct parameters of light power and beam focus are found, opening of capsules is well-tolerated by cells. In particular, as our methods are based on single cells, impaired cells can be discarded from analysis. Nevertheless, as shown herein (Figure 4), our approach did not affect the biological activity of such a notoriously unstable molecule as mRNA. Nonetheless, for triggered-release experiments using the capsules as demonstrated here, interference of cytotoxic effects has to be considered, and only appropriate experiments can be chosen that have no dominant effect on the intracellular metabolism. At the current state, quantitative release is difficult to achieve owing to, for example, inhomogeneous loading of capsules with cargo and Au NPs, dependence on the illumination protocol (power density and illumination time), and incomplete release upon light-mediated opening.[30] Thus, the system is most suited to study the kinetics of reactions in which only the mere presence of the released cargo in the cytosol but not its quantity is of relevance, as it is for example the case for the mRNA experiment shown in Figure 4. Moreover, this approach offers the greatest advantage for reactions that occur on a short time scale, that is, within a couple of hours. For much slower reactions the cargo can be introduced through classical incorporation with polyplexes/lipoplexes, because in this case the uptake and cytosolic delivery would happen on a smaller time scale than the actual reaction and thus would not interfere with the reaction kinetics. We want to emphasize in particular the possibility to release different cargos independently at designated time points within the same cell. One could think of releasing different mRNA molecules at different time points and record interactions of expressed proteins. Thus we believe that the methodology described herein already offers a great potential for numerous in vitro applications. In vivo applications would face further challenges. Even though capsules have been successfully used for vaccination purposes,[31,32] other in vivo applications have to cope with targeting, clearance of capsules by the immune system, and long-term cytotoxic effects. Another issue is that visible light is strongly absorbed by tissue. Even when NIR light in the "biologically friendly window" of the electromagnetic spectrum is used,[33,34] homogeneous illumination of capsules in tissue is a challenge. However, optical excitation of plasmonic NPs could be replaced by radiofrequency excitation of magnetic NPs.[35,36] Modern set-ups for magnetic-resonance imaging (MRI) already allow to follow individual cells in vivo. Sequential opening of different capsules might be even feasible by employing magnetic NPs of different resonance frequencies and different radiofrequency ranges, which in the future may facilitate externally triggered release from capsules also in vivo.

Experimental Section

Polyelectrolyte capsules loaded with different cargo molecules in the inner cavity and magnetic and/or plasmonic nanoparticles within the wall were synthesized according to procedures described in the literature.[17,27,21] In the Supporting Information a detailed explanation of the strategies used to encapsulate the different cargos has been reported. mRNA was produced by in vitro transcription with appropriate plasmids (pGEM4*Z*/*E*GFP/A64 or pBlue-Luc-A50 or pCXCR4).[29] They were first purified using a QIAquick PCR purification kit (Qiagen) and linearized using restriction enzymes (Dra I for plasmid encoding firefly luciferase or Spe I for plasmid encoding GFP or Xba I for plasmid encoding CXCR4). The mRNA concentration was determined by measuring the absorbance at 260 nm. mRNA was stored in small aliquots at −80 °C at a concentration of 1 $\mu g\,\mu L^{-1}$. Lipofectamine lipoplexes loaded with mRNA encoding GFP (mGFP) protein were prepared by mixing Lipofectamine™ 2000 purchased from Invitrogen and mGFP in OptiMem media as it was described.[29] The basic setup for microscopic observation and experimental progress consisted of a wide-field fluorescence microscope Axiovert200M from Zeiss. The microscope was coupled with an 830 nm IR laser. The maximum light power reaching the sample plane on top of the used 63×/1.4 oil immersion Plan-Apochromat objective was approximately 30 mW (continuous output). The light energy is dispersed on an oval spot of about 6 μm^2. With a tunable power supply the output power of the laser can be

varied smoothly from 0 to 30 mW effective light power on the sample plane. Capsules were opened upon irradiation with laser intensities between 2.5 and 3 mW μm^{-2} during 1–2 seconds.

Received: August 18, 2012
Revised: October 25, 2012
Published online: ■■ ■■, ■■■■

Keywords: enzyme catalysis · gene expression · nanoparticles · polymeric capsules

[1] G. Decher, J. D. Hong, *Makromol. Chem. Macromol. Symp.* **1991**, *46*, 321.
[2] G. Decher, J. D. Hong, J. Schmitt, *Thin Solid Films* **1992**, *210*, 831.
[3] E. Donath, G. B. Sukhorukov, F. Caruso, S. A. Davis, H. Möhwald, *Angew. Chem.* **1998**, *110*, 2323; *Angew. Chem. Int. Ed.* **1998**, *37*, 2201.
[4] C. S. Peyratout, L. Daehne, *Angew. Chem.* **2004**, *116*, 3850; *Angew. Chem. Int. Ed.* **2004**, *43*, 3762.
[5] Y. Wang, A. S. Angelatos, F. Caruso, *Chem. Mater.* **2008**, *20*, 848.
[6] T. Mauser, C. Dejugnat, G. B. Sukhorukov, *J. Phys. Chem. B* **2006**, *110*, 20246.
[7] D. G. Shchukin, G. B. Sukhorukov, H. Möhwald, *Adv. Colloid Interface Sci.* **2010**, *158*, 2.
[8] N. A. Kotov, I. Decany, J. H. Fendler, *J. Phys. Chem.* **1995**, *99*, 13065.
[9] F. Caruso, *Chem. Eur. J.* **2000**, *6*, 413.
[10] D. G. Shchukin, G. B. Sukhorukov, H. Möhwald, *Angew. Chem.* **2003**, *115*, 4610; *Angew. Chem. Int. Ed.* **2003**, *42*, 4472.
[11] A. Muñoz Javier, O. Kreft, A. Piera Alberola, C. Kirchner, B. Zebli, A. S. Susha, E. Horn, S. Kempter, A. G. Skirtach, A. L. Rogach, J. Rädler, G. B. Sukhorukov, M. Benoit, W. J. Parak, *Small* **2006**, *2*, 394.
[12] S. De Koker, B. G. De Geest, S. K. Singh, R. De Rycke, T. Naessens, Y. Van Kooyk, J. Demeester, S. De Smedt, J. Grooten, *Angew. Chem.* **2009**, *121*, 8637; *Angew. Chem. Int. Ed.* **2009**, *48*, 8485.
[13] S. De Koker, R. Hoogenboom, B. G. De Geest, *Chem. Soc. Rev.* **2012**, *41*, 2867.
[14] A. P. Esser-Kahn, S. A. Odom, N. R. Sotos, S. R. White, J. S. Moore, *Macromolecules* **2011**, *44*, 5539.
[15] A. Johnston, G. Such, F. Caruso, *Angew. Chem.* **2010**, *122*, 2723; *Angew. Chem. Int. Ed.* **2010**, *49*, 2664.
[16] O. Kreft, A. Muñoz Javier, G. B. Sukhorukov, W. J. Parak, *J. Mater. Chem.* **2007**, *17*, 4471.
[17] W. Tong, Y. Zhu, Z. Wang, C. Gao, H. Mohwald, *Macromol. Rapid Commun.* **2010**, *31*, 1015.
[18] A. Muñoz Javier, O. Kreft, M. Semmling, S. Kempter, A. G. Skirtach, O. Bruns, P. d. Pino, M. F. Bedard, J. Rädler, J. Käs, C. Plank, G. Sukhorukov, W. J. Parak, *Adv. Mater.* **2008**, *20*, 4281.
[19] K. Wang, Q. He, X. Yan, Y. Cui, W. Qi, L. Duan, J. Li, *J. Mater. Chem.* **2007**, *17*, 4018.
[20] B. G. De Geest, S. De Koker, G. B. Sukhorukov, O. Kreft, W. J. Parak, A. G. Skirtach, J. Demeester, S. C. De Smedt, W. E. Hennink, *Soft Matter* **2009**, *5*, 282.
[21] B. Zebli, A. S. Susha, G. B. Sukhorukov, A. L. Rogach, W. J. Parak, *Langmuir* **2005**, *21*, 4262.
[22] A. Muñoz Javier, P. d. Pino, M. Bedard, A. G. Skirtach, D. Ho, G. Sukhorukov, C. Plank, W. J. Parak, *Langmuir* **2009**, *24*, 12517.
[23] B. Radt, T. A. Smith, F. Caruso, *Adv. Mater.* **2004**, *16*, 2184.
[24] A. G. Skirtach, A. M. Javier, O. Kreft, K. Köhler, A. P. Alberola, H. Möhwald, W. J. Parak, G. B. Sukhorukov, *Angew. Chem.* **2006**, *118*, 4728; *Angew. Chem. Int. Ed.* **2006**, *45*, 4612.
[25] R. Palankar, A. G. Skirtach, O. Kreft, M. Bedard, M. Garstka, K. Gould, H. Mohwald, G. B. Sukhorukov, M. Winterhalter, S. Springer, *Small* **2009**, *5*, 2168.
[26] G. C. R. Ellis-Davies, *Nat. Methods* **2007**, *4*, 619.
[27] S. Carregal-Romero, M. Ochs, P. Rivera-Gil, C. Gana, A. M. Pavlov, G. B. Sukhorukov, W. J. Parak, *J. Controlled Release* **2012**, *159*, 120.
[28] C. Hrelescu, J. Stehr, M. Ringler, R. A. Sperling, W. J. Parak, T. A. Klar, J. Feldmann, *J. Phys. Chem. C* **2010**, *114*, 7401.
[29] J. Rejman, G. Tavernier, N. Bavarsad, J. Demeester, S. C. De Smedt, *J. Controlled Release* **2010**, *147*, 385.
[30] M. F. Bedard, B. G. De Geest, A. G. Skirtach, H. Mohwald, G. B. Sukhorukov, *Adv. Colloid Interface Sci.* **2009**, *1*, 1705.
[31] B. G. De Geest, M. A. Willart, B. N. Lambrecht, C. Pollard, C. Vervaet, J. P. Remon, J. Grooten, S. De Koker, *Angew. Chem.* **2012**, *124*, 3928; *Angew. Chem. Int. Ed.* **2012**, *51*, 3862.
[32] M.-L. De Temmerman, J. Rejman, J. Demeester, D. J. Irvine, B. Gander, S. C. De Smedt, *Drug Discovery Today* **2011**, *16*, 569.
[33] R. Weissleder, *Nat. Biotechnol.* **2001**, *19*, 316.
[34] N.-N. Dong, M. Pedroni, F. Piccinelli, G. Conti, A. Sbarbati, J. E. Ramírez-Hernández, L. Martínez Maestro, M. C. Iglesias-de la Cruz, F. Sanz-Rodriguez, A. Juarranz, F. Chen, F. Vetrone, J. A. Capobianco, J. G. Solé, M. Bettinelli, D. Jaque, A. Speghini, *ACS Nano* **2011**, *5*, 8665.
[35] R. Mohr, K. Kratz, T. Weigel, M. Lucka-Gabor, M. Moneke, A. Lendlein, *Proc. Natl. Acad. Sci. USA* **2006**, *103*, 3540.
[36] C.-T. Lin, K.-C. Liu, *Int. Commun. Heat Mass Transfer* **2009**, *36*, 241.

Communications

Intracellular Release

M. Ochs, S. Carregal-Romero, J. Rejman, K. Braeckmans, S. C. De Smedt, W. J. Parak* ——— ■■■■–■■■■

Light-Addressable Capsules as Caged Compound Matrix for Controlled Triggering of Cytosolic Reactions

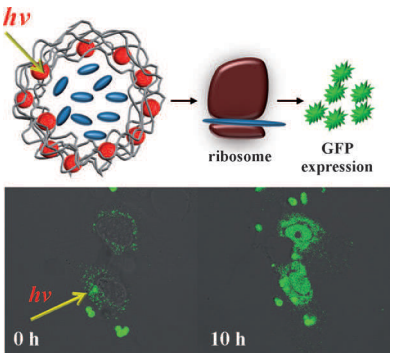

Release me: Polyelectrolyte capsules with different cargo in their cavities and plasmonic and magnetic nanoparticles in their walls were synthesized. Enzymatic reactions were triggered inside cells by light-mediated opening of two individual capsules containing either an enzyme or its substrate, by using photothermal heating. Furthermore, this technique allows controlled release of mRNA from capsules, thereby resulting in synthesis of green fluorescent protein (GFP).